

Special design considerations for precast prestressed hollow core floors

@Seismicisolation



Special design considerations for precast prestressed hollow core floors

Guide to good practice prepared by *fib* Commission 6

Prefabrication

(former FIP Commission 5 with the same title)

January 2000

@Seismicisolation

Subject to priorities defined by the Steering Committee and the Praesidium, the results of *fib*'s work in Commissions and Task Groups are published in a continuously numbered series of technical publications called 'Bulletins'. The following categories are used:

category	minimum approval procedure required prior to publication
Technical Report	approved by a Task Group and the Chairpersons of the Commission
State-of-Art report	approved by a Commission
Manual or Guide (to good practice)	approved by the Steering Committee of <i>fib</i> or its Publication Board
Recommendation	approved by the Council of <i>fib</i>
Model Code	approved by the General Assembly of <i>fib</i>

Any publication not having met the above requirements will be clearly identified as preliminary draft.

This Bulletin N° 6 has been approved as a *fib* Guide to good practice in October 1999 by the Publication Board of the *fib* Steering Committee.

Commission 6 on *Prefabrication* started as a former FIP Commission 5 with the same title. CEB and FIP merged in 1998 into *fib*. This guide, therefore, is published in the new *fib* series of bulletins:

A. Van Acker (Belgium, Chairman), M. Menegotto^⑤ (Italy, Vice-chairman), N. Robbens (Belgium, Secretary), S. Alexander (Norway), J. Beluzsar (Hungary), J. Calavera (Spain), A. Cholewicki^④ (Poland), A. De Chefdebien (France), B. Della Bella^② (Italy), K. S. Elliott^④ (United Kingdom), B. Engström (Sweden), D. Fernandez-Ordonez (Spain), C. Goodchild (United Kingdom), K. Gylltoft^① (Sweden), J. Havinga (South Africa), R. Krömer (Germany), L. Marcaccioli^⑤ (Italy), F. Mönnig (Germany), A. Ramakrishna (Italy), G. Rise^③ (Sweden), H. Romanes (New Zealand), A. Sarja (Finland), L. Sasek (Czech Republic), L. V. Sassonko (Russia), N. L. Scott (USA), A. Skjelle (Norway), A. Suikka (Finland), B. S. Tsoukantas (Greece), J. Vambersky (The Netherlands), C. W. Wilson (USA)

Full affiliation details of Commission members may be found in the *fib* Directory.

①②③④⑤: Chapter number for which this Commission member was the main preparing author. For chapter 3 *Non-rigid supports* the co-operation of W. Bennen (The Netherlands) was highly appreciated.

Cover photo: Underground parking garage with composite beams (Piazza Vittoria, Genova, Italy)

© fédération internationale du béton (*fib*), 2000

Although the International Federation for Structural Concrete *fib* - fédération internationale du béton - created from CEB and FIP, does its best to ensure that any information given is accurate, no liability or responsibility of any kind (including liability for negligence) is accepted in this respect by the organisation, its members, servants or agents.

All rights reserved. No part of this publication may be reproduced, stored in a retrieval system, or transmitted in any form or by any means, electronic, mechanical, photocopying, recording, or otherwise, without prior written permission.

First published 2000 by the International Federation for Structural Concrete (*fib*)

Post address: Case Postale 88, CH-1015 Lausanne, Switzerland

Street address: Federal Institute of Technology Lausanne - EPFL, Département Génie Civil

Tel (+41.21) 693 2747, Fax (+41.21) 693 5884, E-mail fib@epfl.ch

ISSN 1562-3610

ISBN 2-88394-046-0

Printed by Sprint-Druck Stuttgart (2nd edition minor editorial changes, December 2000)



Foreword

In 1987 the Commission on Prefabrication published the FIP Recommendations on the design of "Precast prestressed hollow core floors". The document was highly appreciated by designers and public authorities because of the lack of guidelines elsewhere with respect to some specific features of the product, e.g. the absence of ordinary transverse reinforcement. It has also served as a reference guide for national standards and especially for the CEN product standard on Prestressed Hollow Core Slabs. During the production of the latter it was felt that some design rules were incomplete or missing. Furthermore, research carried out since 1987 has resulted in complementary knowledge on the behavior of hollow core floors, e.g. in combination with slender floor beams. The present Guide to good practice is intended to complement existing recommendations. The scientific research for the different items was carried out at Chalmers University of Technology, Sweden, for chapter 1; Politecnico di Torino, Italy for chapter 2; a Nordic research program carried out at VTT Finland for chapter 3; University of Nottingham, UK and Building Research Institute, Poland for chapter 4; Ist. di scienza e tecnica delle costruzioni dell'universita di Roma for chapter 5. The Commission wishes to thank the International Prestressed Hollowcore Association "IPHA" for its contribution, and particularly Tony Crane, for the work undertaken in the editing of this document.

Arnold Van Acker

Chairman FIB Commission
on Prefabrication

CONTENTS

Introduction	1
1. Transfer of prestressing	3
1.0 Notations	3
1.1 Introduction	4
1.2 Finite element modelling	5
1.2.1 Introduction	5
1.2.2 Material models	5
1.2.3 Calibration of the model	6
1.3 Applications on hollow core slabs	7
1.3.1 Introduction	7
1.3.2 Sensitivity study of influential parameters	9
1.3.3 Limit values of influential parameters	10
1.3.4 Tolerance influences and safety at release	11
1.4 Discussion and conclusions	12
1.4.1 Numerical results	12
1.4.2 Production control parameters	12
1.4.3 Detensioning design procedure	13
1.4.4 Correspondence and relevance to the code	13
1.5 References	13
2. Restrained composite support	15
2.1 Introduction and scope	15
2.2 Basic considerations	15
2.2.1 Restraint: when and why	15
2.2.2 Advantages and inconveniences	19
2.2.3 Examples of applications	20
2.3 Design guidelines	25
2.3.1 General	25
2.3.2 Structural types and schemes	26
2.3.3 Design principles and checks	27
2.3.4 Design analysis and recommendations	28
2.3.5 Detailed design recommendations	31
2.3.5.1 Negative (and positive) bending capacity of the composite member	31
2.3.5.2 Long term effects of the restrained supports	32
2.3.5.3 Anchorage capacity of the reinforcement bar in a filled core	36
2.3.5.4 Interface shear strength of the composite member	36
2.3.5.5 Shear capacity of the composite member, under negative moment, without contribution from prestressing	37
2.3.5.6 Flexural/shear tension capacity, under bending moment and contribution from prestressing	37
2.3.5.7 Anchorage resistance of the prestressing steel	40
2.3.5.8 Negative bending capacity of the hollow-core slab	40
2.3.5.9 Shear capacity at the slab-end section at the support	41
2.3.5.10 Shear and spalling stresses	42

2.4	Detailing of connections	44
2.4.1	General	44
2.4.2	Number and length of grouted cores	44
2.4.3	Simplified rules	46
2.5	References and experimental results	47

Annex A - Examples of calculation

1	General	49
1.1	Basis of calculation	49
1.2	Structural systems and support conditions	50
2.	Example 1 - Two-span floor	52
2.1	Simply supported slab with direct bearings	52
2.2	Slab continuous at center support, simply supported at end supports with direct bearings	56
2.3	Slab restrained at all supports and without direct (normal) bearings	62
3.	Example 2 - Multi-span floor	67
3.1	Simply supported slabs with direct (normal) bearings	67
3.2	Slabs continuous at internal supports with direct (normal) bearings	72
3.3	Slab restrained at all supports and without direct (normal) bearings	79
4.	General conclusion	85
3.	Non-rigid supports	89
3.1	Introduction	89
3.2	The behaviour of hollow core slabs supported on beams	90
3.3	Mechanical behaviour in transverse direction	93
3.4	Design at ultimate limit state	95
3.4.1	Shear tension failure in the hollow core slab	95
3.4.2	Longitudinal cracking of hollow core slabs	96
3.4.3	Design of curvature of the beam	96
3.5	Design in the serviceability limit state	96
3.5.1	Longitudinal cracking of the hollow core slabs	96
3.6	Design calculations	97
3.6.1	Data to be specified for the design	97
3.6.2	Critical cross-sections	97
3.6.3	The composite beam	99
3.6.4	Shear stress in the transverse direction	101
3.6.5	Maximum principal stress and the design criterion	103
3.6.6	Curvature of the beam	103
3.6.7	Serviceability limit state	104
3.7	Examples of calculation	105
3.8	References	116

4. Floor diaphragm action	117
4.1 General	117
4.2 Shear transfer mechanism	121
4.3 Edge profile and tie steel details	123
4.4 Calculation model	126
4.4.1 General	126
4.4.2 Shear wedging/ Shear friction resistance	127
- Strength due to aggregate interlock	
- Tie steel calculation	
- Shear stiffness due to aggregate interlock	
4.4.3 Dowel action	132
- Strength due to dowel action	
- Tie steel calculation due to dowel action	
- Shear stiffness due to dowel action	
4.4.4 Minimum area of tie steel	134
4.5 Shear stiffness of the entire diaphragm	134
4.6 Calculation example	135
4.6.1 Aggregate interlock	135
4.6.2 Dowel action	136
4.6.3 Shear stiffness of the entire diaphragm	137
4.7 Experimental and numerical studies of floor diaphragms	137
Appendix 1: Analytical derivation of τ and σ values and friction factor μ	140
References	142
5. Floors under seismic action	145
5.1 General	145
5.2 Diaphragm action	147
5.3 Seismic diaphragms	149
5.4 Design criteria	151
Appendix: Calculation examples	154

Introduction

Precast prestressed hollow core units are among to the more advanced structural floor systems for all kinds of buildings. The reason for this lies not only in the production technology, which is nearly fully automated , but also in other features such as optimum use of materials, slenderness of the construction, environmental friendliness, etc. Compared to plain concrete floors, hollow core floors can save 50% concrete and 30% steel for the same performances.

Because of the wide use of the product, and the creation of new markets and applications, much research work has been carried out in the past and is still going on, e.g. concerning the transfer of prestressing at the slab end, continuous supports, non-rigid supports, diaphragm action, composite action with the supporting beam, large openings, seismic action, non-static loading etc. The FIP Commission on Prefabrication published in May 1998 a Guide to Good Practice on “Composite floor structures”, in which the interaction between floors and toppings, or between floors and their supporting beam, is dealt with.

The present report gives design guidelines for some of the above mentioned subjects. The first chapter describes the state of knowledge concerning the stress distribution at the slab end, due to the transfer of prestressing. It deals with the splitting, bursting and spalling stresses, for which already calculation formulae were given in the previous FIP Recommendations on the design of hollow core floors. We now have a much better knowledge in this field.

The previous FIP recommendations only dealt with simply supported hollow core floor units. In the mean time, experience has been gained with continuous supports. The second chapter gives guidelines for the design of hollow core floors with restrained supports.

In the third chapter, the problem of decreased shear capacity due to the deflection of non-rigid supporting beams is dealt with. On the basis of an extensive test and research program, a new calculation method has been given to take account of the influence of a non-rigid support on the shear capacity of hollow core floors.

The fourth chapter gives a detailed analysis of the behavior and detailing of floor diaphragms composed of hollow core floor units. In the past, several research programs have been carried out on this subject. The aim of the study was to analyze the existing research and to give recommendations concerning the calculation model and formulae.

Finally the last chapter describes the design philosophy for a hollow core floor, subject to seismic action, and some practical calculation examples. They are intended for designers who are not familiar with this design requirement.

The *fib* commission on Prefabrication is also working on further topics, e.g. design rules for large openings, non static loading, horizontal loading on hollow core floors supported on retaining walls, etc. The *fib* Commission on Prefabrication expects to publish guidelines on these matters in the future.

1. Transfer of prestressing

1.0 Notations

f_{ba}	adhesion strength in the interface
f_{ct}	mean concrete tensile strength
f_{cc}	mean concrete compressive strength
f_{stu}	ultimate tensile strength of the strand
f_{ctk}	characteristic value of concrete tensile strength
$f_{ctk0.05}$	characteristic value of concrete tensile strength at the time of prestress release
$[C]$	elastic material stiffness matrix
E	modulus of elasticity
e_0	eccentricity of prestressing steel, in mm
G	shear modulus
k	core radius taken equal to the ratio of the lower section modulus and the area of the cross section, in mm
P_0	initial prestressing force in the considered web just after release
ε	normal strain
ϕ_p	diameter of strand
γ	total shear strain
γ_p	partial safety factor for prestressing stress
γ_c	partial safety factor for concrete tensile strength
μ	coefficient of friction
σ	normal stress
σ_\perp	normal stress in the interface
σ_γ	expansion stress
σ_{spl}	splitting stress
σ_{sp0i}	initial prestressing stress
σ_{sp0}	prestressing stress after release
σ_{sp0d}	design value of prestressing stress
σ_{sp0k}	characteristic value of prestressing stress
τ	shear stress
τ_i	shear stress in the interface

1.1 Introduction

In the FIP Recommendations [FIP Recommendations 1988], the calculation rules for the analysis of the spalling stresses due to the transfer of prestressing in the transmission zone are conservative and do not correspond to daily practice.

The draft of the European product standard for prestressed hollow core slabs, prEN 1168, gives the following design rules for the resistance to spalling

- for the web in which the highest spalling stress will be generated, or, for the whole section if the strands or wires are essentially well distributed over the width of the slab element, the spalling stress σ_{sp} shall satisfy the following condition:

$$\sigma_{sp} \leq f_{ck0.05} \quad (1.1)$$

$$\text{with } \sigma_{sp} = \frac{P_0}{b_w \cdot e_0} \cdot \frac{15 \cdot \alpha_e^{2.3} + 0.07}{1 + \left(\frac{l_{bp}}{e_0} \right)^{1.5} \cdot (1.3 \cdot \alpha_e + 0.1)}$$

$$\text{and } \alpha_e = \frac{e_0 - k}{h}$$

where:

- $f_{ck0.05}$ is the characteristic value of concrete tensile strength of the concrete at the time the prestress is released, in N/mm²
- P_0 is the initial prestressing force just after release in the considered web, in N
- e_0 is the eccentricity of prestressing steel, in mm
- k is the core radius taken equal to the ratio of the lower section modulus and the area of the cross section, in mm;

- a fracture mechanics design using the method of finite elements shall prove that spalling cracks will not develop, using characteristic values on fracture energy and tensile strength;
- all elements shall be visually inspected before delivery and any element with horizontal spalling cracks rejected.

At the beginning of 1990, a project was initiated at Chalmers University of Technology in Göteborg, to investigate the response and condition in the transmission zone, using a non-linear three-dimensional finite element model. A detailed survey of the study is given hereafter.

The specific bond properties of strands are mainly determined by the number of wires, the pitch, the surface roughness and lack of fit of the strands and of indentations, if any. Typical relations between bond stress and slip for different types of reinforcement are shown in Fig 1.1.

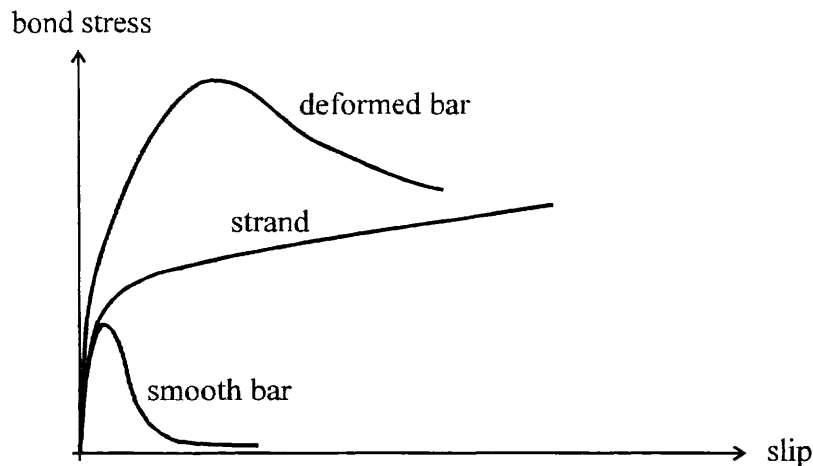


Fig. 1.1 Schematic relations between bond stress and slip for different reinforcement types.

Lack of fit, surface roughness, pitch and indentations are all factors that directly affect the frictional resistance of the strand by increasing the normal pressure when the strand is sliding.

1.2 Finite element modelling

1.2.1 Introduction

The precast hollow core slabs studied in the project are shown in Figure 1.2. The load action concerned is the action due to the release of the prestressing force in the strands. The response of the slab for this action was analysed using a 3-D FE model based on fracture mechanics. The FE code ABAQUS [ABAQUS (1989)] was used. In order to model the response as close as possible, a new nonlinear interface model was developed to describe the interface between the strand and the concrete.

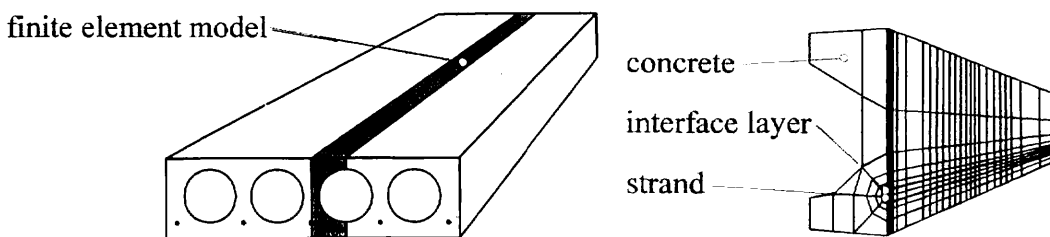


Fig. 1.2 Hollow core slab with 3-D finite element model.

1.2.2 Material models

For the concrete and the strand, the standard options for material modelling in ABAQUS were used. The slip behaviour was simulated with an interface layer around the strand in which the new interface model was used, Figure 1.3.

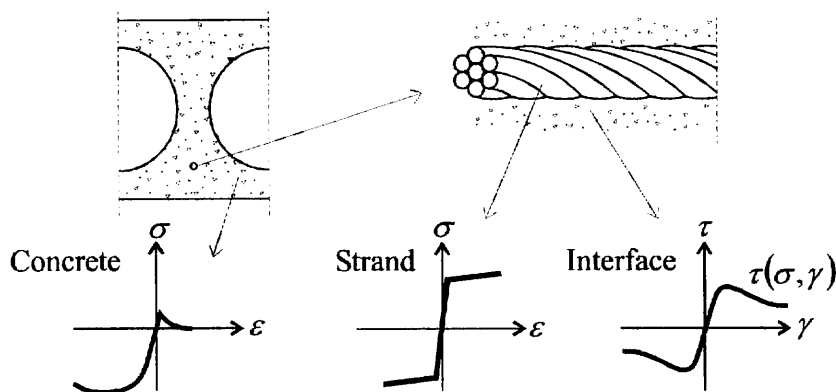


Fig. 1.3 "Materials" used in the finite element model.

The new interface model (here called BOND) made it possible to simulate the slip between the strand and the surrounding concrete. The model is formulated as a conventional elastic-plastic material model with a yield condition, a flow rule and a softening law. BOND defines two arbitrary stress components, σ_\perp and τ_\parallel (the other four are set equal to zero), the slip and the material stiffness matrix $[C]$ with the elements $C_{ij} = \partial\sigma_i / \partial\varepsilon_j$. The parameters of the interface model are a modulus of elasticity E , a shear modulus G , an adhesion capacity f_{ba} , a coefficient of friction μ and an expansion-stress curve $\sigma_\gamma(\gamma)$. The expansion-stress curve is a special feature of the model, which couples the normal stress to the shear strain, i.e., the interface expands when it is subjected to shear deformations. A typical expansion-stress curve, which gives the relation between slip and the normal stress in the interface for fixed interface boundaries in the normal direction is shown in Figure 1.4.

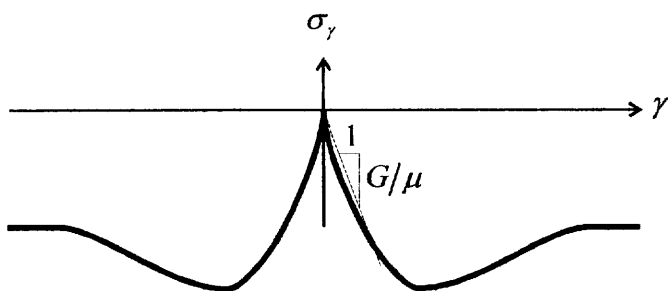


Fig. 1.4 Stress strain relation with associated parameters describing the expansion-stress versus the total shear strain.

1.2.3 Calibration of the model

The numerical experiments performed in the calibration process of the interface model, were divided into two groups. For the first group, the aim was to determine material parameters that could not be established from the literature. This was done through an adjustment process where data from [Gylltoft (1979)] and [Tassi (1988)] was used. The aim of the second group of numerical experiments was to verify the material models with laboratory tests. All FE analyses were performed with ABAQUS.

1.3 Applications on hollow core slabs

1.3.1 Introduction

In the numerical experiments that were performed on hollow core slabs, the material parameters derived and established in the calibration process were used. The study consisted in all of three different groups of analyses. The first group of numerical analyses was a sensitivity study in which the influential parameters of interest were identified. The second group was a study that was intended to establish the limits of the influential parameters with respect to the failure criteria associated with the types of failure studied here (bursting failure, splitting failure or total loss of bond strength around the strand). In this second group, the failure criteria were defined as visible cracks on the concrete surface, crack widths of 0.3 millimetres or more, extremely long transmission length or a draw-in of several millimetres. The third and last group was a study concerning tolerance influence and safety with respect to failure at release of the prestressing force. In the last group of analyses, all influential parameters were given unfavourable values within allowed tolerances. Three different slab types were used in the analyses, a small 215 mm thick slab, a medium 265 mm thick slab and a large 380 mm thick slab, see Figures 1.5 and 1.6. The length of the slabs varied depending on the study performed. The load action in all of the analyses was the prestressing force in the strand and the dead weight of the structures.

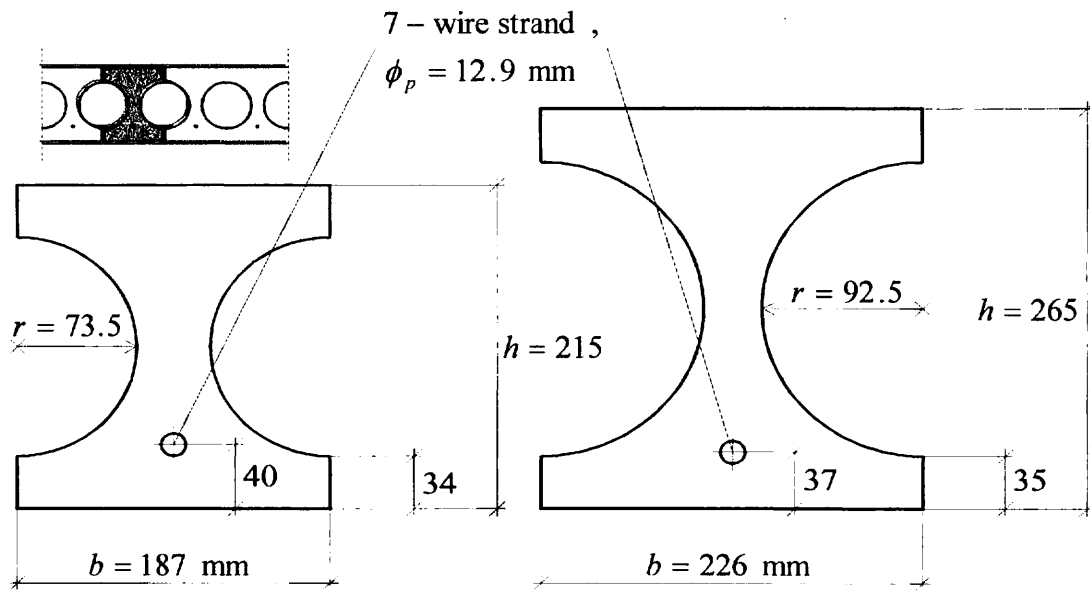


Fig. 1.5 Small and medium hollow core slabs used in the analyses.

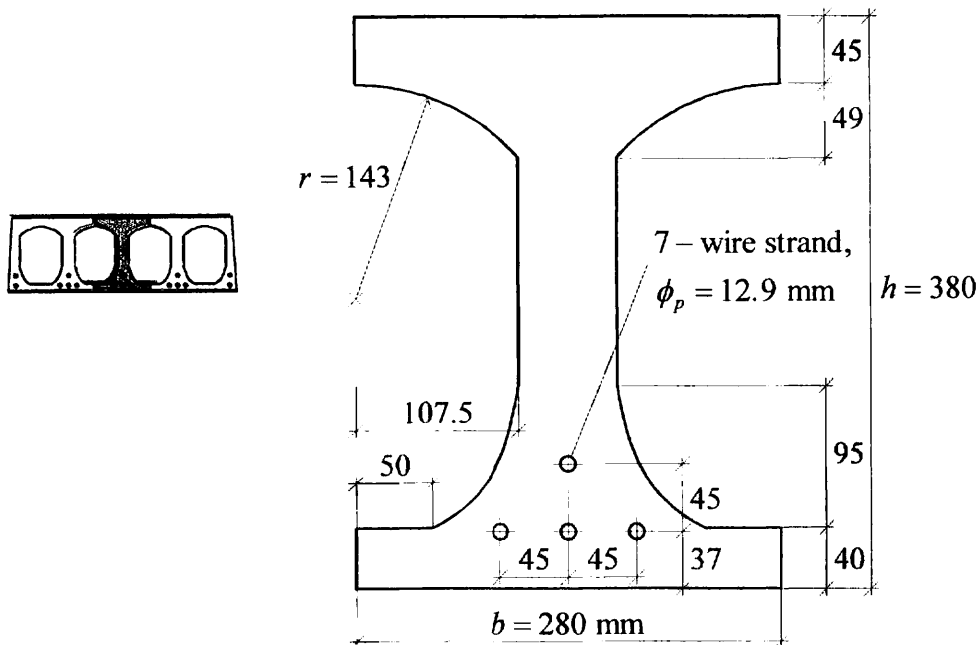


Fig. 1.6 Large hollow core slab used in the analyses.

The expression used, in the second and third group of analyses, for the tensile strength was derived from the measured strength at release, see equation 1.2.

$$f_{ct} = 0.381 \cdot f_{cc}^{2/3} [\text{MPa}] \quad (1.2)$$

In the sensitivity study a simplified bi-linear stress strain relation for the 7-wire strand was used, while the more complex stress strain relation according to [CEB-FIP Model Code (1990)] was used in the study of limit values of influencing parameters and the study of tolerance influences. In both relations, the same ultimate tensile strength $f_{stu} = 1860.0$ MPa was used.

All of the FE analyses, as in the calibration process, were done with the FE code ABAQUS. Post-processing was done with the CAD I-DEAS and with a FORTRAN program developed within the project. With these two post-processing tools, it was possible to visualise output in a simple and understandable way. In Figures 1.7 and 1.8, examples of typical results from a FE-analysis are shown.

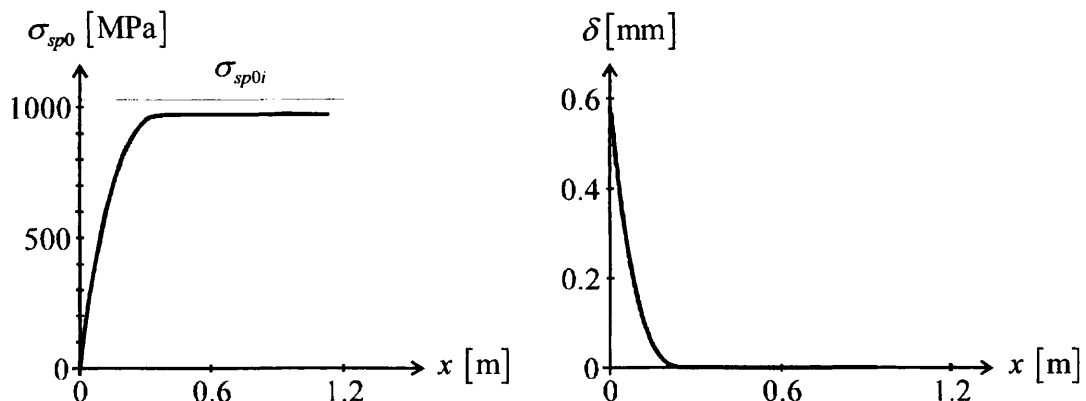


Fig. 1.7 Normal stress and slip distribution along a strand in a hollow core slab after the release of the prestressing force.

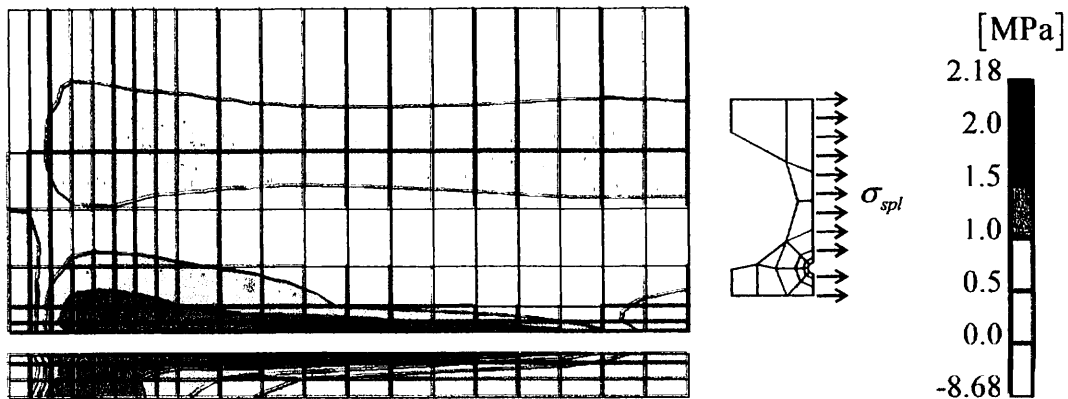


Fig. 1.8 Splitting stress distribution $\sigma_{sp,l}$ in the middle of the section, in a hollow core slab rib after the release of the prestressing force.

1.3.2 Sensitivity study of influential parameters

To study the behaviour of the numerical model and to determine which parameters should be varied in forthcoming analyses (by which the parameter limits allowed would be determined), a sensitivity study was performed on a prestressed hollow core slab rib with a thickness of 215 mm and a length of 2.4 m. Interesting variation parameters were chosen to be the concrete compressive strength f_{cc} , the prestressing stress $\sigma_{sp0,i}$, the radius of the hole r and the concrete cover c , Figure 1.9.

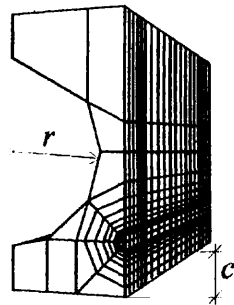


Fig. 1.9 Three-dimensional finite element model used in the sensitivity analysis consisting of 4524 elements with 18 603 degrees of freedom.

To get a well-defined transfer length, a new definition was used. The transfer length was defined as the length to the intersection of a line l_1 , passing through the origin and the point where 90 % of the maximum stress in the strand was reached, and a line l_2 that was derived as the least square solution through the last 10 elements in the FE mesh (i.e., a line through the points for the positions of the last 10 elements and their normal stresses), Figure 1.10.

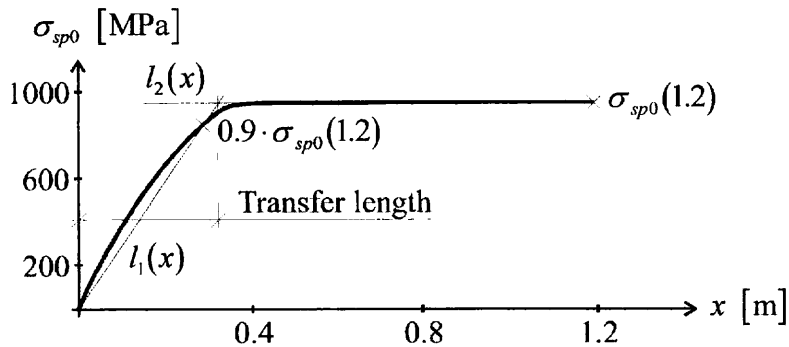


Fig. 1.10 Definition of transfer length in the sensitivity analysis.

The sensitivity study was performed by varying, one by one, the influential parameters around a chosen standard configuration ($f_{cc} = 47.5\text{ MPa}$, $\sigma_{sp0i} = 1000.0\text{ MPa}$, $r = 73.5\text{ mm}$, $A = 100.0\text{ mm}^2$ and $c = 34.36\text{ mm}$). The completed sensitivity analysis showed that the numerical model behaved in a realistic way for all of the influential parameters. The two parameters that had the most influence on the response for transfer length, draw-in and cracking were the compressive concrete strength f_{cc} and the initial prestressing stress σ_{sp0i} .

1.3.3 Limit values of influential parameters

The analyses of the second group were designed with the aim of establishing the failure limits of the influential parameters of interest (which were identified in the sensitivity analyses), i.e., the concrete compressive strength f_{cc} , the prestressing stress σ_{sp0i} , the radius of the hole r and the concrete cover c . In the process of establishing the failure limits, the parameters were varied around a standard configuration one by one until failure occurred. The failure criteria were defined as visible cracks on the concrete surface, extreme transmission length or a draw-in of several millimetres. Two different types of slabs were used in the analyses, the medium 265×6000 mm slab and the large 380×6000 mm slab. The finite element models had 1404 elements with 6042 degrees of freedom and 3402 elements with 12 255 degrees of freedom respectively.

In Table 1.1, the limits of the different influential parameters are shown. The crack widths are the maximum widths for the critical cracks and they are estimated as the normal strain perpendicular to the crack plane multiplied by the relevant length of the element (this way of estimating the crack width was used in all of the slab analyses). The critical cracks are the largest of the cracks that are visible on the concrete surface. For the large slab, the critical crack originated from the lower left strand and propagated towards the centre of the hole whereas, for the medium slab, the critical crack propagated from the strand downwards. Table 1.1 also shows the transfer length that was defined according to the definition in the sensitivity analysis. It should be noted that some of the limits in Table 1.1 were not governed by the failure criteria but also by material and geometrical limitations (i.e., the yield stress in the strand and the width of the hollow core rib).

Type	Transfer length	Draw-in	Crack width
Large slab			
standard: $\begin{cases} f_{cc} = 29.0 \text{ MPa} \\ \sigma_{sp0i} = 1200.0 \text{ MPa} \\ r = 109.0 \text{ mm} \\ c = 31.35 \text{ mm} \end{cases}$	524	1.19	0.006
$f_{cc} = 20.0 \text{ MPa}$	649	1.46	0.012
$\sigma_{sp0i} = 1534.5 \text{ MPa}$	632	1.89	0.019
$r = 134.5 \text{ mm}$	532	1.19	0.009
$c = 20.0 \text{ mm}$	544	1.24	0.010
Medium slab			
standard: $\begin{cases} f_{cc} = 29.0 \text{ MPa} \\ \sigma_{sp0i} = 1200.0 \text{ MPa} \\ r = 92.5 \text{ mm} \\ c = 31.36 \text{ mm} \end{cases}$	458	1.15	0.000
$f_{cc} = 15.0 \text{ MPa}$	613	1.59	0.020
$\sigma_{sp0i} = 1534.5 \text{ MPa}$	512	1.66	0.014
$r = 108.0 \text{ mm}$	466	1.16	0.000
$c = 20.0 \text{ mm}$	486	1.26	0.037

Table 1.1 Failure limits of influential parameters in millimetres.

1.3.4 Tolerance influences and safety at release

In this analysis, the objective was to investigate the condition of three typical slab types after the release of the prestressing force. To get a conservative estimate of the response, a 10 % reduction of concrete material data, a 10 % increased initial prestressing stress and unfavourable geometrical tolerances were used. The tolerances gave a slab height decreased by 4 mm, a radius r increased by 4.0 mm and a concrete cover c decreased by 4 mm. After the first analysis, a failure analysis was performed with the intention to increase the prestressing stress until failure occurred, however, for all three types of slabs the analyses were ended when the strands started to yield. The slabs that were investigated were the two slabs, large and medium, used in the limit analyses, and a small 215×6000 mm slab with $f_{cc} = 29.0 \text{ MPa}$, $\sigma_{sp0i} = 1040.0 \text{ MPa}$, $r = 73.5 \text{ mm}$ and $c = 34.4 \text{ mm}$. The FE model used for the third slab had 754 elements with 3240 degrees of freedom. Table 1.2 shows transfer length, draw-in and maximum crack width for the three slabs; for the failure analysis, the maximum prestressing stress is also shown. The results given in the table, for the failure analysis, are for steel stresses equal to the yield stress in the strand.

Type	Transfer length	Draw-in	Crack width
Safety analysis			
Large	540	1.70	0.005
Medium	504	1.40	0.015
Small	423	1.14	0.000
Failure analysis			
Large/1534.5	719	2.19	0.008
Medium/1534.5	556	1.84	0.020
Small/1534.5	496	1.78	0.000

Table 1.2 Absolute values in mm for transfer length, draw-in, crack width, and for the safety analysis and the failure stress (yield stress) for the large, medium and small slabs, respectively.

1.4 Discussion and conclusions

1.4.1 Numerical results

After the calibration process, numerous comparisons were made between FE results and laboratory results. In all comparisons, material parameters were entered in the FE models and the calculation results were directly compared to the laboratory results without calibration. From the comparisons, it appeared that the material models offer the opportunity to model a variety of problems with reasonably good accuracy. After the calibration and comparisons, numerous analyses of different types of prestressed hollow core slabs were made. They aimed at investigating responses for stress state, cracking, draw-in and transfer length of the slabs. With these data it should be decided whether the slabs need transverse reinforcement to assure sufficient bearing capacity with respect to the types of failure (bursting failure, splitting failure and total loss of bond strength around the strand) studied in this project.

The conclusion that can be drawn from the analyses on hollow core slabs is that there is no danger of bursting failure, splitting failure or total loss of bond stress around the strand under normal conditions as the safety margins are sufficiently high. It should be noted that in none of the slab analyses spalling cracks occurred. The significance of the non-linear analysis models is that they make it possible to take into account softening of the materials and, thereby, to allow for stress redistribution, which cannot be modelled by conventional methods. One example of softening behaviour is cracking in concrete. Normally, in the analyses of the slabs, splitting cracks formed close to the strands but were stopped and did not penetrate to the surface.

1.4.2 Production control parameters

One outcome of all analyses is the feasibility to identify production control parameters enabling to estimate the condition of a hollow core slab in the production process. The criteria to assure that a slab has sufficient load bearing capacity in the transmission zone could be to limit the draw-in to 2.0 mm and no visible cracks on the concrete surface. Given these criteria, the results from chapter 1.3.3 show that the mean concrete compressive strength, f_{cc} , should be at least 20.0 MPa, the concrete cover, c , minimum 20 mm and the initial prestressing stress, σ_{sp0i} , below 1500 MPa (this limit is an estimate from chapter 1.3.4). The suggested limits of the influential parameters, were defined on the basis of analyses in which the influential parameters were varied one by one.



1.4.3 Detensioning design procedure

Detensioning should be performed as an ULS analysis. The design values for the prestressing stress and the material parameters should be $\sigma_{sp0d} = \gamma_p \cdot \sigma_{sp0k}$, $f_{ctd} = \gamma_c \cdot f_{ctk}$ etc., where indices d and k stand for design and characteristic, respectively. The failure criterion in the above mentioned situation should be: limited (stable) deformations in the whole body.

1.4.4 Correspondence and relevance to the code

The overall result from the non-linear FE analyses did show a fairly good correspondence with the results from the studied experiments concerning the slippage and the transfer length. The suggestion of a lowest compressive strength of 20 N/mm^2 is in good correspondence with the numerical results obtained in the present study.

The “minimum thickness” (4.3.1.1) of any web in the slab described in the section of product requirements is exactly in line with the observation from the numerical slab analyses where the same thickness was found to be a lower limit of the thickness with respect to failure.

The requirements for preventing cracking in the transmission zone described in “bursting and splitting” (4.3.3.1), was also in line with the observations from the numerical analyses.

A final concluding remark when comparing the suggestions in the code with the results from the numerical analyses is that the non-linear fracture mechanics based FE modelling technique is a powerful approach when studying the condition of these kinds of objects for the present loading situation. It can also be noted that the suggestions in the code are supported by the numerical results in [Åkesson (1993)].

1.5 References

FIP Recommendations - Precast prestressed hollow core floors (1988): FIP Commission on Prefabrication, Thomas Telford, London, England.

ABAQUS Theory manual version 4.8 (1989): HKS, Hibbit, Karlsson and Sorensen INC., HKS, Providence, USA, 341 pp.

Gylltoft K. (1979): Bond properties of strands in fatigue loading, Luleå University of Technology, Division of Structural Engineering, Research report TULEA 1979:22, Luleå, Sweden, 73 pp.

Tassi G. (1988): Bond properties of prestressing strands, Proceedings of the FIP symposium, Jerusalem, Israel, 8 pp.

CEB-FIP Model Code 1990 First draft No 196 (1990): Comité Euro-International du Beton, Lausanne, Switzerland, 461 pp.

Åkesson M. (1993): Fracture mechanics analysis of the transmission zone in prestressed hollow core slabs, Chalmers University of Technology, Division of Concrete Structures, Göteborg, Sweden, 62 pp.



Seite

(14)

bleibt
wiss.

@Seismicisolation

Copyright fib, all rights reserved. This PDF copy of fib Bulletin 6 is intended for use and/or distribution only by National Member Groups of fib.

2 Restrained composite support

2.1 Introduction and scope

The FIP Recommendations [1] are mainly restricted to simply supported floors units. However during the past 20 years, experience has also been gained with restrained support conditions, especially in combination with cast in-situ beams and walls, or in mixed composite structures. These applications are fairly common in some buildings, and in seismic designs mainly in Italy, Spain and Turkey.

The present chapter deals with the analysis, the design rules and the detailing for hollow core units with restraint at support. They may act compositely with the supporting beam, which is usually assumed to be rigid. In the case of non-rigid support, additional stresses due to the composite action with the beam should be taken into account according to Chapter 3 "Non-rigid supports".

The analysis of hollow-core floors with restraint at the support, should be carried out for all critical sections in the vicinity of the support, taking into account the structural scheme and the two loading conditions

- a) Temporary condition with simple bearings and dead loadings prior to the hardening of in situ concrete.
- b) Final condition taking account of restrained bearings and imposed live loadings.

Basic considerations about the advantages and disadvantages of such an application, requiring additional in-situ concrete and steel reinforcement within a certain number of open cores at the slab end, are also given.

The design guidelines in the present chapter refer frequently to the new European Standard "Eurocode 2 – Design of concrete structures". The reason thereto lies not only in the fact that this standard is largely based on the CEB-FIP Model Code, and thus reflects the latest state of knowledge on the matter, but also because it contains an extensive part dealing with precast concrete elements and structures.

2.2 Basic considerations

2.2.1 Restraint: when and why

Hollow core floor units have been used until 70's mainly as simple floor units in combination with precast or steel structures with simple and dry connections, minimizing any additional in-situ concrete or steel reinforcement. Hollow core floor elements were therefore normally applied according to a "free or simple bearing" scheme without any restraint at the supports, as is still frequently the case to-day in totally precast concrete structures.

Since the 70's however hollow core units have been largely applied in residential and office buildings and in car parks designed or hybrid (mixed) structures where the monolithic design characteristics normally associated with traditional cast in-situ structures is achieved.

However restraint is "recommended", and requires a careful design of connections, to meet the requirement of a monolithic structure (i.e. for mixed- composite and for seismic buildings).



In such buildings the additional in-situ concrete and reinforcement will not normally constitute any additional problem for the contractor, since part of building structure is already cast in-situ (e.g. columns, staircases and basement walls, and often also beams and floor topping).

Restraint is a "must" when hollow core floor units are to be used in a totally cast in-situ structure with frames or walls, to avoid large beams or walls (see fig. 2-1,2-2,2-3,2-4). In the case of flat beams, the limitations for non-rigid supports should also be considered (see chapter 3).

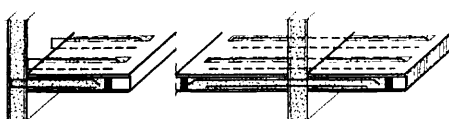


Fig. 2-1: Wall system

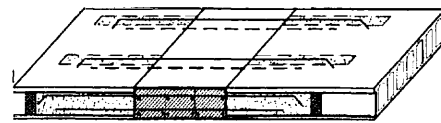


Fig. 2-2: Flat beam

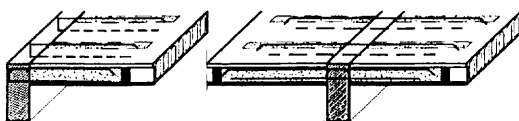


Fig. 2-3: Traditional beams

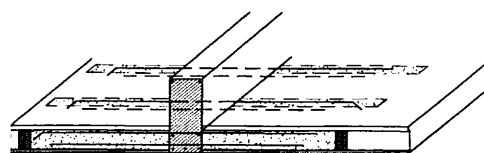


Fig. 2-4: Up stand beam

Restraint or continuity is also a "must" when the floor finishing is such that no large cracks are allowed at the intermediate supports and when deflection under live and long-term loads has to be minimized (see fig. 2-5,2-6).

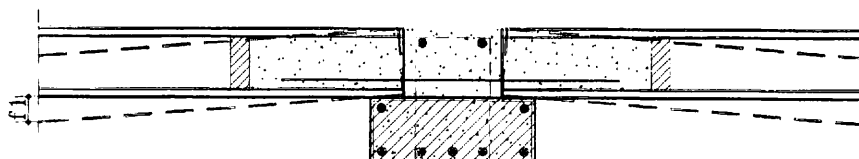


Fig. 2-5: Simple support: large cracks and higher deflection ($f_1 = 2-5 f_2$)

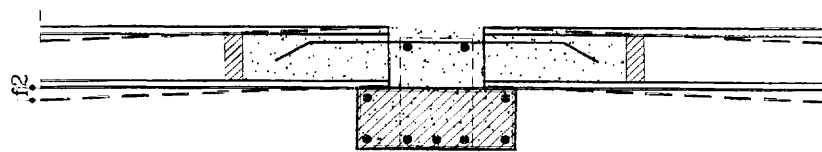


Fig. 2-6: Restrained support and floor continuity: no large cracks and minimum deflection

Restraint is also "recommended" when, to increase the stiffness, the compression flange of the beam, has to be enlarged between the ends of hollow core slabs. The latter functions as the compression flange of a complete composite structure (see fig. 2-7,2-8).

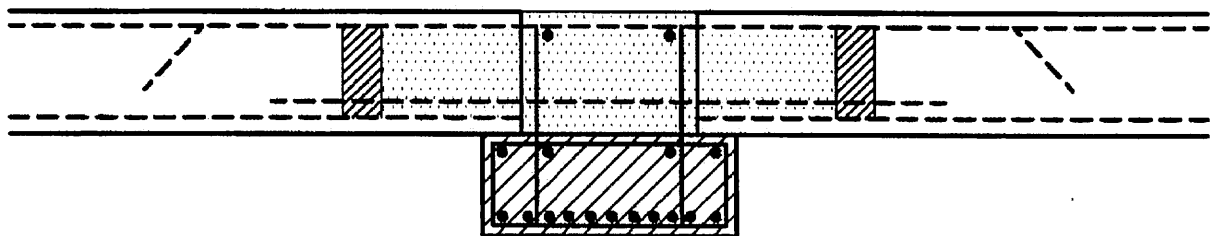


Fig. 2-7: Compression flange of composite beam

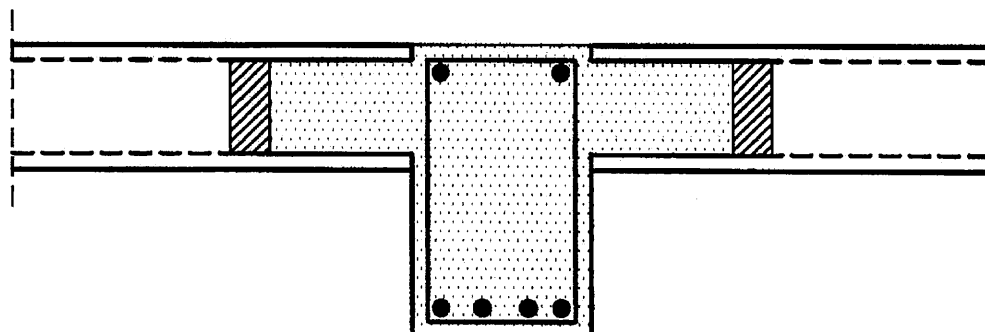


Fig. 2-8: Compression flange of in-situ beam

Finally, restraint is an intended design or unintended "consequence", which the designer has to recognise when particular construction conditions occur (i.e. floor slabs restrained between lower and upper walls, or slabs with a reinforced topping, see fig. 2-9,2-10).

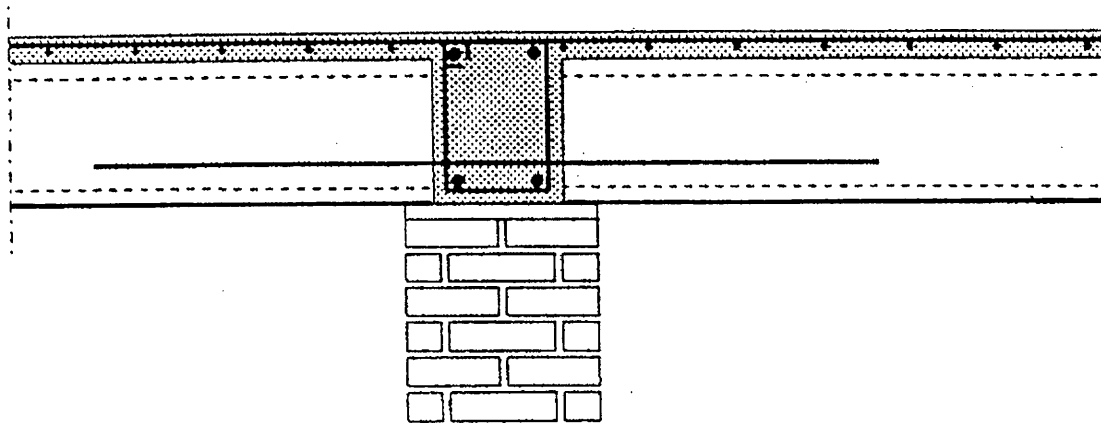


Fig. 2-9: Unintended floor continuity

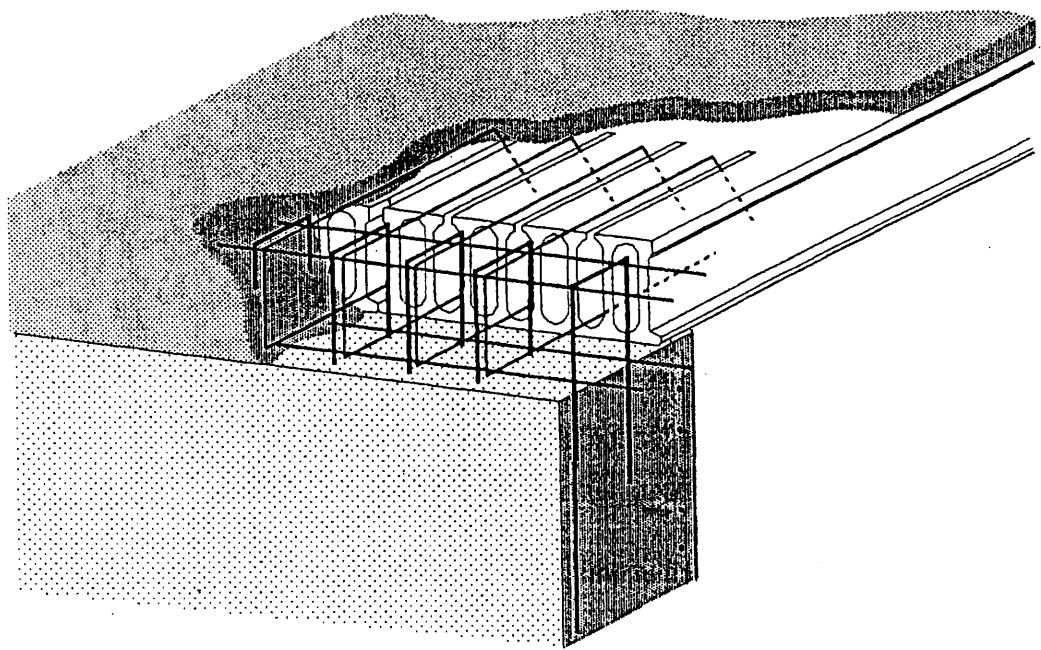
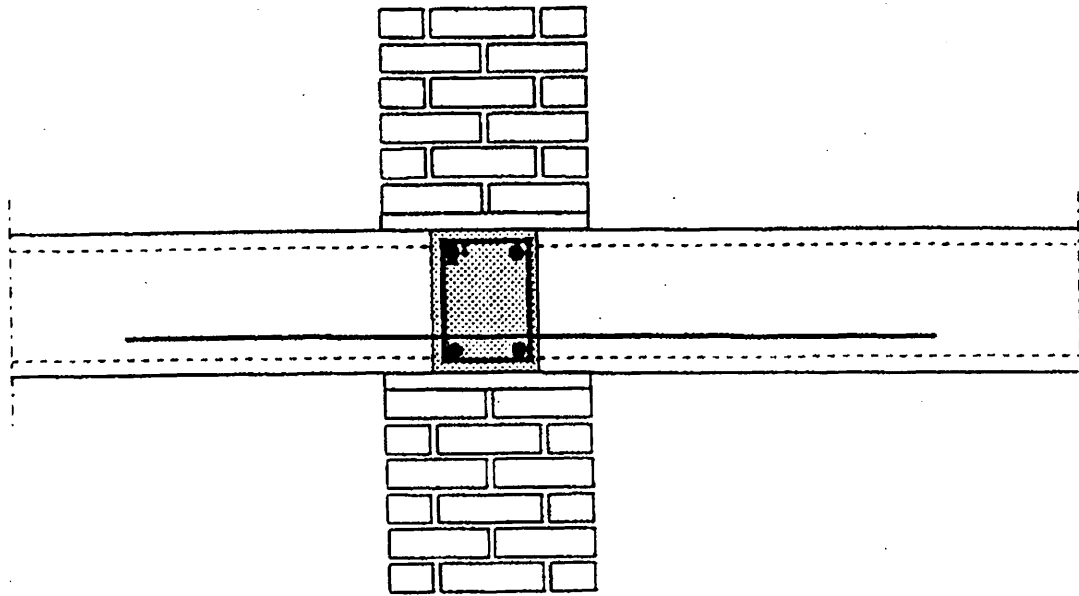


Fig. 2-10: Unintended wall restraintment

@Seismicisolation

2.2.2 Advantages and inconveniences

In designing hollow-core floors with negative moment at supports, the following technical and economical aspects should be taken into account and evaluated, compared to the traditional way to design based on a simple support scheme.

<u>Requirement</u>	<u>Advantages</u>	<u>Disadvantages</u>
1. Moment and (shear) resistance at SLS and ULS	<ul style="list-style-type: none"> - Higher values (up to 30%) with same hollow-core section and prestressing reinforcement With regard to shear it depends on the number of cores filled in-situ with concrete. 	<ul style="list-style-type: none"> - Higher incidence of additional reinforcement and in-situ concrete (up to 3 Kg/m² steel and 30 lt/m², concrete) for connections at supports - Provision of a minimum number of upper strand and open cores at upper face of slab ends - Provision of plugs inside cores at a stated distance from the support - Limitation of max H.C. prestressing reinforcement to avoid excess of compression stresses into the bottom flange - Higher design shear value to be supported by beam - Additional shear stresses in the webs due to composite action and necessity of filling of cores
2. Fire resistance	<ul style="list-style-type: none"> - Higher value (up to 30 %) with the same H.C. section and prestressing reinforcement 	<ul style="list-style-type: none"> - See point 1)
3. Seismic design of prefabricated structures with H.C. floor slabs	<ul style="list-style-type: none"> - Higher value of the behavior factor "q", due to higher structural ductility and energy dissipation 	<ul style="list-style-type: none"> - See point 1)
4. Minimum elastic and long term deflection under live and permanent loads	<ul style="list-style-type: none"> - The requirement is met with lower deflection values (up to 2-5 times) with the same H.C. section 	<ul style="list-style-type: none"> - See point 1)
5.(Absence) or minimizing of upper cracks at supports in multispan floors	<ul style="list-style-type: none"> - The requirement is met and no (large) cracks will occur by adequate design of number, size and spacing of reinforcement. 	<ul style="list-style-type: none"> - See point 1)
6. Increase of beam stiffness	<ul style="list-style-type: none"> - The requirement is met due to the contribution of a larger compression flange 	<ul style="list-style-type: none"> - See point 1)
7. Application of H.C. slabs supported by cast in-situ beams without direct support	<ul style="list-style-type: none"> - Application is possible 	<ul style="list-style-type: none"> - See point 1) - The design of H.C. slab cross section requires a larger total web thickness (normally 400 mm.) and lower prestressing reinforcement, to minimize suspension and spalling stresses
H.C. = Hollow core		

The extra cost related to the manufacturing of hollow-core slabs designed for application with negative moments at supports, necessary to meet the above requirements "1" to "6" may be estimated in the range of 0-5%; but in some cases a saving up to 5% may be achieved by the reduction of bottom strands and/or slab depth.

On the other hand the extra cost necessary to meet the requirement "7", involving a heavier section and higher slab depth, may be estimated in the range of 5-15%.

The extra costs, related to the additional in-situ concrete and reinforcement at the supports, for all cases "1" to "7", is normally limited to the range 2-6%. In the case of a cast in-situ load bearing structure, as case "7", and also for prefabricated buildings in seismic areas, as case "3", the saving related to the lower cost of the bearing structure compared to the floor (normally in excess of 10-15%) and the aesthetic and architectural advantages more than compensates for the extra cost.

In conclusion, the application of hollow core units with restrained supports is normally of no benefit in prefabricated building in non seismic area. It may be of benefit in mixed constructions and in the case of seismic design. Finally it is strongly recommended and even essential in cast in-situ buildings or in specific design situations.

2.2.3 Examples of applications

During the last 20 years, numerous applications of hollow-core floors with restrained support have been experienced in residential buildings and underground parking garages, and in seismic areas, where hyperstatic behaviour and limitations of structural depth and width of composite or cast in-situ beams are important requirements for structural and architectural reasons.

In underground parking garages and in seismic design particularly, a monolithic behaviour and continuity of the floor structure are also important for the overall structural robustness and for a better response to very large horizontal forces originating from retaining walls or seismic action.

Construction examples and details normally used in such buildings are presented in the following figures.

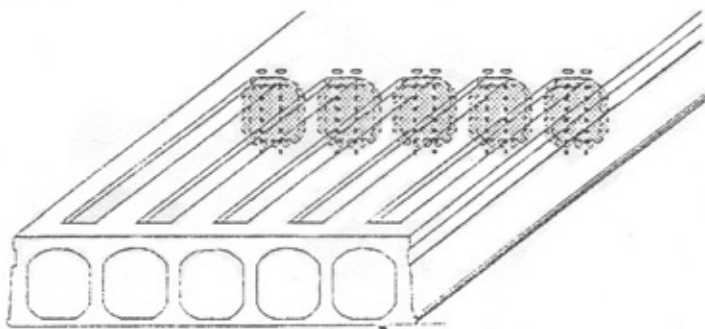
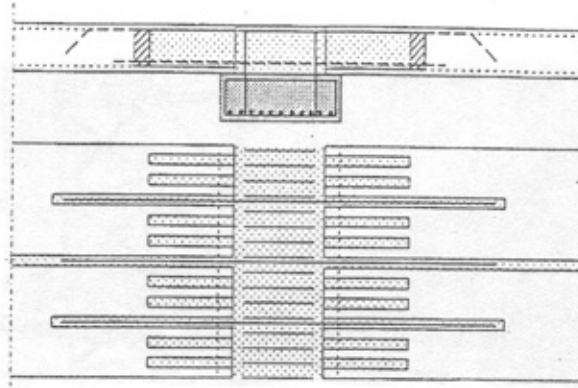


Fig. 2-11: Composite beam with enlarged composite flange.

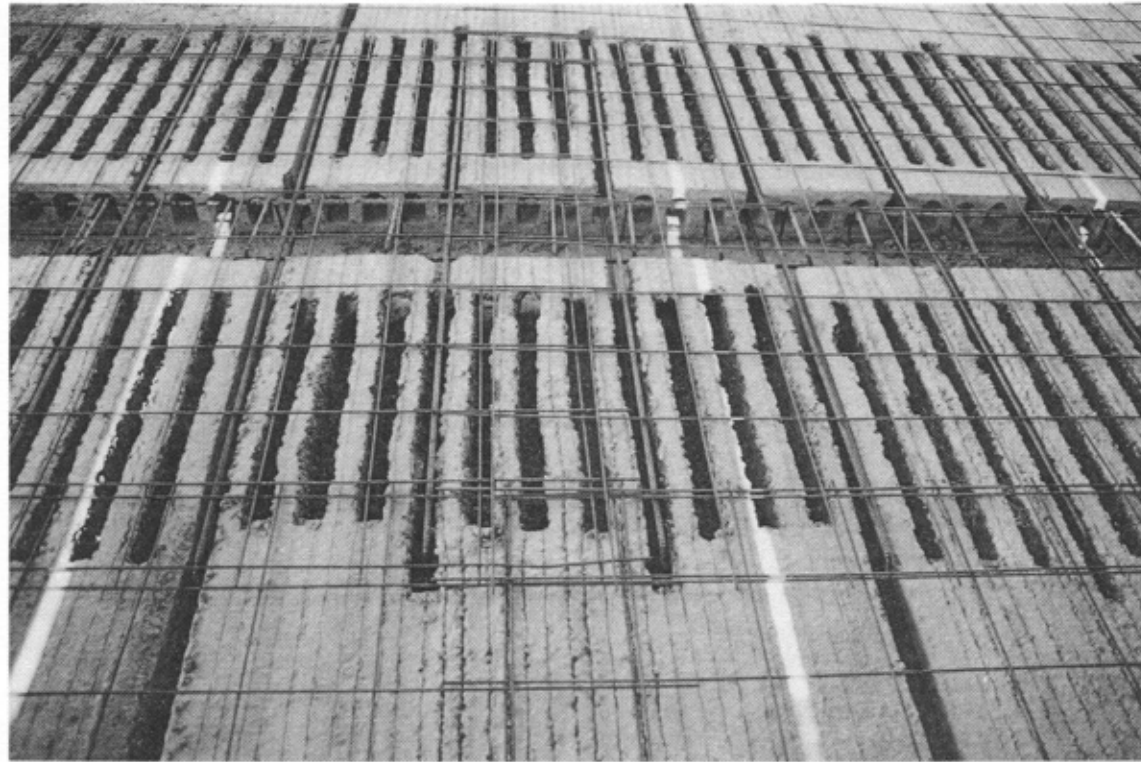


Fig. 2-12: Slab end with open cores

@Seismicisolation

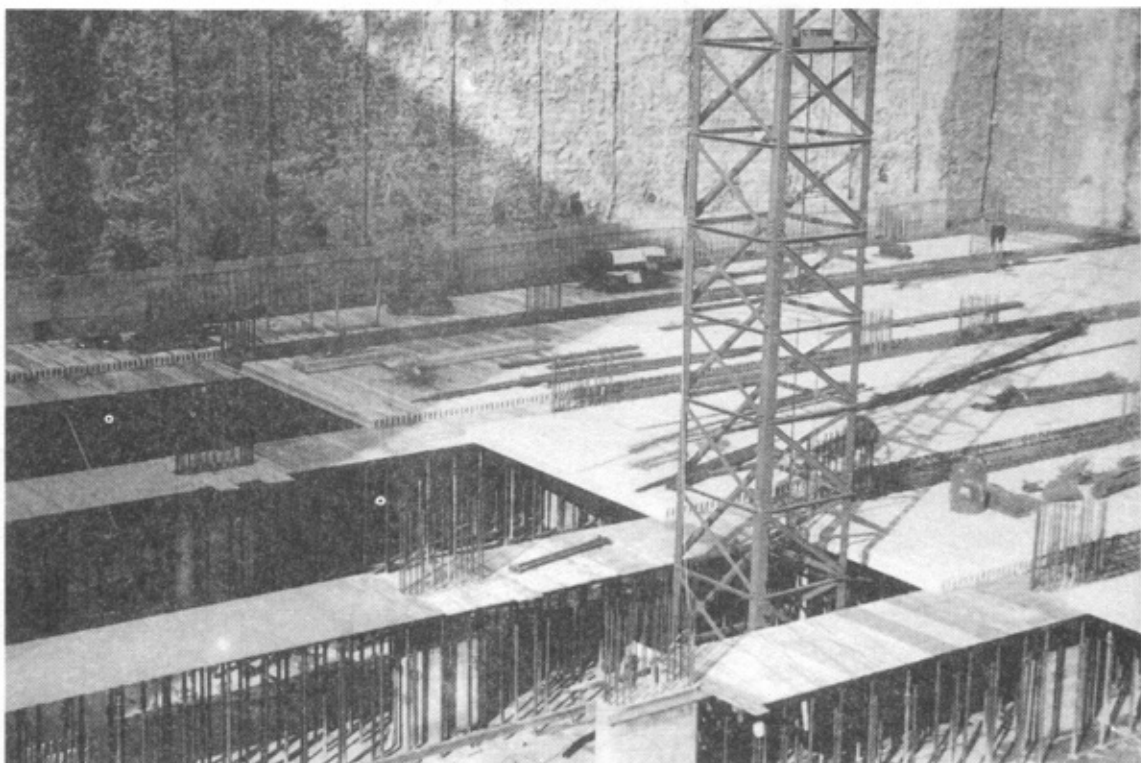


Fig. 2-13: Underground parking garage with flat cast in-situ beams P.le Facchinetti - Busto Arsizio (Italy)

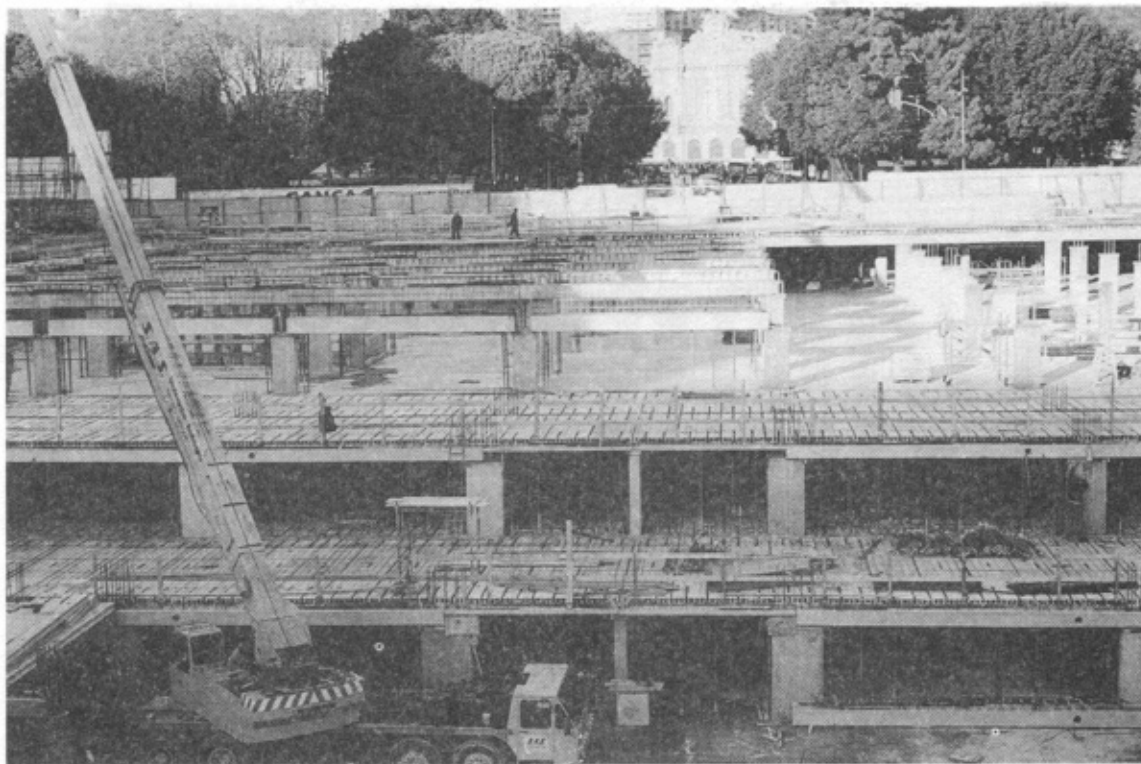


Fig. 2-14: Underground parking garage with composite beams P.zza Vittoria - Genova (Italy)

@Seismicisolation

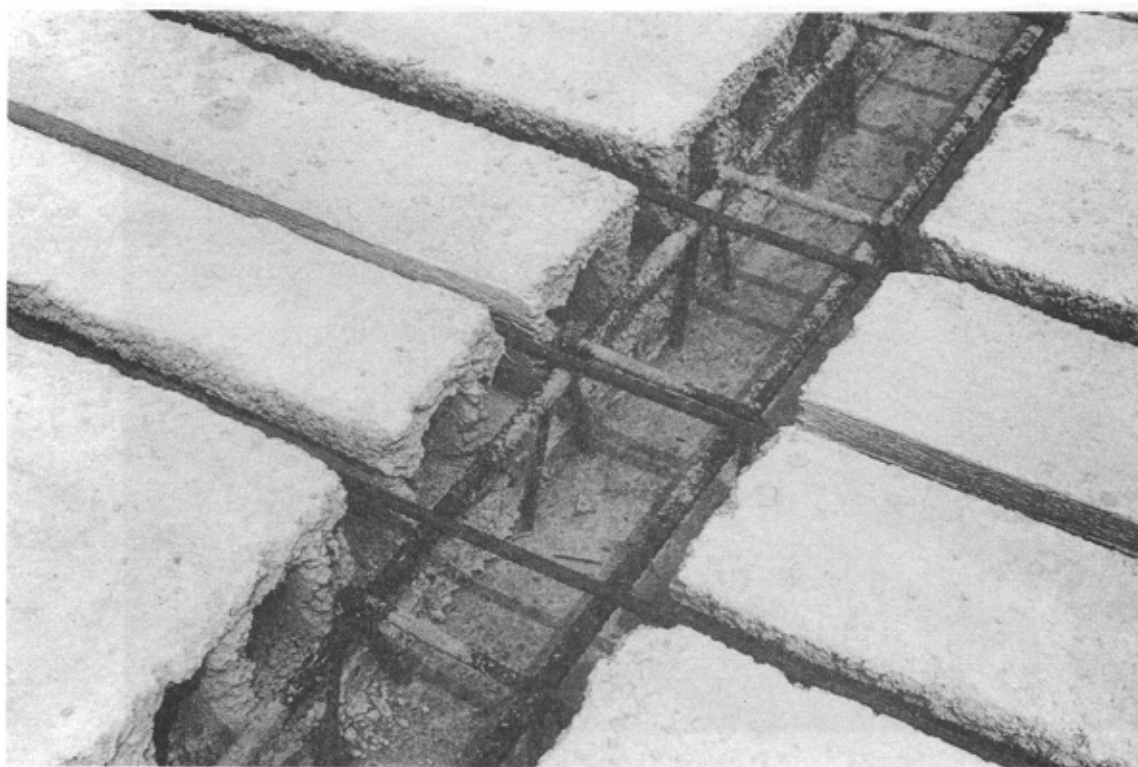


Fig. 2-15: Hollow-core floor/beam reinforcement at support

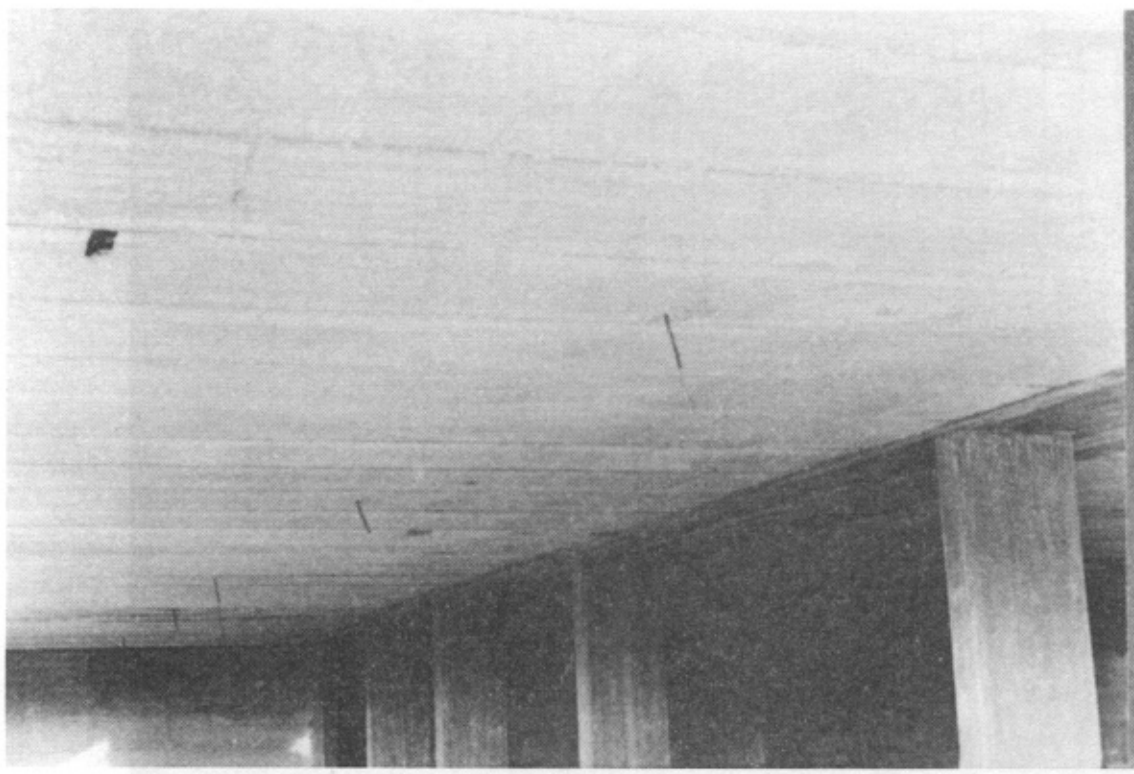


Fig. 2-16: Cast in-situ residential building with flat beam

@Seismicisolation



Fig. 2-17: Cast in-situ residential building with projecting beam

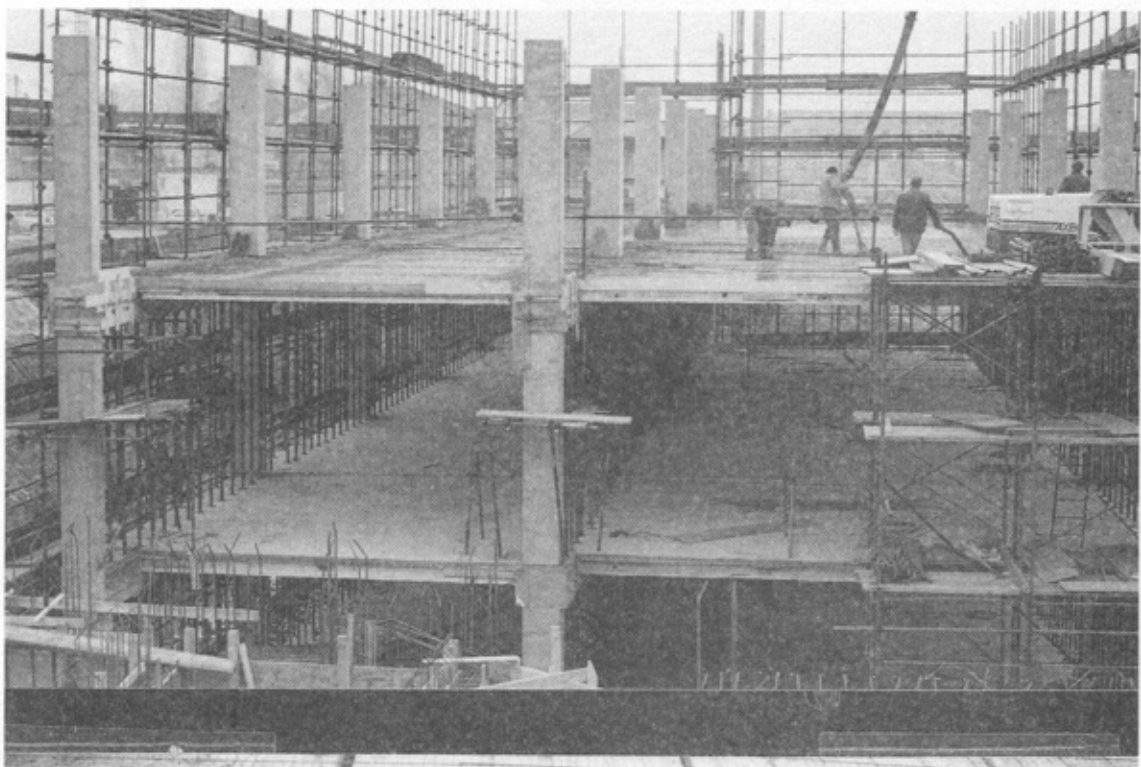


Fig 2-18: Hybrid (mixed) construction for residential building

@Seismicisolation

2.3 Design guidelines

2.3.1 General

The longitudinal continuity at the support zone of prestressed hollow core units can be achieved by adequate design of the slab end and suitable reinforcement to withstand negative moments. In addition to the function of anchoring the reinforcement, the core concrete filling also provides additional shear resistance to the precast element.

The core filling is not always necessary in case of hollow core floor with reinforced topping.

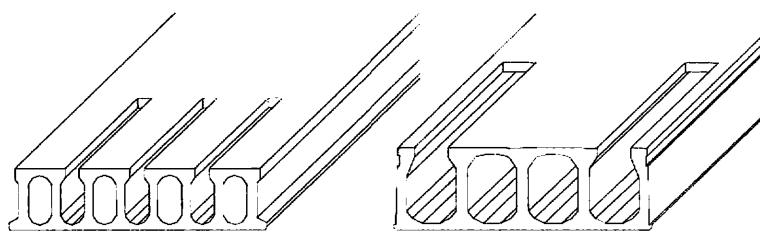


Fig. 2-19: Open cores in hollow-core units at supports.

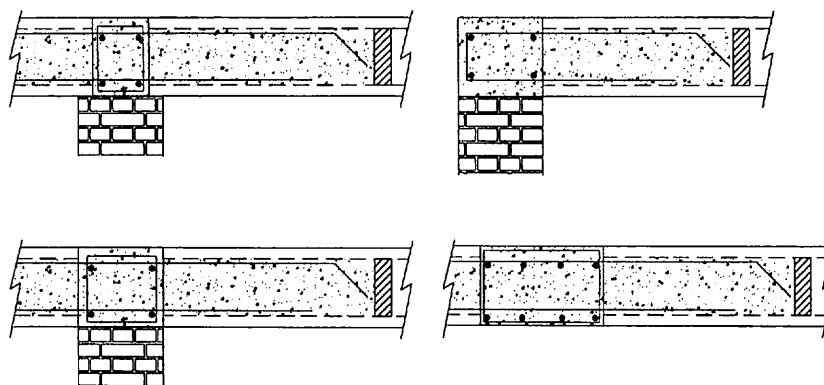


Fig. 2-20: Arrangement of hollow-core units with restraint at support.

This arrangement meets the requirement set out in Eurocode 1992.1.1 [2] par. 4.3.2.3 concerning elements with no shear reinforcement.

A simply supported hollow core slab is characterized by a critical zone in the vicinity of the support, which is subject to the simultaneous presence of tangential bond stresses between prestressing steel and concrete, transversal forces due to the diffusion of the prestressing force and shear actions. As for bond stresses and the effects of their diffusion, there is the positive contribution due to the presence of the compression strut inside the web.

For elements in which continuity at support is provided, the situation is substantially improved in all respects by the presence of compressive forces of considerable intensity at the lower flange.

For continuous elements, the possibility of cracks forming in the area of negative moment will prevent the formation of two concrete arch and tie mechanisms with concavities pointing in opposite directions (upward at the support and downward at the center line). This is due to the simultaneous presence of compression struts in the two systems, preventing the extension of cracks, induced by bending moments of opposite sign. (see fig. 2-21).

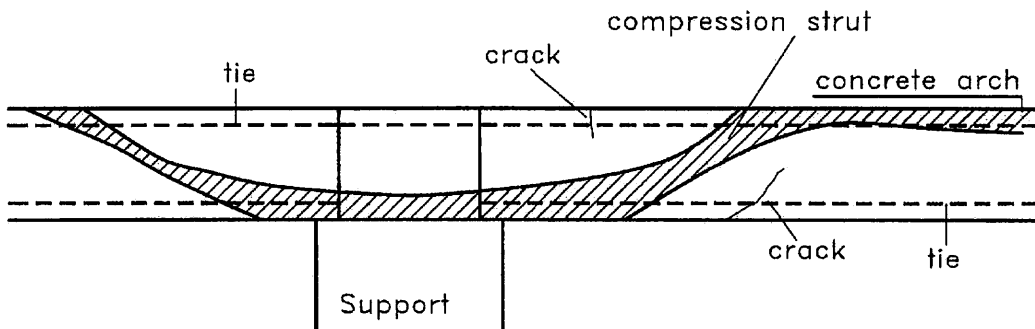


Fig. 2-21: Arch and tie mechanism at support in continuous elements.

2.3.2 Structural types and schemes

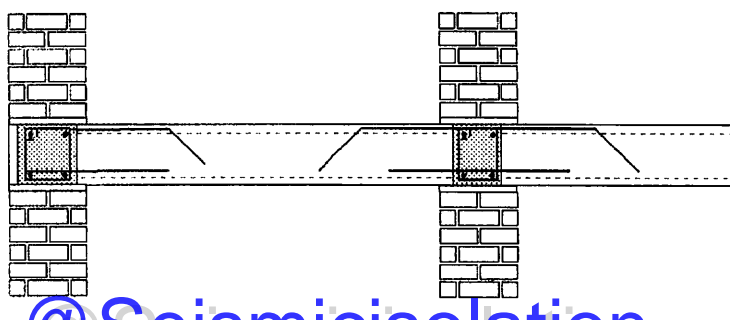
In the design analysis of hollow-core floors with restraint and composite action at the support, the following points should be considered:

- The different geometric and static characteristics of the cross sections: the element itself, and the composite structure with filled cores at support and with or without in-situ topping.
- Design shear and moment resistance V_{Rd} and M_{Rd} for each section of the composite member, as applicable:
 - * At the support edge
 - * At the distance $d/2$ (d is the effective depth of the cross section) from the support end.
 - * At the slab section where the added steel reinforcement is no further anchored.
 - * At the end of the filled cores.
- The two loading conditions: self weight + in situ concrete carried by the element itself, + construction loading if applicable, and the additional loads carried by the composite structure.

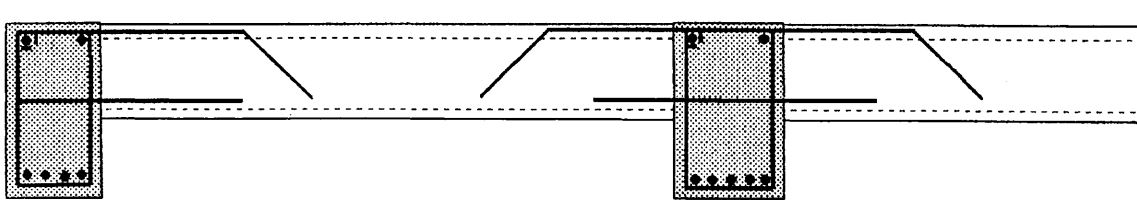
The following two support conditions represent possible combinations of structural systems and schemes. They will be analysed in detail, on the assumption of a rigid support.

In fact the considerations relevant to non-rigid supports (see chapter 3 of this Guide) are also applicable in case of restraint at support, with the advantage that the situation is improved by the presence of a compressive force at the bottom flange.

CASE I: Negative support moment due to floor continuity or restraint (intentional or not), with normal support length.



CASE II: Negative support moment due to floor continuity or restraint (always intentional), with composite support (no direct support under the precast slab)



2.3.3 Design principles and checks

Transversal sections and member design should be analysed according to section 4 of Eurocode 1992.1.1 [2] and 1992.1.3 [3] and to European standard EN1168 [4].

In addition, the relevant specific rules and checks, as detailed in the following paragraphs, should be carried out for the two basic cases I and II, described in § 2.3.4

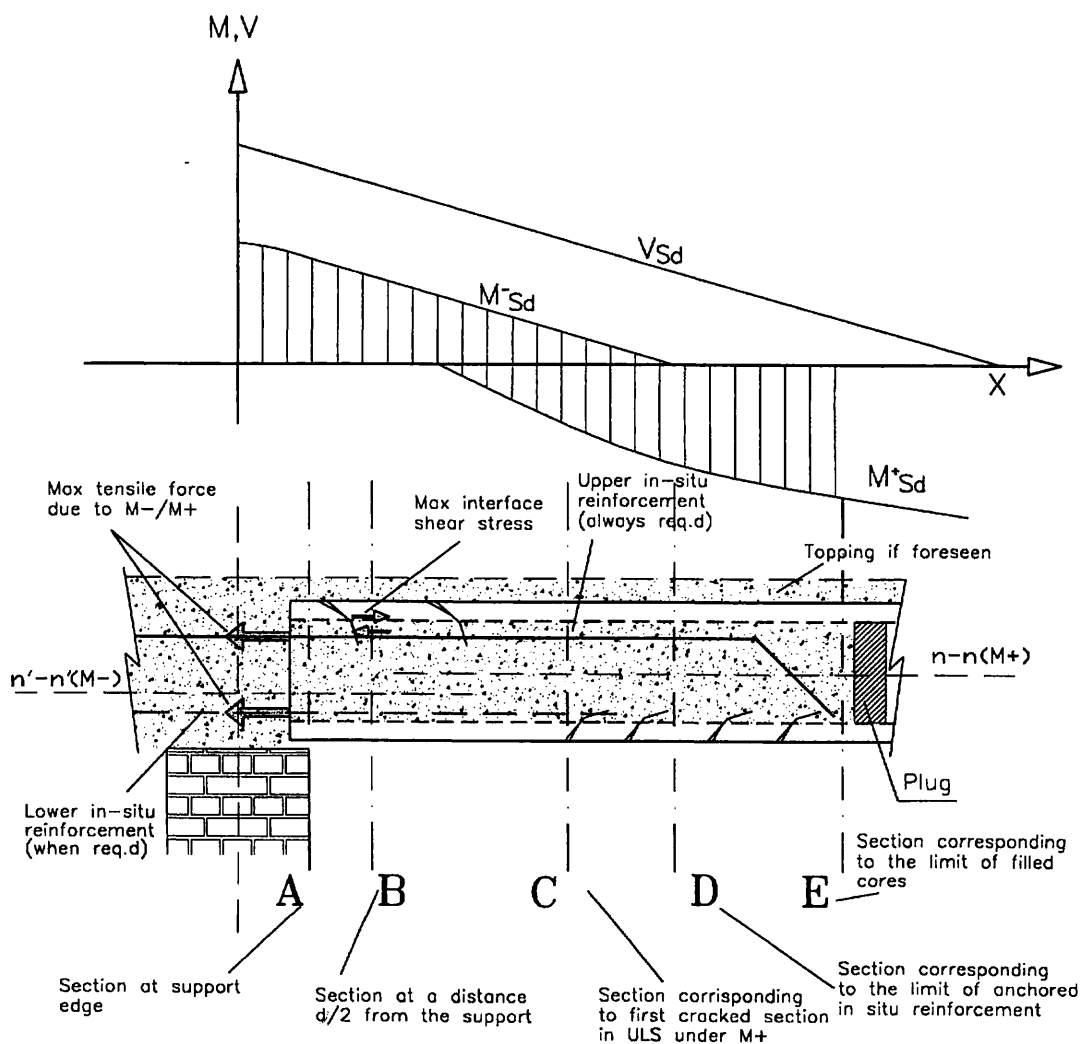


Fig. 2-22: Critical sections and design checks on the composite member at restrained support of a hollow core slab.

Specific design checks will refer in particular to:

- a) In-situ concrete interface shear capacity, under loads carried by the composite structure
- b) Interface shear capacity or anchorage to precast structure, of in-situ concrete filled cores, under tensile force due to additional reinforcement placed in the core and anchored at support.
- c) In-situ concrete shear resistance under loads carried by the composite structure.
- d) Flexural and tension shear capacity of the composite prestressed member and/or shear capacity of the composite member with additional in-situ reinforcement assuming no prestress contribution.
- e) In case of composite support (no direct support under precast slab), the precast concrete strength at the interface section due to shear and spalling stresses, and in-situ concrete shear capacity.
- f) Negative (and positive) bending capacity of the composite member at support, restrained by additional reinforcement, under the design bending moment, which should take into account also the long term effects of creep and shrinkage.
- g) Negative bending capacity of the hollow core composite cross section, corresponding to the limit of the anchorage of the upper in-situ reinforcement.

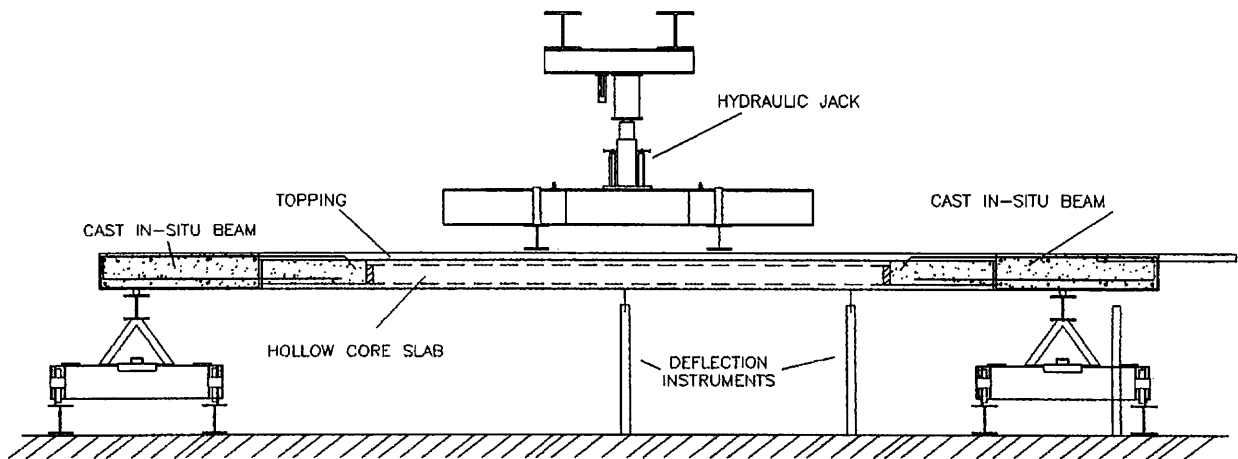


Fig. 2-23: Test of hollow-core slab with composite support (no direct support under the precast slab) [10].

2.3.4 Design analysis and recommendations

In the following, the design principles are dealt with for the two typical support conditions given in § 2.3.2. For each case, first the critical sections and design procedures are explained. Then in § 2.3.5 a detailed procedure is given for the various analysis as to be carried out at the design.

Case I: negative moment with direct support

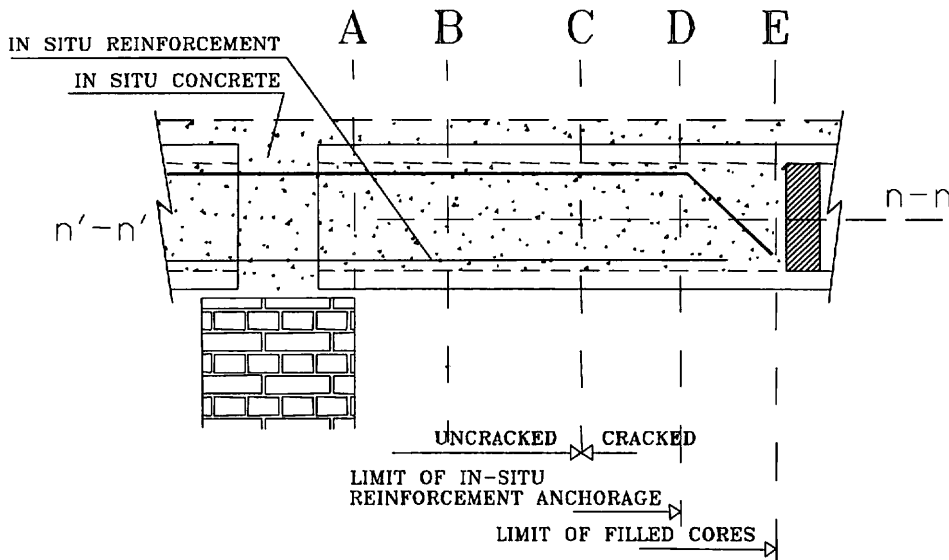


Fig. 2-24: Critical sections in case I of normal (direct) support

a) CRITICAL SECTIONS AND DESIGN PROCEDURE

SECTION A At support edge, the following design calculations should be carried out:

- Bending capacity of the composite member, under the negative (or positive) design moment M_{sd} , and no prestress contribution, according to 2.3.5.1.
- Anchorage resistance of in-situ reinforcement bar, (upper and lower also, if necessary), with respect to long term effects according to 2.3.5.2, and interface anchorage strength of core, with respect to pull-out force of in-situ reinforcement, according to 2.3.5.3.

SECTION B At a distance $d/2$ (half of the effective depth of the section) from the support, the following calculations should be carried out:

- Interface shear capacity of cast in-situ/precast concrete, according to 2.3.5.4.
- Shear capacity of the composite member, under negative moment and no prestress contribution, according to 2.3.5.5.

SECTION C At the first cracked section, in ULS under positive bending moment, nearest to the support, the following calculations should be carried out:

- Flexural/tension shear capacity of composite member, under positive moment and prestress contribution, according to 2.3.5.6.
- Anchorage resistance of prestressing steel, according to 2.3.5.7.

SECTION D At the end of the anchored in-situ upper reinforcement, the following calculations should be carried out:

- Bending capacity of prestressed hollow-core element under the negative design moment M_{sd} (D), according to 2.3.5.8
- Flexural/tension shear capacity of composite member, under negative moment and prestress contribution, according to 2.3.5.6
- Anchorage resistance of upper prestressing steel, according to 2.3.5.7.

SECTION E At the end of the filled cores, the following calculations should be carried out:

- Flexural/tension shear capacity of non-composite member, according to 2.3.5.6.

b) GENERAL DESIGN RECOMMENDATIONS

In case I, upper prestressing strand reinforcement of the hollow-core slab is generally required, overlapping the upper in-situ normal reinforcement to limit the length of this additional reinforcement and of the corresponding open cores. The upper prestressing strands also limit the depth and the width of negative moment bending cracks. Furthermore the additional in-situ reinforcement and the upper strands should be well distributed over the slab width, to avoid stress concentrations.

The amount of the in-situ reinforcement should take into account the long term effects of the combination of permanent and prestressing forces.

It is necessary to pay attention also to the shortening of the hollow-core elements due to prestressing and creep with respect to the differential shrinkage between precast and cast in-situ structure.

The lengths of reinforcement bars should be calculated according to the anchorage requirements and the design diagram of M_{sd} . Therefore the bars are often designed in 2 or 3 lengths, but the minimum length should not be less than the transmission length l_{bp} of the prestressing tendons.

The maximum diameter of reinforcement bar should be limited according to the interface shear resistance between the core and precast concrete, taking into account the effective interface of the core (no contribution should be considered from the bottom surface of the core because of the presence of debris due to top concrete removal).

The calculated length of the core filling should be increased by the total thickness of the slab.

More details on the above recommendations are given in paragraph 2.4 “Detailing of Connection”

Case II: Negative moment without direct support

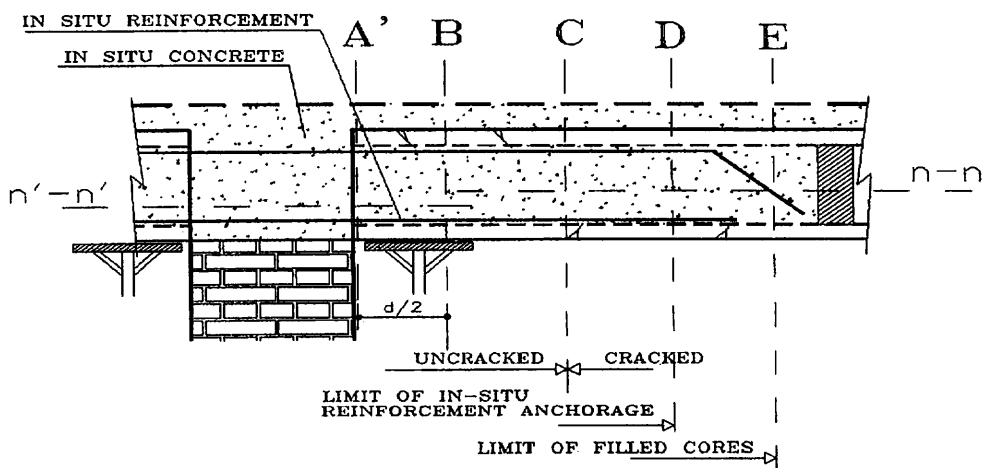


Fig. 2-25: Critical sections at support (no direct support under the precast slab)

a) CRITICAL SECTIONS AND DESIGN PROCEDURE

SECTION A' At the interface between hollow-core slab and cast in-situ concrete beam or wall, the following design calculations should be carried out, in addition to those listed for the direct support in para 2.3.4.: Case I

- Interface shear capacity of cast in-situ/precast concrete, according to 2.3.5.4
- Shear capacity at the slab end for both sides, member and support side, according to 2.3.5.5 and 2.3.5.9.
- Shear and spalling stresses, according to 2.3.5.10

SECTION B No need to be checked since relevant design calculations are covered by section A'

SECTIONS C,D,E: See design procedures for direct support, in para 2.3.4.: Case I

b) GENERAL DESIGN RECOMMENDATIONS

In addition to the general recommendations given for the "direct" support Case I, it is necessary for Case II to provide additional in-situ reinforcement at the bottom level with adequate anchorage length. Reinforced filled cores should be provided in the slab width (at 300-400 mm centres) and it may be necessary to add ordinary shear reinforcement in the cast in-situ cores.

The in-situ concrete should penetrate into all the cores, including those without additional reinforcement bars, over a length at least equal to the total depth of the slab. Stopping is needed in each core to ensure a good concrete compaction.

The span/depth ratio l/h of the hollow-core slab has to be minimised (normally $l/h \leq 30-35$) and the total web width increased (normally 400 mm min.) to limit the spalling stress and the shear stress so that the resulting value will not exceed the ULS value of the concrete tensile strength.

2.3.5 Detailed design recommendations

The following practical design rules refer to the design principles given in the previous chapter, for the two main support conditions of the hollow core floors subjected to negative moments.

2.3.5.1 Negative (and positive) bending capacity of the composite member (Section A and A')

The design negative (and positive) moment value M_{sd} and the capacity M_{Rd} of the composite member at the support, corresponding to negative (and positive) reinforcement A_s , should be calculated in ULS and SLS according to EC-2 principles (ENV 1992-1.1) [2]. For the evaluation of M_{Rd} only the ordinary reinforcement A_s should be considered, together with the effective developed prestress in the considered section, provided that anchorage failure of the prestressing steel is prevented according to 2.3.5.7.

The contribution of in situ concrete shall be homogenised with the precast concrete taking into account the ratio E_c/E_p .



The negative (or positive) design moment M_{Sd} refers to the design moment M_{Sdq} , relevant to the imposed loading Q on the composite structure, eventually increased by the moment due to the long term effects of the combined permanent and prestressing forces. The design moment M_{Sdq} is calculated at the support edge section, after redistribution of the moments due to the plasticity of the connection and the different modulus of elasticity at support.

$$M_{Sd} = M_{Sdq} + M'_{S(p,G)d} \quad (2-1)$$

$$M^+_{Sd} = M^+_{Sdq} + M'_{S(p,G)d} \quad (2-2)$$

Where:

$M'_{S(p,G)d}$ the design moment due to second order effects, (see chapter 2.3.5.2), to be considered only in case of increasing the value of M_{Sdq} .

M_{Sdq}/M^+_{Sdq} the design negative/positive moment due to the imposed loading Q. (see fig. 2-26)

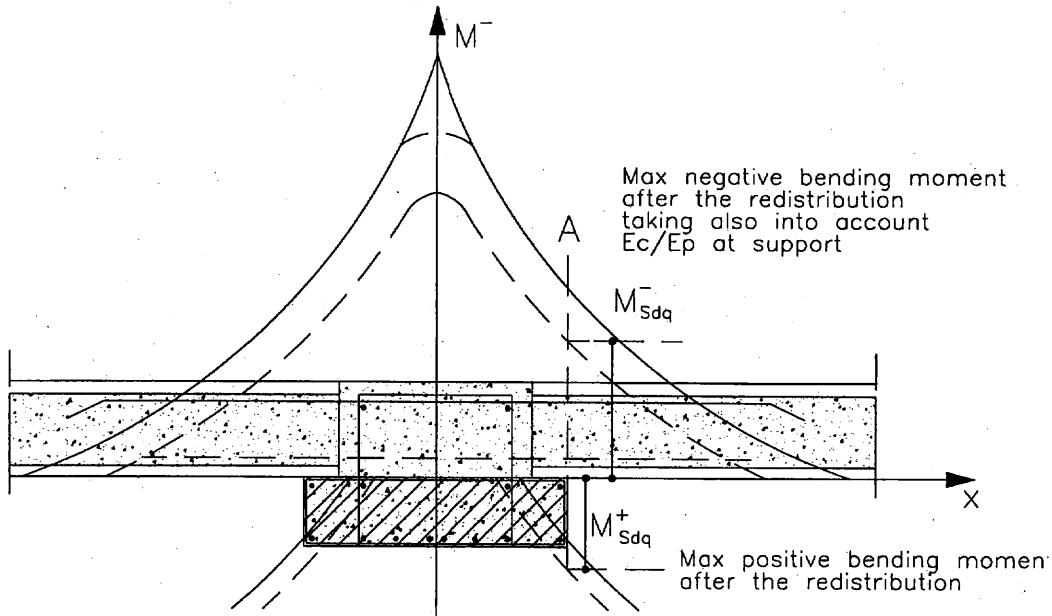


Fig. 2-26: Design negative/positive moment due to the imposed loading Q at the support edge section.

2.3.5.2 Long term effects of restrained supports (Section A and A')

Whilst, under the long term effects of the combined permanent and prestressing forces, the in-situ steel reinforcement will restrict the free rotation of the slab end-section. The flexural moment capacity of the composite member should be able to take up the additional design moment $M'_{S(p,G)d}$, calculated below for two floor schemes. For intermediate conditions, interpolation should be carried out.

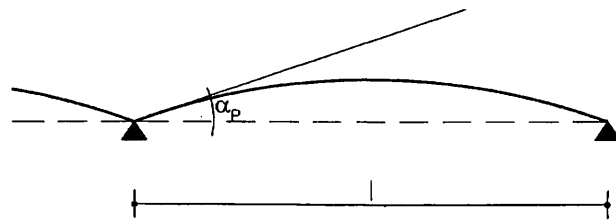
This calculated moment should be added to the design negative moment for the imposed loading Q if it increases the total negative design moment (if it decreases the total moment, it should be neglected).

In the latter case, this value has to be taken into account for the design of the lower in-situ reinforcement at section A/A' for the positive bending moment at support.

Case A) Two span floor with free rotation at the end supports.

α_p = rotation of the slab end section, due to the prestressing moment

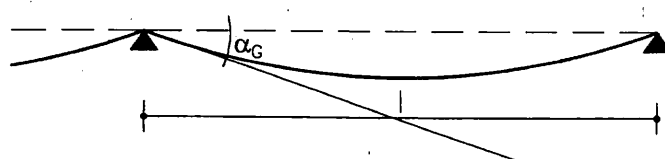
$$\alpha_p = -\frac{1}{2} \frac{P_{t_0} l_e}{E_c I'_c}$$



Where

P_{t_0}	the prestressing force at time t_0 of in-situ concrete hardening
P_{t_0}	$= P_o - \Delta P_{t_0}$
e	the eccentricity of the prestressing force
P_o	the prestressing force just after release
ΔP_{t_0}	the prestressing losses due to creep shrinkage and relaxation at time t_0 $\Delta P_{t_0} = (P_\infty - P_o)\alpha_{t_0}$
P_∞	the final prestressing force after occurrence of all losses
α_{t_0}	proportion of actual losses at time t_0 (see Fig. 2-27)
E_c	the modulus of elasticity of the precast concrete
I'_c	the second moment of area of the current cross section of the hollow core floor slab (including homogenized contribution of the in-situ concrete)
l	the floor length
α_G	rotation of the slab end section, due to the permanent load Σ_{G_i} , applied before in situ concrete hardening and development of continuity

$$\alpha_G = \frac{1}{24} \frac{\Sigma_{G_i} l^3}{E_c I'_c}$$



$$\text{If } \alpha_p > \alpha_G \text{ it is } \frac{1}{2} \frac{P_{t_0} e l}{E_c I'_c} > \frac{1}{24} \frac{\Sigma_{G_i} l^3}{E_c I'_c} \text{ and then } \frac{3}{2} M_p > M_G$$

Where

Σ_{G_i}	the permanent loads applied before development of continuity
M_p	the bending moment at support due to the prestressing force ($M_p = P_{t_0} e l$)
M_G	the bending moment at support due to the restriction of the rotation induced by the permanent loads Σ_{G_i} ($M_G = \Sigma_{G_i} l^2/8$)

In this case the restricted rotation of the slab end section at support may induce a design moment as follows:

$$M'_{S(p,G)d} = \frac{(3 M_{p,d} - M_{G,d}) \varphi(\infty, t_0)}{2^2 + \rho \varphi(\infty, t_0)} \quad (2-3)$$

where

- ρ the ageing coefficient of the precast concrete (normally $\rho = 0.8$)
 $\varphi(\infty, t_0)$ the creep value of the precast concrete of the hollow core slab from the time to of the in-situ concrete hardening (normally in the range 1-1.5)

$M_{p,d}$ and $M_{G,d}$ the design values of bending moments at support due to prestressing and permanent loads with appropriate partial safety factor for action ($\gamma_p = 0.9$ or 1.2 and $\gamma_G = 1.35$ or 1.0)

The creep value to be taken into account for the precast element, is the residual value from the time "t₀" of the in-situ concrete hardening which may be calculated according to the basic relationship of shrinkage and creep vs. time, depending on the concrete section and ambient characteristics. A typical example is shown in Fig. 2-27.

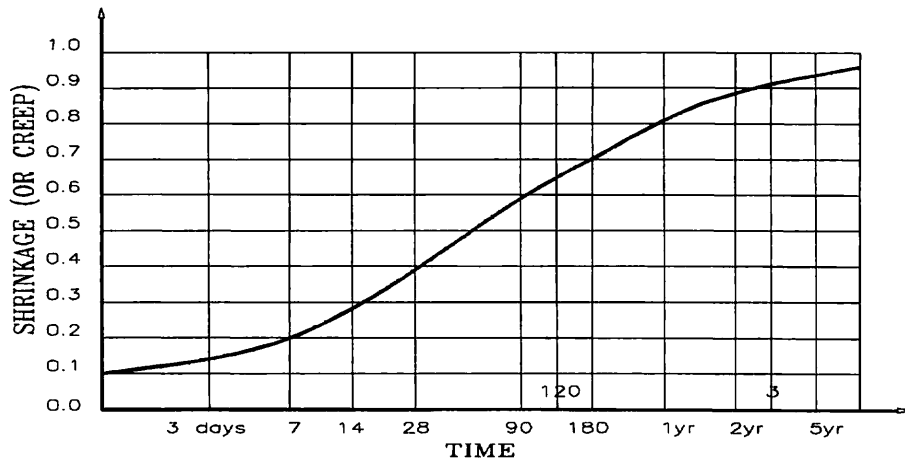


Fig. 2-27: Typical example of proportion of the final shrinkage or creep vs time

Assuming $\varphi_{(\infty,0)} = 2.5$ and a relationship as per Fig. 2-27

If $t_0 = 1$ month

$$\varphi_{(\infty,t_0)} = 0.6 \times 2.5 = 1.50$$

$t_0 = 2$ month

$$\varphi_{(\infty,t_0)} = 0.5 \times 2.5 = 1.25$$

$t_0 = 3$ month

$$\varphi_{(\infty,t_0)} = 0.4 \times 2.5 = 1.00$$

Case B) Multispan floor with restraint at 2nd support (multispan floor).

Using the same procedure, and with restraint at both ends of the slab we have:

$$M'_{S(p,G)d} = \frac{(M_{p,d} - 2 M_{G,d})}{3} \frac{\varphi_{(\infty,t_0)}}{1 + \rho \varphi_{(\infty,t_0)}} \quad (2-4)$$

NOTE: In the presence of a topping, the effect of the differential shrinkage depends on the age of the hollow core slab with respect to the cast in-situ concrete. This effect should also be taken into account, and the relevant moment M_S has to be evaluated as follows:

where

$\varepsilon_{s(\infty,t_0)}$ the differential shrinkage of the cast in-situ concrete versus the precast concrete from the time "t₀" of the in-situ concrete hardening.

Assuming $\varepsilon_{s(\infty,0)} = 0.0004$ and a relationship as per Fig. 2-27, the following values of $\varepsilon_s(\infty,t_0)$ may be calculated depending on time to:

$$\begin{aligned} t_0 = 1 \text{ month} & \quad \varepsilon_{s(\infty,t_0)} = 0.4 \times 0.0004 = 0.00016 \\ t_0 = 2 \text{ months} & \quad \varepsilon_{s(\infty,t_0)} = 0.5 \times 0.0004 = 0.00020 \\ t_0 = 3 \text{ months} & \quad \varepsilon_{s(\infty,t_0)} = 0.6 \times 0.0004 = 0.00024 \end{aligned}$$

A_c, E'_c the area and the modulus of elasticity of the cast in-situ topping

x_{nn} the distance from the neutral axis of the cross section of the cast in-situ topping to the neutral axis of the composite cross section.

In the presence of a topping, the restricted rotation of the slab end section at support will induce a design moment $M'_{S(p,G)d}$ as follows

$$M'_{S(p,G)d} = \frac{(3 M_{p,d} - M_{G,d}) \varphi(\infty, t_0)}{2 + \rho \varphi(\infty, t_0)} - \frac{3 M_s}{2} \frac{1}{1 + \rho \varphi(\infty, t_0)} \quad \text{for case "A"} \quad (2-5)$$

$$M'_{S(p,G)d} = \frac{(M_{p,d} - 2 M_{G,d}) \varphi(\infty, t_0)}{3 + \rho \varphi(\infty, t_0)} - M_s \frac{1}{1 + \rho \varphi(\infty, t_0)} \quad \text{for case "B"} \quad (2-6)$$

Case C) Restraint due to slab shortening

Generally no special considerations are needed in designing the hollow core slab in this respect, because the time from hollow core slab production to in-situ concrete hardening normally exceeds 1 month, and initial shortening has taken place. In fact the differential shrinkage of the cast in-situ concrete is larger than the shortening of the precast hollow core slab due to creep under prestressing.

That is $\varepsilon_{p(\infty,t_0)} = \frac{P_{to}}{A'_c E_c} \varphi(\infty, t_0) \leq \varepsilon_{s(\infty,t_0)}$

where

$\varepsilon_p(\infty, t_0)$ the shortening of the hollow core slab due to the prestressing creep.

A'_c the area of the cross section of the hollow core floor slab (including the homogenized contribution of the in-situ concrete)

$P_{to}, E_c, \varphi(\infty, t_0), \varepsilon_s(\infty, 0)$ see notation of the points A), B)

Assuming $\varphi_{(0,\infty)} = 2.5$ $\varepsilon_{s(0,\infty)} = 0.0004$ $E_p \approx 40.000 \text{ N/mm}^2$

and a relationship as in Fig. 2-27 the following minimum hardening times of the precast element and the relevant maximum average prestressing have to be stated in order to meet the requirement:

$$t_0 = 1 \text{ month} \quad \sigma_p = P_{to}/A'_c \leq 4.2 \text{ N/mm}^2$$

$$t_0 = 2 \text{ months} \quad \sigma_p = P_{to}/A'_c \leq 6.4 \text{ N/mm}^2$$

$$t_0 = 3 \text{ months} \quad \sigma_p = P_{to}/A'_c \leq 9.6 \text{ N/mm}^2$$

The total shortening of the slab of a whole floor cannot take place freely when restrained by walls, central cores or facades. In this case the long term effects have to be taken into account in the design of the additional reinforcement at support.

In special cases, when no shrinkage shortening is expected between rigid and separate stair or walls cores, provisions have to be made to avoid excessive tensile forces by means of a free joint at the final support or by providing adequate reinforcement at the slab end (after having taken into account the plasticity of the in-situ support connection). In this latter case the additional reinforcement has to be designed for the following additional tensile force $\Delta F'_s$

$$\Delta F'_s = (\varepsilon_{p(\infty, t_0)} - \varepsilon_{s(\infty, t_0)}) E_c A'_c \frac{1}{1 + \rho \Phi_{(\infty, t_0)}} \quad (2-7)$$

The reinforcement should be extended over at least 1.5 times l_{bp} , and should well distributed over the floor width.

2.3.5.3 Anchorage capacity of the reinforcement bar in a filled core (Section A' and B)

The tensile stress f_{sd} of the reinforcement in ULS, due to the design bending moment M_{sd} and increased by the stress due to restraint due to slab shortening for long term effect, shall not exceed the design steel strength.

$$f_{sd(M_{sd}, \Delta F'_s)} \leq f_{td} = \Sigma A_s f_y / \gamma_s \quad (2-8)$$

where

f_{sd} and f_{td}	the design tensile force and resistance of the reinforced steel in ULS in section A/A'
ΣA_s	the total area of the tension reinforcement extending not less than $l_{b,net}$ beyond the section considered
f_y	$l_{b,net}$ is the required anchorage length according to ENV 1992.1.1 [2]
γ_s	yield strength of reinforcement.
	partial safety factor of reinforcement ($\gamma_s = 1.15$)

The anchorage length of the bars, either at support side and at the hollow-core slab side, should be calculated according to Eurocode 2, ENV 1992.1.1 [2]. The anchorage of the concreted core within the precast element shall be verified according to ENV 1992.1.3. 4.5.3.3 [3]

2.3.5.4 Interface shear strength of the composite member (Section A' and B)

At the interface between the cast in-situ and the precast concrete, the max interface shear stress should be checked, due to f_{sd} (see point 2.3.5.3) and to V_{sd} , assuming for K_T the corresponding value for smooth surfaces ($K_T = 1.4$) according to 4.5.3.3 of Eurocode2 1992-1-3 [3].

$$\tau_{sdj} = \tau'_{sd} + \tau''_{sd} = f_{sd}/\Sigma S_c l_s + V_{sd}/0.9d' \Sigma S_c \leq \tau_{Rdj} = K_T \tau'_{Rd} \quad (2-9)$$

where

τ_{sdj} and τ_{Rdj}	the interface design shear stress and resistance between the cast in-situ and the precast concrete
τ'_{sd}	the average longitudinal shear stress at the interface between the hollow-core and the in-situ concrete of the filled cores, due to M_{sd} and long term effects

τ''_{sd}	the interface shear stress due to V_{sd}
V_{sd}	the shear due to the additional loads Q only for direct support (case I), or the total design shear for non-direct support (case II)
τ'_{rd}	shear resistance of the in-situ concrete.
d'	the effective depth of the composite cross section.
S_c	the interface perimeter of the in-situ concrete in the core section (without taking into account the bottom side of the core when debris may be present); approximately $S_c \approx 2 h$ with h the hollow-core depth.
l_s	the length of the reinforcement in the filled core.

The average longitudinal shear stress in the longitudinal joints should be limited to 0.1 N/mm².

$$\tau'_{rdj} \leq 0.1 \text{ N/mm}^2$$

This check is not needed when the reinforcement bar is placed over the joint into the reinforced topping, with a direct bond within the joint.

2.3.5.5 Shear capacity of the composite member, under negative moment, without contribution from prestressing (Section A' and B)

When sufficiently anchored reinforcement is placed in the filled cores in the tensile zone of the composite member, the design shear resistance V'_{rd1} may be calculated as follows, according to ENV 1992.1.1 [2], assuming no contribution from prestressing:

$$V'_{rd1} = 0.25 f_{ctd} b'_{w} d' k (1.2 + 40\rho_1) \leq V_{rd2} \quad (2-10)$$

where

$$\begin{aligned} \rho_1 &= \Sigma A_s / b'_{w} d' \\ V_{rd2} &= 1/2 v f_{cd} b'_{w} 0.9 d' \end{aligned}$$

$$k = 1.6 - d' \geq 1$$

$$v = 0.7 - f_{ck}/200 \geq 0.5.$$

f_{ctd} the design tensile strength of the precast concrete.

b'_{w} the total web width of the composite section with filled cores $b'_{w} = b_w + n_{bc} E_c/E_p$

ΣA_s the total area of tension reinforcement, adequately anchored.

n and b_c the number and width of the filled core.

E_c/E_p the ratio of the modulus of elasticity of the in-situ and precast concrete

d' the effective depth of the composite cross section.

f_{ck} the characteristic cylinder compressive strength of the precast concrete.

2.3.5.6 Flexural/shear tension capacity, under bending moment and contribution from prestressing. (Sections C, D, E)

The shear capacity of a composite member with contribution from prestressing, under positive or negative bending moment, should be evaluated as follows:

- for non-cracked sections, by the shear tension capacity (i).
- for cracked sections, the lower value of flexural (ii) and shear tension capacity

calculated according to the two procedures given hereafter, and provided that anchorage failure of prestressing steel is prevented according to 2.3.5.7.

If the anchorage of the prestressing steel is not satisfied, the shear capacity of the composite member, under positive or negative bending moment, should be calculated according to 2.3.5.5., ignoring the prestressing, and taking into account only the additional in-situ reinforcement.

i) Shear tension capacity

The shear tension capacity of a hollow-core slab with or without topping and/or with a number of filled cores can be calculated according to the procedures given in the ANNEX F of prEN 1168 [4].

a) Hollow core unit

$$V_{Rdt} = \frac{1}{S} b_w \sqrt{f_{ctd}^2 + \alpha \sigma_{cpm} f_{ctd}} \quad (2-11)$$

b) Hollow core unit with topping

Since $\tau_{Sd} \leq \tau_{Rd}$

$$\begin{aligned} \tau_{Sd} &= V_{Sdg} S/b_w l + V_{Sdq} S'/b_w l' \leq \tau_{Rd} = \sqrt{f_{ctd}^2 + \alpha \sigma_{cpm} f_{ctd}} \\ V_{Rdt} &= V_{Rdt} \underline{\frac{S}{S'} \frac{l}{l'}} + V_{Sdg} (1 - \underline{\frac{S}{S'} \frac{l}{l'}}) \geq V_{Rdt} \end{aligned} \quad (2-12)$$

c) Hollow core unit with a number of filled cores

- Assuming simultaneous shear failure in ULS of the in-situ and precast concrete:

$$V'_{Rdt} = V_{Rdt} + \frac{2}{3} n b_c h_c f'_{ctd} \quad (2-13 \text{ a})$$

Note: this is an upper limit condition, which rarely occurs, since normally V_{Sdq} is limited by in-situ concrete failure or by precast concrete failure, that is $V'_{Rdt} = V_{Rdg} + V_{Rdq \min} \geq V_{Rdt}$

- Assuming a limited value of V_{Sdq} due to the in-situ concrete failure

(assuming $V_{Rdg} = V_{Sdg}$)

$$V'_{Rdt} = V_{Sdg} + \frac{b'_w l' f'_{ctd}}{S' E'_c} \geq V_{Rdt} \quad (2-13 \text{ b})$$

- Assuming a limited value of V_{Sdq} due to the precast concrete failure:

$$V'_{Rdt} = V_{Sdg} + \frac{b'_w l' S}{b_w l S'} (V_{Rdt} - V_{Sdg}) \geq V_{Rdt} \quad (2-13 \text{ c})$$

d) Hollow core unit with topping and a number of filled cores

- Assuming simultaneous shear failure in ULS of the in-situ and precast concrete (assuming $V_{Rdg} = V_{Sdg}$):

$$\overline{V'_{Rdt}} = V_{Rdt} \underline{\frac{S}{S'} \frac{l}{l'}} + V_{Sdg} (1 - \underline{\frac{S}{S'} \frac{l}{l'}}) + \frac{2}{3} n b_c h_c f'_{ctd} \geq \overline{V_{Rdt}} \quad (2-14 \text{ a})$$

Note: as per point "c" above this is an upper limit, since V_{Sdq} is limited by in-situ or precast concrete failure, which means:

$$V'_{Rdt} = V_{Sdg} + V_{Sdq \ min} \geq V_{Rdt}$$

Assuming a limited value of V_{Sdg} due to in-situ concrete failure:

$$\frac{-}{V'_{Rdt}} = V_{Sdg} + b'_w \frac{E_c l'}{E_c' S'} f'_{ctd} \geq V_{Rdt} \quad (2-14 b)$$

Assuming a limited value of V_{Sdg} due to precast concrete failure:

$$\frac{-}{V'_{Rdt}} = V_{Sdg} + \frac{b'_w l' S}{b_w l' S'} (V_{Rdt} - V_{Sdg}) \geq V_{Rdt} \quad (2-14 c)$$

ii) Flexural shear capacity

The flexural shear capacity of a slab with topping and/or with a number of filled cores can be calculated according to the procedures given in ANNEX F of prEN1168 [4]:

a) Hollow core unit

$$V_{Rdf} = 0.25 f_{ctd} b_w d k (1.2 + 40\rho_1) + 0.15 \sigma_{cpm} b_w d \leq V_{Rd2} \quad (2-16)$$

b) Hollow core unit with topping

$$V_{Rdf} = 0.25 f_{ctd} b_w d' k' (1.2 + 40\rho'_1) + 0.15 \sigma_{cpm} b_w d' \leq V'_{Rd2} \quad (2-17)$$

c) Hollow core unit with a number of filled cores

$$V'_{Rdf} = 0.25 f_{ctd} b'_w d k (1.2 + 40\rho'_1) + 0.15 \sigma_{cpm} b_w d \leq V'_{Rd2} \quad (2-18)$$

d) Hollow core unit with topping and a number of filled cores

$$V'_{Rdf} = 0.25 f_{ctd} b'_w d' k' (1.2 + 40\rho'_1) + 0.15 \sigma_{cpm} b_w d' \leq V'_{Rd2} \quad (2-19)$$

where

V_{Rdt} and V'_{Rdt} shear tension and flexural shear capacity of the hollow-core slab
 V_{Rdt} and V_{Rdf} shear tension and flexural shear capacity of the hollow-core slab with topping

V'_{Rdt} and V'_{Rdf} shear tension and flexural shear capacity of the hollow-core slab with topping and filled cores.

V_{Sdg} and V_{Rdg} design shear and capacity of the hollow-core floor due to the dead loads carried on the hollow-core itself before composite section development

V_{Sdq} design shear force due to the additional loads (variable and permanent) carried by the composite hollow-core slab.

τ_{Sd} and τ_{Rd} design shear stress and resistance of precast concrete.

f_{ctd} and f'_{ctd} the design tensile strength of precast and in-situ concrete.

b_w and b'_w the total web width of the precast hollow-core slab and of composite section with filled cores $b'_w = b_w + n b_c E_c / E_p$

A_p the cross section of the prestressing steel $k = 1.6 - d \geq 1$ and $k' = 1.6 - d' \geq 1$

$V_{Rd2} = 1/2 v f_{cd} b_w 0.9 d$ and $V'_{Rd2} = 1/2 v f_{cd} b'_w 0.9 d'$

$v = 0.7 - f_{ck}/200 \geq 0.5$

f_{ck} the characteristic cylinder compressive strength of the precast concrete

ρ_1 and $\rho'_1 =$ specific reinforcement of the precast and composite hollow-core

section $\rho_1 = A_p/b_w d$ $\rho'_1 = A_p/b'_w d'$

$\alpha \sigma_{cpm}$ the average concrete compressive stress due to the effective prestressing force.

$$\alpha = l_x/l_{bpd}$$

$$\sigma_{cpm} = P_{\text{eff}}/A$$

l_x the distance of the section x from the slab end

l_{bpd}	the design value of the transmission length $l_{bpd} = 1.2\beta\phi = 1.2 \cdot 70\phi$ when $f_{cj} = 30 \text{ N/mm}^2$.
P_∞	the final prestressing force after all losses
A	the cross section area of the precast hollow-core slab
S and S'	first moment of the cross section of the hollow core and composite hollow core slab.
I and I'	second moment of the cross section of hollow core and composite hollow core slab.
d and d'	effective depth of the hollow core and composite hollow core cross section
n, b_c and h_c	number, width and depth of the filled cores when related to an equivalent rectangular section
E_c/E_p	the ratio of the modulus of elasticity of in-situ to precast concrete.

2.3.5.7 Anchorage resistance of the prestressing steel (Section C)

According to pr EN1168 [4] and to Eurocode ENV 1992.1.3 [3], in the nearest section to the support (at the distance x from the slab end) in which the tensile stress reaches f_{ctd} under M_{sd} , the following condition should be satisfied

$$T_{dx} = M_{Sdx}/z + V_{Sdx} \cot\theta \leq F_{px} \quad (2-20)$$

where

T_{dx}	the design value of the tensile force in the prestressing steel at section x
M_{Sdx}	the design value of bending moment at section x
z	the lever arm
V_{Sdx}	the design value of shear force at section x
x	distance of section x from the slab end
θ	the angle of the concrete strut. For a hollow core slab without shear reinforcement $\cot\theta = 1$
F_{px}	the ultimate resisting force provided by prestressing tendons in a cracked anchorage zone. $F_{px} = P_o x/l_{bpd} \leq A_p f_{p,0.1k}/\gamma_s$
P_o	the initial force at the active end of the tendons immediately after stressing
l_{bpd}	the design value of transmission length. $l_{bpd} = 1.2\beta\phi = 1.2 \cdot 70\phi$ when $f_{cj} = 30 \text{ N/mm}^2$.
A_p	the cross section area of the prestressing steel
$f_{p,0.1k}$	characteristic 0.1% proof-stress of prestressing steel
γ_s	the partial safety factor for the prestressing steel ($\gamma_s = 1.15$)

2.3.5.8 Negative bending capacity of the hollow-core slab (Section D)

The negative design moment value M_{sd} and the capacity M_{Rd} of the hollow-core composite cross section, limited by the anchorage of the in situ negative reinforcement, should be evaluated in ULS according to the principles of ENV 1992.1.1 [2]. The contribution of the prestressing steel A_p at the upper level only and the effective precast concrete stresses due to prestress at the relevant section, should also be considered.

The additional contribution of the in-situ concrete to the precast concrete should be calculated for the homogenised section, according to the ratio E_c/E_p .

The negative design moment M_{sd} refers to all loads on the composite structure resulting from the bending diagram at section D, increased by the moment due to the second order effects of combined permanent and prestressing forces, given in § 2.3.5.2.



2.3.5.9 Shear capacity at the slab-end section at the support (Section A')

The design shear resistance V'_{Rd1} shall be calculated at the support, according to ENV 1992.1.1 [2] taking into account the effective in-situ concrete cross section adjacent to the hollow core slab end.

$$V'_{Rd1} = 0.25 f'_{ctd} \Sigma b_c d'' k (1.2 + 40 \rho'_1) \leq V'_{Rd2} \quad (2-21)$$

where

ρ'_1	$= \Sigma A_s / \Sigma b_c d''$
V'_{Rd2}	$= 1/2 v f'_{ctd} \Sigma b_c 0.9 d''$
k	$= 1.6 - d'' \geq 1$
v	$= 0.7 - f'_{ck}/200 \geq 0.5$
f'_{ctd}	the design tensile strength of the in-situ concrete
ΣA_s	the total area of tension reinforcement adequately anchored
Σb_c	the total width of the in-situ concrete cross section adjacent to the hollow core slab end
d''	the effective depth of the in-situ concrete cross section, at support side
f'_{ck}	the characteristic cylinder compressive strength of the in-situ concrete

In case that $V_{sd} > V'_{Rd1}$ a specific shear reinforcement has to be provided in the cast in-situ section at the support (see fig 2-29)

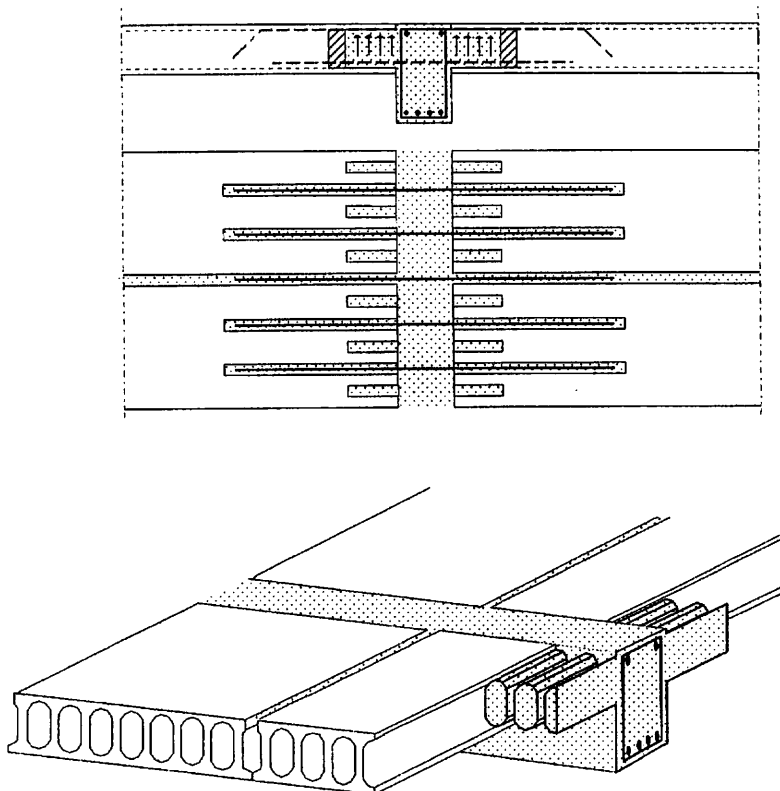


Fig. 2-28: Arrangement of a composite connection between hollow-core slab and in-situ beam

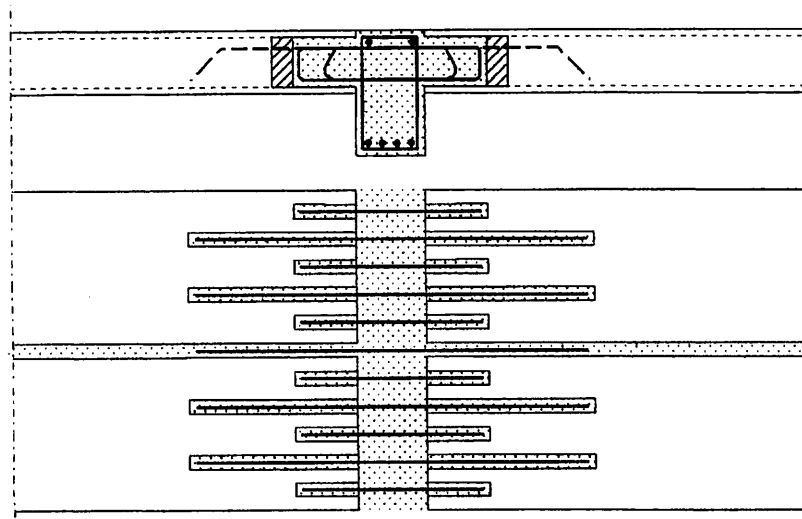


Fig. 2-29: Specific shear reinforcement of in-situ concrete

2.3.5.10 Shear and spalling stresses (Section A')

In the case of composite support (without direct support under the precast slab) the shear capacity at the slab end section is limited by the simultaneous presence of shear and spalling stresses.

The principal design stress in ULS in the most critical web should be checked for the cross section at the slab end, in order to avoid horizontal cracking under combined design stresses. The result should never exceed the design tensile strength of the precast concrete.

In the case of non rigid support the resulting additional shear stresses should be considered when evaluating τ_{sd} .

$$\sigma_{t,d} = \frac{\sigma_{Spi,d(t)} + \tau_{sd} \cos 2\beta}{2} + \sqrt{(\tau_{sd} * \sin 2\beta)^2 + \left(\frac{\sigma_{Spi,d(t)} + \tau_{sd} \cos 2\beta}{2} \right)^2} \leq f_{ctd} \quad (2-22)$$

τ_{sd} the design value of shear stress $\tau_{sd} = V_{sd}/0.9d'b'_w$
 $\sigma_{Spi,d(t)}$ the design value of spalling stress at time t $\sigma_{Spi,d(t)} = \gamma_p \sigma_{Spi} P_{m,t}/P_{m,o}$
 in the most critical web

where

$\sigma_{t,d}$ the max design value of the principal tensile stress in the most critical web
 f_{ctd} the design tensile strength of precast concrete
 V_{sd} the design value of shear force in section A'
 β the angle of spalling stress with respect to shear force (approximately $\beta \approx 20 \div 25^\circ$ and therefore $\cos 2\beta \approx 0.7$)
 b'_w the total web width of composite section taking into account the number of filled cores with additional lower and upper in-situ reinforcement
 $b'_w = b_w + n b_c E_c'/E_c$.
 n and b_c number and width of the filled cores with steel reinforcement.
 E_c'/E_c the ratio of the modulus of elasticity of in-situ to precast concrete.

d'	the effective depth of the composite cross section.
γ_p	the partial safety factor of prestressing force for ULS ($\gamma_p = 1.2$)
b_i and b_w	the width of the most critical web " i " of the precast hollow-core slab subject to spalling stress and the total web width
σ_{Spi}	the spalling stress at detensioning in the most critical web " i ", calculated according to clause 4.3.1.6 of pr EN 1168 [4].

$$\sigma_{Spi} = \frac{P_o}{b_i e_o} \frac{15\alpha_c^{2.3} + 0.07}{1 + (l_{bp}/e_o)^{1.5} (1.30\alpha_c + 0.1)}$$

P_o	the initial prestressing force just after release.
e_o	the eccentricity of the prestressing steel.
α_c	eccentricity coefficient $\alpha_c = (e_o - k)/h$.
k	the core radius, the ratio of the lower section modulus and the area of the cross section of the precast hollow core slab $k = J/x_{mn}A$.
l_{bp}	the transmission length for tendon with diameter ϕ $l_{bp} = \beta_b \phi = 70 \phi$ in case of $f_{ej} = 30 \text{ N/mm}^2$ (according to clause 4.2.3.5.6 ENV 1992.1.1 [2]).
h	the depth of hollow core slab.
P_t	the mean value of prestressing force at time t $P_t = P_o - \Delta P_t$.
ΔP_t	the loss due to creep, shrinkage and relaxation at time t $\Delta P_t = (P_o - P_\infty)\alpha_t$.
P_∞	the final prestressing force after occurrence of all losses.
α_t	proportion of actual losses to time according to Fig. 2-27 as per 2.3.5.2.
t	the time passed from the time $t = 0$ when prestressing force is released and the time t when design actions will occur.

$t = 2 \text{ months } \alpha_t = 0.5$

$t = 3 \text{ months } \alpha_t = 0.6$

$t = 6 \text{ months } \alpha_t = 0.7$

$t = 1 \text{ year } \alpha_t = 0.8$

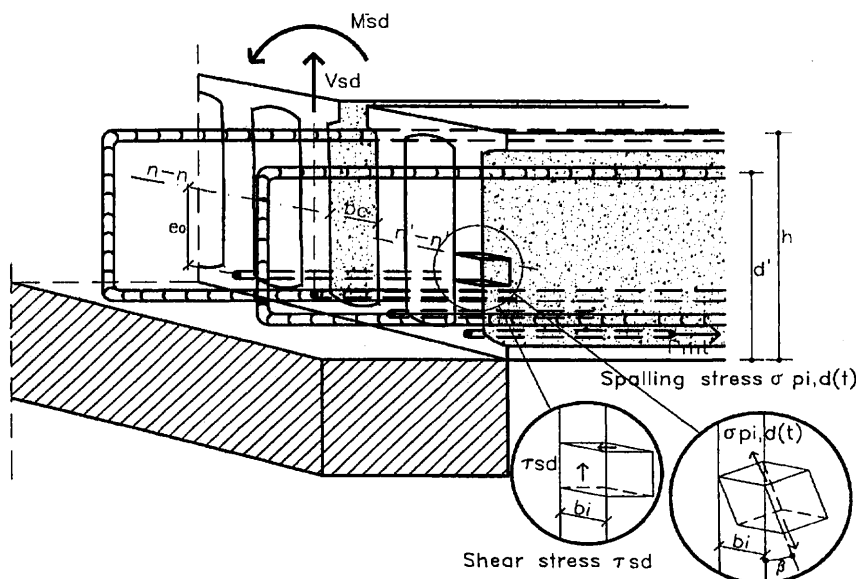


Fig. 2-30: Shear and spalling stresses at interface between hollow-core slab and cast in-situ concrete at support.

2.4 Detailing of connections

2.4.1 General

The detailing of the connection at support has to fulfill specific requirements, depending upon the structural philosophy of the specific structure. In all cases, tie arrangements at support should be able to provide the structural integrity with regard to loads and restrained deformations.

Openings in a hollow core unit for concreting the cores and for placement of the additional in-situ reinforcement can be in form of holes or slots.

The anchorage length of the bottom and top reinforcement bars should be calculated individually and should be sufficient to anchor the yield load; the anchorage length should be at least equal to

$$L_s = L_{cr} + \Delta L_b \quad \text{where:}$$

L_{cr} = length from the support to the nearest flexural crack which causes anchorage failure of the prestressing strands (bottom or top strands, according to the ultimate strain relevant to the appropriate design bending moment)

ΔL_b = additional anchorage length for ribbed tie bars to be provided with regard to the resistance against progressive collapse (see F.I.P. Recommendations [1]).

The shape and width of joints and cores in which in-situ reinforcement is to be anchored, the positioning of the reinforcement, and the concrete filling of the joint or cores, should meet the requirements given at point 4.3 of prEN 1168 [4].

It is recommended to provide a suitable plug or other devices at the end of the design length of each core in order to ensure adequate filling of the core with well compacted in-situ concrete.

2.4.2 Number and length of grouted cores

When hollow core slabs are designed for direct support conditions (See Fig. 2-31) it is recommended to provide at least two grouted cores with tie bars in each slab unit of 1.20 m width, or one core with a tie bar and the other tie reinforcement in the longitudinal joint.

In the case of non-direct support, the minimum number of grouted cores should be 3, or alternatively 2 grouted cores together with a tie bar in the longitudinal joint (See Fig. 2-32).

The length of the reinforcement bars in the cores should be calculated according to the design moment and shear requirements given in § 2.3.5, but it should not be less than the minimum length given in § 2.4.1 (See Fig. 2-33).

The number and length of filled cores without steel reinforcement should be calculated according to the design shear requirements as given in chapter 2.3.5.

The filling length should be at least equal to the core height or 50% l_{bp} , whichever is greater. (See Fig. 2-34)



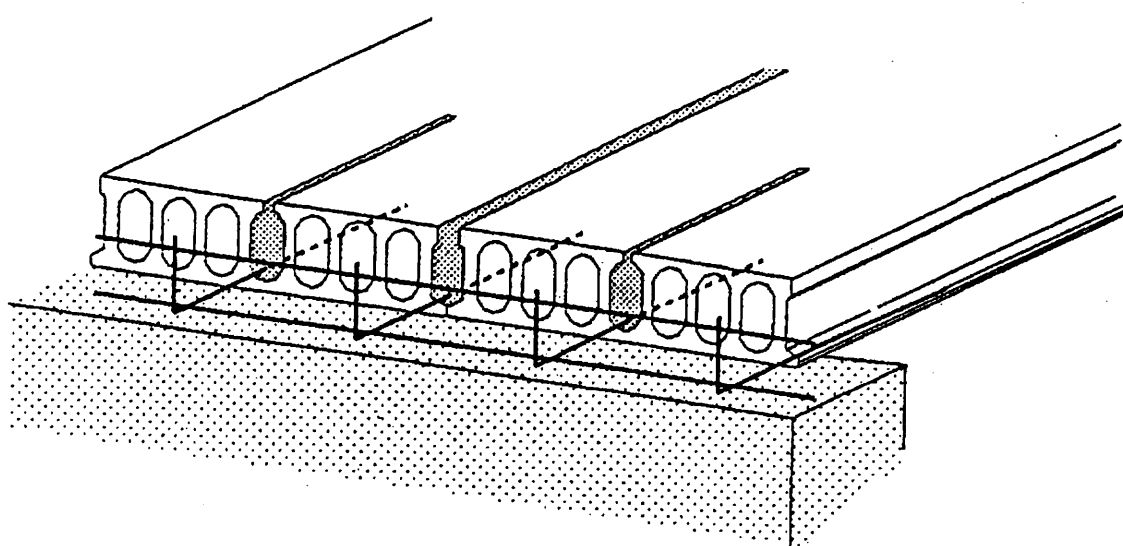


Fig. 2.31 - Normal (direct) support length N° 2 ties per slab

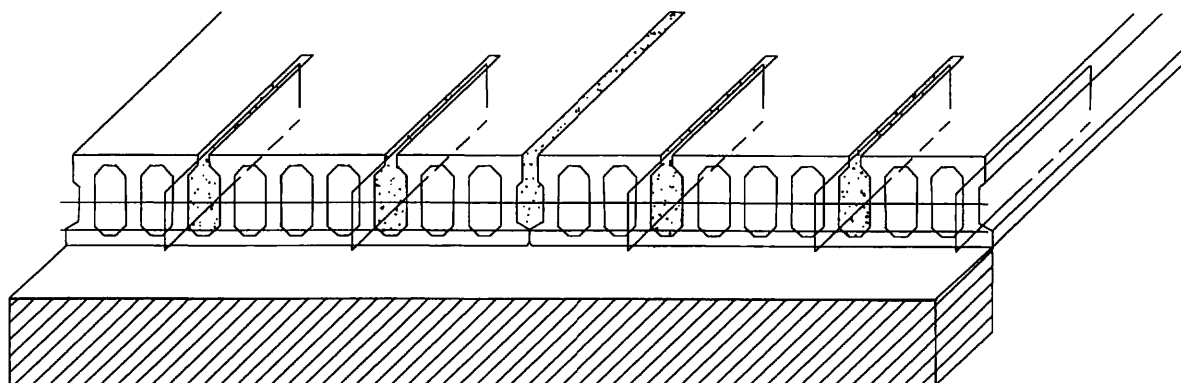


Fig. 2.32: Composite (non-direct) support length N° 3 ties per slab

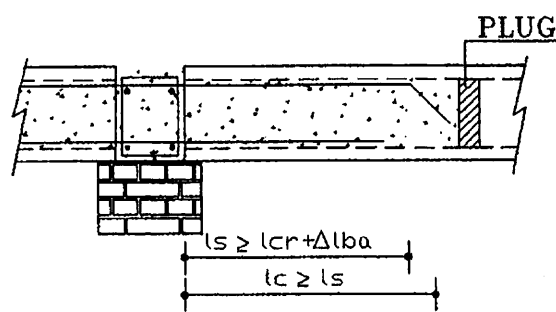


Fig. 2.33: Core with steel reinforcement

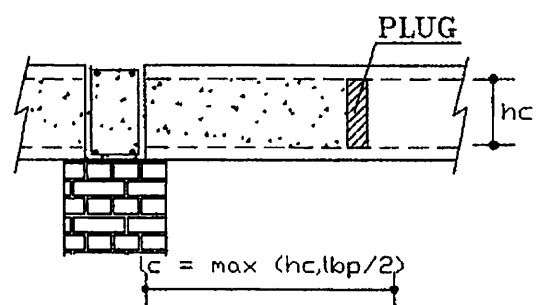


Fig. 2.34: Grouted core without steel reinforcement

2.4.3 Simplified rules

For the preliminary design of a floor and its connections, the following recommendations, derived from normal applications of hollow core slabs with continuity or restrained supports, may be used to calculate number, length and diameter of the reinforcement bars and the grouted cores.

The final design should be carried out according to the rules set out in chapters 2.3.3, 2.3.4 and 2.3.5.

The following simplified rules refer to Negative Moment M^- (kNm) and Shear V (kN) values calculated at S.L.S. before redistribution at support, and with normally distributed permanent + variable load in the range of 4.0-8.0 kN/m²

	Normal support	Composite support
- Floor Length/depth l/h	-	30-35
- Required precast web thickness Σbw	-	380-420 mm
- Max No of 1/2" strands per web	2-3	1
- Number of cores with reinforcement		
l≤6.0 m	2-3	3
6.0 < l ≤ 10.0 m	3	3-4
10.0 < l m	3-4	4
- Length of cores with reinforcement (ls)		
l≤6.0 m	One bar (normally in the joint) ls≈1.4 m other bars ls≈1.0 m.	One bar (normally in the joint) ls≈1.4 m other bars ls≈1 m.
l>6.0 m	One bar (normally in the joint) ls=0.20-0.25 l other bars ls≈1.2-1.5 m	One bar (normally in the joint) ls=0.20-0.25 l other bars ls≈1.2-1.5 m.
- In-situ bottom reinforcement (total section As per slab and Ø max)	Usually none	As=5 V (mm ²) Ø max≈2+h/25 (mm)
- In-situ top reinforcement (total section As per slab and Ø max)	As=5000 M ² /h (mm ²) Ø max≈6+h/25 (mm)	As=5000 M ² /h (mm ²) Ø max≈6+h/25 (mm)
- No/Length of additional filled cores (l _c) without reinforcement	Usually none	All remaining/ l _c =300-400 mm

2.5 References and experimental results

- [1] FIP Recommendations "Precast prestressed hollow core floors", Fip Commission on Prefabrication, Thomas Telford, London 1988.
- [2] ENV 1992.1.1. - Eurocode 2 - General rules and rules for buildings
- [3] ENV 1992.1.3. - Eurocode 2 - Precast concrete, elements and structures.
- [4] Pr EN 1168 - European Standard - Precast concrete - Hollow core slabs for floors
- [5] [B. Lewicki, Soltan (1984)]. Pannelli alveolari precompressi. Calcolo delle capacità portanti a taglio secondo le normative CEB/FIP e di diversi paesi. "La Prefabbricazione" n. 3 e 4.
- [6] [F. Levi, P.G. De Bernardi, (1986)]. Prove di continuità longitudinale di solai di tipo alveolare privi di cappa di completamento. "La Prefabbricazione" n. 4.
- [7] [C. Bosco, A. Carpinteri, P.G., De Bernardi, (1990)]. Minimum reinforcement in high strength concrete. "Journal of Structural Engineering" (ASCF) Vol. 116.
- [8] [C. Bosco, P.G. De Bernardi, (1990)]. Indagine sulla continuità strutturale di solai alveolari prodotti col metodo slipform "L'Edilizia" n. 11.
- [9] [M. Grzybowski, B. Westerberg, (1991)]. Prestressed Concrete Hollow Core Slabs Subjected to Negative Moment, Royal Institute of Technology, Stockholm, SWEDEN.
- [10] [F. Mola, (1992)]. Prove sperimentali di collaudo di solai alveolari portati da travi in spessore.

The purpose of the experimental investigation was to assess the behaviour of structural elements designed in accordance with the methods described in the previous paragraph. The tests were carried out on hollow core slabs which were connected at the supporting beam (beam depth equal to and greater than slab thickness) by means of a reinforcement specially designed to withstand the negative moment. The loading programme was defined to simulate the actual distribution of load-effects as well as to bring about the reversal of moment sign. Both static actions and cyclic actions were applied till failure.

No anomaly was observed in the behaviour of the slabs in service conditions. The failure of the connection invariably occurred through the yielding of the upper in situ reinforcement, at the point of maximum negative moment.

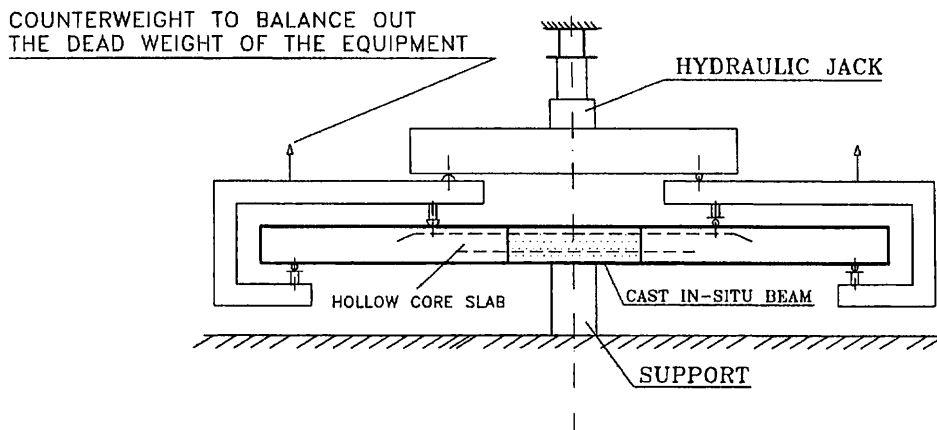


Fig 2-35: Test of flat beam/hollow-core connection [6]

Annex A - Examples of calculation.

1 General

1.1 Basis of calculation

All calculations in the following examples are carried out according to Eurocode 2 ENV 1992.1.1, ENV 1992.1.3 and to European Standard pr EN 1168 "Precast prestressed hollow core elements".

The following material characteristics, prestressing stresses and losses, and partial safety factors are taken as the basis for all calculations.

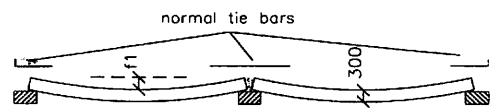
<u>Concrete characteristics</u>	<u>Precast concrete</u>	<u>In-situ concrete</u>
Strength class	C 45/55	C25/30
Concrete strength at release	f_{cj} 30	(N/mm ²)
Lower characteristic tensile strength	$f_{ctk0.05}$ 2.7	(N/mm ²)
Design value of tensile strength	f_{ctd} 1.8	(N/mm ²)
Design value of shear strength	τ_{Rd} 0.44	(N/mm ²)
Modulus of elasticity	E_{cm} 36	(N/mm ²)
<u>Steel characteristics</u>		
Characteristic tensile strength of prestressing steel	f_{pk} 1860 (MPa)	
Characteristic 0.1% proof stress of prestressing steel	$f_{p0.1k}$ 1670 (MPa)	
Initial prestressing stress applied to the tendons	σ_0 1350 (MPa)	
Prestressing stress immediately after transfer	$\sigma_{pm,0}$ 1250 (MPa)	
Effective final stress after loss of prestress at $t \rightarrow \infty$	$\sigma_{p,\infty}$ 1100 (MPa)	
In-situ reinforcement characteristic yield strength	f_{yk} 500 (MPa)	
Ductility class		High
<u>Partial safety factors</u>		
For actions, permanent G and variable Q	$\gamma_G = 1.35$	$\gamma_Q = 1.5$
For prestressing	$\gamma_p = 0.9$	or 1.2
For materials, concrete and steel	$\gamma_c = 1.5$	$\gamma_s = 1.15$
<u>Creep, shrinkage and time dependent factors</u>		
Ageing coefficient	$\rho = 0.8$	
Creep coefficient	$\phi(\infty,0) = 2.5$	
Shrinkage coefficient	$\epsilon_s(\infty,0) = 0.0004$	
Time passed between precast element cutting and in-situ concrete hardening	$t_o = 2$ month ($\alpha_{t_0} = 0.5$)	

1.2 Structural systems and support conditions

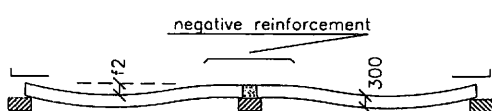
Example 1 - Two span floor

Two spans of hollow core slabs, with depth 300 mm and width 1200 mm and no topping, supported by one intermediate and two external beams at 10.0 m centres, are designed and calculated according to the following three schemes, for two typical hollow core sections.

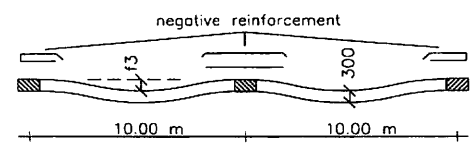
**Scheme 1 - Simply supported slabs,
with direct (normal) bearings**



**Scheme 2 - Slab continuous at centre support,
simply supported at end supports
with direct (normal) bearings.**



**Scheme 3 - Slab restrained at all supports
and without direct (normal) bearings**



The service loads are as follows:

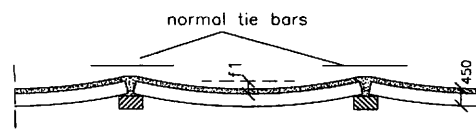
Dead load of hollow core floor	G	4.00 kN/m ²
Permanent load	G'	2.00 kN/m ²
Variable load	Q	6.00 kN/m ²
<hr/>		
Total load	<hr/>	
	$\Sigma_{G,Q}$ 12.00kN/m ²	

Linear design load at USL $q_u = 1.2[1.35(4.0+2.0)+1.5*6.0] = 20.52 \text{ kN/m}$

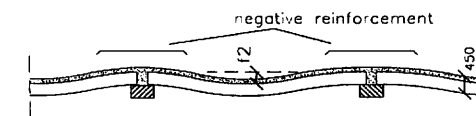
Example 2 - Multispan floor

Multispan hollow core floor slab with depth 400 mm and width 1200 mm and 50 mm topping, supported by beams at 10.0 m. centres, are designed and calculated according to the following three schemes, for two typical hollow core sections.

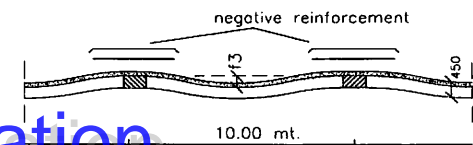
**Scheme 1 - Simply supported slabs,
with direct (normal) bearings**



**Scheme 2 - Slab continuous at internal supports,
with direct (normal) bearings**



**Scheme 3 - Slab restrained at all supports
and without direct (normal) bearings**



The service loads are as follows:

Dead load of hollow core with topping	G	6.00	kN/m ²
Permanent load	G'	4.00	kN/m ²
Variable load	Q	15.00	kN/m ²
Total load	$\Sigma_{G,Q}$	25.00	kN/m ²

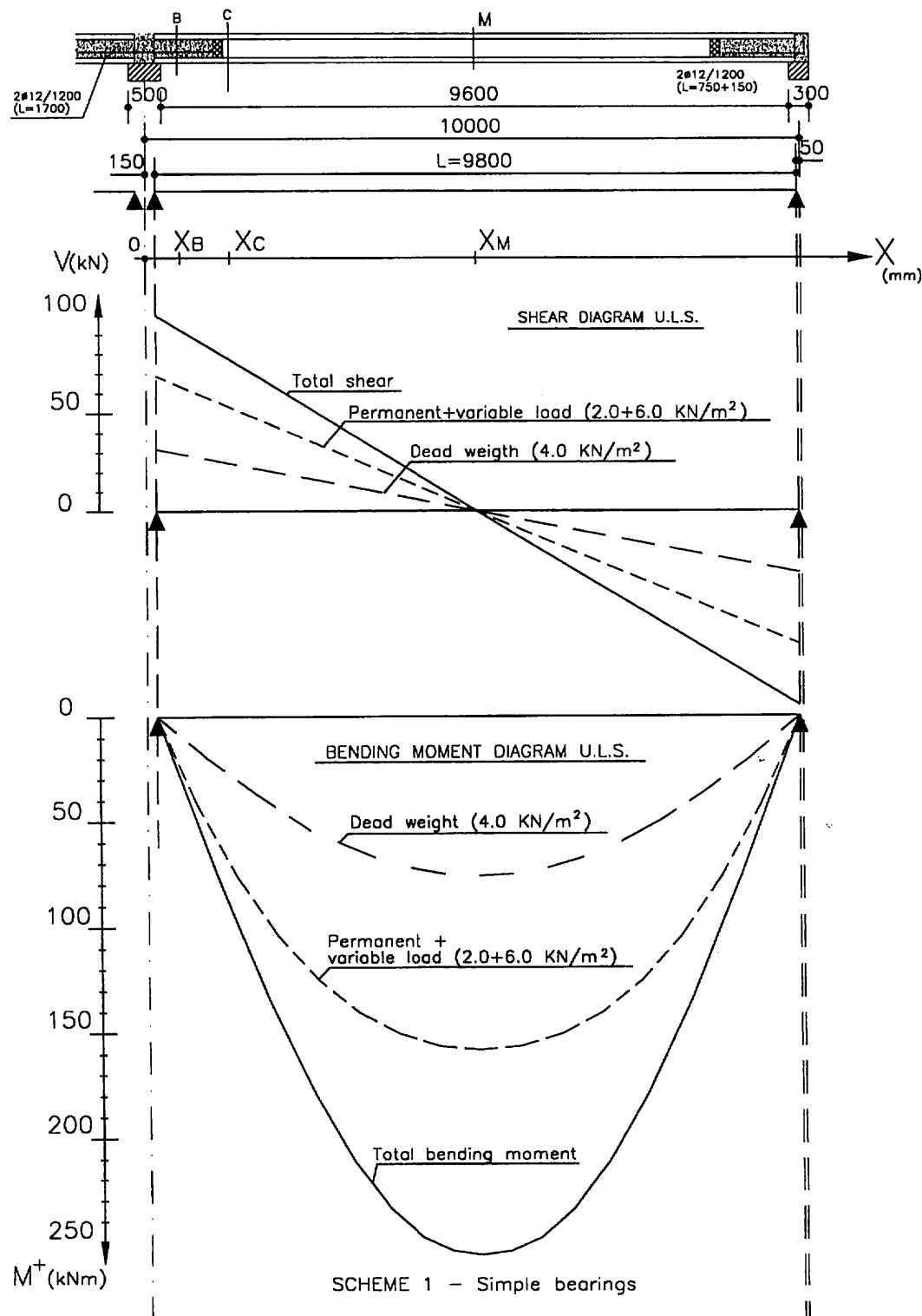
$$\text{Linear design load at USL } q_d = 1.2[1.35(6.0 + 4.0) + 1.5 \cdot 15.0] = 43.2 \text{ kN/m}$$

The purpose is to evaluate for both examples 1 and 2 and each structural scheme the relevant load capacity, with regard to bending moment and shear, the deflection value and the amount of additional in-situ concrete and reinforcement and finally to compare the results in a summary (See point 4. General conclusions).

2 Example 1 - Two span floor

2.1 Simply supported slab with direct (normal) bearings

a) Design actions and sections to be checked



- **Section A ($x_A = 250$):** No need to be checked
- **Section B ($x_B = 250+d/2 = 378$):** Uncracked section, closest to support where shear tension capacity and interface shear strength should be checked

- $\underline{V'_{Rdt}} \geq V_{Sd} = \frac{20.52(4900+150-378)}{1000} = 95.9 \text{ kN}$
- $\underline{\tau_{Rdj}} > \underline{\tau_{Sdj}} = f_{Sd}/\Sigma S_c l_s + V_{Sd}/0.9d \Sigma S_c = 0 + 0.17 = 0.17 \text{ N/mm}^2$
 $f_{Sd} = 0$
 $\Sigma S_c = 1200 + 2*600 = 2400 \text{ mm}$

- **Section C ($x_c = 1120$):** First cracked section where shear flexural capacity should be checked

- $\underline{V'_{Rdf}} \geq V_{Sd} = \frac{20.52(4900+150-1120)}{1000} = 78.1 \text{ kN}$
 $q_d * L/2 x - q_d x^2/2 = f_{ctd} I/x_{nn} + M_p$ (Equation to be solved for x_c calculation)

$$x_c = x_o + q_d L/2 - \sqrt{(q_d L/2)^2 - 2q_d(M_p + f_{ctd} I/x_{nn})}$$

$$M_p = \gamma_p e \sigma_{p,\infty} A_p = 0.9 * 73 * 1100 * 871.2 * 10^6 = 62.96 \text{ kNm}$$

$$x_o = 150 \text{ mm} \quad L = 9800 \text{ mm} \quad q_d L/2 = 100.5 \text{ kN}$$

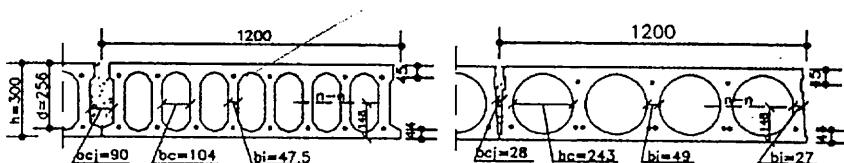
$$x_c = 150 + \frac{100.5 - \sqrt{100.5^2 - 2 * 20.52(62.96 + 1.8 * 205260 * 10^2 / 148)}}{20.52 * 10^3} = 1120 \text{ mm}$$

- **Section D:** No need to be checked
 - **Section E:** No need to be checked
 - **Section M ($x_M = 150+4900 = 5050$):** Where positive bending capacity should be checked
- $\underline{M'_{Rd}} \geq M'_{Sd} = 20.52 * 9.8^2 / 8 = 246.3 \text{ kN m}$

b) Hollow-core unit cross section and characteristics

- **Cross section (Sect C,M)**

Cracked sections, and subject to positive moment

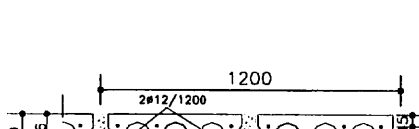
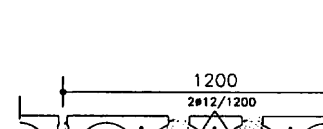


Prestressing reinforcement

Upper	No 6 str. 3φ3 mm	Fs 127.2 mm ²	No 2 str 3/8" + 1 str 3φ3 Fs 125 mm ²
Lower	No 8 str. 0.5"	Fi 744 mm ²	No 8 str 0.5" Fi 744 mm ²

Tot = 871 mm² @Seismicisolation

Tot = 869 mm²

	Hollow core type I	Hollow core type II
<u>Section properties</u>		
$A(\text{cm}^2)/I(\text{cm}^4)/S(\text{cm}^3)$	1820/205260/9000	1730/195830/8720
$b_w/b'_w/e(\text{mm})$	380/455/73	200/223/73
- Cross section at slab end (Sect A,B)		
Uncracked sections, and subject to positive moment		
<u>Prestressing reinforcement</u>		
Upper No 6 str. 3φ3 mm	Fs 127.2 mm ²	No 2 str 3/8" + 1 str 3φ3 Fs 125 mm ²
Lower No 8 str. 0.5"	Fi 744 mm ²	No 8 str 0.5"
	Tot = 871 mm ²	Tot = 869 mm ²

Section properties

$I'(cm^4)/S'(cm^3)$	217920/9950	224390/11280
b'_w/d' (mm)	541/256	628/256
$b_c/b_{cj}/h_c$ (mm)	104/90/200	243/28/200
Support length a (mm)	140	140

c) Calculations

- Section B ($V_{sd} = 95.9$ kN, $\tau_{sdj}=0.17$ N/mm 2 , M^+)
($x_B=378$ mm)

$$\begin{aligned}
 V_{Rdt} &= \frac{I_b w}{S} \sqrt{f_{ctd}^2 + \alpha \sigma_{cpm}} f_{ctd} \quad (\text{kN}) & 207.1 & 108.3 \\
 \alpha &= l_x/l_{bpd} = (a+x_B-x_A)/l_{bpd} & 0.29 & 0.29 \\
 &= (140 + 128)/1.2 * 70 * 10.9) \\
 \sigma_{cpm} &= \gamma_p \sigma_{p,\infty} A_p/A \quad (\text{N/mm}^2) & \underline{0.9*1100*871.2=4.740.9*1100*869=4.94} \\
 && 182000 & 173000
 \end{aligned}$$

$$V_{sdG} = \frac{1.2 * 4.00 * 1.35 * 4900 + 450 - 378}{1000} = 30.3 \text{ kN}$$

V_{sdq} max due to in-situ concrete failure is such that:

$$\tau'_{sd} = \frac{V_{sdq} * S'}{b'_w I' E_p / E_c} = f'_{ctd} = 1.2 \text{ N/m}^2$$

$V_{sdq} = f'_{ctd} b'_w I' / S' E_p / E_c$	(kN)	170.6
		179.9

$$V_{sdq} \text{ max due to precast concrete failure is such that: } \tau_{sd} = \frac{V_{sdG} S}{b_w I} + \frac{V_{sdq} S'}{b'_{w'} I'} = \tau_{Rd}$$

Hollow core type I	Hollow core type II
--------------------	---------------------

$\tau_{Rd} = \sqrt{f_{ctd}^2 + \alpha \sigma_{cpm} f_{ctd}}$	(N/mm ²)	2.39	2.41
$\tau_G = V_{SdG} \frac{S}{b_w I}$		0.35	0.67
$V_{Sdq} = (\tau_{Rd} - \tau_G) b' w \frac{I'}{S'}$	(kN)	241.7	217.4

Since V_{Sdq} is limited by in-situ concrete failure, the shear tension capacity of the composite section has to be evaluated as follows, but can never be lower than V_{Rdt} of the hollow-core itself

- $V'_{Rdt} = V_{SdG} + V_{Sdq} \min < V_{Rdt}$ (kN) $30.3 + 170.6 = 200.9 \geq 207.1 = 210.2 \geq 108.3$
- $\tau_{Rdj} = k_t * \tau'_{Rd} = 1.4 * 0.3 \text{ N/mm}^2$ 0.42 0.42

$$q_d \text{ max when } V'_{Rdt} = V_{Sd} \quad (\text{kN/m}) \quad 44.4 \quad 44.9$$

- **Section C ($V_{Sd} = 78.1 \text{ kN}$, M^+)**
($x_C = 1120 \text{ mm}$)

$$\begin{aligned} \bullet \quad V'_{Rdf} &= 0.25 f_{ctd} b' w d k (1.2 + 40 \rho' 1) + \\ &+ 0.15 \sigma_{cpm} b_w d (\text{kN}) \quad 102.5 + 69.2 = \underline{171.7} \quad 62.1 + 37.2 = \underline{99.3} \\ k &= 1.6 - d \quad (\text{m}) \quad 1.344 \quad 1.344 \\ \rho' 1 &= A_p / b' w d \quad 744/455*256 = 0.00639 \quad 744/223*256 = 0.0150 \\ \sigma_{cpm} &= \sigma_{p,\infty} A_p / A \quad (\text{N/mm}^2) \quad 4.74 \quad 4.84 \\ q_d \text{ max when } R = S & \quad (\text{kN/m}) \quad 43.7 \quad 26.1 \end{aligned}$$

- **Section M ($M^+_{Sd} = 246.3 \text{ kNm}$, M^+)**
($x_M = 5050$)

$$\bullet \quad M^+_{Rd} \quad (\varepsilon_s = 1\%) \quad (\text{kNm}) \quad \underline{290} \quad \underline{290}$$

$$q_d \text{ max when } M^+_{Rd} = M^+_{sd} \quad (\text{kN/m}) \quad 24.2 \quad 24.2$$

$$\begin{aligned} \text{Max deflection at SLS under variable} \\ \text{load } Q \quad f = \underline{5} \quad Q \cdot 1.2 \cdot L^4 / EI \quad (\text{mm}) \quad 11.7 \quad 12.2 \\ 384 \end{aligned}$$

d) Conclusions

The load capacity is governed by moment resistance and $q_d \text{ max} = 24.2 \text{ kN/m}$ for both hollow-core types.

The quantities of additional in-situ concrete and reinforcement and possible saving in prestressing reinforcement for a tight design without any margin, are as follows for the both types:

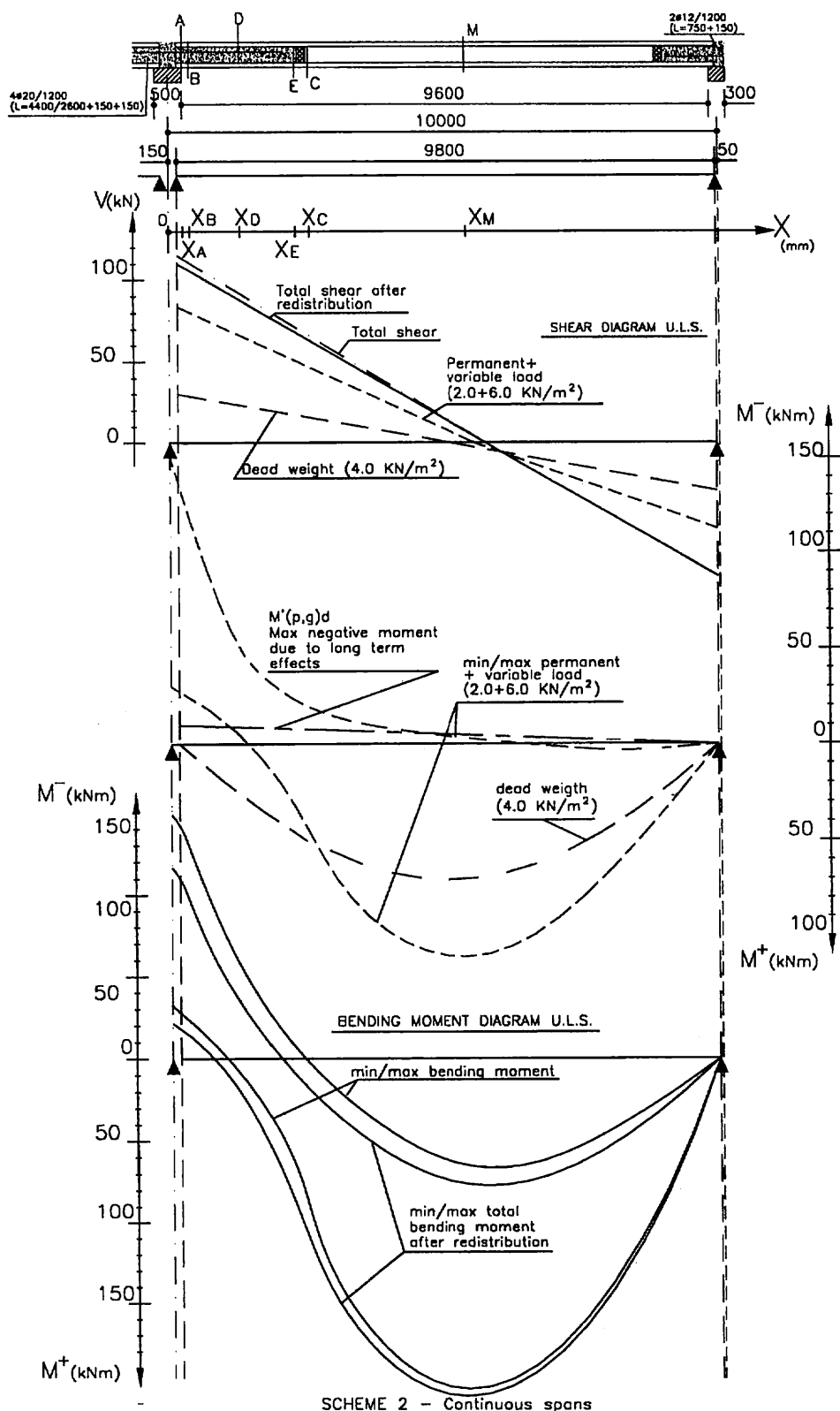
In-situ concrete: $0.015 \text{ m}^3/\text{m}^2$ Additional reinforcement: 0.3 Kg/m^2

Possible saving in prestressing reinforcement (without upper prestressing and minimizing lower prestressing): 1.6 Kg/m^2

Elastic deflection due to variable load 6.00 kN/m^2 is 12 mm approx. for both hollow-core types.

2.2 Slab continuous at centre support, simply supported at end supports with direct (normal) bearings

- a) Design actions and sections to be checked



- **Section A ($x_A = 250$, M):** The anchorage of in-situ reinforcement in the concreted core within the precast slab should be checked in the zone of negative bending moment.

- $\underline{M}_{Rd} \geq \underline{M}_{Sd}$ = $M_{Sdq} + M'_{(p,G)d} = 108.0 + 0 = \underline{108}$ kNm
 M_{Sdq} = 108.0 kNm from bending moment diagram with redistribution

- $M'_{(p,G)d}$ = $\frac{(3 M_p - M_G)}{2} \frac{\varphi(\infty, t_0)}{1 + \rho \varphi(\infty, t_0)}$ long term effect of the restrained support due to prestressing and permanent loads ($\Sigma G_i = G = 4 \text{ kN/m}^2$) with appropriate partial safety factor ($\gamma_p = 0.9$ or 1.2 and $\gamma_G = 1.35$ or 1.0), to be neglected if positive.

$$\frac{(3 \cdot 1.2 \cdot 74.7 - 1.0 \cdot 57.6)}{2} \cdot 0.625 = +48 \text{ kNm (max pos. value)}$$

- $M'_{(p,G)d}$ = $\frac{(3 \cdot 0.9 \cdot 74.7 - 1.35 \cdot 57.6)}{2} \cdot 0.625 = 14.42 \text{ kNm (min pos value)}$

- M_p = $\gamma_p e [P_o - (P_o - P_\infty) \alpha_{t_0}] = 73 \cdot 871 [1250 - (1250 - 1100) 0.5] \gamma_p \cdot 10^{-6}$
 $= 74.7 \gamma_p \text{ kNm}$

- M_G = $\gamma_G \sum G_i L^2 / 8 = \gamma_G 4.0 \cdot 1.2 \cdot 9.8^2 / 8 = 57.6 \gamma_G \text{ kNm}$
 $\varphi(\infty, t_0)$ = $\frac{0.5 \cdot 2.5}{1 + 0.8 \cdot 0.5 \cdot 2.5} = 0.625$

- $f_{ld} \geq f_{sd}$ = $f_{ld}(M_{Sd}) + f_{ld}(\Delta F'_s) = 444.4 + 0 = \underline{444.4}$ kN

- $f_{sd}(M_{Sd})$ ≈ $M_{Sd} / 0.9 d' = 108000 / 0.9 \cdot 270 = 444.4$ kN
 $f_{sd}(\Delta F'_s)$ = 0 assuming no restraint due to slab shortening

- $\underline{\tau}'_{Rd} \geq \underline{\tau}'_{Sd}$ = $A_s f_{sd} / S_c l_s = \frac{314}{\Sigma A_s} \cdot 444400 / 600 \cdot 2300 = \frac{0.08}{1256}$

- ΣA_s = 1256 mm²
 A_s = $A_s (\phi 20) = 314 \text{ mm}^2$
 V_{Sd} = 110.6 kN from shear diagram

- **Section B ($x_B = 250 + d/2 = 378$, M):** The flexural capacity of the composite member under negative moment, and the interface shear strength should be checked

- $\underline{V}'_{Rd1} \geq V_{Sd}$ = 108 kN from shear diagram

- $\underline{\tau}'_{Rd1} \geq \underline{\tau}'_{Sd1}$ = $\tau'_{Sd} + \tau''_{Sd} = 0.08 + 0.19 = \underline{0.27}$ N/mm²
 $\tau'_{Sd} = f_{sd} / \Sigma S_c l_s = 444400 / 600 \cdot 4 \cdot 2300 = 0.08 \text{ N/mm}^2$
 $\tau''_{Sd} = V_{Sd} / 0.9 d' \Sigma S_c = 108.000 / 0.9 \cdot 270 \cdot 600 \cdot 4 = 0.19 \text{ N/mm}^2$

- **Section C** ($x_c = 250 + \Delta x_a = 2483$, M^+): first cracked section, under positive bending moment where shear flexural capacity and anchorage failure of prestressing steel should be checked:

- $V'_{Rd} \geq V_{Sd} = 64.8 \text{ kN}$ from shear diagram at $x = 2483$

$$\Delta X_A = \frac{V_{SdA} - \sqrt{V_{SdA}^2 - 2q_d(M_{SdA} + M_p + f_{ctd} I/X_{nn})}}{q_d}$$

$$= \frac{110.6 - \sqrt{110.6^2 - 2*20.52(108+62.9+1.8*205260*10^{-2}/148)}}{20*52*10^{-3}} = 2233 \text{ mm}$$

$$M_p = \gamma_p * e \sigma_{p,\infty} A_p = 0.9 * 1100 * 871.2 * 73 * 10^{-6} = 62.9 \text{ kNm}$$

$$V_{SdA} = 110.6 \text{ kN} \quad \text{from shear diagram}$$

- $F_p \geq T_d = M^+_{Sd}/z + V_{Sd} \cot\theta = 539.1 + 64.8 = 604 \text{ kN}$

$$M^+_{Sd} = 124 \text{ kNm} \quad \text{from bending moment diagram with redistribution}$$

$$z = 0.9 d = 230 \text{ mm.}$$

- **Section D** ($x_D = 1300$, M^-): limit of in-situ reinforcement anchorage in the zone of negative moment. The flexural/tension shear capacity under negative moment and anchorage failure of upper prestressing steel should be checked at this section.

- $M'_{Rd} \geq M'_{Sd} = M'_{Sdq,G} + M'_{(p,G)}d = 2.6 + 0 = 2.6 \text{ kNm}$

$$M'_{Sdq,G} = 2.6 \text{ kNm} \quad \text{from bending moment diagram with redistribution}$$

$$M'_{(p,G)}d = \frac{(3 M_p - M_G) \varphi(\sigma, to)}{2(1 + \rho \varphi(\infty, to)) L} =$$

$$= \frac{0.625(3 * 0.9 * 74.7 - 1.35 * 57.6) * (9800 - 1150)}{2(9800 - 100)} = 12.8 \text{ kNm (Positive)}$$

- $V'_{Rdf} \geq V_{Sd} = 89.1 \text{ kN}$ from shear diagram

- $F_{p,D} \geq T_{d,D} = M'_{Sd,D/z} + V_{sd,D} \cot\theta = 2.6/0.229 + 89.1 = 100.4 \text{ kN}$

$$z = 0.9 * d = 0.9 * 255 = 229 \text{ mm}$$

- **Section E** ($x_E = 2300$, M^+): limit of in-situ filling of concrete in the cores where flexural/tension capacity of hollow-core slab should be checked.

- $V_{Rdf} \geq V_{Sd} = 68.6 \text{ kN}$ from shear diagram

- **Section M** ($x_M = 5530$, M^+) where positive bending capacity should be checked

- $M_{Rd} \geq M'_{Sd} = M'_{Sdq,G} + M'_{(p,G)}d = 193 + 12.8 = 205.8 \text{ kNm}$

$$M'_{Sdq,G} = 193 \text{ kN} \quad \text{from bending moment diagram with redistribution}$$

$$M'_{(p,G)}d = \frac{(9800 - 5280)(3 * 1.2 * 74.7 - 1.35 * 57.6) * 0.625}{9800 - 100} = 12.8 \text{ kNm}$$

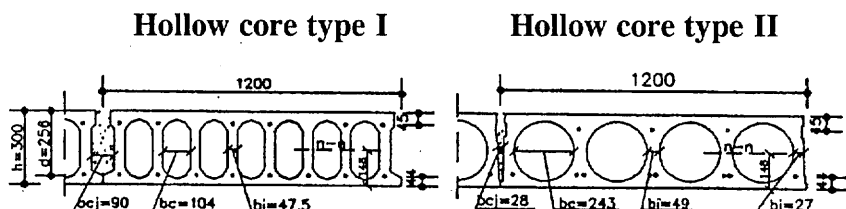
$$\approx 12.8 \text{ kNm}$$



b) Hollow core unit cross section and characteristics

- Cross sections
(Sect E,C,M)

Cracked sections
and subject to
positive moment



Prestressing reinforcement

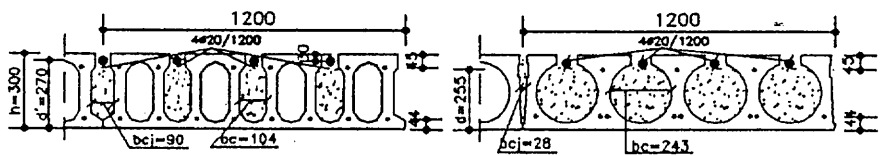
Upper	No 6 str. 3φ3 mm	Fs 127.2 mm ²	No 2 str 3/8" + 1 str 3φ3 Fs 125 mm ²
Lower	No 8 str. 0.5"	Fi 744 mm ²	No 8 str 0.5" Fi 744 mm ²
Tot = 871 mm ²			Tot = 869 mm ²

Section properties

A(cm ²)/I(cm ⁴)/S(cm ³)	1820/205260/9000	1730/195830/8720
b _w /b' _w /e(mm)	380/455/73	200/223/73

- Cross section at slab end
(Sect A,B,D)

Cracked sections
and subject to
negative moment



Prestressing properties

Upper	No 6 str. 3φ3 mm	Fs 127.2 mm ²	No 2 str 3/8" + 1 str 3φ3 Fs 125 mm ²
Lower	No 8 str. 0.5"	Fi 744 mm ²	No 8 str 0.5" Fi 744 mm ²
Tot = 871 mm ²			Tot = 869 mm ²

Section properties

I'(cm ⁴)/b' _w (mm)	217920/715	210890/1033
A _s max/ΣA _s (mm ²)	314 (φ20)/1256	314(φ20)/1256
d'(Sect A,B)/d(Sect D) (mm)	270/255	270/255
S _c /l _s /hc (mm)	600/2300/200	600/2300/200

c) Calculations

- Section A ($M_{sd} = 108 \text{ kNm}$, $f_{sd} = 444.4 \text{ kN}$, $\tau'_{sd} = 0.08 \text{ N/mm}^2$)
($x_A = 250$)

• M_{Rd} ($\epsilon_s = 1\%$)	(kNm)	<u>138.6</u>	<u>138.6</u>
• $f_{td} = \Sigma A_s f_y / \gamma_s$	(kN)	$\frac{1256 * 500 / 1.15}{1000} = 546$	<u>546</u>
• τ'_{Rd} (joint)	(N/mm ²)	<u>0.1</u>	<u>0.1</u>
q_d max when $S=R$	(kN/m)	<u>23.0</u>	<u>23.0</u>

- **Section B** ($V_{sd}=108.0 \text{ kN}$, $\tau_{sdj}=0.27 \text{ N/mm}^2$, M^+)
($x_A=378$)

	Hollow core type I	Hollow core type II
● $\frac{V'_{Rd1}}{*(1.2+40\rho_1)} = 0.25 f_{ctd} b'_w d' k * 0.25 * 1.8 * 715 * 270 * 1.33 * 1000 \geq V_{Rd2}$ (kN)	$*(1.2+40*0.0065) = 168.7$	$0.25 * 1.8 * 1033 * 270 * 1.33 * 1000$
$k = 1.6-d'$ (m)	1.33	1.33
$\rho_1 = \sum A_s / b'_w d'$ (m)	1256/715*270=0.0065	0.0045
$V_{Rd2} = 1/2 v f_{cd} b'_w 0.9 d'$ (kN)	<u>1</u> 0.5*45 715*0.9*2 1.5	
	$*270/1000=1303$	1882
$v = 0.7-f_{ck}/200 \geq 0.5$	0.7-45/200=0.475→0.5	0.5
● $\tau_{Rdj} = K_t \tau'_{Rd}$ (N/mm ²)	<u>1.4*0.3=0.42</u>	<u>0.42</u>
$q_d \text{ max when } S=R$	32.0	34.4
- Section C ($V_{sd}=64.8 \text{ kN}$, $T_d=604 \text{ kN}$, M^+) ($x_c=2483$)		
● $\frac{V'_{Rdf}}{*(1.2+40\rho_1)+0.15*} = 0.25 f_{ctd} b'_w d K^*$ (kN)	$102.5+69.2=\underline{171.7}$	$59.3+37.9=\underline{97.2}$
$*\sigma_{cpm} b_w d \geq V_{Rd2}$		
$k = 1.6-d$ (m)	1.344	1.344
$\rho_1 = \sum A_p / b'_w d$	744/455*256=0.00639	744/223*256=0.0130
$V_{Rd2} = 1/2 v f_{cd} b'_w 0.9d$ (kN)	786	385
$v = 0.7-f_{ck}/200 \geq 0.5$	0.7-45/200=0.475→0.5	0.5
$\sigma_{cpm} = \sigma_\infty A_p / A$	<u>0.9*1100*871.5=4.74</u>	<u>0.9*1100*869=4.94</u>
	$1820*10^2$	$1730*10^2$
● $F_p = P_o x / l_{bpd} \leq A_p f_{p0,1} k / \gamma_s$	<u>1080</u>	<u>1080</u>
$P_o x / l_{bpd}$ (kN)	<u>1350</u> *744*(2636-160)=2696	2696
$l_{bpd} = 1.2 * 70 * \phi$	1000	915
$A_p f_{p0,1} k / \gamma_s$ (kN)	<u>744</u> *1670/1.15= <u>1080</u>	<u>1080</u>
$q_d \text{ max when } S=R$ (kN/m)	1000	
	36.7	30.8
- Section D ($M^+_{sd}=2.6 \text{ kN}$, $V_{sd}=89.1 \text{ kN}$, $T_d=100.4 \text{ kN}$) ($x_D=1300$)		
● $M^+_{Rd} (\varepsilon_s=1\%)$ (kNm)	<u>52.3</u>	<u>51.5</u>
● $\frac{V'_{Rdf}}{*(1.2+40\rho_1)+} + 0.15 \sigma_{cpm} b_w d$ (kN)	$135.5+68.9=\underline{204.4}$	$124.3+37.8=\underline{232.1}$
$k = 1.6-d$ (m)	1.345	1.345
$\rho_1 = \sum A_p \text{ sup } / b'_w d$	127/715*255=0.00069	125/1033*255=0.00047
σ_{cpm}	4.74	4.94

		Hollow core type I	Hollow core type II
• $F_p = P_o x / l_{bpd} \leq A_p f_{p0,1} k / \gamma_s$ (kN)		<u>184.4</u>	<u>181.5</u>
$P_o x / l_{bpd}$		<u>1350 * 1190 + 127 / 1000</u>	<u>1350 * 1190 * 125 / 1000</u>
$A_p f_{p0,1} k / \gamma_s$ (kN)		<u>127 * 1670 / 1.15 = 184.4</u>	<u>181.5</u>
q_d max when $S=R$ (kN/m)		37.7	37.1
- Section E ($V_{sd}=68.6$ kN, M^+) ($x_E=2300$)			
• $V'_{Rdf} =$ (as per sect C) (kN)		<u>102.5 + 69.2 = 171.7</u>	<u>59.3 + 37.9 = 97.2</u>
q_d max when $S=R$ (kN/M)		51.3	29.1
- Section M ($M^+_{sd}=205.8$ (kNm) ($x_M=5530$)			
• M^+_{Rd} ($\varepsilon_s=1\%$) (kN/m)		<u>290</u>	<u>290</u>
q_d max when $S=R$ (kN/m)		28.9	28.9
Max deflection at SLS under variable load Q (mm)		4.9	4.9

d) Conclusions

The load capacity is governed by in-situ reinforcement area and length in section A with $q_d \text{max} = 23$ kN/m for both hollow core types.

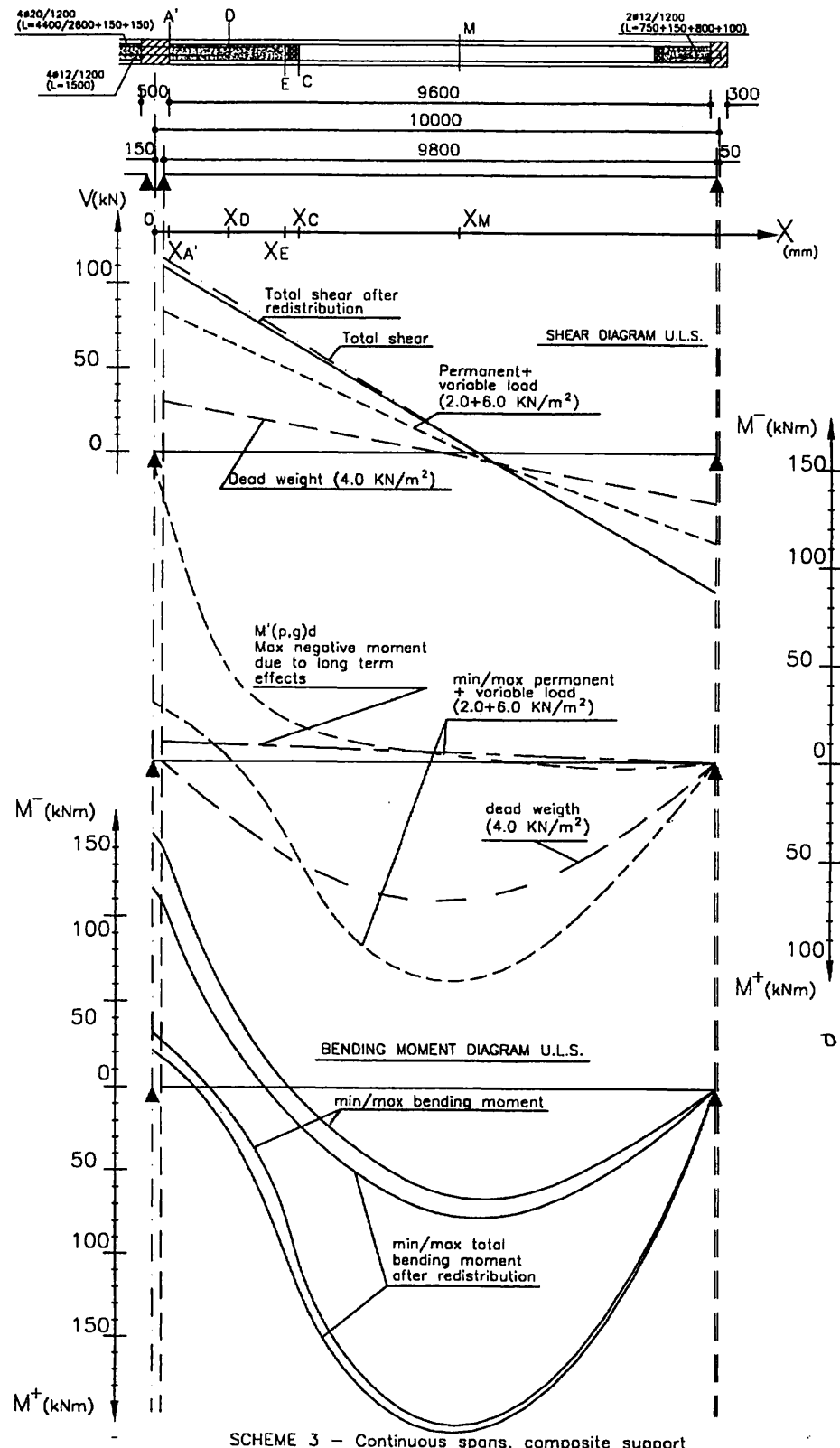
With a small increase of upper reinforcement (only 0.4 Kg/m²), the load capacity could be increased to $q_d = 29$ kN/m, governed by positive bending moment resistance.

The quantities of additional in-situ concrete and reinforcement and possible saving in prestressing reinforcement for a tight design without any margin, are as follows for both types:

- In situ concrete	(m ³ /m ²)	0.030	0.045
- Additional reinforcement	(Kg/m ²)	2.0	2.0
- Possible saving in prestressing reinf.	(Kg/m ²)	1.6	1.6
- Elastic deflection due to variable load (6.00 kN/m ²)	(mm)	4.9	4.9

2.3 Slab restrained at all supports and without direct (normal) bearings.

- a) Design actions and sections to be checked



- **Section A' ($x_{A'}=250, M'$):** Where in addition to the design calculations as per scheme2, sect A, the shear capacity at the slab end section, at both member and support sides, as well as the shear and spalling stresses should also be checked.

- $M'_{Rd} \geq M'_{Sd}$ = 108 kN/m (see scheme 2, sect A)
- $f_{cd} \geq f_{Sd}$ = 444.4 kN/m (see scheme 2, sect A)
- $\tau'_{Rd} \leq \tau'_{Sd}$ = 0.08 N/m² (see scheme 2, sect A)
- V'_{RdI} (member and support side) $\geq V_{Sd} =$ 110.6 kN from shear diagram
- $\tau'_{Rdj} \geq \tau'_{Sdj}$
 τ'_{Sd} = $\tau'_{Sd} + \tau''_{Sd}$ = $0.192 + 0.08 =$ 0.27 N/mm²
 τ''_{Sd} = $f_{Sd}/\sum S_c l_s$ = $444400/600*4*2300 = 0.08$ N/mm²
 $= V_{Sd}/0.9 d' \sum S_c$ = $110600/0.9 * 270 * 600 * 4 = 0.192$
 $=$ 1.18 N/mm² (Hollow core type I)
- $f_{cd} \geq \sigma_{I,d} =$
 $=$ 1.93 N/mm² (Hollow core type II)

$\sigma_{I,d}$ = principal tensile stress

$$= \frac{\sigma_{Spi, d(t)} + \tau_{Sd} \cos 2\beta}{2} + \sqrt{(\tau_{Sd} \sin 2\beta)^2 + \left(\frac{\sigma_{Spi, d(t)} + \tau_{Sd} \cos 2\beta}{2} \right)^2} =$$

$$= 0.55 + 0.63 =$$
 1.18 N/mm² (Hollow core Type I)
 $=$

$$= 0.94 + 0.99 =$$
 1.93 N/mm² (Hollow core type II)

since $2\beta = 45^\circ$ $\sin 2\beta = \cos 2\beta = 0.7$

$$\tau_{Sd} \sin 2\beta = \tau_{Sd} \cos 2\beta = 0.7 V_{Sd} / 0.9 d' b'_w =$$

$$= 0.7 * 110600 / 0.9 * 1061 * 270 = 0.7 * 0.43 = 0.30$$
 N/mm² (Hollow core type I)
 $=$

$$= 0.7 * 110600 / 0.9 * 1033 * 270 = 0.7 * 0.44 = 0.31$$
 N/mm² (Hollow core type II)

$\sigma_{Spi, d(t)}$ = the design value of spalling stress at time t = $\gamma_p \sigma_{Spi} P_t / P_o =$

$$= 1.2 * 0.73 * 1152 / 1250 = 0.80$$
 N/mm² (Hollow core type I)
 $=$

$$= 1.2 * 1.42 * 1152 / 1250 = 1.570$$
 N/mm² (Hollow core type II)
$$= 0.73$$
 N/mm² (Hollow core type I)

σ_{Spi} = the spalling stress at detensioning =

1.42 N/mm² (Hollow core type II)

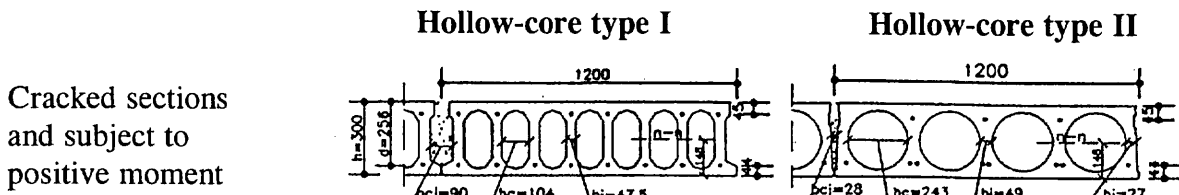
$P_t = P_o - (P_o - P_\infty) \alpha_t = 1250 - (1250 - 1100) 0.65 = 1152$ MPa

$\alpha_t = 0.65$ (assuming that design action occurs after 2 months from cast-in situ, that is after 4 months from prestressing release)

- **Section B:** No need to be checked
- **Section C ($x_c = 2483$, M^+):** (see scheme 2, sect C)
 - $V'_{Rdf} \geq V_{Sd}$ = 64.8 kN (see scheme 2, sect C)
 - $F_p \geq T_d$ = 604 kN (see scheme 2, sect C)
- **Section D ($x_D = 1300$, M^-):** (see scheme 2, sect D)
 - $M^-_{Rd} \geq M^-_{Sd}$ = 2.6 kNm (see scheme 2, sect D)
 - $V'_{Rdf} \geq V_{Sd}$ = 89.1 kN (see scheme 2, sect D)
- **Section E ($x_E = 2300$, M^+):** (see scheme 2 sect E)
 - $V_{Rd} f \geq V_{Sd}$ = 68.6 kN (see scheme 2 sect E)
- **Section M ($x_M = 5530$):** (see scheme 2, sect M)
 - $M^+_{Rd} \geq M^+_{Sd}$ = 205.8 kNm (see scheme 2, sect M)

b) Hollow core unit cross section and characteristics

- **Cross section (Sect E,C,M)**



Prestressing reinforcement

Upper	No 6 str. 3φ3 mm	Fs 127.2 mm ²	No 2 str 3/8" + 1 str 3φ3	Fs 125 mm ²
Lower	No 8 str. 0.5"	Fi 744 mm ²	No 8 str 0.5"	Fi 744 mm ²

Tot = 871 mm²

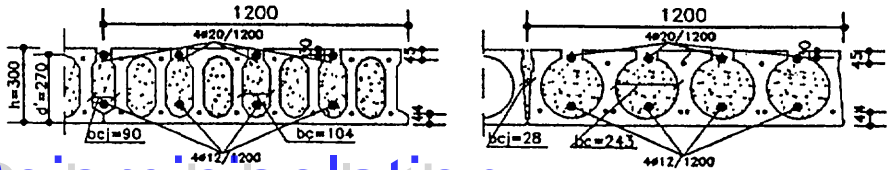
Tot = 869 mm²

Section properties

A(cm ²)/I(cm ⁴)/S(cm ³)	1820/205260/9000	1730/195830/8720
b _w /b'/e(mm)	380/455/73	200/223/73

- **Cross sections at slab end (Sect D)**

Cracked section and subject to negative moment



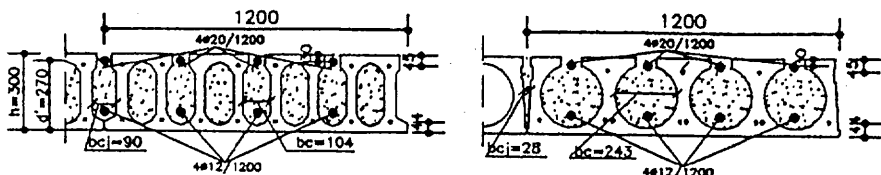
Hollow-core type I				Hollow-core type II	
Prestressing reinforcement					
Upper	No 6 str. 3φ3 mm	F _s 127.2 mm ²	No 2 str 3/8" + 1 str 3φ3	F _s 125 mm ²	
Lower	No 8 str. 0.5"	F _i 744 mm ²	No 8 str 0.5"		F _i 744 mm ²
Tot = 871 mm ²				Tot = 869 mm ²	

Section properties

I' (cm)/b' _w (mm)	217 920/715	210890/1033
A _s max/ΣA _s upper (mm ²)	314 (φ20)/1256	314/(φ20)/1256
d (under M ⁻) (mm)	255	255

- Cross section at slab end
(Sect A')**

Cracked section
and subject to
negative moment

**Section properties**
(composite member side)

d'(under M ⁻)/b' _w (mm)	270/1061	270/1033
A _s max/ΣA _s upper (mm ²)	314(φ20)/1256	314(φ20)/1256
A _s max/ΣA _s lower (mm ²)	113(φ12)/452	113(φ12)/452
S _c /l _s /h _c (mm)	600/2300/200	600/2300/200

Section properties
(support side, cast-in situ concrete)

d''(under M ⁻)/Σb _c (mm)	230/820	230/1000
A _s max/ΣA _s upper (mm ²)	314(φ20)/1256	314(φ20)/1256
A _s max/ΣA _s lower (mm ²)	113(φ12)/452	113(φ12)/452

c) Calculations

- Section A':** (M_{sd} = 108 kNm, f_{sd} = 444.4 kN, τ'_{sd} = 0.08 N/mm², V_{sd} = 110.6 kN (x_A = 250) τ_{sdj} = 0.27 N/mm² σ_{l,d} = 1.18 N/mm² for type I, σ_{l,d} = 1.93 N/mm² for type II)

● <u>V'_{Rd1}</u> (Hollow core slab side (kN) see same procedure of sect B, scheme 2)		
= 0.25f _{ctd} b' _w d'k(1.2+40ρ' ₁)		<u>168.7</u>
● <u>M'_{Rd}</u> (ε _s = 1%)	kN	<u>138.6</u>
● <u>f_{ld}</u> (same procedure of sect A, scheme 2)	kN	<u>546</u>

		Hollow-core type I	Hollow-core type II
● τ'_{Rd}	(N/mm ²)	0.1	0.1
● V''_{RdI} (Support side) =	(kN)	113.5	134.2
$= 0.25f'ctd \sum bcd''k(1.2+40\rho'1)$		$0.25*1.2*230*820*1.37*$ 1000 $*(1.2+40*0.0066)=113.5$ $1256/820*230=0.00666$	$0.25*1.2*1000*230*1.37*$ 1000 $*(1.2+40*0.0053)=134.2$ $1256/1000*230=0.0053$
$\rho' = \sum A_s / \sum b_c d''$		1.37	1.37
$k = 1.6 - 0.23$			
● f_{ctd}	(N/mm ²)	$1.8 > \sigma I, d = 1.18$	$1.8 < \sigma I, d = 1.93$
		Acceptable	<u>Not acceptable</u>
$q_d \text{max when } S=R$ (kN/m)		≈ 21 kN/m without specific shear reinforcement of in situ concrete; ≈ 29 kN/m as per scheme 2 with additional in-situ reinforcement (about 1.0 Kg/m ² in addition)	≈ 18 kN/m due to limited positive bending capacity with reduction in prestressing strand (only one 1/2" strand per web)
● Section C,D,E,M:	same calculations and considerations as scheme 2		

d) Conclusions

The same values of load capacity, as per scheme 2, are applicable for hollow-core type I with its larger total web width. Hollow-core type II is limited, by spalling and shear stresses, to approx 90% of the required design capacity

For hollow-core type I, with a small increase of upper reinforcement (only 0.4 Kg/m² in addition), the load capacity could be increased to $q_d = 30$ kN/m, governed by positive bending moment resistance.

The quantities of additional in-situ concrete and reinforcement and possible saving in prestressing reinforcement for a tight design without any margin, are as follow for both types:

- In situ concrete	(m ³ /m ²)	0.042	0.045
- Additional reinforcement	(Kg/m ²)	2.5	2.5
- Possible saving in prestressing reinf.	(Kg/m ²)	1.6	1.9 (with load capacity limited to 91% of the specified one)
- Elastic deflection due to variable load (6.00 kN/m ²)	(mm)	<<< 4.9(*)	<<< 4.9(*)

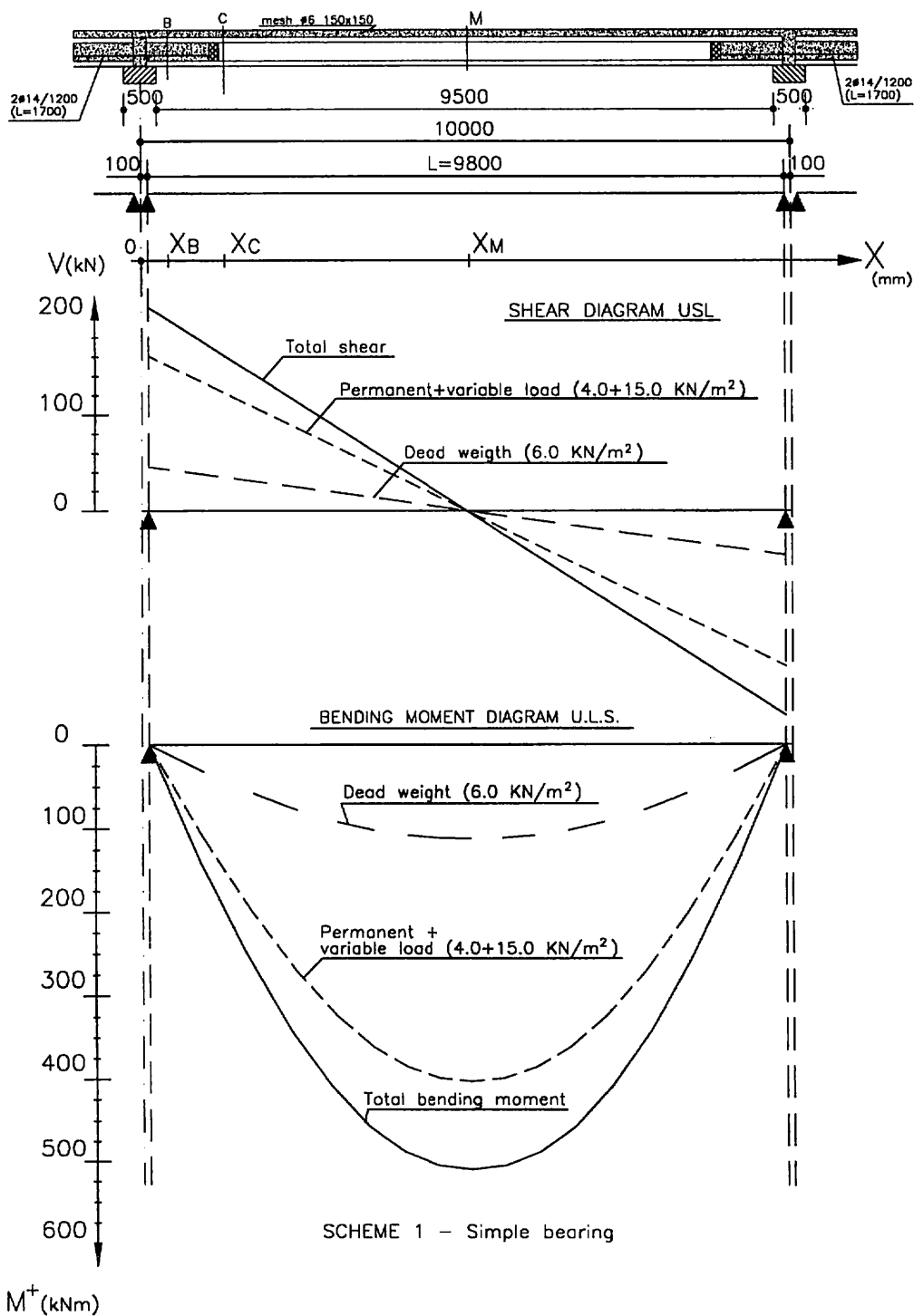
(*) taking into account partial restraint at 2° support also.



3 Example 2 - Multispan floor

3.1 Simply supported slabs with direct (normal) bearings

- a) Design actions and sections to be checked



- **Section A ($x_A=250$):** No need to be checked
- **Section B ($x_B=250+d/2=453$):** Uncracked section, close to support where shear tension capacity and interface shear strength should be checked.
- $\underline{V'_{Rd}} \geq V_{Sd} = 43.2 \frac{(5000-453)}{1000} = 196.4 \text{ kN}$
- $\underline{\tau_{Rdj}} \geq \tau_{Sdj} = f_{Sd}/\sum S_c l_s + V_{Sd}/0.9d' \sum S_c = 0 + 0.19 = 0.19 \text{ N/mm}^2$
 $f_{Sd}=0$
 $\sum S_c = 1200 + 2*800 = 2800 \text{ mm}$
- **Section C ($x_C=978$):** First cracked section where shear flexural capacity has to be checked
- $\underline{V'_{Rd}} \geq V_{Sd} = 43.2 \frac{5000-1084}{1000} = 169.2 \text{ kN}$

$$q_d L/2x - q_d x^2/2 = f_{ctd} I'/x_{n'n'} + M_p \text{ (equation to be solved for } x_c \text{ calculation)}$$

$$x_c = x_o + q_d L/2 - \sqrt{(q_d L/2)^2 - 2q_d (M_p + f_{ctd} I'/x_{n'n'})}$$

$$M_p = \gamma_p \text{ e } \sigma_{p,\infty} A_p = 0.9 * 105 * 1100 * 1099.6 * 10^{-6} = 114.3 \text{ kNm}$$

$$x_o = 100 \text{ mm} \quad L = 9800 \text{ mm} \quad qdL/2 = 211.7 \text{ kN}$$

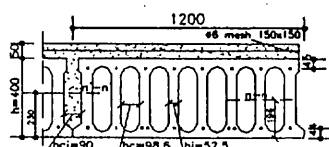
$$x_c = 100 + \frac{211.7 - \sqrt{211.7^2 - 2 * 43.2 (114.3 + 1.8 * 702540 * 10^{-2} / 230)}}{43.2 * 10^{-3}} = 978 \text{ mm}$$

- **Section D:** No need to be checked
- **Section E:** No need to be checked
- **Section M ($x_M=5000$):** Where positive bending capacity should be checked
- $\underline{M_{Rd}^+} \geq M_{Sd}^- = 43.2 * 9.8^2 / 8 = 518.6 \text{ kNm}$

b) Hollow-core unit cross section and characteristics

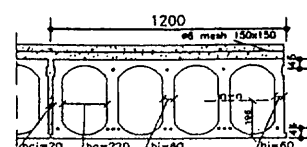
- **Cross section**
(Sect C,M)

Hollow-core type I



Cracked sections,
and subject to
positive moment

Hollow-core type II



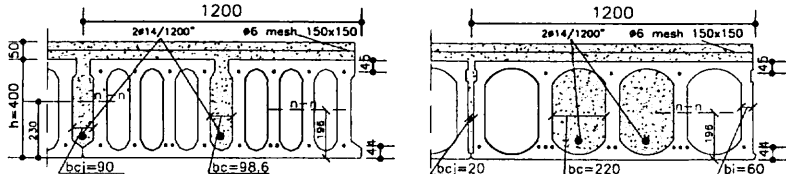
Hollow core type I			Hollow core type II	
<u>Prestressing reinforcement</u>				
Upper	No 8 str. 3φ3 mm	Fs 169.6 mm ²		No 3 str 3/8" Fs 156 mm ²
Lower	No 10 str. 0.5"	Fi 930 mm ²		No 10 str 0.5" Fi 930 mm ²
		Tot = 1099.6 mm ²		Tot = 1086 mm ²

Section properties

A(cm ²)/I(cm ⁴)/S(cm ³)	2450/463600/15110	2200/452090/14600
b _w /b' _w /e/d'(mm)	420/495/105/406	300/317/105/406
A'(cm ²)/I'(cm ⁴)/S'(cm ³)	3175/702540/20700	2750/673.000/20060
n-n/n'-n' (mm)	196/230	196/230

- Cross section at slab end
(Sect A,B)

Uncracked sections,
and subject to
positive moment

Section properties

I'(cm ⁴)/S'(cm ³)	717.940/21620	755500/25090
b' _w /d' (mm)	576/406	683/406
b _c /b _{ci} /h _c (mm)	98.6/90/300	220/20/300
Support length a (mm)	140	140

c) Calculations

- Section B: (V_{Sd}=196.4 kN, τ_{Sdj}=0.19 N/mm², M⁺)
(x_B=453)

Shear tension capacity of
hollow-core slab itself

$$V_{Rdt} = \frac{S}{I} b_w \sqrt{f_{ctd}^2 + \alpha \sigma_{cpm} f_{ctd}} (kN) \quad 320.9 \quad 236.9$$

$$\alpha = l_x / l_{bpd} = a + (x_B - x_C) / l_{bpd} = \frac{140 + 203}{1.2 * 70 * 10.9} = 0.375 \quad 0.375$$

$$1.2 * 70 * 10.9$$

$$\sigma_{cpm} = \gamma_p \sigma_{p,\infty} A_p / A \quad (\text{N/mm}^2) \quad \frac{0.9 * 1100 * 1099.6}{2450 * 10^2} = 4.44 \quad \frac{0.9 * 1100 * 1086}{2200 * 10^2} = 4.89$$

Shear tension capacity with
50 mm topping

$$\bar{V}_{Rdt} = V_{Rdt} \frac{S}{I} \frac{I'}{S} + V_{Sdg} \left(1 - \frac{S}{S'} \frac{I'}{I} \right) \geq V_{Rdf}$$

@Seismicisolation

Hollow core type I	Hollow core type II
$320.9 * 1.082 + 44.2$ $(1-1.082) = 343.6$	$236.9 * 0.972 + 44.2$ $(1-0.972) = 231.5 \rightarrow 236.9$

$$V_{Sdg} = \frac{1.2 * 6.00 * 1.35 * (5000 - 453)}{1000} = 44.2 \text{ (kN)}$$

V_{Sdq} max due to in-situ concrete failure is such that

$$\tau'_{sd} = \frac{V_{Sdq} * S'}{b'_w l' E_p / E_c} = f'_{ct} = 1.2 \text{ N/mm}^2$$

$$V_{Sdq} = \frac{f'_{ctd} b'_w l' E_p}{S E_c} \quad (\text{kN}) \quad 275.4 \quad 296.2$$

V_{Sdq} max due to precast concrete failure is such that

$$\tau_{sd} = \frac{V_{Sdg} * S'}{b_w l} + \frac{V_{Sdq} * S'}{b'_w l'} = \tau_{Rd} =$$

$$\sqrt{f'_{ctd}^2 + \alpha \sigma_{cpm} f_{ctd}} \quad (\text{N/mm}^2) \quad 2.49 \quad 2.55$$

$$\tau_G = \frac{V_{sdg} * S}{b_w l} = \quad (\text{N/mm}^2) \quad \underline{44200 * 15110} = 0.35 \quad \underline{44200 * 14600} = 0.48$$

$$420 * 463600 * 10 \quad 300 * 452090 * 10$$

$$V_{Sdq} = (\tau_{Rd} - \tau_G) b'_w \frac{l}{S} \quad (\text{kN}) \quad \underline{(2.49 - 0.35) 576 * 717940 * 10} \quad \underline{(2.55 - 0.48) 683 * 755500 * 10}$$

$$21620 * 1000 \quad 25090 * 1000$$

$$= 409.3 \quad = 425.7$$

Since V_{Sdq} is limited by in-situ concrete failure, the shear tension capacity of the composite section has to be evaluated as follows, but can never be lower than V_{Rdt} of the hollow-core itself.

- $\overline{V'_{Rdt}} = V_{Sdg} + V_{Sdq} \min \geq V_{Rdt} \quad (\text{kN}) \quad 44.2 + 275.4 \quad 44.2 + 296.2 =$
- $\underline{\underline{\tau_{Rdj}}} = k_t * \tau'_{Rd} = 1.4 * 0.3 \quad \text{N/mm}^2 \quad \underline{\underline{0.42}} \quad \underline{\underline{0.42}}$

$$q_d \text{ max when } V'_{Rdt} = V_{Sd} \quad (\text{kN/m}) \quad 75.4 \quad 74.8$$

- Section C ($V_{Sd} = 169.2 \text{ kN}$, M^+)
($x_C = 978 \text{ mm}$)

- $\overline{V'_{Rdf}} = 0.25 f_{ctd} b'_w d' k' (1.2 + 40 \rho'_1) +$
 $+ 0.15 \sigma_{cpm} b_w d' \quad (\text{kN}) \quad 149.6 + 106.7 = \underline{283.3} \quad 102.9 + 84.9 = \underline{197.1}$
- $k' = 1.6 - d' \quad (\text{m}) \quad 1.194 \quad 1.194$

	Hollow core type I	Hollow core type II
$\rho'_1 = A_p/b'_w d'$	$930/495*406=0.00463$	$930/317*406=0.00722$
$\sigma_{cpm} = \sigma_{p,\infty} A_p/A$	(N/mm ²)	4.44
q_d max when $R = S$	(kN/m)	72.3
- Section M ($M^+_{sd}=518.6$ kNm): ($x_M=5000$)		
● M^+_{Rd} ($\epsilon_s=1\%$)	(kNm)	<u>548</u>
q_d max when $M^+_{Rd}=M^+_{sd}$	(kN/m)	45.6
Max deflection at SLS under variable load Q	$f=\frac{5}{384} Q L^4/EI$ (mm)	8.6
		8.6

d) Conclusions

The load capacity is governed by moment resistance and q_d max=45.6 kN/m for both hollow-core types.

The quantities of additional in-situ concrete and reinforcement and possible saving in prestressing reinforcement for a tight design without any margin, are as follow for both types:

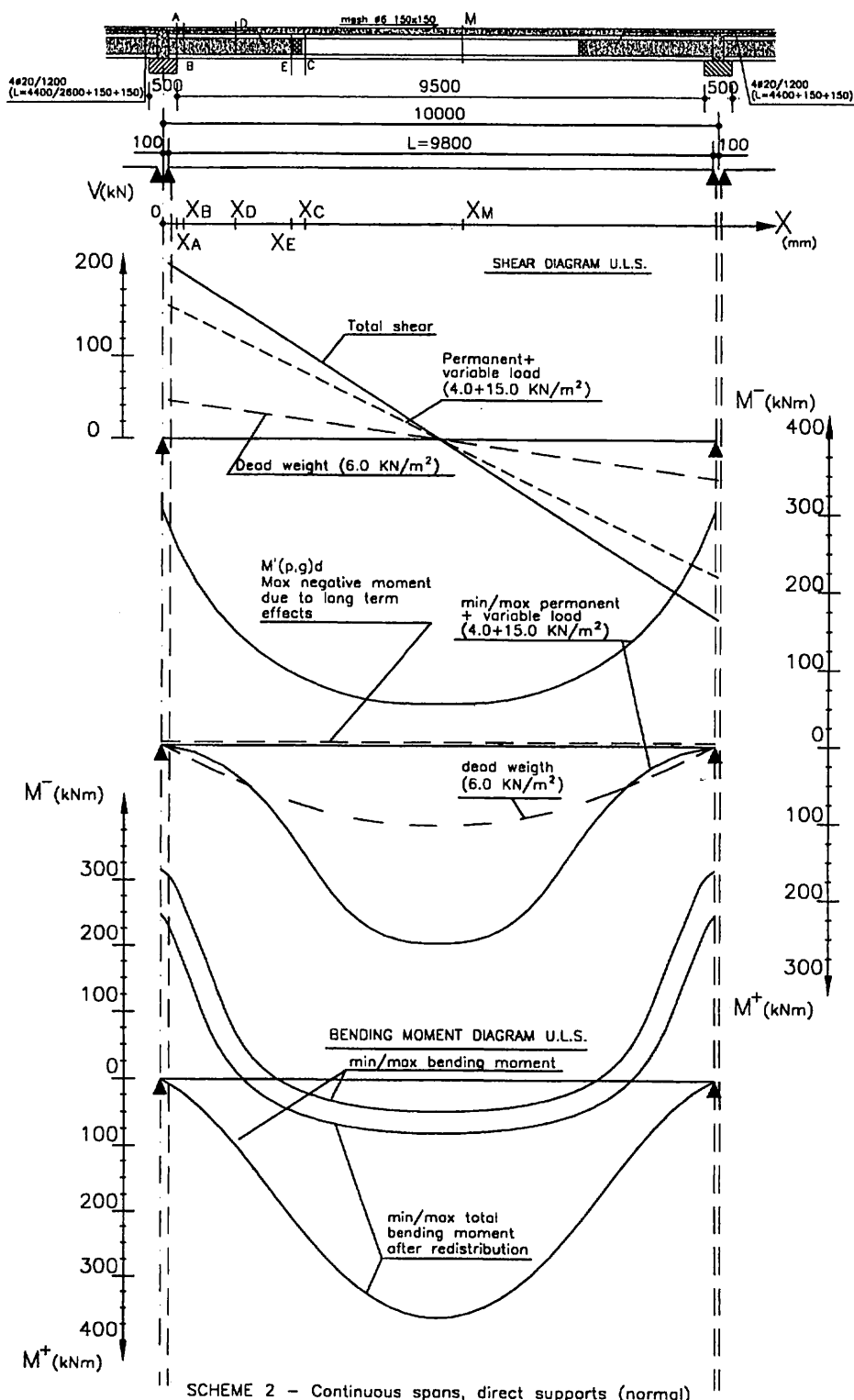
In-situ concrete: 0.058 m³/m² Additional reinforcement: 0.4 Kg/m²

Possible saving in prestressing reinforcement (without upper prestressing and minimizing lower prestressing): 1.4 Kg/m²

Elastic deflection due to variable load 15.00 kN/m² is 9 mm approx. for both hollow-core types.

3.2 Slabs continuous at internal supports with direct (normal) bearings

a) Design actions and sections to be checked



- **Section A ($x_A = 250$, M^-):** Where bending capacity under negative moment and anchorage reinforcement should be checked

- $M_{Rd} \geq M_{Sd}$ $= M_{Sdq} + M'_{(p,G)}d = 239.7 + 7.4 = \underline{247.1} \text{ kNm}$
 M_{Sdq} $= 239.7 \text{ kNm}$ from bending moment diagram with redistribution

- $M'_{(p,G)}d$ $= \frac{(M_p - 2 M_s) \underline{\varphi(\infty, t_0)}}{3} - \frac{M_s}{1 + \rho \varphi(\infty, t_0)} \frac{1}{1 + \rho \varphi(\infty, t_0)}$ long term
 effect of the restrained

support due to prestressing and permanent loads ($\Sigma G_i = G = 6.0 \text{ kN/m}^2$) with appropriate partial safety factor ($\gamma_p = 0.9$ or 1.2 and $\gamma_G = 1.35$ or 1.0), to be neglected if positive

$$(1.2 * 135.6 - 1.0 * \underline{2} * 86.4) \frac{0.625}{3} - 70.2 * 0.5 = 30.6 \text{ kNm}$$

(max pos. value)

- $M'_{(p,G)}d$ $= (0.9 * 135.6 - 1.35 * \underline{2} * 86.4) \frac{0.625}{3} - 70.2 * 0.5 = -7.4 \text{ kNm}$
 (max neg. value)

- M_p $= \gamma_p e [P_o - (P_o - P_\infty) \alpha t_o] = 105 * 1099 [1250 - (1250 - 1100) * 0.5] \gamma_p * 10^{-6} = 135.6 * \gamma_p \text{ kNm}$

- M_G $= \gamma_G \Sigma G_i L^2 / 8 = \gamma_G 6.0 * 1.2 * 9.8^2 / 8 = 86.4 * \gamma_G \text{ kNm}$
 $\underline{\varphi(\infty, t_0)}$ $= \frac{0.5 * 2.5}{1 + 0.8 * 0.5 * 2.5} = 0.625$
 M_s $= \epsilon_s(\infty, t_o) A_c E_c \Delta X_{mn} = 0.0002 * 50 * 1200 * 30 * \frac{(425 - 230)}{1000} = 70.2 \text{ kNm}$

- $\frac{1}{1 + \rho \varphi(\infty, t_0)}$ $= 0.5$

- V_{Sd} $= 205.2 \text{ kNm}$ from shear diagram

- $f_{ld} \geq f_{Sd}$ $= f_{Sd}(M_{Sd}) + f_{Sd}(\Delta F'_s) = 634 + 0 = \underline{634} \text{ kN}$

- $f_{Sd}(M_{Sd})$ $\approx M_{Sd} / 0.9 d' = 239700 / 0.9 * 420 = 634 \text{ kN}$
 $f_{Sd}(\Delta F'_s)$ $= 0$ assuming no restraint due to slab shortening

- **Section B ($x_B = 250 + d/2 = 453$, M^-):** The flexural capacity of the composite member under negative moment, and the interface shear strength should be checked

- $\overline{V'}_{Rd1} \geq V_{Sd}$ $= \underline{196.4} \text{ kN}$ from shear diagram

- $\tau'_{Rdj} \geq \tau''_{Sd}$ $= \tau'_{Sd} (f_{Sd}) + \tau''_{Sd} (V_{Sd}) = 0.063 + 0.118 = \underline{0.181} \text{ N/mm}^2$
 τ'_{Sd} $= f_{Sd} / \sum S_c l_s = 634000 / 4400 * 2300 = 0.063 \text{ N/mm}^2$
 τ''_{Sd} $= V_{Sd} / 0.9 d' \sum S_c = 196400 / 0.9 * 420 * 4400 = 0.118 \text{ N/mm}^2$
 $\sum S_c$ $= 800 + 4 * 1200 = 4400 \text{ mm}$

- **Section C ($x_c = 250 + \Delta x_a = 3095$, M^+):** First cracked section, under positive bending moment where shear flexural capacity and anchorage failure of prestressing steel should be checked:

- $\overline{V}'_{Rd} \geq V_{Sd} = 82.3 \text{ kN}$ from shear diagram at $x = 3095$

$$\begin{aligned}\Delta x_A &= \frac{V_{SdA} - \sqrt{V_{SdA}^2 - 2q_d(M_{SdA} + M_p + f_{ctd} I' / x'_{nn})}}{q_d} = \\ &= \frac{205.2 - \sqrt{205.2^2 - 2 * 43.2(239.7 + 114.3 + 1.8 * 702540 * 10^2 / 230)}}{43.2 * 10^3} = 2845 \text{ mm}\end{aligned}$$

$$\begin{aligned}M_p &= \gamma_p * e \sigma_p, \infty A_p = 0.9 * 1100 * 1099.6 * 105 * 10^6 = 114.3 \text{ kNm} \\ V_{SdA} &= 205.2 \text{ kN} \quad \text{from shear diagram}\end{aligned}$$

- $F_p \geq T_d = M^+_{Sd}/z + V_{Sd} \cot\theta = 959 + 83.2 = 1041.3 \text{ kN}$

$$\begin{aligned}M^+_{Sd} &= 350 \text{ kNm from bending moment diagram with redistribution} \\ z &= 0.9 d' = 0.9 * 0.406 = 0.365\end{aligned}$$

- **Section D ($x_D = 1300$, M^-):** Limit of in-situ reinforcement anchorage in the zone of negative moment. The flexural tension shear capacity under negative moment and anchorage failure of upper prestressing steel should be checked at this section.

- $\overline{M}'_{Rd} \geq M_{Sd}$ $= M_{Sdq,G} + M'_{(p,G)d} = 19.7 + 7.4 = 27.1 \text{ kNm}$
 $M_{Sdq,G}$ $= 19.7 \text{ kNm from bending moment diagram with redistribution}$
 $M'_{(p,G)d}$ $= 7.4 \text{ kNm}$

- $\overline{V}'_{Rd} \geq V_{Sd} = 159.8 \text{ kN}$ from shear diagram

- $F_{p,D} \geq T_{d,D} = M_{Sd,D}/z + V_{Sd,D} \cot\theta = 19.7 / 0.319 + 159.8 = 221.5 \text{ kN}$
 $z = 0.9d = 0.9 * 355 = 319 \text{ mm}$

without taking into account contribution of 6 mm mesh 150x150

- **Section E ($x_E = 2300$, M^+):** Limit of in-situ filling of concrete in the cores where flexural/tension capacity of hollow-core slab should be checked.

- $\overline{V}'_{Rd} \geq V_{Sd} = 116.6 \text{ kN}$ from shear diagram

- **Section M ($x_M = 5000$, M^+):** Where positive bending capacity should be checked

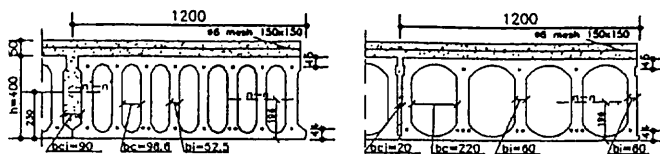
- $\overline{M}'_{Rd} \geq M^+_{Sd} = M^+_{Sdq,G} + M'_{(p,G)d} = 370.0.0 + 31 = 401 \text{ kNm}$
 $M^+_{Sdq,G}$ $= 370 \text{ kN from bending moment diagram with redistribution}$
 $M'_{(p,G)d}$ $= (1.2 * 135.6 - 1.0 * 86.4 * 2) * 0.625 - 70.2 * 0.5 = 31 \text{ kNm}$

b) Hollow core unit cross section and characteristics

- Cross sections
(Sect E,C,M)

Hollow core type I Hollow core type II

Cracked sections
and subject to
positive moment



Prestressing reinforcement

Upper	No 8 str. 3φ3 mm	Fs 169.6 mm ²	No 3 str 3/8"	Fs 156 mm ²
Lower	No 10 str. 0.5"	Fi 930 mm ²	No 10 str 0.5"	Fi 930 mm ²

Tot = 1099.6 mm²

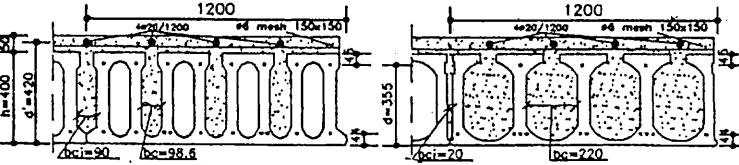
Tot = 1096 mm²

Section properties

A(cm ²)/I(cm ⁴)/S (cm ³)	2450/463600/15100	2200/452090/14600
b _w /b' _w /e/d' (mm)	420/495/105/406	300/317/105/406
A' (cm ²)/I' (cm ⁴)/S' (cm ³)	3175/702540/20700	2750/673000/20060
n-n/n'-n' (mm)	196/230	196/230

- Cross section at slab end
(Sect A,B,D)

Cracked sections
and subject to
negative moment



Prestressing reinforcement

Upper	No 8 str. 3φ3 mm	Fs 169.6 mm ²	No 3 str 3/8"	Fs 156 mm ²
Lower	No 10 str. 0.5"	Fi 930 mm ²	No 10 str 0.5"	Fi 930 mm ²

Tot = 1099.6 mm²

Tot = 1086 mm²

Section properties

b' _w (mm)	741	1050
Asmax/ΣAs(mm ²)	314(φ20)/1482	314(φ20)/1482
d'(Sect A,B)/d(Sect D) (mm)	420/355	420/355
ΣSc/ls/hc (mm)	4400/2300/300	4400/2300/300

c) Calculations

- Section A ($M_{su} = 247.1 \text{ kNm}$, $f_{sd} = 634 \text{ kN}$)
($x_A = 250$)

- M_{Rd} ($\epsilon_s = 1\%$) (kNm) 258.4 258.4

		Hollow core type I	Hollow core type II
●	$f_{td} = \sum A_s f_y / \gamma_s$ (kN)	$\frac{1482*500/1.15}{1000} = 644$	<u>644</u>
	q_d max when $S=R$ (kN/m)	43.9	43.9
-	Section B: ($V_{sd}=196.4$ kN, $\tau_{sdj}=0.181$ N/mm ² , M^+) ($x_B=453$)		
●	$\underline{V'_{Rd1}} = 0.25 f_{ctd} b'_w d' k'^*$ $*(1.2+40\rho'_1) \geq V_{Rd2}$ (kN)	$0.25*1.8*741*420*1.18*$ $*(1.2+40*0.0047) = 229.8$ 1000	$0.25*1.8*1050*420*1.18*$ $*(1.2+40*0.0033) = 312.8$ 1000
	$\bar{k}' = 1.6-d'$ (m)	1.18	1.18
	$\varphi'_1 = \sum A_s / b'_w d'$ (m)	$1482/741*420 = 0.00476$	0.00336
	$V_{Rd2} = 1/2 v f_{cd} b'_w 0.9 d'$ (kN)	$\underline{1} 0.5*45 741*0.9*$ 2 1.5 $*420/1000 = 2100$	
	$v = 0.7-f_{ck}/200 \geq 0.5$	$0.7-45/200 = 0.475 \rightarrow 0.5$	2975 0.5
●	$\underline{\tau_{Rdj}} = K_t \tau'_{Rd}$ (N/mm ²) q_d max when $S=R$	$1.4*0.3 = 0.42$ 50.5	<u>0.42</u> 68.7
-	Section C: ($V_{sd}=82.3$ kN, $T_d=1041.3$ kN, M^+) ($x_c=3095$)		
●	$\underline{V'_{Rdf}} = 0.25 f_{ctd} b'_w d' K^*$ (kN) $*(1.2+40\rho'_1)+0.15^*$ $*\sigma_{cpm} b'_w d' \leq V_{Rd2}$	$149.5+133.8 = 283.3$	$102.9+94.2 = 197.1$
	$k = 1.6-d'$ (m)	1.194	1.194
	$\rho'_1 = \sum A_p / b'_w d'$	$930/495*406 = 0.0046$	$930/317*406 = 0.072$
	$V_{Rd2} = 1/2 v f_{cd} b'_w 0.9 d'$ (kN)	786	385
	$v = 0.7-f_{ck}/200 \geq 0.5$	$0.7-45/200 = 0.475 \rightarrow 0.5$	0.5
	$\sigma_{cpm} = \sigma_\infty A_p / A$	$0.9*1100*1099 = 4.44$ $2450*10^2$	$0.9*1100*1086 = 4.88$ $2200*10^2$
●	$F_p = P_o x / l_{bpd} \leq A_p f_{p0.1} k / \gamma_s$ $P_o x / l_{bpd}$ (kN)	$\underline{1350}$ 1350 * 930 * (2890-160) = 3746 1000 915	$\underline{1350}$ 3746
	$l_{bpd} = 1.2*70*\phi$	1.2*70*10.9 = 915	
	$A_p f_{p0.1} k / \gamma_s$ (kN)	$\underline{930}$ * 1670 / 1.15 = <u>1350</u> 1000	<u>1350</u>
	q_d max when $S=R$ (kN/m)	56.0	56.0
-	Section D: ($M_{sd}=27.1$ kNm, $V_{sd}=159.8$ kN, $T_d=221.5$ kN) ($x_D=1300$)		
●	$\underline{M_{Rd}}$ ($\epsilon_s = 1\%$) (kNm)	<u>92.5</u>	<u>85.1</u>

	Hollow core type I	Hollow core type II
• $\underline{V}'_{Rdf} = 0.25 f_{ctd} b'_{w} dk^*$ *(1.2+40 ρ'_1)+ $+0.15 \sigma_{cpm} b_w d$ $k=1.6-d$ $\rho_1 = \sum A_p sup/b'_{w} d$ σ_{cpm}	(kN) 177.6+99.3= <u>276.9</u> (m) 1.345 $169.6/741*355=0.00064$ 4.44	254.1+77.9= <u>332</u> 1.345 $156/1050*355=0.00042$ 4.88
• $F_p = P_o x / l_{bpd} \leq A_p f_{p0,1} k / \gamma_s$ (kN)	<u>246.3</u>	<u>226.5</u>
$P_o x / l_{bpd}$	<u>1350</u> *890*169.6 1000 $/1.2*70*5.2=466$	<u>1350</u> *890*156 1000 $/1.2*70*8.1=275$
$A_p f_{p0,1} k / \gamma_s$	(kN) <u>169.6</u> *1670/1.15=246.3 1000	226.5
q_d max when $S=R$	(kN/m) 48.0	44.2
- Section E ($V_{sd}=116.6$ kN, M^+) ($x_E=2300$)		
• $\underline{V}'_{Rdf} =$ (as per sect C) (kN)	<u>149.5</u> +133.8= <u>283.3</u>	<u>102.9</u> +94.2= <u>197.1</u>
q_d max when $S=R$	(kN/M) 104.9	73.0
- Section M ($M^+_{sd}=401$ kNm) ($x_M=5000$)		
• M^+_{Rd} ($\varepsilon_s=1\%$)	(kN/m) <u>548</u>	<u>548</u>
q_d max when $S=R$	(kN/m) 59	59
Max deflection at SLS under variable load Q		
$f = \frac{1}{384} Q 1.2 L^4 / EI$	(mm) 1.7	1.7

d) Conclusions

The load capacity is governed by in-situ reinforcement area and length in section A with $q_{dmax}=44$ kN/m for both hollow core types.

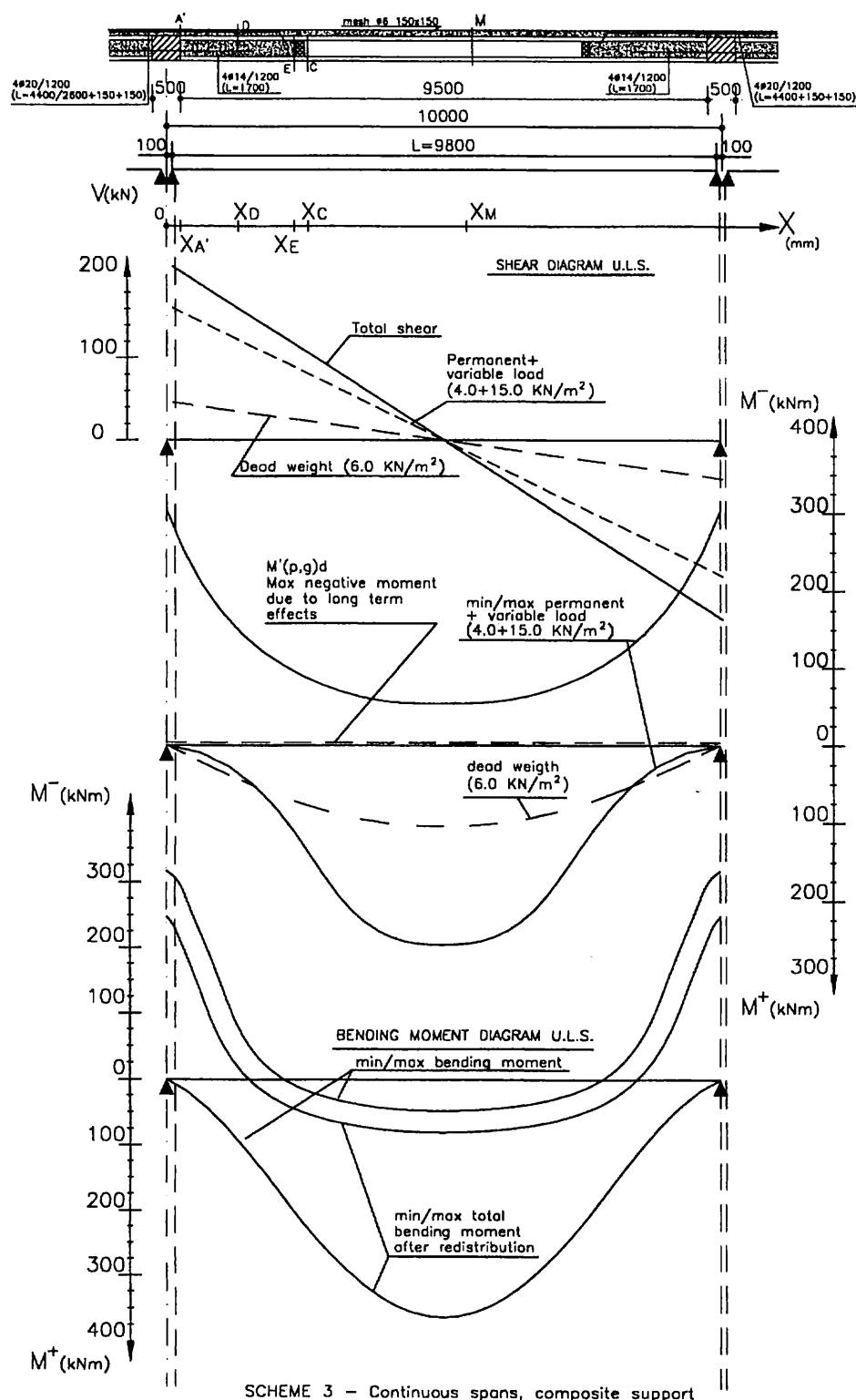
With a small increase of upper reinforcement (only 1.0 Kg/m²), the load capacity could be increased to $q_d = 59$ kN/m, governed by positive bending moment resistance.

The quantities of additional in-situ concrete and reinforcement and possible saving in prestressing reinforcement for a tight design without any margin, are as follow for both types:

		Hollow core type I	Hollow core type II
- In situ concrete	(m ³ /m ²)	0.086	0.095
- Additional reinforcement	(Kg/m ²)	3.9+φ6 mesh	3.9+φ6 mesh
- Possible saving in prestressing reinf.	(Kg/m ²)	1.5	1.5
- Elastic deflection due to variable load (15.0 kN/m ²)	(mm)	1.7	1.7

3.3 Slab restrained at all supports and without direct (normal) bearings

- a) Design actions and sections to be checked



- **Section A'** ($x_{A'} = 250$, M'): Where in addition to the design calculations as per scheme 2, sect A, shear capacity at the slab end section, at both member and support sides the shear and spalling stress as should also be checked.

	Hollow core type I	Hollow core type II
• $M'_{Rd} \geq M'_{Sd}$	$= 247.1 \text{ kN/m}$	(see scheme 2, sect A)
• $f_{ld} \geq f_{Sd}$	$= 634 \text{ kN/m}$	(see scheme 2, sect A)
• $V'_{Rd1} (\text{member and support side}) \geq V_{Sd} = 205.2 \text{ kN}$	from shear diagram	
• $\tau'_{Rdj} \geq \tau'_{Sd}$	$= \tau'_{Sd} + \tau''_{Sd} = 0.123 + 0.063 = 0.186 \text{ N/mm}^2$	
τ'_{Sd}	$= f_{Sd} / \sum S_c l_s = 634000 / 4400 * 2300 = 0.063 \text{ N/mm}^2$	
τ''_{Sd}	$= V_{Sd} / 0.9 d' \sum S_c = 205200 / 0.9 * 420 * 4400 = 0.123$	
	$= 2.74 \text{ N/mm}^2$ (Hollow core type I)	
• $f_{cid} \geq \sigma_{I,d} =$	$= 3.47 \text{ N/mm}^2$ (Hollow core type II)	

$$\sigma_{I,d} = \text{principal tensile stress} = \frac{\sigma_{Spi,d(t)} + \tau_{Sd} \cos 2\beta + \sqrt{(\tau_{Sd} \sin 2\beta)^2 + (\sigma_{Spi,d(t)} + \tau_{Sd} \cos 2\beta)^2}}{2} =$$

$$1.35 + 1.39 = 2.74 \text{ N/mm}^2 \text{ (Hollow core Type I)}$$

$$=$$

$$1.72 + 1.75 = 3.47 \text{ N/mm}^2 \text{ (Hollow core type II)}$$

since $2\beta = 45^\circ$ $\sin 2\beta = \cos 2\beta = 0.7$

$$\tau_{Sd} \sin 2\beta = \tau_{Sd} \cos 2\beta = 0.7 V_{Sd} / 0.9 d' b' w =$$

$$0.7 * 205200 / 0.9 * 1070 * 420 = 0.7 * 0.507 = 0.35 \text{ N/mm}^2 \text{ (Hollow core type I)}$$

$$=$$

$$0.7 * 205200 / 0.9 * 1050 * 420 = 0.7 * 0.517 = 0.36 \text{ N/mm}^2 \text{ (Hollow core type II)}$$

$$\sigma_{Spi,d(t)} = \text{the design value of spalling stress at time } t = \gamma_p \sigma_{Spi} P_t / P_o =$$

$$1.2 * 2.13 * 1152 / 1250 = 2.35 \text{ N/mm}^2 \text{ (Hollow core type I)}$$

$$=$$

$$1.2 * 2.80 * 1152 / 1250 = 3.09 \text{ N/mm}^2 \text{ (Hollow core type II)}$$

$$\sigma_{Spi} = \text{the spalling stress at detensioning} =$$

$$2.13 \text{ N/mm}^2 \text{ (Hollow core type I)}$$

$$2.80 \text{ N/mm}^2 \text{ (Hollow core type II)}$$

$$P_t = P_o - (P_o - P_\infty) \alpha_t = 1250 - (1250 - 1100) 0.65 = 1152 \text{ MPa}$$

$$\alpha_t = 0.65 \text{ (assuming that design action occurs after 2 months from cast-in situ, that is after 4 months from prestressing release)}$$

- **Section B:** No need to be checked

- **Section C ($x_c = 3095, M^+$):** (see scheme 2, sect C)
- $V'_{Rdf} \geq V_{Sd}$ = 82.3 kN (see scheme 2, sect C)
- $F_p \geq T_d$ = 1041.3 kN (see scheme 2, sect C)

- **Section D ($x_D = 1300, M^+$):** (see scheme 2, sect D)
- $M'_{Rd} \geq M'_{Sd}$ = 27.1 kNm (see scheme 2, sect D)
- $V'_{Rdf} \geq V_{Sd}$ = 159.8 kN (see scheme 2, sect D)

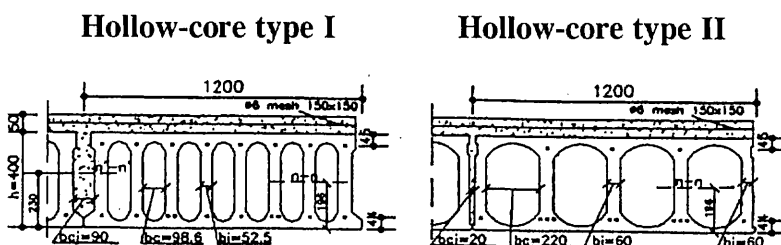
- **Section E ($x_E = 2300, M^+$)** (see scheme 2 sect E)
- $V_{Rdf} \geq V_{Sd}$ = 116.6 kN (see scheme 2 sect E)

- **Section M ($x_M = 5000$)** (see scheme 2, sect M)
- $M^+_{Rd} \geq M^+_{Sd}$ = 401 kNm (see scheme 2, sect M)

b) Hollow core unit cross section and characteristics

- Cross section
(Sect E,C,M)

Cracked sections
and subject to
positive moment



Prestressing reinforcement

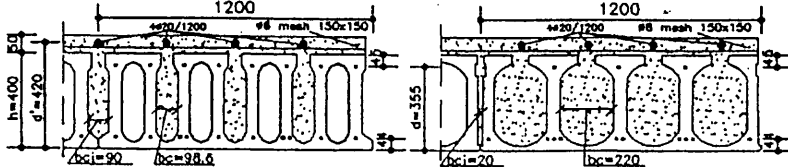
Upper	No 8 str. 3φ3 mm	Fs 169.6 mm ²	No 3 str 3/8"	Fs 156 mm ²
Lower	No 10 str. 0.5"	Fi 930 mm ²	No 10 str 0.5"	Fi 930 mm ²
Tot = 1099.6 mm ²			Tot = 1096 mm ²	

Section properties

A(cm ²)/I(cm ⁴)/S(cm ³)	2450/463600/15100	2200/452090/14600
b _w /b' _w /e(mm)	420/495/105	300/317/105
A' (cm ²)/I(cm ⁴)/S(cm ³)	3175/702540/20700	2750/673000/20060
n-n/n'-n' (mm)	196/230	196/230

- Cross section at slab end
(Sect D)

Cracked section
and subject to
negative moment



Prestressing reinforcement

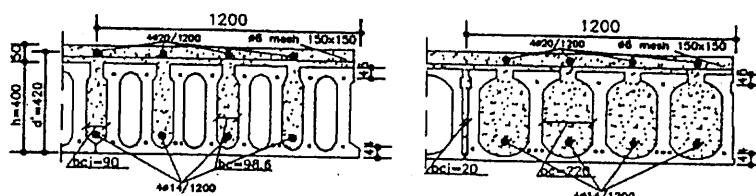
Upper	No 8 str. 3φ3 mm	Fs 169.6 mm ²	No 3 str 3/8"	Fs 156 mm ²
Lower	No 10 str. 0.5"	Fi 930 mm ²	No 10 str 0.5"	Fi 930 mm ²
Tot = 1099.6 mm ²			Tot = 1086 mm ²	

Section properties

b' _w (mm)	741	1050
A _s max/ΣA _s upper (mm ²)	314 (φ20)/1482	314/(φ20)/1482
d (under M') (mm)	355	355

- Cross section at slab end
(Sect A')

Cracked section
and subject to
negative moment



		Hollow-core type I	Hollow-core type II
<u>Section properties</u>			
(composite member side)			
d'(under M')/b' _w		420/1070	420/1050
A _s max/ΣA _s upper	(mm ²)	314(ϕ20)/1182	314(ϕ20)/1482
A _s max/ΣA _s lower	(mm ²)	154(ϕ14)/616	754(ϕ14)/616
S _c /l _s /h _c	(mm)	800/2300/300	800/2300/300
<u>Section properties</u>			
(support side, cast-in situ concrete)			
d"(under M')/Σb _c	(mm)	280/780	380/900
A _s max/ΣA _s upper	(mm ²)	314(ϕ20)/1482	314(ϕ20)/1482
A _s max/ΣA _s lower	(mm ²)	154(ϕ14)/616	113(ϕ14)/616

c) Calculations

- **Section A':** ($M_{sd} = 247.1$ kNm, $f_{sd} = 634$ kN, $V_{sd} = 205.2$ kN
 $(x_A = 250)$ $\tau_{sdj} = 0.19$ N/mm² $\sigma_{l,d} = 2.74$ N/mm² for type I, $\sigma_{l,d} = 3.47$ N/mm² for type II)

- V'_{Rd1} (Hollow core slab side (kN)
see same procedure
of sect B, scheme 2)

$$\begin{array}{lll}
 = 0.25f_{ctd} b' w d' k' (1.2 + 40\rho') & 229.8 & 312.8 \\
 \bullet M'_{Rd} (\varepsilon_s = 1\%) & 258.4 & 258.4 \\
 \bullet f_{ld} (\text{same procedure} \\ \text{of sect A, scheme 2}) & 644 & 644 \\
 \bullet \tau'_{RdG} = k_t \tau'_{Rd} & (N/mm^2) \quad 0.42 & 0.42 \\
 \bullet V''_{Rd1} (\text{Support side}) = & (kN) & \\
 = 0.25f'_{ctd} \sum b c d'' k (1.2 + 40\rho' 1') & 0.25 * 1.2 * 380 * 780 * 1.22 * & 0.25 * 1.2 * 380 * 900 * 1.22 * \\
 & 1000 & 1000 \\
 & *(1.2 + 40 * 0.005) = 151.9 & *(1.2 + 40 * 0.0043) = 171.7 \\
 \rho' = \sum A_s / \sum b c d'' & 1482 / 780 * 380 = 0.005 & 1482 / 900 * 380 = 0.0043
 \end{array}$$

$$k = 1.6 - 0.38$$

$$\begin{array}{lll}
 \bullet f_{ctd} & (N/mm^2) & \\
 & 1.22 & 1.22 \\
 & \text{Not acceptable} & \text{Not acceptable} \\
 & 1.8 < \sigma_{l,d} = 2.74 & 1.8 < \sigma_{l,d} = 3.47 \\
 & \text{Not Acceptable} & \text{Not acceptable}
 \end{array}$$

$$\begin{array}{lll}
 q_d \text{max when } S=R \text{ (kN/m)} & \approx 48 \text{ kN/m with} \\
 & \text{Additional specific shear} \\
 & \text{reinforcement of in situ} \\
 & \text{concrete} \\
 & (\text{about } 1.0 \text{ Kg/m}^2 \text{ in} \\
 & \text{addition}) \text{ and with} \\
 & \text{reduction in prestressing} \\
 & \text{strand (only one } \frac{1}{2} \text{ "} \\
 & \text{strand per each web)} & \approx 30 \text{ kN/m due to limi-} \\
 & \text{ted positive bending} \\
 & \text{capacity with reduction} \\
 & \text{in prestressing strand} \\
 & (\text{only one } \frac{1}{2} \text{ "} \\
 & \text{strand per each web})
 \end{array}$$

- Section C,D,E,M = same calculations and considerations as scheme 2

d) Conclusions

The same values of load capacity, as per scheme 2, are applicable but only for hollow-core type I with its larger total web width. Hollow-core type II is limited, by spalling and shear stresses, to approx 80% of the required design capacity

For hollow-core type I, with a small increase of upper reinforcement (only 1.0 Kg/m² in addition) and reduction in prestressing, the load capacity could be increased to $q_d = 48$ kN/m, governed by positive bending moment resistance.

The quantities of additional in-situ concrete and reinforcement and possible saving in prestressing reinforcement for a tight design without any margin, are as follows for both types:

		Hollow core type I	Hollow core type II
-	In situ concrete	(m ³ /m ²)	0.090
-	Additional reinforcement	(Kg/m ²)	4.6 + $\phi 6$ mesh
-	Possible saving in prestressing reinf.	(Kg/m ²)	2.5
-	Elastic deflection due to variable load (15.0 kN/m ²)	(mm)	1.7
			1.7
			(with load capacity limited to 70% of the specified one)

4 General conclusion

In the following tables the results for each scheme and for the two different hollow-core sections are reported and compared, with reference to the concrete and steel content, to the shear and moment extra capacity, and to the deflection values.

- Summary Table 1 for the Example 1: two span hollow-core slabs.
- Summary Table 2 for the Example 2: multispan hollow-core slabs.

Comparing the Summary Tables it is evident that for both examples and both hollow-core sections the scheme 2 (continuity) requires a larger content of in-situ concrete (+0.015-0.030 m³/m²) and reinforcement (+2.0-3.0 Kg/m²) compared to scheme 1 (simple bearing); but at the same time it shows an extra bending capacity of 20-25% and a consistent reduction of elastic deflection (2-4 times lower).

For hollow-core type 1, scheme 2 shows a lower extra shear capacity (35-60%), but this has to be related to the minimum number of narrow filled cores specified in the examples (3 no. only with $\Sigma b_c \approx 400$ mm. for type 1, 4 no. with $\Sigma b_c \approx 900$ for type 2).

If a larger shear capacity is required, this can be easily obtained by providing one or two more filled cores, with a negligible increase of in-situ concrete.

Comparing the results of type 1 hollow core with those of type 2, it is evident that type 1 allows higher values of shear capacity and negative bending moment since it is possible to utilize a higher number of filled cores with steel reinforcement (it has to be noted that in any core normally it is not allowed to install more than No 1φ20-24 reinforcement bar, due to max interface shear capacity). Furthermore, for the same negative moment, type 1 requires less in-situ concrete and allows a better distribution of in-situ steel reinforcement unless a reinforced topping is specified.

In conclusion it is demonstrated that hollow core with section type 1 is normally more suitable for floors with negative moments or restrained supports.

For scheme 3 (composite non-direct support) with regard to material content, bending capacity and deflection the same considerations as per scheme 2 apply, but, for this structural scheme without any direct support under the precast slab, special attention has to be paid to shear capacity related to the in-situ concrete at support and to suspension capacity limited by spalling stresses.

In fact it is shown by the examples that this structural scheme is not always possible due to limited shear and spalling stresses at support.

For both examples the hollow-core type 1 shows higher capacity (+50% and more) with respect to hollow-core type 2, and this is due to the higher number of precast webs and to the larger web width (+40% and more), from which lower spalling stresses are developed by the same prestressing force.

For both types of hollow-core sections scheme 3 should be adopted only with special attention and after having carefully checked not only the number and distribution of prestressing strands (normally no more than one 0.5" strand in each web), but also the shear resistance of the in-situ concrete at support side which is often the limiting design factor, and the creep and long term effects which may affect the shear capacity of the composite support.

In final conclusion, comparing the results of type 1 hollow core with those of type 2, it can be seen that type 1 allows higher suspension and shear stresses and is normally more suitable for hollow-core floor connection to cast in-situ beams or walls without direct support, taking into account also that the considerations relevant to the negative moment and restraint for scheme 2, apply also for scheme 3.

Hollow-core type 1		SCHEME 1 - Simple Bearing
Hollow-core type 2		SCHEME 2 - Continuous spans, direct support
		SCHEME 3 - Continuous spans, non-direct support
Scheme 2 vs. Scheme 1		
- In-situ contents		
- Concrete:	+0.015-0.030 m ³ /m ²	(lower incidence for H.C. type 1)
- Reinforcement:	+2.0-3.0 Kg/m ²	(for both H.C. types)
- Bending capacity		
	+20-25% extra capacity (for both H.C. types)	(additional +30-50% extra capacity for H.C. type 1 with filled and reinforced cores)
- Deflection		
	1/2-1/4	(for both H.C. types)
- Shear capacity		
	no max capacity reduction due to filled cores	(higher shear values for H.C. type 1)
Scheme 3 vs. Scheme 1		
- In situ incidence		
- Concrete	+0.015-0.030 m ³ /m ²	(lower incidence for H.C. type 1)
- Reinforcement	+2.0-4.0 Kg/m ²	(for both H.C. types)
- Bending capacity		
	+20-25% extra capacity (for both H.C. Types)	(additional +30-50% extra capacity for H.C. type 1 with more reinf. Cores)
- Deflection		
	1/2-1/4 (for both H.C. types)	
- Shear capacity		
(due to spalling stresses)	30-50% reduction of max capacity (for both H.C. types)	(higher shear values +50% and more, for H.C. type 1)

SUMMARY TABLE 1 - TWO SPAN HOLLOW-CORE SLABS

TWO SPAN HOLLOW-CORE SLABS

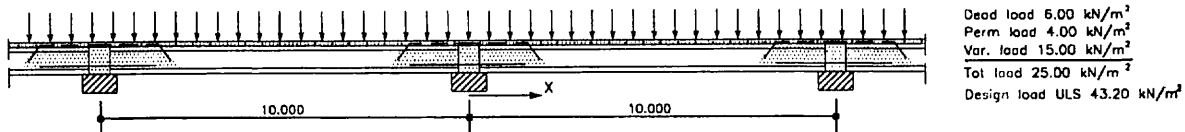
Dead load 4.00 kN/m²
 Perm load 2.00 kN/m²
 Var. load 6.00 kN/m²
 Tot load 12.000 kN/m²
 Design load ULS 20.52 kN/m²

HOLLOW CORE TYPE	HOLLOW CORE TYPE I			HOLLOW CORE TYPE II		
CROSS SECTION	 1200 mm width			 1200 mm width		
Prestressing reinforcement						
Upper	1. Simple bearing	2. Cont spans ordinary supp (direct)	3. Cont spans composite supp (non-direct)	1. Simple bearing	2. Cont spans ordinary supp (direct)	3. Cont spans composite supp (non-direct)
Lower	No 6 str. 3Ø 3 mm Fs 127 mm ² No 8 str. 0.5" Fi 744 mm ²	No 2 str. 3/8" + 1 st 3 Ø 3 Fs 125 mm ² No 8 str. 0.5" Fi 744 mm ²				
STRUCTURAL SCHEME	1. Simple bearing	2. Cont spans ordinary supp (direct)	3. Cont spans composite supp (non-direct)	1. Simple bearing	2. Cont spans ordinary supp (direct)	3. Cont spans composite supp (non-direct)
ARRANGEMENT AT SUPPORT	1 + joint 700 2Ø12	3 + joint 2300/1400 4Ø20	3 + joint 4/450 2300/1400 4Ø20 (+4Ø12)	2 700 2Ø12	4 (all) 2300/1400 4Ø20	4 (all) 2300/1400 4Ø20 (+4Ø12)
Concrete content m ³ /m ²	0.015 0.3	0.030 2.0	0.042 2.5	0.015 0.3	0.045 2.0	0.045 2.5
BENDING (kNm)	246 at 5050 290 + 18%	206 at 5530 290 + 41%	206 at 5530 290 + 41%	246 at 5050 290 + 18%	206 at 5530 290 + 41%	206 at 5530 290 + 41%
- Max Pos. M _{sd} at dist x(mm)	1.6 (100% up + 15% low)	1.6 (32% lower)	1.6 (32% lower)	1.6 (100% up, 15% low)	1.6 (32% lower)	1.9 (38% lower with 90% of design capacity)
- Capacity M _{rd} (kNm)						
- Extra capacity% $\frac{M_{rd}-M_{sd}}{M_{sd}}$						
- Possible saving in prestressing reinf. (Kg/m ²)						
Max neg. M _{sd} at supp (kNm)		108	108		108	108
Capacity M _{rd} at supp (kNm)		139	139		139	139
Extra capacity% $\frac{M_{rd}-M_{sd}}{M_{sd}}$		+ 28% (+ 90% with 6Ø20 in 6 filled cores)	+ 28% (+ 90% with 6Ø20 in 6 filled cores)		+ 28%	+ 28%
SHEAR (kNm)						
- Max V _{sd} at support (kN)	96	108	111	96	108	111
- Capacity V' _{rd} (kN)	207	169	169	210	230	230
- Capacity V' _{rd1} supp. side (kN)	-	-	113	-	-	134
- Max V _{sd} at 1° crack sect (kN)	78 at 1120 172	65 at 2483 172	65 at 2483 172	78 at 1120 99	65 at 2483 97	65 at 2483 97
- Capacity V' _{rd1} (kN)	Not applicable	89 at 1300 204	89 at 1300 204	Not applicable	89 at 1300 232	89 at 1300 232
- Max V _{sd} at limit of reinf. (kN)	-					
- Capacity V' _{rd1}						
- Max V _{sd} at limit of cores (kN)	Not applicable	69 at 2300 172	69 at 2300 172	Not applicable	69 at 2300 97	69 at 2300 97
- Capacity V' _{rd1} (kN)	-					
- Extra capacity% $\frac{V_r-V_d}{V_d}$	115% (+ 100% with 2 more filled cores)	+ 56% (+ 100% with 2 more filled cores)	+ 2% (+ 50% with shear reinf. of in-situ concrete)	+ 27%	+ 38%	+ 20% (+ 50% with shear reinf. of in-situ concrete)
SHEAR + SPALLING STRESSES						
- σ _{l,D} (N/mm ²)	Not applicable	Not applicable	1.18	Not applicable	Not applicable	1.93
- Extra capacity% $\frac{1.8-\sigma_{l,D}}{\sigma_{l,D}}$	-	-	+ 50%	-	-	Not acceptable -9% (with one 0.5" / web)
ELASTIC DEFLECTION (mm) (var. load)	≈ 23	≈ 5	≈ 5	≈ 12	≈ 5	< 5

@Seismicisolation

SUMMARY TABLE 2 - MULTI SPAN HOLLOW-CORE SLABS

MULTI SPAN HOLLOW-CORE SLABS



HOLLOW CORE TYPE		HOLLOW CORE TYPE I			HOLLOW CORE TYPE II		
CROSS SECTION							
Prestressing reinforcement							
Upper	No 6 str. 3Ø 3 mm Fs 169.6 mm ²				No 3 str. 3/8" Fs 156 mm ²		
Lower	No 8 str. 0.5"	Fi 930 mm ²			No 10 str. 0.5" Fi 930 mm ²		
STRUCTURAL SCHEME	1. Simple bearing	2. Cont spans ordinary supp (direct)	3. Cont spans composite supp (non direct)	1. Simple bearing	2. Cont spans ordinary supp (direct)	3. Cont spans composite supp (non direct)	
ARRANGEMENT AT SUPPORT							
- Open cores with reinforcement	1 + joint	3 + joint	3 + joint 4/450	2	4 (all)	4 (all)	
- Additional filled cores No/Length (mm)	700	2300/1400	2300/1400	-	2300/1400	2300/1400	
- Length of filled cores with reinf. (mm)	2Ø14	4Ø20	4Ø20 (+4Ø14)	2Ø14	4Ø20	4Ø20 (+4Ø14)	
- Add. Reinforc. excluding Ø 6 mesh (Add. lower reinf. if req.d)							
- Concrete content m ³ /m ²	0.058	0.086	0.090	0.058	0.095	0.095	
- Add. reinf. Content Kg/m ²	0.4 + Ø6 mesh	3.9 + Ø6 mesh	4.6 + Ø6 mesh	0.4 + Ø6 mesh	3.9 + Ø6 mesh	4.6 + Ø6 mesh	
BENDING (kNm)							
- Max Pos. M ⁺ _{Sd} at dist x(mm)	519 at 5000	401 at 5000	401 at 5000	519 at 5000	401 at 5000	401 at 5000	
- Capacity M ⁺ _{Rd} (kNm)	548	548	548	548	548	548	
- Extra capacity% $\frac{M^+_{Rd} - M^+_{Sd}}{M^+_{Sd}}$	+ 6%	+ 37%	+ 37%	+ 6%	+ 37%	+ 37%	
- Possible saving in prestressing reinf. (Kg/m ²)	1.5 (100% up + 5% low)	1.5 (24% lower)	1.5 (24% lower)	1.5 (100% up, 5% low)	1.5 (24% lower)	3.1 (50% lower with 70% of design capacity)	
- Max neg. M _{Sd} at supp (kNm)	-	247	247	-	247	247	
- Capacity M ['] _{Rd} at supp (kNm)	-	258	258	-	258	258	
- Extra capacity% $\frac{M'_{Rd} - M'_{Sd}}{M'_{Sd}}$	-	+ 4% (+ 60% with 6Ø20)	+ 4% (+ 60% with 6Ø20)	-	+ 4%	+ 4%	
SHEAR (kNm)							
- Max V _{Sd} at support (kN)	196	196	205	196	196	205	
- Capacity V ['] _{Rd} (kN)	344	230	230	340	313	313	
- Capacity V ['] _{Rd} at supp. side (kN)	-	-	152	-	-	172	
- Max V _{Sd} at 1° crack sect (kN)	169 at 978	82 at 3095	82 at 3095	169 at 978	82 at 3095	82 at 3095	
- Capacity V ['] _{Rd} (kN)	283	283	283	197	197	197	
- Max V _{Sd} at limit of reinf. (kN)	Not applicable	160 at 1300	160 at 1300	Not applicable	160 at 1300	160 at 1300	
- Capacity V ['] _{Rd}	-	277	277	-	332	332	
- Max V _{Sd} at limit of cores (kN)	Not applicable	117 at 2300	117 at 2300	Not applicable	117 at 2300	117 at 2300	
- Capacity V ['] _{Rd} (kN)	-	283	283	-	197	197	
- Extra capacity% $\frac{V'_R - V_D}{V_D}$	+ 67%	+ 17% (+ 60% with all filled cores)	-26% (+ 12% with shear reinf. of in situ concrete)	+ 17%	+ 60%	-16% (+ 2.5% with shear reinf. of in situ concrete)	
SHEAR + SPALLING STRESSES							
- σ _{1,0} (N/mm ²)	Not applicable	Not applicable	2.74 Not acceptable + 12% (with one 0.5"/web)	Not applicable	Not applicable	3.47 Not acceptable -30% (with one 0.5"/web)	
- Extra capacity%	-	-	-	-	-	-	
ELASTIC DEFLECTION (mm) (under variable load)	≈ 9	≈ 2	≈ 2	≈ 9	≈ 2	≈ 2	

@Seismicisolation

3. Non-rigid supports

3.1 Introduction

The application of hollow core slabs is still growing. New ways to create an optimal structural design are developed continuously. Shallow steel and concrete beams became efficient solutions for floors. New developments always demand the awareness of the designer. In this paper the behaviour of a floor structure with beams is reviewed. Attention is paid to interactions between hollow core units and supporting beams.

Hollow core slabs are reinforced by pretensioned strands or wires parallel to the cores and the slab is usually designed as a simply supported structural element. The analyses of the slab are in general based on 2-dimensional stress distributions. This is theoretically valid when the slab is subjected to symmetrical and uniformly distributed loading and is supported on a rigid bearing, such as a wall or a deep beam, under the assumption that the supports are parallel and the angle between span direction and support direction is 90°. Under these conditions no torsional stresses are acting.

To achieve a minimum structural depth, and provide a clear route for services, new types of beams are introduced in the past period of time. So, in many cases hollow core slabs are now supported on steel or prestressed / reinforced concrete beams of moderate stiffness - shallow beams- and designed as non-composite beams as shown in Figure 3.1.

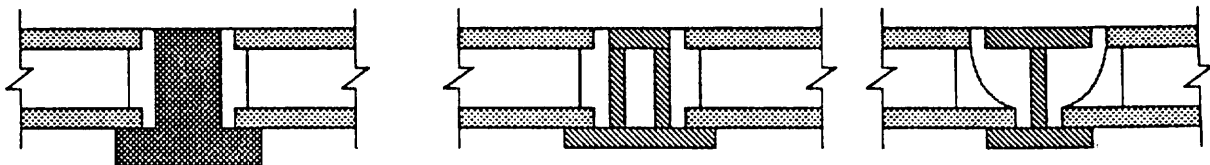


Fig.3.1: Different types of shallow beams.

When slabs are supported on beams with moderate stiffness the deformation of the beam will cause a composite action between slab and beam. This action alters the mode of behaviour of the structure and will introduce stresses in the transversal direction of the slab, not only in cases like those illustrated in Fig. 3.1, but also when the slabs are supported on the top of the beams. These transversal stresses need to be considered in the design.

This paper shows how the interaction between slab and beam can be taken into account in the design of the hollow core slab and the supporting beam. Research on this issue has been carried out in Scandinavia [1]. The hollow core floors designed according to the guidelines given in chapter 2 of this guide are not considered here. It is likely that the strong upper reinforcement and long filling in the cores reduce the transversal stresses in the web so effectively that they can be ignored in the design.

3.2 The behaviour of hollow core slabs supported on beams.

Consider a floor in which hollow core slabs are supported on beams. When the floor is loaded, both the slabs and the beams will deflect. The deflection in the middle of the span of the slab is depending on both the deflection of the beam and the slab (Figure 3.2). Figure 3.3 shows how the slab tends to move when there is no composite action between slab and beam.

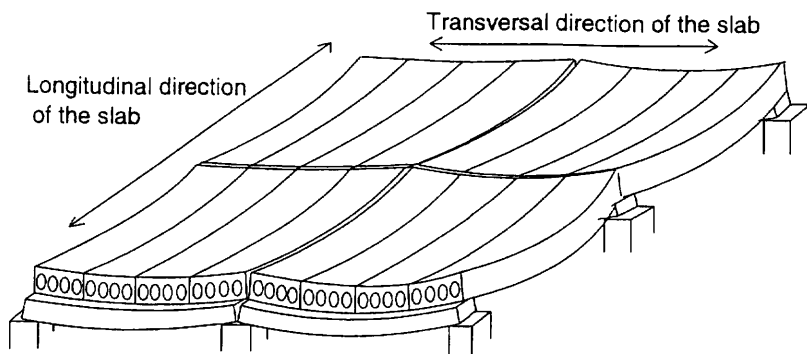


Fig 3.2 Deformed floor of hollow core slabs

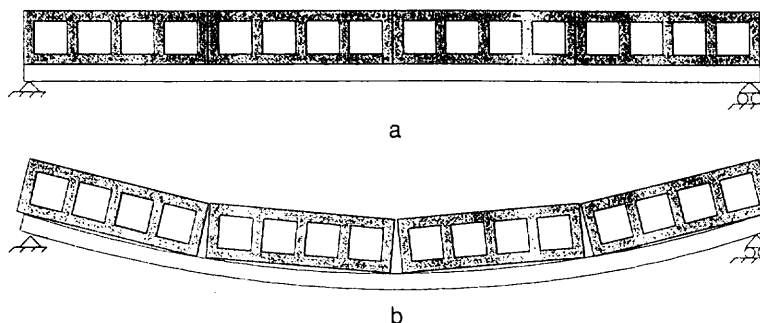


Fig 3.3 Hollow core slabs on a beam without friction between slab and beam.

composite action, shear flow v

In practice the chemical and mechanical bond as well as friction between the slab ends, the cast in situ concrete, and the beam tend to prevent this movement, as shown in Figure 3.4 c. The webs serve as a kind of connector between the compression forces in the flange and the rest of the section. This - kind of Vierendeel effect - will introduce a shear flow v in the webs of the hollow core slabs in transverse direction. The shear flow v has to be considered as additional to those acting when the hollow core slab is rigid supported. In fact, it is impossible to avoid a certain degree of sliding between the bottom side of the slab and the interface of the supporting beam. If the slab is not fully tied or otherwise integral with the beam, the sliding action will decrease the shear flow v , see Figure 3.4 d.

imposed load

The shear flow is depending on the shear force due to the *imposed load*; the load acting after the in situ concrete in the connection between slab and beam is casted and hardened.

When a topping is casted after the joints between hollow core slab ends and the beam have been casted and hardened, the self weight of the topping has to be seen as an imposed load. This is not the case when the structural topping and the joints between hollow core units and beam are casted in one casting operation.

When the beam is propped during that casting the self-weight of the propped structure has to be considered as an imposed load as well.

cracks in longitudinal direction

It is also possible that cracks appear in the bottom flange of the slab when the bottom of the slab is situated in the tensile zone of the beam as indicated in Figure 3.4a. These cracks may influence the bond between concrete and prestressing strand or wire. In fact, the effective prestressing force will decrease in the supporting zone.

cracks in transverse direction, parallel to the axis of the beam

Cracks will also develop in the transverse interface, Figure 3.4b, which will decrease the composite action. These cracks will open due to shrinkage and rotation of the slab ends under loading. The crack width can be decreased by adding top reinforcement across the interface into milled slots in the slabs or by adding reinforcement into the longitudinal joints between the slabs.

Another possibility to control the crack width and to increase the stiffness of the floor structure is to add a composite reinforced concrete topping.

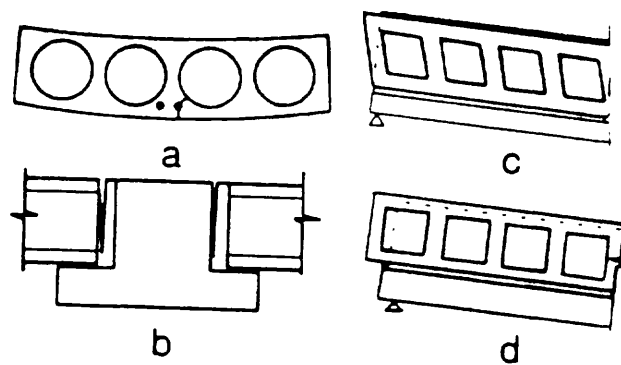


Fig 3.4 a) Longitudinal cracks along strands
 b) Cracks at the interface of beam and in situ concrete or in situ concrete and end of the hollow core unit
 c) Shear deformation of the hollow core slab
 d) Sliding of hollow core slab along the beam

the research and recommendations concern mainly:

- the stress criterion for the stresses in the webs.
- the magnitude of the shear flow, depending on the structural concept and
- the effective prestressing force, that has to be taken into account

stresses in the web

As shown in Figure 3.5, in the web act the following stresses:

- σ_1 , due to the effective prestressing force,
- τ_1 , due to the vertical shear force and
- τ_2 , due to the shear flow in transversal direction, caused by imposed load.

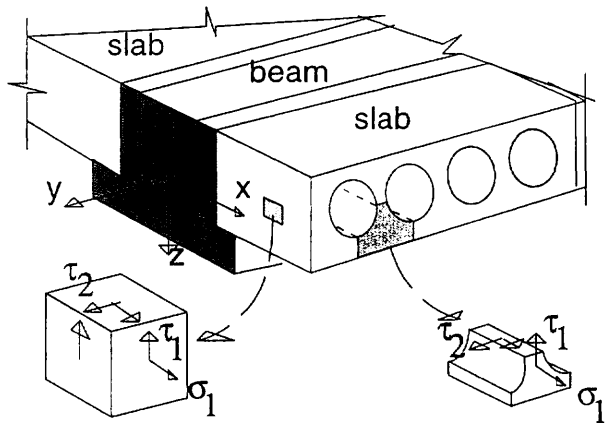


Fig. 3.5 Stress components in the web

failure criterion

Failure will take place when the maximum principle tensile stress σ_{ps} becomes equal to the characteristic tensile strength f_{ctk} of the concrete. So the design criterion will be:

$$\sigma_{ps} \leq f_{ctd}, \text{ the design tensile strength of the concrete} \quad (1)$$

To simplify the calculations, a modified principle stress σ_{ps} is used:

$$\sigma_{ps} = \frac{\sigma_1}{2} + \sqrt{\left(\frac{\sigma_1}{2}\right)^2 + \tau_1^2 + \tau_2^2} \quad (2)$$

The magnitude of the additional shear stress τ_2 is depending on:

- type of beam
- type of slab
- continuous or free supported beam
- span of both beam and slab
- curvature profile of beam
- tie steel arrangement
- penetration of in situ infill concrete into the hollow cores
- presence of a composite reinforced concrete topping

the research and the theoretical model

Most of these influencing factors have been studied experimentally and numerically using slabs 265 and 400 mm deep respectively and a range of beams similar to those in Figure 3.1, but there were also two tests with slabs supported on the top of rectangular concrete beams. The model described in the following chapters is based on the theoretical model calibrated by the results obtained in 10 full-scale tests.

3.3 Mechanical behaviour in transverse direction

the shear flow v

The -partial- composite action between slab and beam will consequently cause a compression force in the upper parts of the hollow core slab. Since the webs in the hollow core slabs have to serve as connectors between the compression flange and the rest of the section, a transverse shear force will act in the webs in the direction parallel to the beam axis. This causes a shear flow v in the hollow core unit transverse to the webs, see Fig. 3.6. This shear flow which causes transversal shear stress, can be calculated assuming only contact between the slab and the beam in the supporting area. Thus the vertical joint between the beam and the slab is considered as completely cracked and frictionless.

The horizontal shear stresses have to be combined with the vertical shear stress, which will reduce the shear capacity of the slab compared with rigid supported hollow core slabs

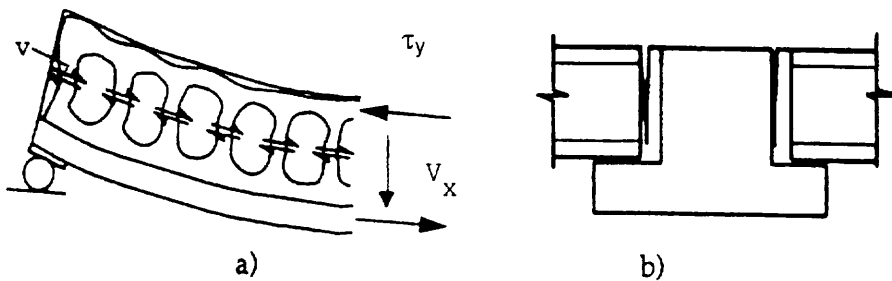


Fig. 3.6 Shows the shear forces in a composite structure when the cracks in b) cannot transfer any stresses.

the beam model and the effective width of the hollow core slabs

For the analyses, an elastic beam model is applied. The 'composite beam', used for the analyses, includes a certain width of the hollow core slab, the effective width b_{eff} , determined by calibrating the test results. Figure 3.7 shows the cross section of the 'composite beam'. The basic values to calculate $b_{eff,0}$ are presented in Table 3.1. The values are based on a basic span of the beam of $L_0 = 5$ m. The value for b_{eff} has to be calculated as follows for a beam with a span length L or $L = L_{cf}$, an equivalent span, (the distance in meters along the beam between the two consecutive points with zero bending moments):

$$b_{eff} = b_{eff,0} \cdot (L / 5\text{m}), \quad (\text{for a continuous beam } L = L_{cf}) \quad (3)$$

In a continuous beam the shear forces shall be calculated only for sagging beam moments. The resulting value of the effective width of the hollow core slab obtained from a test depends on the transfer of the prestressing force, tensile strength and elasticity modulus of the concrete etc., used in the calibration process.

Therefore the formulae used when determining the effective width from the tests should also be used when applying the model for other cases. Nevertheless it can be necessary to determine the effective width by additional tests.

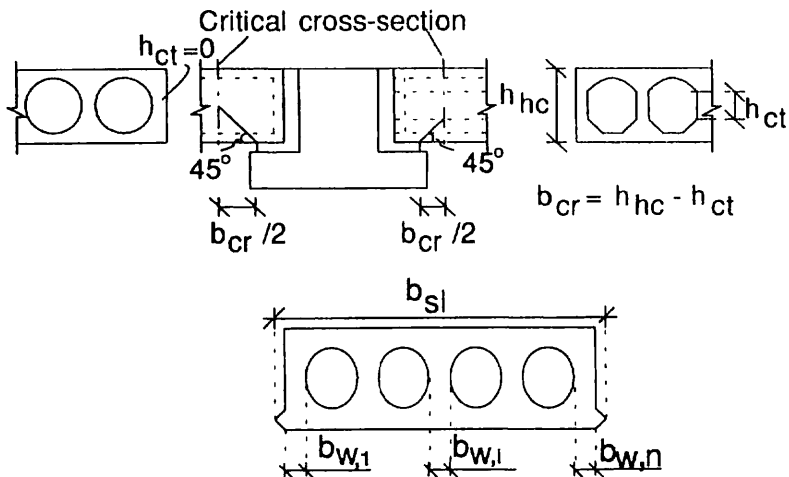


Fig 3.7 Critical cross-section and symbols used.

critical length; b_{cr}

Taking account of the effective width of the hollow core slabs in the composite cross-section and following the elastic beam theory the transverse compression stress σ_y acting in the flange of the hollow core slab, and the transverse shear force τ_y in a web can be calculated. This force will cause shear stresses τ_2 in the webs, as explained previously. Since the distribution of σ_y and τ_2 are unknown, simplifying assumptions must be made. Failure is governed by a local stress state. The shear stress τ_2 at the critical point may be calculated as

$$\tau_2 = \frac{3}{2} \frac{\tau_y}{b_w \cdot 2(b_{cr})} = \frac{3}{2} \cdot \tau_{2,av} \quad (4)$$

where b_{cr} is a parameter called critical length, determined experimentally.

The factor 3/2 arises from the fact that the maximum value of the shear stress is 3/2 times the mean value and b_w = the width of one web at the centroidal axis of the slab.

The distance

$$b_{cr} = h_{hc} - h_{ct} \quad (5)$$

where h_{hc} denotes the thickness of the hollow core slab and h_{ct} the depth of the web with constant thickness ($h_{ct} = 0$ for circular voids), has been found to correlate well with the experimental failure loads.

3.4 Design at ultimate limit state.

3.4.1 Shear tension failure in the hollow core slab

The following design principles are adopted:

The basic design method is developed for simply supported beams and slabs. Other cases are designed by modifying the basic design method.

When calculating the slab the three-dimensional behaviour is modelled by superimposing the stresses calculated separately in the direction of the slab and in the direction of the beam.

The action effects in the longitudinal direction of the hollow core slab are calculated as if the slabs are supported on a wall-like (rigid) support.

In the -partly- composite beam the effective width of the hollow core slabs will be taken into account, as well as the reinforced concrete topping, when present. The effective width for continuous beams is based on the distance between the points with zero moments. The basic shear stress τ_2 , due to the interaction of hollow core slab and beam, is directly depending on the magnitude of the shear force due to the imposed load and a span equal to L for simply supported beams or L_{cf} , an equivalent span, for continuous beams.

In the hollow core slab, failure takes place when the modified maximum principal stress σ_{ps} , calculated from the design loads, becomes equal to the characteristic tensile strength of the concrete f_{ctk} as shown previously.

In the basic formula (2) the basic shear stress value τ_2 can be modified to include explicitly the influences of:

- the infill at the ends of the hollow cores, by using the correction factor β_f which is depending on the depth of the slab and the length of the infill, as shown in Table 3.2 and
- the presence of a structural reinforced concrete topping by using the correction factor σ_{top} , which can be calculated as shown in 3.6.4.

$$\sigma_{ps} = \left(\frac{\sigma_1}{2} \right) + \sqrt{\left(\frac{\sigma_1}{2} \right)^2 + \tau_1^2 + [\beta_f (\tau_{2,top} + \beta_{top} \cdot \tau_{2,imp})]^2} \quad (6)$$

Where $\tau_{2,top}$ is calculated from the shear flow due to the weight of the topping concrete.

$\tau_{2,imp}$ is calculated from the shear flow due to the imposed load.

The visco-elastic behaviour of the concrete results in redistribution of the stresses. This reduces the peak stresses within the concrete consequently, the shear stresses due to the long-term transversal shear flow are reduced with time. To be on the safe side, τ_2 is calculated without taking this time independence into account. For the same reason, σ_1 is calculated at $t = 50$ years. This makes it unnecessary to consider different time points.



3.4.2 Longitudinal cracking of hollow core slabs.

In the ultimate limit state the weakening of the bond between strand and concrete due to longitudinal cracking can be modelled by assuming that a certain number of strands are debonded at the end of the hollow core slab for a certain length. This debonding is taken into account when the transverse tensile stress of the bottom fibre of the slab is greater than the design tensile strength of the slab concrete. The transverse tensile stress of the bottom fibre of the hollow core slab may be calculated from the composite beam model. The cracking and debonding will act in the zone with the maximum bending moment, so not where the maximum shear flow is acting.

The number of debonding strands, per slab and per web can be taken from Table 3.3. When wires are used a similar estimation as for strands can be adopted.

3.4.3 Design of curvature of the beam

Limiting the curvature of the beam axis is necessary for the following reasons:

- The empirical values of $b_{eff,0}$ have been determined in tests in which neither yielding strain of the steel, nor crushing strain of the concrete were exceeded in the beams.
- Extensive yielding of the beams results in large deformations and enables the differences in deflection to grow large between adjacent beams which in its turn results in high torsion within the slab units. The stresses due to torsion are not taken into account in the failure criterion.

Thus the maximum curvature for the sagging moments due to the characteristic values of the imposed load shall be limited to $0,027 \text{ m}^{-1}$.

The actual contribution of the slabs to the stiffness of the beam may be included when calculating the curvature

3.5 Design in the serviceability limit state.

3.5.1 Longitudinal cracking of the hollow core slabs

The longitudinal cracking of the hollow core slab in the serviceability limit state shall be limited to prevent corrosion of strands. The estimation of the crack width is based on an artificial strain ε_2 at the bottom side of the hollow core slab. This strain shall be lower than a critical strain ε_{cr} , corresponding with the allowed crack width w_k . The relationship between ε_{cr} and w_k is given in Table 3.4.

3.6 Design calculations

3.6.1 For the design the following data have to be specified:

- the material parameters of all parts of the composite beam, including the data required for calculating the transfer length of the strands in the hollow core unit.
- the loads and safety factors.
- the dimensions of the beam, the span of the beam, continuous or simply supported.
- the data concerning the hollow core slab, such as:

- b_{sl} width of the slab unit
- h_{hc} height of hollow core slab
- $b_{w, sl}$ sum of the web widths in the axis; sometimes written as $\sum b_{w,i}$
- h_{ct} depth of the web with constant thickness
- A_c cross-sectional area of the slab
- e_{sl} distance from centroid to bottom fibre slab
- S_{sl} first moment of area with respect to the centroid axis of the slab
- I_{sl} second moment of area
- f'_{ct} characteristic compression strength of slab concrete at release of the prestressing force
- ϕ diameter of strands or wires
- A_p cross-sectional area of strands
- σ_{po} initial prestress
- σ_p prestress after $t = 50$ years

3.6.2 Critical cross-section; magnitude of σ_1 and σ_{1c} .

- critical width,

$$\begin{aligned} b_{cr} &= h_{hc} - h_{ct} \\ h_{hc} &= \text{depth of the hollow core slab, see also Fig. 3.7.} \\ h_{ct} &= \text{depth of the web with constant thickness, for circular voids } h_{ct} = 0 \end{aligned} \quad (5)$$

- location of the critical cross-section

The critical cross-section is located at a distance from the slab end equal to

$$\begin{aligned} L_{cr} &= L_{supp,hc} + b_{cr}/2 \\ L_{supp,hc} &= \text{support length of the hollow core slab} \end{aligned} \quad (7)$$

- prestress in strands at the critical cross section

$$\begin{aligned} \sigma_{p, cr} &= \alpha \cdot \gamma_p \cdot \sigma_p \\ \alpha &= \text{factor } \leq 1 \text{ that takes in account the transfer of the prestressing force at} \\ &\quad \text{the critical cross-section according to Eurocode 2} \\ \gamma_p &= \text{safety factor for the prestressing force, lower value} \\ \sigma_p &= \text{fully transferred prestress in strands after losses in 50 years} \end{aligned} \quad (8)$$

- the normal stress σ_1 in the critical cross-section

$$\sigma_1 = -\sigma_{p,cr} \cdot A_p / A_c \quad (9)$$

- the shear force in the critical section and the calculation of τ_1

For the location of the critical cross-section see Fig. 3.7.

- without the application of a reinforced concrete topping:

weight of the slab and joint concrete	g_k
imposed load, live load	q_k
q design for the weight of the slab	$q_{d,g,slab} = \gamma_g \cdot g_k$
q design for the imposed load	$q_{d,imp} = \gamma_k \cdot q_k$

the distance between the critical cross-section and the centre of the support is equal to $0,5 L_{supp,hc} + 0,5 b_{cr}$, see also Figure 3.7

the distance between the mid of the slab to the critical section is equal to

$$L_{mid-crit} = 0,5 L_{sl} - (0,5 L_{supp,hc} + 0,5 b_{cr}), \quad (10)$$

where L_{sl} = span of hollow core slab.

$$V_{d,g,slab} = q_{d,g,slab} \cdot b_{sl} \cdot L_{mid-crit} \quad (11)$$

$$V_{d,imp} = q_{d,imp} \cdot b_{sl} \cdot L_{mid-crit} \quad (12)$$

$$\tau_1 = \frac{(V_{d,g,slab} + V_{d,imp}) \cdot S_{sl}}{b_{w,sl} \cdot l_{sl}} \quad (13a)$$

- with the application of a reinforced concrete topping.

In the case a composite reinforced concrete topping is applied, which is *casted together with the joint concrete*, the self weight of the topping can be taken in account as the weight of the slab, not acting on the composite structure;

The imposed load however is acting on the total cross-section, topping included.

$$\tau_1 = \frac{V_{d,g,slab} \cdot S_{sl}}{l_{sl} \cdot b_{w,sl}} + \frac{V_{d,imp,sl} \cdot S_{sl+top}}{l_{sl+top} \cdot b_{w,sl}} \quad (13b)$$

In the case a composite reinforced concrete topping is applied, which is casted after the joint concrete between the slabs and the beam has hardened, the self weight of the topping has to be taken in account as an imposed load! The formula (13b) is applicable

3.6.3 The composite beam

- *effective width*

$$b_{\text{eff}} = b_{\text{eff},0} \cdot (L / L_0) \quad (\text{see Fig. 3.7 + 3.9}) \quad (3a)$$

$b_{\text{eff},0}$ effective width in mm' for a beam with a basic span $L_0 = 5 \text{ m}'$,
see Table 3.1,

L span of the simply supported beam in m'
 L_0 basic span = 5 m

for a continuous beam

$$b_{\text{eff}} = b_{\text{eff},0} \cdot (L_{\text{ct}} / L_0) \quad (3b)$$

L_{ct} distance between the zero moment points in the beam.

Table 3.1: Effective width $b_{\text{eff},0}$ in mm for beams with a span width $L_0 = 5.0 \text{ m}$.

The  values have been calculated from test results. The other values have been obtained either by interpolation or by extrapolation.

h	Voids	voids	concrete beam	top hat beam
	Circular	non-circular		or equivalent
200	X		150	80
265	X		(185)	(90)
320		x	270	100
400		x	(400)	(115)

 Values determined in tests

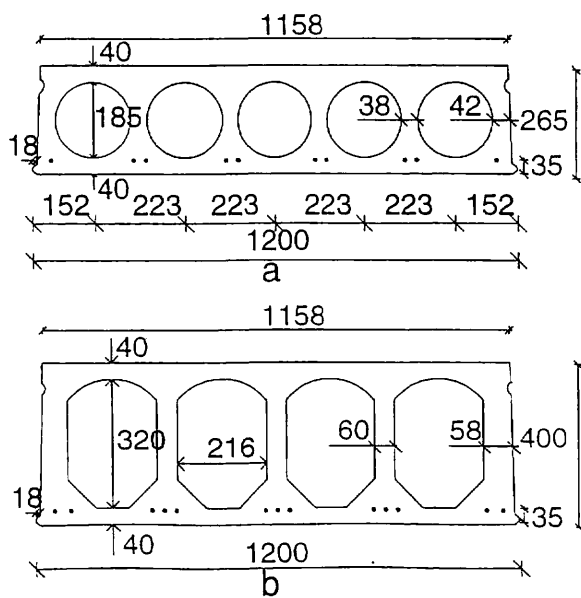


Fig. 3.8 Cross-section of hollow core slabs

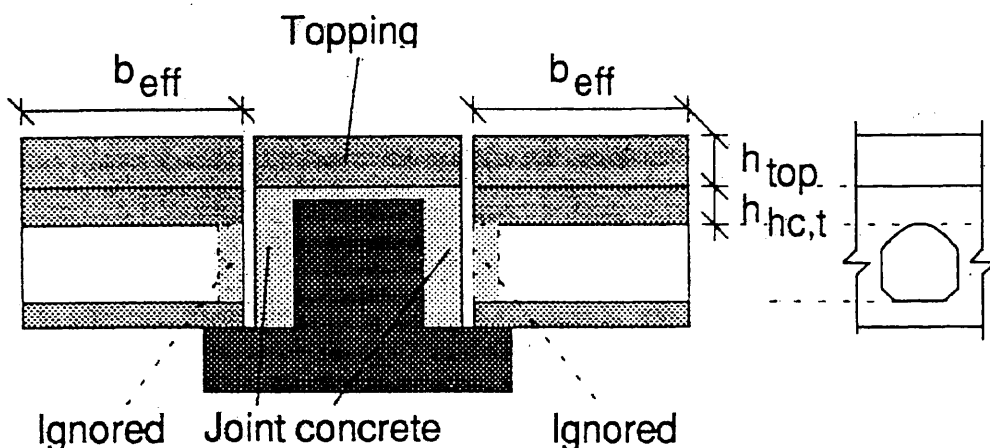


Fig. 3.9 The composite structure used in the calculation of transverse shear stresses

- *Cross-section and characteristics*

Now the cross-section of the composite beam is determined, see Figure 3.9

When the characteristics of the components are known as well, one can calculate:

(EA)_{0-top}, e_{0-top}, and (EI)_{0-top} for the composite section without a concrete topping and .
(EA)₀, e₀, and (EI)₀ for the composite section with a topping, when applied.

- $e_{0-top} =$ distance from the centroid axis of the cross-section, without a topping, to the bottom fibre of the beam
- $e_0 =$ distance from the centroid axis of the cross-section, topping included, to the bottom fibre of the beam

The first moment of area of the top flanges of the hollow core slabs, *without a topping*

$$(ES)_{hc,t} = E_{hc} \cdot h_{hc,t} \cdot 2 b_{eff} \cdot e_{hc,t} \quad (14)$$

- E_{hc} E modulus of the hollow core slab.
- $h_{hc,t}$ thickness of the top flange of the hollow core slab.
- $e_{hc,t}$ the distance of the centroid of the top flange of the hollow core slab from the centroid axis of the concrete cross-section, topping excluded.

The first moment of area of the top flanges of the hollow core slabs and the topping,

$$(ES)_f = (EA)_f \cdot e_f \quad (15)$$

- $(EA)_f$ the axial stiffness of the whole upper flange (shaded area in Fig. 3.9) including concrete topping.

- e_f centroidal distance of the top of the flange from the centroidal axis of the whole composite cross-section.

3.6.4 Shear stress τ_2 in transverse direction

- *shear flow v*
for a composite cross-section without a structural topping

$$v = \frac{(ES)_{hc,t} \cdot V_{x,imp}}{(EI)_{0-top}} \quad (16)$$

$V_{x,imp}$ = Maximum shear force acting in the beam due to imposed loading, in the case the beam is continuous, the maximum shear force for the length of the beam with sagging moments.

for a composite cross-section with a structural topping, casted after the joint concrete between the slabs and the beam is hardened.

$$v = \frac{(ES)_{hc,t} \cdot V_{x,top}}{(EI)_{0-top}} + \frac{(ES)_f \cdot V_{x,imp}}{(EI)_0} \quad (17)$$

$V_{x,top}$ = Maximum shear force acting in the beam due to the self-weight of the reinforced concrete topping, in the case the beam is continuous, the maximum shear force for the length of the beam with sagging moments.

- *The shear stress τ_2 and the correction factors β_f and β_{top}*

$$\tau_2 = \frac{3 \cdot v \cdot b_{sl}}{4b_{cr}b_{w,sl}} \quad (18)$$

factor β_f

In the case the ends of the hollow cores are filled with concrete to a certain length the value of τ_2 may be multiplied with a correction factor $\beta_f \leq 1$, as presented in Table 3.2.

Table 3.2 β_f

Slab thickness	200	265	320	400
Filling length < 50 mm	1.0	1.0	1.0	1.0
Filling length at least equal to the Depth of void. All voids filled (Fig. 10)	0.7	0.7	0.5	0.5

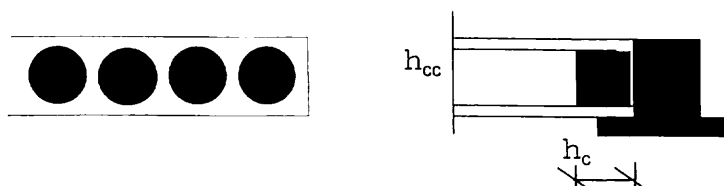


Fig. 3.10 Filling of hollow cores

factor β_{top}

When a floor is provided with reinforcement in the upper level of the hollow core slab or reinforcement in the topping, the β_{top} factor can be calculated in the following way.

$$\beta_{\text{top}} = \frac{F_{\text{web}}}{F_{\text{top}} + F_{\text{web}}} \quad (19)$$

$$F_{\text{top}} = b_{\text{sl}} \cdot \frac{A_{\text{sv}} \cdot f_{\text{yk}}}{S} \mu \cdot 2 \quad (20a)$$

or

$$F_{\text{top}} = 0.2 f_{\text{ck}} \cdot h_{\text{top}} \cdot b_{\text{sl}} \quad (20b)$$

whichever is smaller and

$$F_{\text{web}} = \frac{4}{3} \cdot b_{\text{sl}} \cdot \frac{b_{w,\text{sl}}}{b_{\text{sl}}} \cdot b_{\text{cr}} \cdot \sqrt{2} \cdot \frac{f_{\text{ctm}}}{\beta_f} = \frac{4}{3} \cdot b_{w,\text{sl}} \cdot b_{\text{cr}} \cdot \sqrt{2} \frac{f_{\text{ctm}}}{\beta_f} \quad (21)$$

where

b_{sl} length of the considered structural element in beam direction (slab width)

$\frac{A_{\text{av}}}{S}$ cross-sectional area of the topping reinforcement perpendicular to the beam per lengths

f_{yk} characteristic yield strength of the topping reinforcement perpendicular to the beam

f_{ck} characteristic strength of the topping concrete

f_{ctm} mean axial tensile strength of slab concrete

h_{top} thickness of concrete topping at support area

μ friction coefficient (=2.0)

β_f coefficient for core filling according to Table 3.2

- *the influence of longitudinal cracking of the hollow core slab on σ_I .*

As explained in 3.4.2, longitudinal cracks in the bottom zone of the hollow core slabs along prestressing strands or wires will reduce the bond capacity. These cracks may be expected when the transverse tensile stress in the bottom fibre of the hollow core slab, calculated in the composite cross-section, is greater than the design tensile stress of the slab concrete. In Table 3.3 one can find the reduction of the number of strands due to debonding.

Table 3.3: Debonding of strands

Strands per web	1	2	3
Number of debonded strands per slab unit	1		
Number of debonded strands per web		0.5	0.5
Length of debonding mm	500	500	500

The rate of reduction of the number of strands is the same as for the prestressing force and σ_1 .

3.6.5 The maximum principle stress σ_{ps} and the design criterion.

The values of σ_1 , τ_1 and τ_2 as well as the possible correction factors are known.

$$\sigma_{ps} = \left(\frac{\sigma_1}{2} \right) + \sqrt{\left(\frac{\sigma_1}{2} \right)^2 + \tau_1^2 + [\beta_f (\tau_{2,top} + \beta_{top} \cdot \tau_{2,imp})]^2} \quad (6)$$

where $\tau_{2,top}$ is calculated from the shear flow due to the weight of the topping concrete
 $\tau_{2,imp}$ is calculated from the shear flow due to the imposed load.

criterion

$\tau_{ps} \leq f_{ctd}$, the design tensile strength of the slab concrete.

3.6.6 Curvature of the beam

The curvature can be calculated with respect to the composite cross-section, for sagging moments, taking account of characteristic values of the imposed load.

The curvature shall not exceed $0,027 \text{ m}^{-1}$, see also 3.4.3.

3.6.7 Serviceability limit state.

The longitudinal cracking of the hollow core slabs in serviceability limit state shall be limited to prevent corrosion of the strands or wires.

Estimation of the crack width is based on an artificial transverse strain ε_2 at the bottom fibre of the hollow core slab.

$$\varepsilon_2 = \frac{M_{k,top} \cdot Z'_{hcb}}{(EI)_{o-top}} + \frac{M_{k,imp} \cdot Z_{hcb}}{(EI)_o}$$

$M_{k,top}$ bending moment of the beam due to the weight of the optional topping in serviceability limit state (SLS)

$M_{k,imp}$ bending moment of the beam due to the imposed load in SLS

Z'_{hcb} z' coordinate of bottom fibre of hollow core without topping

Z_{hcb} z coordinate of bottom fibre of hollow core with topping

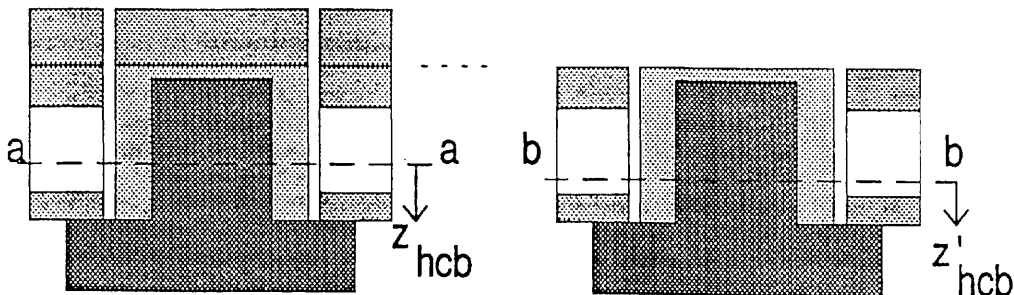


Fig. 3.11 Definition of z and z' coordinate. a – a is the centroidal axis of the whole composite cross-section , b – b the centroidal axis of the composite section without topping.

- *Criterion*

In SLS $\varepsilon_2 < \varepsilon_{cr}$

where the critical strain ε_{cr} is given in Table 3.4

Table 3.4: Critical value ε_{cr} for bottom fibre of hollow core slab.
 w_k is the allowed crack width

w_k	ε_{cr}
0.1	$0.4 \cdot 10^{-3}$
0.2	$0.7 \cdot 10^{-3}$
0.3	$1.0 \cdot 10^{-3}$
0.4	$1.3 \cdot 10^{-3}$

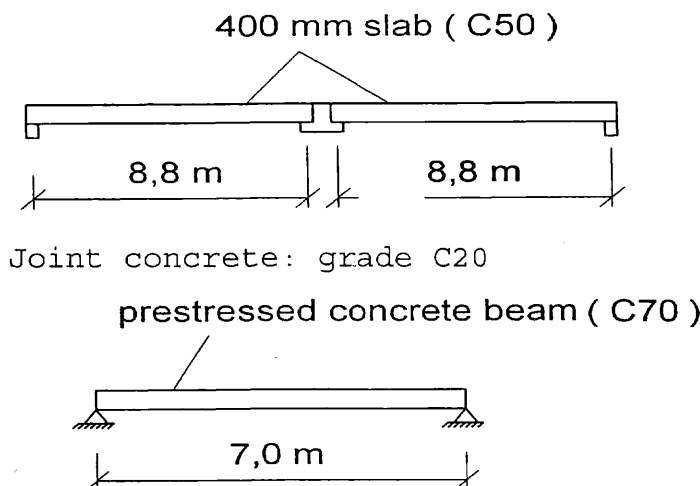
3.7 Examples of calculation

Example 1A: 400 mm slab on prestressed concrete beam

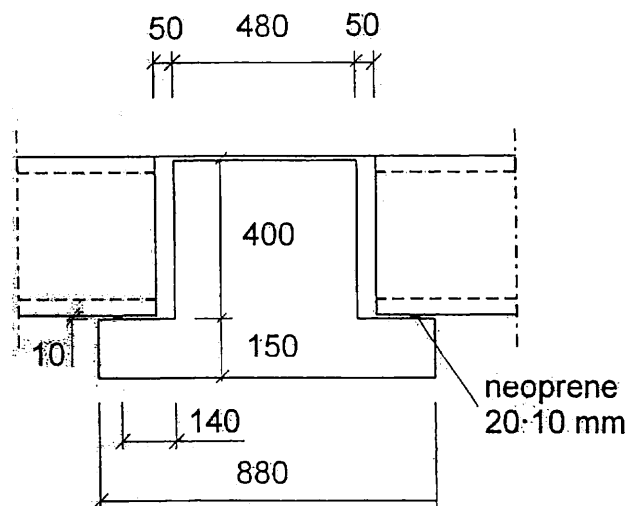
- **Eurocode**

Design loads, prestressing, material parameters etc. according to Eurocodes (ENV 1991 and ENV 1992).

Evenly distributed live load $q_k = 3,0 \text{ kN/m}^2$



- **prestressed concrete beam**



- **material parameters (ENV 1992 – 1 – 1 chapter 3)**

$$\text{C20} \Rightarrow E_c = 28,9 \text{ GPa}$$

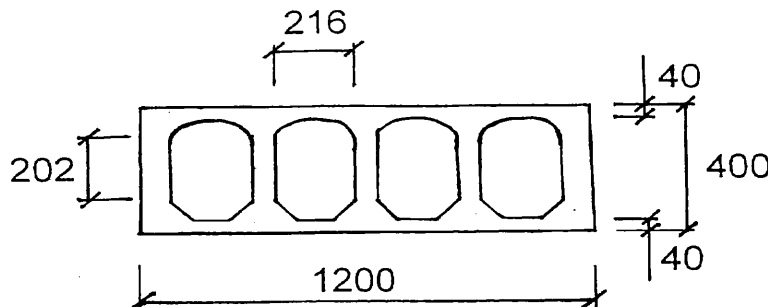
$$\text{C50} \Rightarrow E_c = 36,8 \text{ GPa} \quad f_{ctk} = 2,9 \text{ MPa}$$

$$f_{ctd} = \frac{f_{ctk}}{\gamma_c} = \frac{2,9}{1,5} = 1,93 \text{ MPa}$$

$$\text{C70} \Rightarrow E_c = 40,6 \text{ GPa}$$

$$\text{Prestressing steel} \Rightarrow E_p = 190 \text{ GPa}$$

- hollow core slab



Cross-sectional area	$A_c = 0,217 \text{ m}^2$
Distance from centroid to bottom fibre	0,199 m
Second moment of area	$I_{sl} = 4,41 \cdot 10^{-3} \text{ m}^4$
First moment of area with respect to the centroidal axis of the slab	$S_{sl} = 14,2 \cdot 10^{-3} \text{ m}^3$
Sum of web widths	$\sum b_{w,i} = 0,296 \text{ m}$
Depth of the web with constant thickness	$h_{ct} = 0,202 \text{ m}$
Strength of concrete at release of prestress	35 MPa
Strands	7 Ø 12,5 mm
Cross-sectional area of strands	$A_p = 7 \cdot 93 \text{ mm}^2$
Prestress after 50 years	$\sigma_p = 870 \text{ MPa}$

- transverse web shear failure

Design criterion: $\sigma_p \leq f_{ctd}$

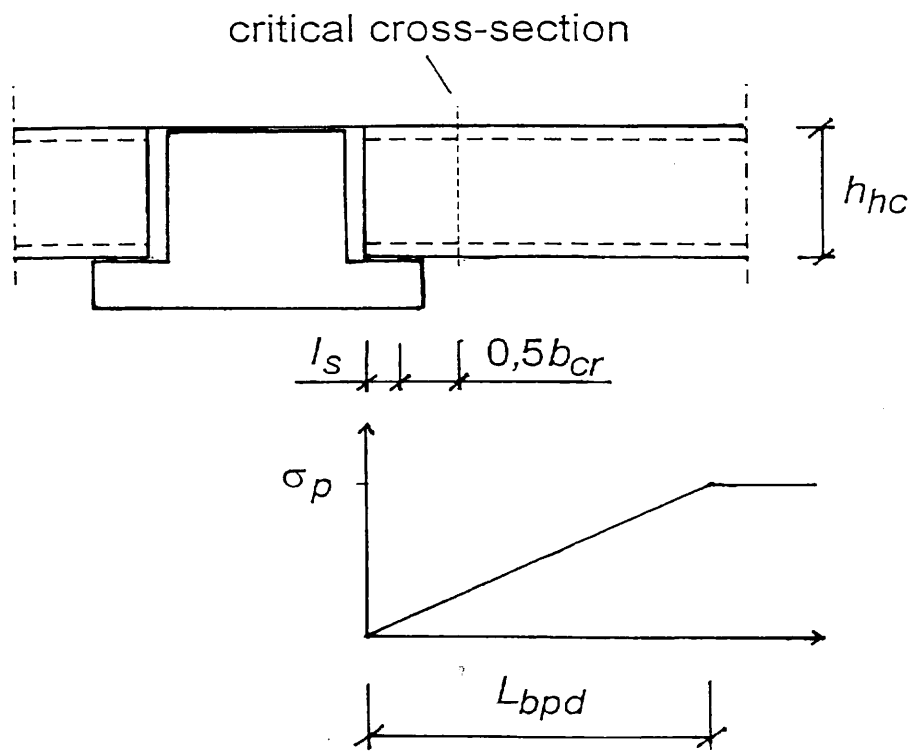
$$\sigma_p = \frac{\sigma_1^2}{2} + \sqrt{\frac{\sigma_1^2}{4} + \tau_1^2 + \tau_2^2}$$

σ_1 , τ_1 and τ_2 are calculated from design loads, at the critical cross-section.

- σ_1 – normal stress in the hollow core slab due to prestress

σ_1 is calculated according to the elementary beam theory

$$\sigma_1 = \frac{\alpha \cdot \gamma_p \sigma_p \cdot A_p}{A_c}$$



I_s = support length

L_{bpd} = transfer length (ENV 1992-1-1, chapter 4.2.3.5.6.)

$$\alpha = \frac{I_s + 0,5b_{cr}}{L_{bpd}}$$

$$b_{cr} = h_{hc} - h_{ct} = 400 - 2052 = 198 \text{ mm}$$

$$L_{bpd} = 0,8 \cdot \beta_b \varnothing \text{ or } 1,2 \cdot \beta_b \varnothing \text{ whichever is less favorable.}$$

$$\text{Cylinder strength at release} = 35 \text{ MPa} \Rightarrow \beta_b = 65$$

$$\varnothing = 12,5 \text{ mm} \Rightarrow L_{bpd} = 1,2 \cdot 65 \cdot 12,5 = 975 \text{ mm}$$

Support length: $I_s = 90 \text{ mm}$

$$\Rightarrow \alpha = \frac{90 + 0,5 \cdot 198}{975} = 0,194$$

$$\gamma_p = 0,9 \text{ (ENV 1991)}$$

$$\sigma_1 = \frac{\alpha \cdot \gamma_p \cdot \sigma_p \cdot A_p}{A_c} = -\frac{0,194 \cdot 0,9 \cdot 870 \cdot 10^6 \cdot 7 \cdot 93 \cdot 10^{-6}}{0,217}$$

\Rightarrow

$$\boxed{\sigma_1 = -0,46 \text{ MPa}}$$

@Seismicisolation

□ **τ_1 – longitudinal shear stress in the hollow core slab**

τ_1 is calculated according to the elementary beam theory

$$\tau_1 = \frac{V_{d,sl} \cdot S_{sl}}{I_{sl} \cdot \sum b_{w,i}}$$

Weight of slab + joint concrete: $g_k = 4,8 \text{ kN/m}^2$

Imposed load: $q_k = 3,0 \text{ kN/m}^2$

Design load q_d (ENV 1991)

$$q_d = \gamma_G \cdot g_k + \gamma_Q \cdot q_k$$

with partial safety factors $\gamma_G = 1,35$ and $\gamma_Q = 1,50$

$$q_d = 1,35 \cdot 4,8 + 1,5 \cdot 3,0 = 11,0 \text{ kN/m}^2$$

$$0,5l_s + 0,5b_{cr} = 0,5 \cdot 90 + 0,5 \cdot 198 = 144 \text{ mm}$$

⇒ distance between the critical cross-section and the support reaction = 144 mm

Design shear force in the hollow core slab at the critical cross-section.

$$V_{d,sl} = 1,2 \cdot 11,0 \cdot (4,4 - 0,144) = 56 \text{ kN}$$

$$\tau_1 = \frac{V_{d,sl} \cdot S_{sl}}{I_{sl} \cdot \sum b_{w,i}} = \frac{56 \cdot 10^3 \cdot 14,2 \cdot 10^{-3}}{4,41 \cdot 10^{-3} \cdot 0,296}$$

$$\Rightarrow \boxed{\tau_1 = 0,61 \text{ MPa}}$$

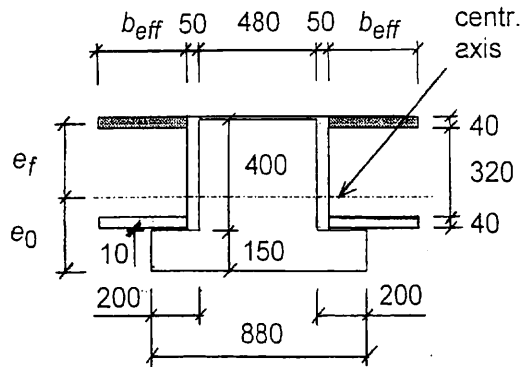
□ **τ_2 – transverse shear stress on the hollow core slab**

$$\tau_2 = \frac{3}{2} \cdot \frac{v(y)}{2b_{cr}} \cdot \frac{b_{sl}}{\sum b_{w,i}}$$

$v(y)$ = transverse shear flow

b_{sl} = slab width

$v(y)$ is calculated by applying the elementary beam theory to the composite beam given on next page.



$$(EI)_0 = 560 \text{ MNm}^2 \quad e_0 = 0,267 \text{ m}$$

$$v(y) = \frac{e_f \cdot (EA)_f \cdot V_{d,imp,b}}{(EI)_0}$$

$(EI)_0$ = bending stiffness of the total composite cross section
 $(EA)_f$ = axial stiffness of the upper flange (shaded area)

From eq. 1 + table 1 in Design Recommendations [1]

$$b_{eff} = \frac{L}{L_0} \cdot b_{eff,0} = \frac{7,0}{5,0} \cdot 400 = 560 \text{ mm}$$

$$(EA)_f = 2 \cdot 36,8 \cdot 10^9 \cdot 0,56 \cdot 0,040 = 1,64 \cdot 10^9 \text{ N}$$

$V_{d,imp,b}$ = shear force of beam at the support due to imposed load (design value)

Design load $q_{d,imp}$ (ENV 1991)

$$q_{d,imp} = \gamma_Q \cdot q_k = 1,5 \cdot 3,0 = 4,5 \text{ kN/m}^2$$

$$V_{d,imp,b} = q_{d,imp} \cdot (4,40 + 0,67 + 4,40) \cdot 3,5$$

$$\Rightarrow V_{d,imp,b} = 149 \text{ kN}$$

$$e_f = 150 + 10 + 400 - 20 - e_0 = 540 - 267 = 273 \text{ mm}$$

$$v(y) = \frac{e_f \cdot (EA)_f \cdot V_{d,imp,b}}{(EI)_0} = \frac{0,273 \cdot 1,64 \cdot 10^9 \cdot 149}{560 \cdot 10^6}$$

$$\Rightarrow v(y) = 119 \text{ kN/m}$$

$$\tau_2 = \frac{3}{2} \cdot \frac{119 \cdot 10^3}{2 \cdot 0,198} \cdot \frac{1,2}{0,296}$$

$$\Rightarrow \boxed{\tau_2 = 1,83 \text{ MPa}}$$

□ Design criterion

$$\sigma_{ps} = \frac{\sigma_1}{2} + \sqrt{\frac{\sigma_1^2}{4} + \tau_1^2 + \tau_2^2} \leq f_{ctd}$$

$$\sigma_{ps} = -\frac{0,46}{2} + \sqrt{\frac{0,46^2}{4} + 0,61^2 + 1,83^2} \Rightarrow \boxed{\sigma_p = 1,71 \text{ MPa}}$$

$$\boxed{\sigma_{ps} < f_{ctd} = 1,93 \text{ MPa} \Rightarrow \text{OK}}$$

□ Longitudinal cracking

Ultimate limit state:

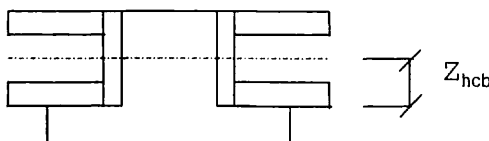
σ_2 = transverse tensile stress of the bottom fibre of the slab

$$\sigma_2 = \frac{E_{hc} \cdot M_{d,imp} \cdot Z_{hcb}}{(EI)_0}$$

$M_{d,imp}$ = bending moment due to $q_{d,imp} = 4,5 \text{ kN/m}^2$

$$M_{d,imp} = 4 \cdot 5(4,40 + 0,67 + 4,40) \cdot \frac{7^2}{8}$$

$$\Rightarrow M_{d,imp} = 261 \text{ kNm}$$



$$Z_{hcb} = 267 - 160 = 107 \text{ mm}$$

$$\sigma_2 = \frac{36 \cdot 8 \cdot 10^9 \cdot 261 \cdot 10^3 \cdot 0,107}{560 \cdot 10^6}$$

$$\Rightarrow \sigma_2 = 1,84 \text{ MPa}$$

$$\Rightarrow \sigma_2 \leq f_{ctd} \Rightarrow \text{no debonding}$$

If $\sigma_2 \leq f_{ctd}$ debonding according to table 3 has to be taken into account. The effect of this is checked with conventional design methods.

Serviceability limit state:

Estimate the crackwidth

$$\varepsilon_2 = \frac{M_{k,imp} \cdot Z_{hcb}}{(EI)_0}$$

$M_{k,imp}$ = bending moment due to $q_k = 3,0 \text{ kN/m}^2$

$$M_{k,imp} = (4,40 + 0,67 + 4,40) \frac{7^2}{8}$$

$$\Rightarrow M_{k,imp} = 174 \text{ kNm}$$

@Seismicisolation

$$\varepsilon_2 = \frac{174 \cdot 10^3 \cdot 0,107}{560 \cdot 10^6} = 0,03 \cdot 10^{-3}$$

Table 3.4 \Rightarrow crack width less than 0,1 mm.

Design of the beam

Curvature of the beam cross-sections subjected to sagging bending moment due to q_k shall not exceed $0,027 \text{ m}^{-1}$. This is checked with conventional design methods.

Example 1b: Structure as in example 1

Question: Will the structure meet the requirement when the live load is 5 kN/m^2 (was 3 kN/m^2) and for separation walls $1,5 \text{ kN/m}^2$ has to be taken into account.

The values calculated previously will be used.

$\sigma_1 = -0,46 \text{ MPa}$, not depending on q_d .

$q_d = 1,35 \times 4,8 + 1,35 \times 1,5 + 1,50 \times 5,0 = 16,0 \text{ kN/m}^2$
(q_d was 11 kN/m^2 , $\tau_1 = 0,61 \text{ MPa}$)

$$\Rightarrow \tau_1 = (16/11) \times 0,61 = 0,89 \text{ MPa}$$

The imposed load $q_{d,imp} = 1,35 \times 1,5 + 1,5 \times 5,0 = 9,5 \text{ kN/m}^2$
($q_{d,imp}$ was $4,5 \text{ kN/m}^2$, $\tau_2 = 1,83 \text{ MPa}$)

$$\Rightarrow \tau_2 = (9,5/4,5) \times 1,83 = 3,86 \text{ MPa}$$

$$\sigma_{ps} = \frac{-0,46}{2} + \sqrt{\left(\frac{0,46}{2}\right)^2 + 0,89^2 + 3,86^2} =$$

$$= -0,23 + 3,97 = 3,74 \text{ MPa}$$

$$\sigma_{ps} > f_{ctd} = 1,93 \text{ MPa}$$

Is it possible to fill the ends of the hollow core slabs. According to Table 2, $\beta_2 = 0,5$ for a slab deep 400 mm and a filling length equal to the depth of the void.

$$\sigma_{ps} = \frac{-0,46}{2} + \sqrt{\left(\frac{0,46}{2}\right)^2 + 0,89^2 + (0,5 \cdot 3,86)^2} = -0,23 + 2,13 = 1,90 \text{ MPa}$$

The check on longitudinal cracking shows that $\sigma_2 > f_{ctd}$. In total 2,5 of 7 strand per slab are debonded over a length of 500 mm. This is in the middle of the span, of the beam where τ_2 is nihil.

Example 2: based on computerprogram from Strängbetong Sweden

Beam:	steel girder	span	6,0 m
	cross-section	height	300 mm
	web	dim	8 x 200 mm ²
	top flange	"	200 x 40 mm ²
	bottom flange	"	400 x 22 mm ²
	distance between beams		10 m

Slab: HD/F 120/27 A 5.1

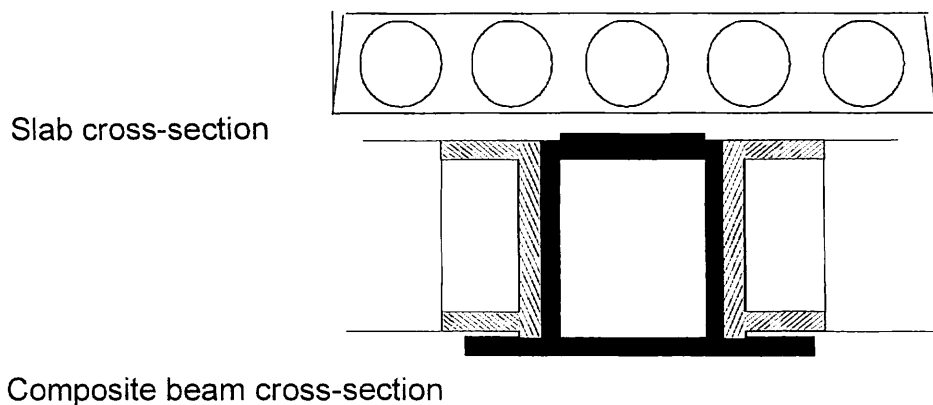
Ultimate loading except self weight 8,00 kN/m²

No topping

Variant 2A

Joint details:

Ultimate limit state: stresses in MPa, f_{ctd} = 1,6



Composite beam cross-section

σ ₁	σ ₂	τ ₁	τ _{2,eff}	σ _{ps}	σ _{ps} /f _{ctd}	Remarks
- 0,439	0,000	1,340	0,000	1,139	0,712	if rigid beam
- 0,365	18,030	1,340	0,000	1,170	0,731	at beam span
- 0,439	0,000	1,340	1,985	2,186	1,366	at beam support

$$\beta_f = 1,0 \text{ (no infill)} \quad \beta_{top} = 1,0 \text{ (no reinforcement)}$$

$$\tau_{2,top} = 0 \text{ MPa} \quad \tau_{2,imp} = 1,985 \text{ MPa}$$

$$\sigma_{ps}/f_{ctd} = 1,366 > 1,0 \rightarrow \text{too high}$$

The output has to be read as follows:

An effective transverse shear stress τ_{2,eff} is introduced, which is defined as

$$\tau_{2,eff} = \beta_f \cdot (\tau_{2,top} + \beta_{top} \cdot \tau_{2,imp})$$

The first line shows σ_1 and τ_1 , the stresses acting when the slab is rigid supported: be aware $\tau_2 = 0$. The condition $\sigma_{ps} \leq f_{ctd}$ is shown as $\sigma_{ps/fctd} \leq 1$.

The second line shows the stresses in the mid of the span of the beam as explained previously in this paper; debonding may be expected when $\sigma_2 > f_{ctd}$. The value is shown. The number of debonded strands is calculated according Table 3. The value of σ_1 shows whether there is a reduced prestressing force. The line is indicated as: at beam span.

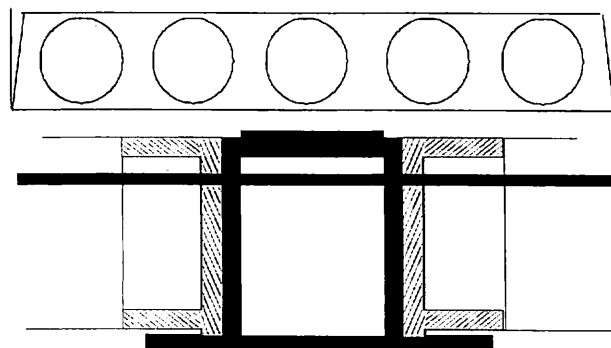
The third line shows the stress components acting in the critical cross-section considering the effects of flexible support of the hollow core slabs. The line is indicated as: at beam support. The maximal shear force due to imposed load is taken into account. When the ratio $\sigma_{ps} / f_{ctd} > 1$ additional actions or modifications in design are required. When reinforcing bars, infill of cores or a structural topping are taken into account, one can notice that $\beta \cdot \tau_2$ is changing. β is the correction factor for the influence of the previously mentioned modifications. As concluded from the first output, additional measurements are required.

Variant 2B

Joint details:

reinforcement 1 Ø 12 mm / 1,2 m

Slab cross-section



Composite beam cross-section

σ_1	σ_2	τ_1	$\tau_{2,eff}$	σ_{ps}	$\sigma_{ps/fctd}$	Remarks
-0,439	0,000	1,340	0,000	1,139	0,712	if rigid beam
-0,365	18,030	1,340	0,000	1,170	0,731	at beam span
-0,439	0,000	1,340	1,262	1,635	1,022	at beam support

$$\beta_f = 1,0 \text{ (no infill)} \quad \beta_{top} = 0,636 \text{ (reinforcement)}$$

$$\tau_{2,top} = 0,0 \text{ MPa} \quad \tau_{2,imp} = 1,985 \text{ MPa}$$

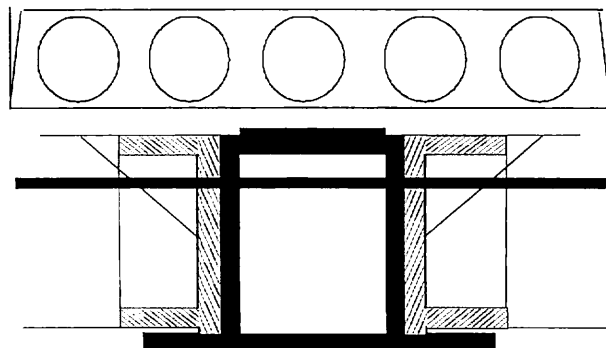
$$\sigma_{ps/fctd} > 1 \rightarrow \text{too high}$$

Variant 2C

Joint details:

reinforcement 1 Ø 12 mm / 1,2 m
 Partly filled with hollow cores.

Slab cross-section



Composite beam cross-section

σ_1	σ_2	τ_1	$\tau_{2,\text{eff}}$	σ_{ps}	σ_{ps}/f_{ctd}	Remarks
-0,439	0,000	1,340	0,000	1,139	0,712	if rigid beam
-0,365	18,030	1,340	0,000	1,170	0,731	at beam span
-0,439	0,000	1,340	0,992	1,463	0,914	at beam support

$$\beta_f = 0,7 \text{ (infill)} \quad \beta_{top} = 0,714 \text{ (reinforcement)} \\ \tau_{2,top} = 0,0 \text{ MPa} \quad \tau_{2,imp} = 1,985 \text{ MPa}$$

This solution meets the requirements.

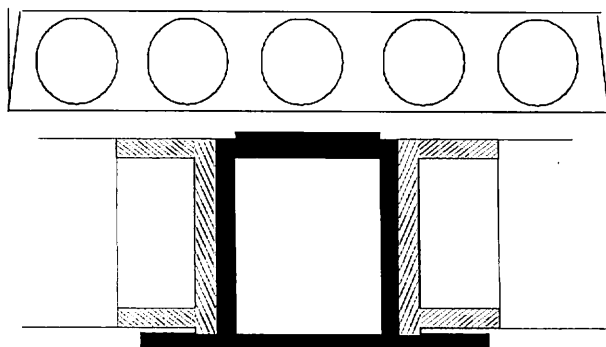
Example 3: based on computer program from Strängbetong Sweden

Data beam, slab, etc., are equal to those used in example 2.

Variant 3A

Ultimate loading except self weight: 8,00 kNm
 Topping (non structural) 50 mm

Slab cross-section



Composite beam cross-section

Joint details:

σ_1	σ_2	τ_1	$\tau_{2,\text{eff}}$	σ_{ps}	σ_{ps}/f_{ctd}	Remarks
-0,439	0,000	1,476	0,000	1,273	0,796	if rigid beam
-0,365	20,060	1,476	0,000	1,304	0,855	at beam span
-0,439	0,000	1,476	1,909	2,204	1,377	at beam support

> 1 too high

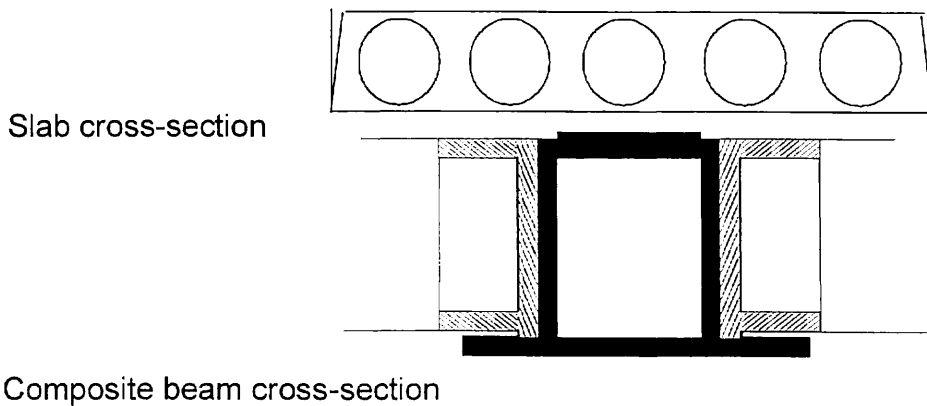
$$\beta_f = 1,0 \text{ (no infill)} \quad \beta_{top} = 1,0 \text{ (no reinforcement)}$$

$$\tau_{2,top} = 0,091 \text{ MPa} \quad \tau_{2,imp} = 1,618 \text{ MPa}$$

Variant 3B

Ultimate loading except self weight: 8,00 kNm
Topping (structural) 50 mm

Joint details: reinforcement in topping 125 mm²/m



σ_1	σ_2	τ_1	$\tau_{2,\text{eff}}$	σ_{ps}	σ_{ps}/f_{ctd}	Remarks
-0,439	0,000	1,329	0,000	1,128	0,705	if rigid beam
-0,365	19,640	1,329	0,000	1,159	0,724	at beam span
-0,439	0,000	1,329	-0,105	1,132	0,707	at beam support

$$\beta_f = 1,0 \text{ (no infill)} \quad \beta_{top} = 0,568 \text{ (reinforcement)}$$

$$\tau_{2,top} = 0,291 \text{ MPa} \quad \tau_{2,imp} = -0,326 \text{ MPa}$$

The structure meets the requirements.

3.8 References

Leskelä, M.V. (1993). "Slim-Floor Beams: Design Criteria and Structural Behaviour." *Proc., The Engineer. Found. Confer. Construction II, Potosi, Missouri, ASCE*, 182 - 197.

Leskelä, M.V. (1994). "Shear Flow Calculations for Slim-Type Composite Beams Supporting Hollow-Core Slabs." *Proc., Concrete 95 Conference: Steel-Concrete Composite Structures, Bratislava, ACCS*, 299-302.

Leskelä, M.V. & Pajari, M. (1995). "Reduction of the Vertical Shear Resistance in Hollow-Core Slabs when Supported on Beams." *Proc., Concrete 95 Conference*, Vol. 1, Brisbane, 559 - 568.

Pajari, M. & Yang, L. (1994). "Shear Capacity of Holow Core Slabs on Flexible Supports." Technical Research Centre of Finland, Espoo, VTT Research Notes 1587, 111 p + app. 26 p.

Pajari, M. (1995a). "Shear Resistance of Prestressed Hollow Core Slabs on Flexible Supports". Technical Research Centre of Finland, Espoo, VTT Publications 228, 132 p + app. 25 p.

Pajari, M. (ed.) (1995b). "Design Recommendations for Hollow Core Slabs Supported on Beams." Technical Research Centre of Finland, Espoo, Internal Report RTE37-IR-2/1995,22 p + app. 17 p.

Pajari, M. & Koukkari, H. "Shear Resistance of Prestressed Hollow Core Slabs Supported on Beams: Part: Tests." Accepted for publication by ASCE, Journal of Structural Engineering.

Pajari, M. " Shear Resistance of Prestressed Hollow Core Slabs Supported on Beams: Part II: Analysis." Accepted for publication by ASCE, Journal of Structural Engineering.

4 Floor Diaphragm Action

4.1 General

The stability of precast concrete buildings is provided in two ways. First the horizontal loads due to wind are transmitted to shear walls or moment resisting frames by the floor (or roof). In most instances this consists of individual precast concrete hollow core units, 1.2 m in width, as shown in Fig. 4-1. Secondly, the reaction forces resulting from the floor at each level are transmitted to the foundation. Where the distance between the shear walls is large, say more than 6 to 8 m, the floor has to be designed as a plate, or so called 'diaphragm', which must sustain shear forces and (frequently) bending moments. To achieve this, a 'ring beam', or series of 'ring beams', as shown in Fig. 4-1, is formed around the precast floor units to effectively clamp the slabs together to ensure the diaphragm action.

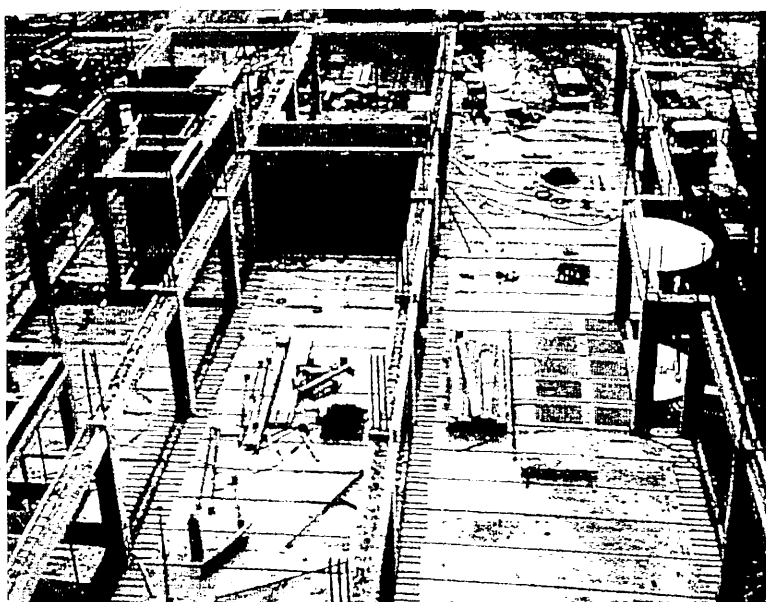


*Fig. 4-1: Precast concrete hollow core floor diaphragm in multi-storey construction.
(Courtesy Reinforced Concrete Council, UK)*

This chapter shows how to recognise such a diaphragm, how to determine the forces acting on it, and how to calculate its structural strength and stiffness. The results are validated by full scale experimental testing.

The way in which the diaphragm behaves depends on the plan geometry of the floor. The diaphragm may behave either as a truss, (Fig. 4-2 a) or Vierendeel girder, (Fig. 4-2 b), or more usually as a deep horizontal beam having a compression arch and tensile chord as shown in Fig. 4-2 c. It is assumed that no out-of-plane deformations are present; in this case these would be vertical deflections, and therefore seismic behaviour is excluded from the analysis presented here. As well as to wind loading, the floor diaphragm may also be subjected to additional horizontal forces, such as:

- horizontal forces due to lack of verticality of the structure which may be manifested as small restoring forces between the stabilising walls,
- temperature and shrinkage effects,
- in-plane, or catenary, forces as a consequence of abnormal loading, accidental damage etc.

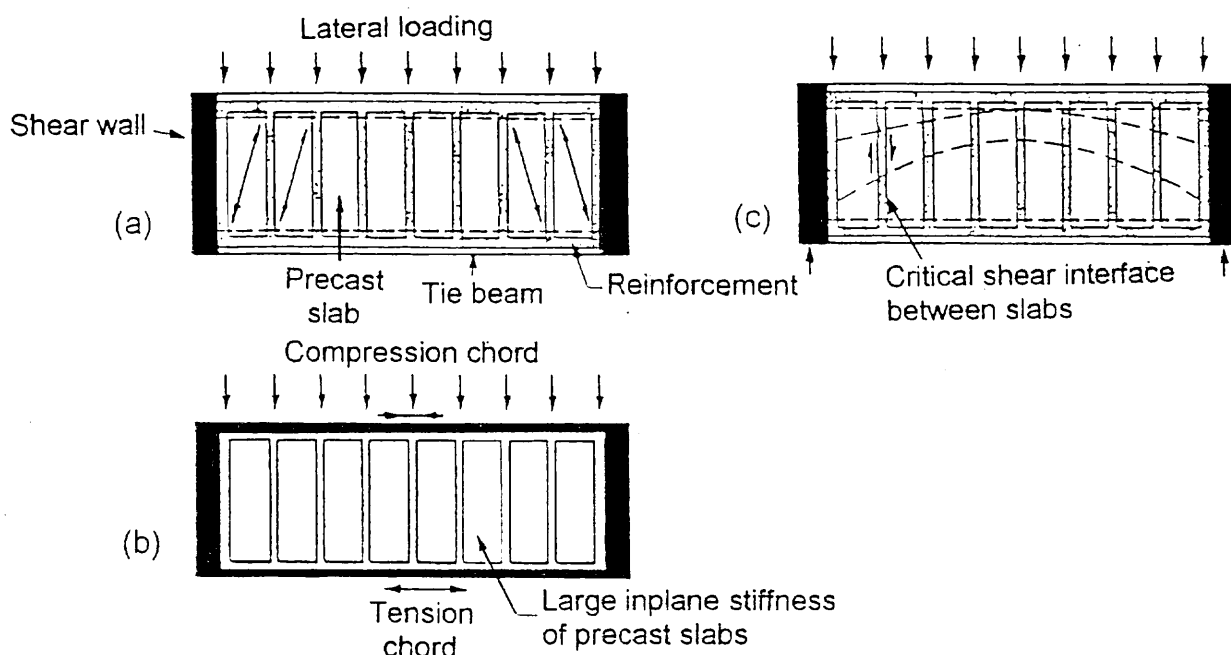


Fig. 4-2: Structural models used to analyse floor diaphragms.
(a) Diagonal truss, (b) Vierendeel girder, (c) Deep horizontal beam.

The structural walls or stabilising frames are supports for this analogous *deep beam* and the lateral loads are transmitted to these supports as reactions, which may be determined from any statical method of analysis. Besides the common situation of a single bay diaphragm supported on two end walls, several other examples of building layout are possible, as shown in Fig. 4-3 a. The diaphragm bending moments and shear forces may be calculated for the cases cited in Fig. 4-3 a and are as shown in the distributions in Fig. 4-3 b. The diaphragm must be checked in both directions, i.e. x and y planes, because the complementary shear stresses perpendicular to the direction of loading may be equally as important as those in the direction of the load.

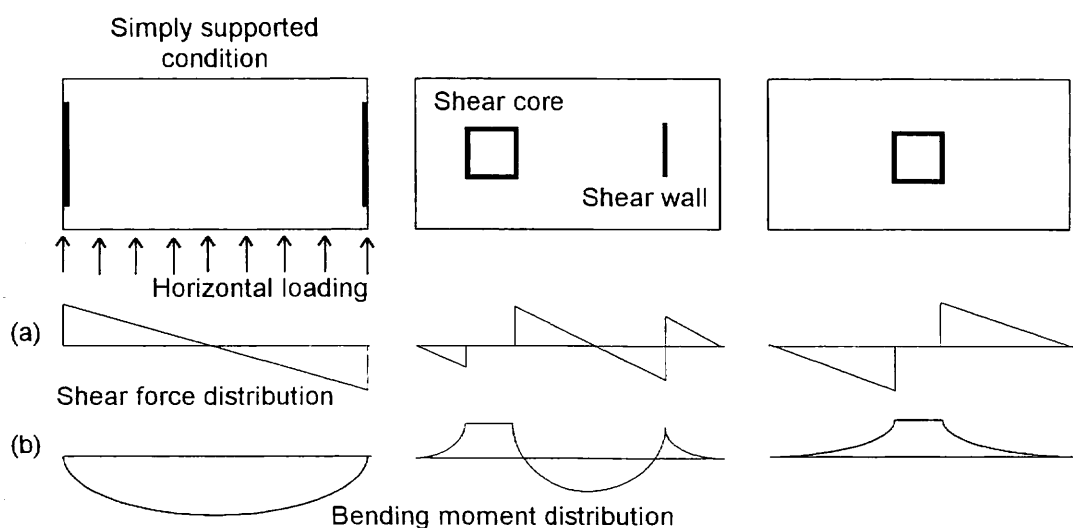


Fig. 4-3: (a) Plan geometry of floor diaphragms,
(b) Floor diaphragm shear forces and bending moments diagrams.

In multi-bay floors, where the slabs are spanning parallel to the direction of the applied load, as in Fig. 4-4 a, the shear flow V_h at the interior support between span l_1 and l_2 is given by:

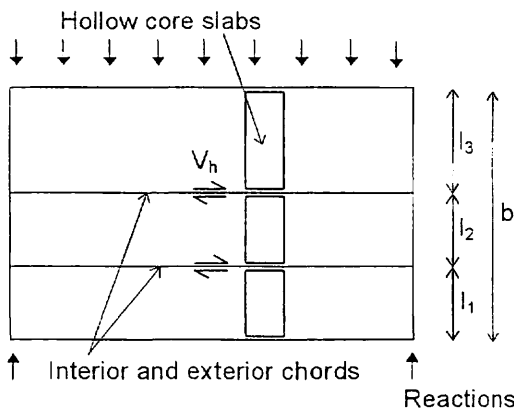
$$V_h = \frac{VS}{I} = \frac{6V(b - l_1)l_1}{b^3} \quad (4-1)$$

for $l_1 > l_3$, where V is the applied design shear force, S and I are the first and second moments of area at the joint concerned and b is the total length of the slabs in the diaphragm.

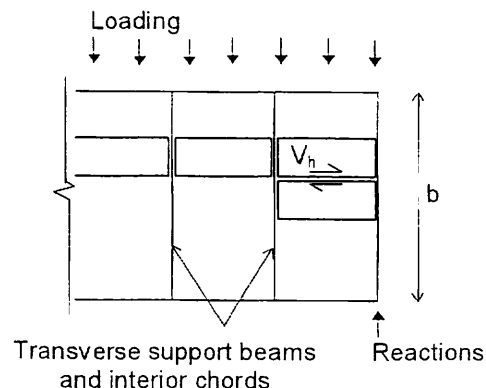
Where the slabs are spanning perpendicular to the direction of the applied load, (Fig. 4-4 b), it is assumed that the stiffness of the floor diaphragm is large and that the behaviour is similar to that of a rigid plate. In this case the maximum transverse shear flow between the slabs V_h occurs at the neutral axis of the entire floor diaphragm and is given by:

$$V_h = \frac{VS}{I} = 1.5 \frac{V}{b} \quad (4-2)$$

[a]



[b]



Shear force diagram

Shear force (V) diagram

(a) Floor span parallel to load

Fig. 4-4: Shear stresses in floor diaphragms

(b) Floor span perpendicular to load

If the floor diaphragm is subjected to horizontal bending, as shown in Fig. 4-5, the internal equilibrium is maintained by tension and compression chords. The forces in the chords may be mobilised either by adding *insitu* tie steel in the joints between the precast units, as described in Section 4.2, or may be provided as part of the supporting floor beams, e.g. steel UB, precast beam, RC beam, but ONLY if a mechanical connection is made between the slabs and beams. The tie force resisting bending is given by F_{tM} as follows:

$$F_{tM} = \frac{M_h}{z} \quad (4-3)$$

where M_h is the applied diaphragm moment and z is the lever arm. The value of z depends on the aspect ratio for the floor, and on the magnitude of the bending moment. Maximum values for z/b at the points of maximum bending are as follows [Bruggeling 1991¹]

b/l	z/b
< 0.5	0.9
$0.5 < 1.0$	0.8

Walraven [Walraven 1990²] proposes a constant value for $z/b = 0.8$, which is used in this document.

Where the aspect ratio $b/l > 1$ the behaviour will be closer to the strut and tied arch than either the deep beam or truss models. The tie force is given by:

$$F_{tM} = \frac{0.5V}{b/l} \quad (4-4)$$

as a diagonal compressive strut will develop across the floor.

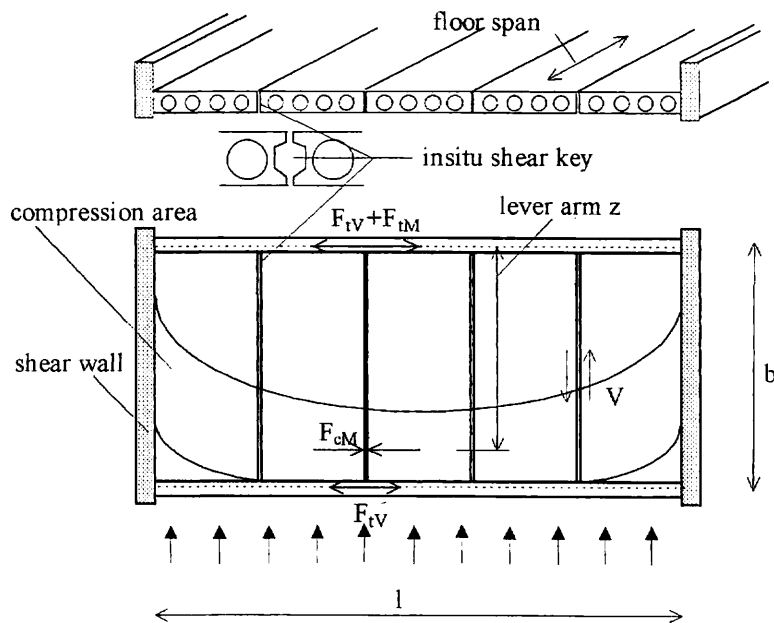


Fig. 4-5: Forces acting in a precast concrete floor diaphragm (according to deep beam theory).

The ties prevent the slabs from moving apart and simultaneously generate the clamping force F_{tV} , when the diaphragm is subjected to shear forces V , as shown in Fig. 4-5. The tie force is given by F_{tV} as follows:

$$F_{tV} = \frac{V}{2\mu} \quad (4-5)$$

where μ is the friction factor active in the longitudinal joints between the slabs, as given for the joints without indentations (plain joints) in Appendix 1.

If there are a number of floor bays resisting the shear force, it is assumed (owing to absence of confirmed data) that the tie force is shared equally between each of them.

In combined bending and shear, the maximum tie force is given by:

$$F_t = F_{\text{tr}} + F_{\text{M}} = \frac{V}{(n+1)\mu} + \frac{M_h}{z} \quad (4-6)$$

where: n is the number of floor bays resisting the shear force.

In a simply supported situation the maximum force occurs at a distance X from the nearest stabilising wall, where X is given by:

$$X = \frac{l}{2} - \frac{z}{n\mu} \quad (4-7)$$

Where: l is the distance between the stabilising walls.

The condition at this point is critical because precast units are often tied to the framing elements at the ends of the diaphragm in order to satisfy the structural stability requirements of the frame. This means that it is the interior joints which rely on the shear mechanism in the longitudinal joints. Finite element results have shown that the first and second interior joints are likely to fail before the end joint [de Roo, Straman 1991³].

The part of the supporting beam which is below the floor plate is ignored in computing shear resistances. Experiments have shown a much reduced capacity if the tie steel is placed below the floor [Svensson 1988⁴].

4.2 Shear Transfer Mechanism

Various structural models, including the finite element method, can be applied to model the shear transfer mechanism between the diaphragm and the stabilising walls (or frames). The behaviour of a precast hollow core floor diaphragm is different to that of a solid slab because the precast unit has large in-plane stiffness relative to that of the joints.



*Fig. 4-6: Cored section of the longitudinal joint between two precast units.
Note the segregation of aggregate at the bottom of the joint.*

Small shrinkage cracks appear at the interface between the precast and insitu concretes, as shown in Fig. 4-6, and the width of this crack (δ_{ti}) influences the effective shear area in the joint. The value of δ_{ti} depends on several factors, but the most influential are:

- the age of the precast units at the time the insitu concrete is placed
- the size of the longitudinal gap between the units
- the shrinkage of the insitu infill.

Table 4-1 gives data for δ_{ti} which are validated in tests [Elliott, Davies, Bensalem 1993⁵] where 50 %, 70 % and 80 % of the total shrinkage has taken place over the first 7, 28 and 90 days, respectively. The free shrinkage strain taken for the insitu infill is 600×10^{-6} .

Thus, the design of the diaphragm is essentially a problem of ensuring force transfer in the narrow precracked joints, as shown in Fig. 4-7. By considering the precast units as rigid ones (characterized by shear modulus G), an 'effective shear modulus' for the floor diaphragm may be computed, see Section 4.5.

Table 4-1. Initial crack widths to be used in the calculation of diaphragm strength and stiffness.

Age of precast unit when insitu concrete is cast (days)	Precast unit width (mm)	Width of longitudinal joint (mm)	Initial crack width δ_{ti} (mm)
< 7	1200	25	0.215
		50	0.230
	600	25	0.115
		50	0.130
28	1200	25	0.135
		50	0.150
	600	25	0.075
		50	0.090
90	1200	25	0.095
		50	0.110
	600	25	0.055
		50	0.070

Notes. 1. Infill concrete is of medium to high workability with a water to cement ratio of less than 0.6.
2. Linear interpolation permitted.

Shear resistance R (see Fig. 4-7) is a combination of:

- aggregate interlock in cracked concrete, by so called 'wedging action' and 'shear friction'. Fig. 4-7 b or global uneveness of slab edges; this is given by R_V
- dowel action through kinking and shear capacity of tie bars placed in the chords, given by R_d . Fig. 4-7 c.

Wedging action and shear friction mechanisms are much magnified in case of sinusoidal (wave like) shaped shear keys, like in the solution of M. Menegotto [Menegotto 1989 and 1988^{6,7}], see Section 4.7. Shear strength and stiffness is provided by aggregate interlock, and the structural integrity by dowel action of the reinforcing bars crossing the cracked interface. Aggregate interlock may be separated into two distinct phases, namely 'shear wedging' where the inclined surfaces either side of the crack are in contact, and 'shear friction' where the contact surfaces are being held in contact by the normal stress generated by the transverse tie force ΣF_{tw} .

Shear wedging provides a very high shear resistance, but is present only if the interfaces between the precast units and the insitu infill is intact. It relies on the adhesion and bond between the precast to insitu concrete interface and is exhausted when the width of the interface cracks is sufficient to cause an increase in the tie force ΣF_{tv} . It is influenced by the surface roughness of the slabs and shrinkage of the cast insitu infill concrete in the joints.

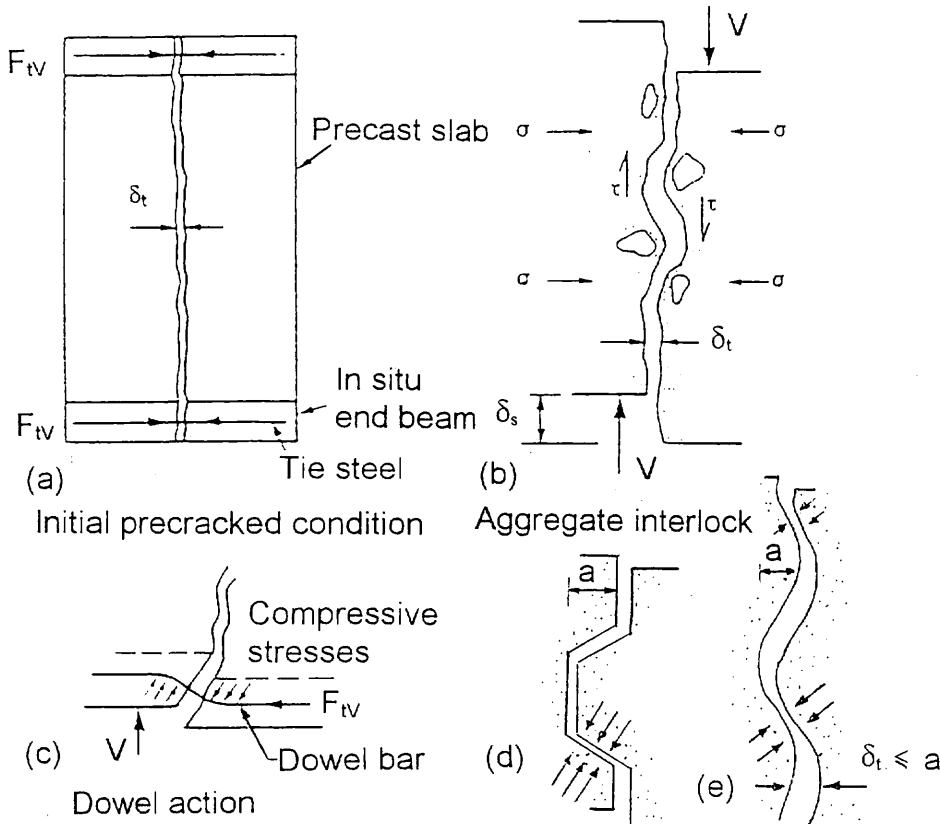


Fig. 4-7: Definitions of shear transfer mechanism, (a) Initial precracked condition, (b) Aggregate interlock mechanism, (c) Dowel action action mechanism, (d, e) Compressive strut mechanism

Shear friction also provides a high shear resistance. It is present when the both crack width and the tie force ΣF_{tv} are increasing. It too is influenced by the surface roughness of the slabs, but more by the amplitude of the crevices than by the profile. Except in the case of keyed profiles (Fig. 4-7d, e) friction is exhausted when the crack width exceeds a certain value; experimental tests show that this limit corresponds to about 2 to 3 mm, and is roughly equal to the amplitude of the surface crevices [Elliott, Davies 1993⁵].

Dowel action provides lower strength than the above but greater deformation capacity and ductility. It is influenced by the ability of the tie steel in the chords to resist shear forces by bending and kinking, and is dependent on the manner in which the tie steel is anchored to the precast slab and tied into the floor diaphragm. The edge profile of the precast slab has no influence on dowel action.

4.3 Edge Profile and Tie Steel Details

The most important feature of the floor diaphragm is the edge profile, shown in Fig. 4-8. The edge is not made deliberately rough, but the drag of the casting machine on the semi-dry mix creates a surface roughness vital to diaphragm action. These units have edge profiles, according to the details in Fig. 4-9, which permit the placement of insitu concrete (or grout) in

the longitudinal joints between adjacent units. Although different strengths of *insitu* concrete are used in practice, the lowest grade is usually B20 (cylinder strength) or C25 (cube strength). For the purpose of limiting shear stress, the joints may be considered 'plain' (i.e. uncastellated) and 'unreinforced'.

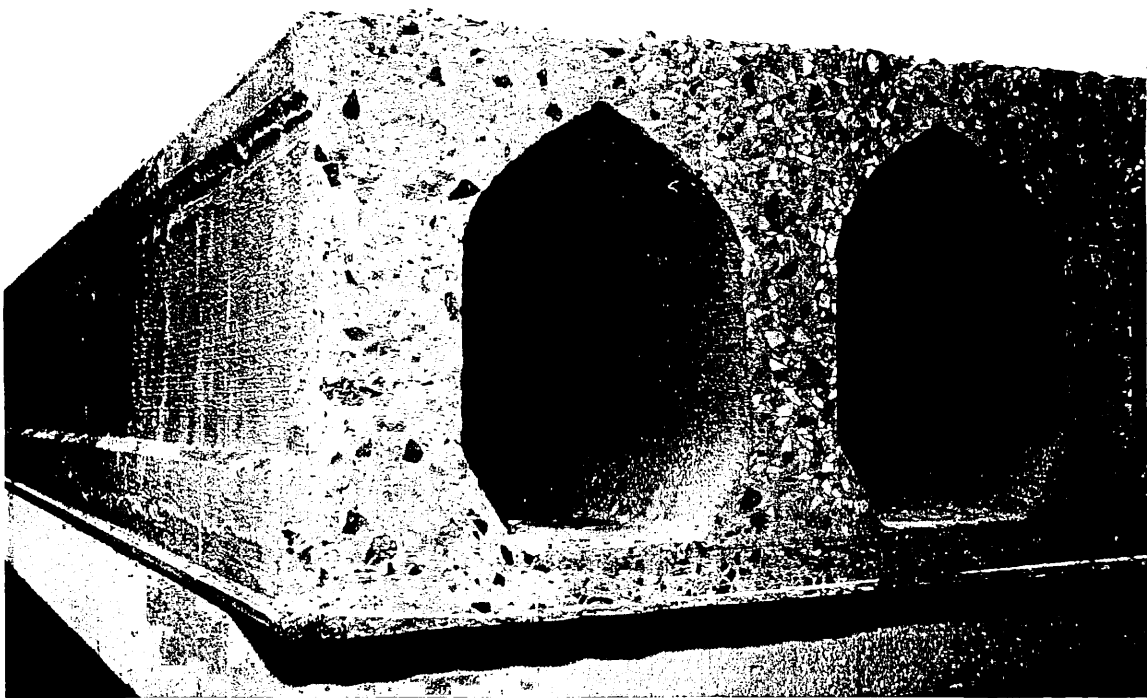


Fig. 4-8: Edge profile of slip-formed hollow core slab.

The precast units should be placed side by side such that there is no 'appreciable' gap between the units to allow shear-tension failure in the unreinforced *insitu* concrete. The size of this gap is not known, but its existence is thought to alter the shear failure mechanism by allowing diagonal tension to develop across gap which are more than 60 mm wide [Abdul-Wahab, Sarsam 1988⁸].

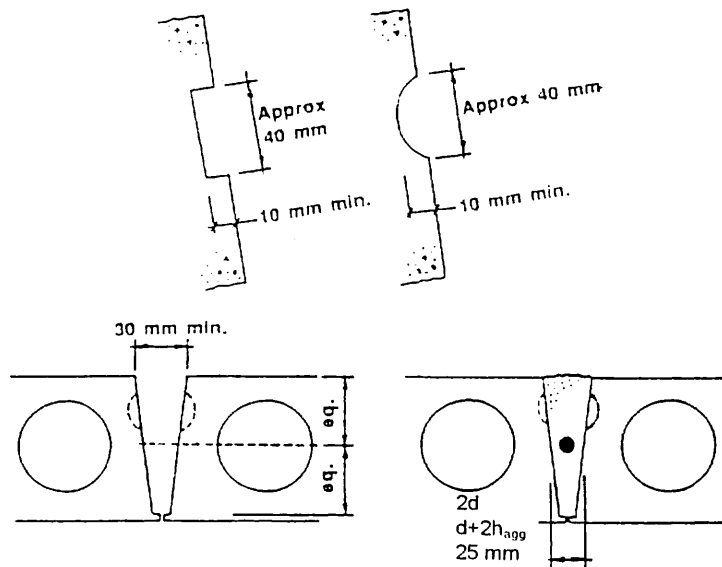


Fig. 4-9: Details of conforming longitudinal joints.

Tie steel is usually concentrated as one or two bars, placed at the mid height of the slab, see (Fig. 4-10 a). L-shape coupling bars should be tied to the continuous reinforcement, otherwise U-shape or straight bars should pass over the top of the tie bars. One leg of the coupling bar should be concreted into milled slots in the slabs, at positions which coincide with the second (or third) hollow core from the edges of the unit. A full bond length of at least $30 \times$ diameter of bar should be specified, and hooked ends used if the length of slot is excessively large, say more than 600 mm. The size of bar should be at least 10 mm diameter, and not more than 25 mm diameter. To prevent premature bond failure in the top of the insitu concrete infill the top cover to the bars should be at least 25 mm. Further details are shown in the FIP Handbook [FIP 1994⁹].

Details at longitudinal edges are shown in Fig. 4-10b where cut outs need to be made in the edges of the precast units at centres of between 2 m and 3 m, depending on the overall frame stability tie force requirements.

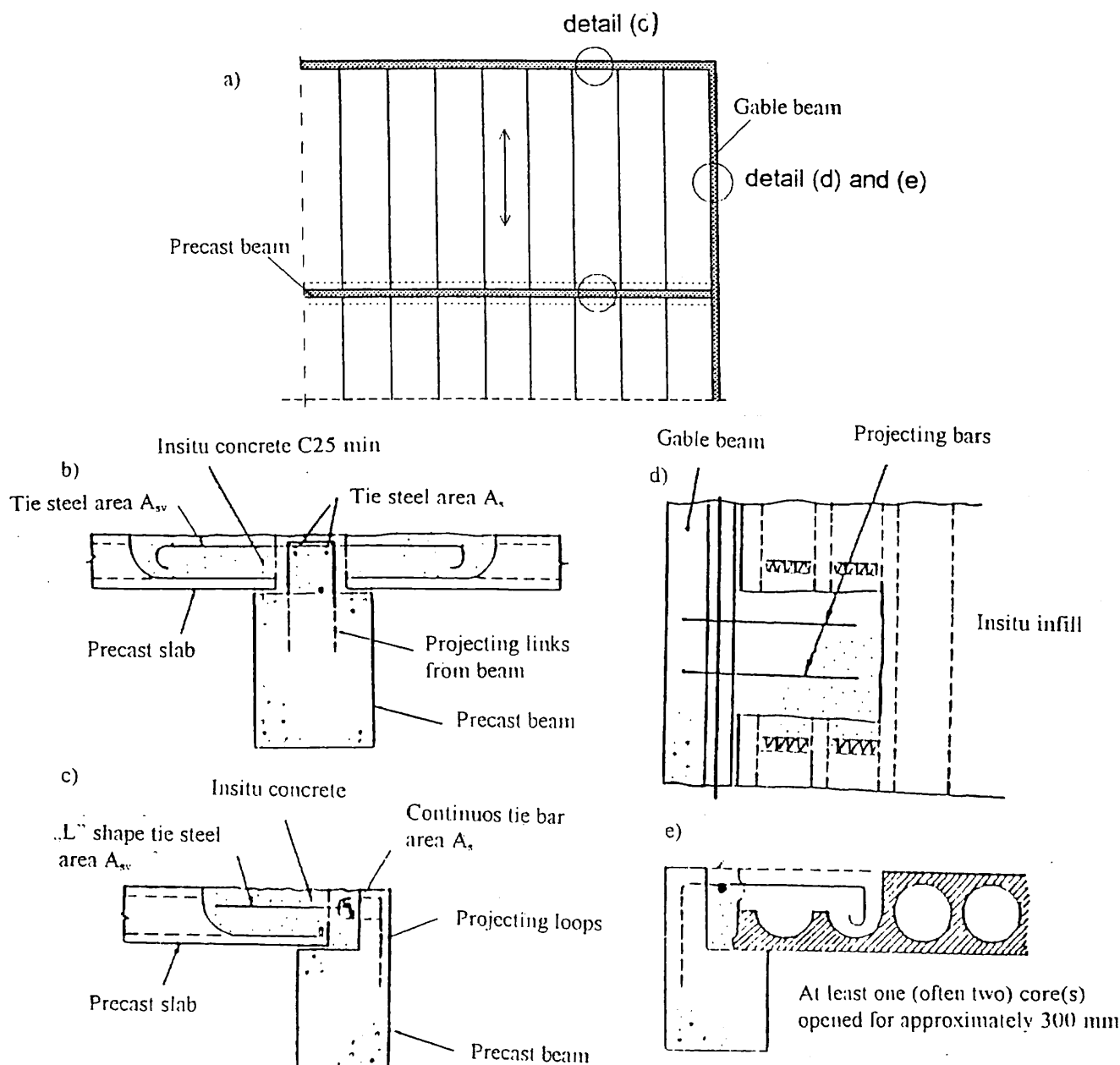


Fig. 4-10: Connection details to structural frame members (a) Plan of floor diaphragm (b, c) At ends of slab (d, e) At edges of slab

Although high tensile deformed bar (grade 410 to 500 MPa) is used mainly for the tie bars in the tension chord, it is becoming increasingly popular to reinforce the insitu perimeter strip using 7-wire helical prestressing strand (grade 1750 MPa). The favourable mechanical properties of this type of strand and long lengths available on site make it an attractive alternative to high tensile bar.

4.4 Calculation Model

4.4.1 General

The following sections explain how to calculate the horizontal resistance and stiffness of the floor diaphragm. The method is adopted from the theoretical work published in ref [Cholewicki¹⁰]. The aim of the calculation, concerning the ultimate limit state, is as follows:

- dimensioning of tie bars, of area A_s , to resist the peripheral or internal chord forces: the first ones are occurring due to combined action of the shear force V and horizontal moment M_h in the plane of diaphragm, the second ones are occurring due to action of shear force V only,
- dimensioning of the coupling bars, of area A_{sv} , to resist the transverse (complementary) shear forces,
- determination of the horizontal shear force resistance R_v and resistance to horizontal moment M_h in the plane of the diaphragm.

Concerning the serviceability limit state, the aim of the calculation is as follows:

- determination of the longitudinal shear stiffness K_s in the joints,
- determination of the horizontal shear modulus G of the floor,
- determination of crack widths δ_t in the joints between the precast floor units,
- analysis of local displacements and curvature deformations in the floor for use in conjunction with exterior facade tolerances, limitations etc.

The following input data are required:

- depth of hollow core floor slab t (this calculation is restricted to a floor diaphragm of constant depth),
- the total length b of the longitudinal joint, or the lever arm length z in the case of combined bending and shear,
- initial crack width δ_{ti} ,
- a wedging factor v , derived using experimental data,
- material properties f_c and μ' for the infill concrete in the longitudinal joint.

The calculation of the shear resistance involves the separate actions of:

- (i) shear wedging and shear friction, and
- (ii) dowel action.

Constitutive relationships shown in Fig. 11 explain the substantial differences between the shear wedging / shear friction model and the dowel action one (Section 4.2). Shear wedging / shear friction action is dominating within the range of very small transverse displacement (in the domain A to C). Walraven *et al* [Walraven, Reinhardt 1981¹¹] and Millard *et al* [Millard, Johnson 1984¹²] and Münger *et al* [Münger, Wicke, Rndl 1997¹³] show that the combined mechanism of aggregate interlock and dowel action may be used to predict the response of cracked concrete subjected to a shearing force. However, when calculating the areas of tie steel A_s and A_{sv} , (Fig. 4-10), the two effects are not additive.

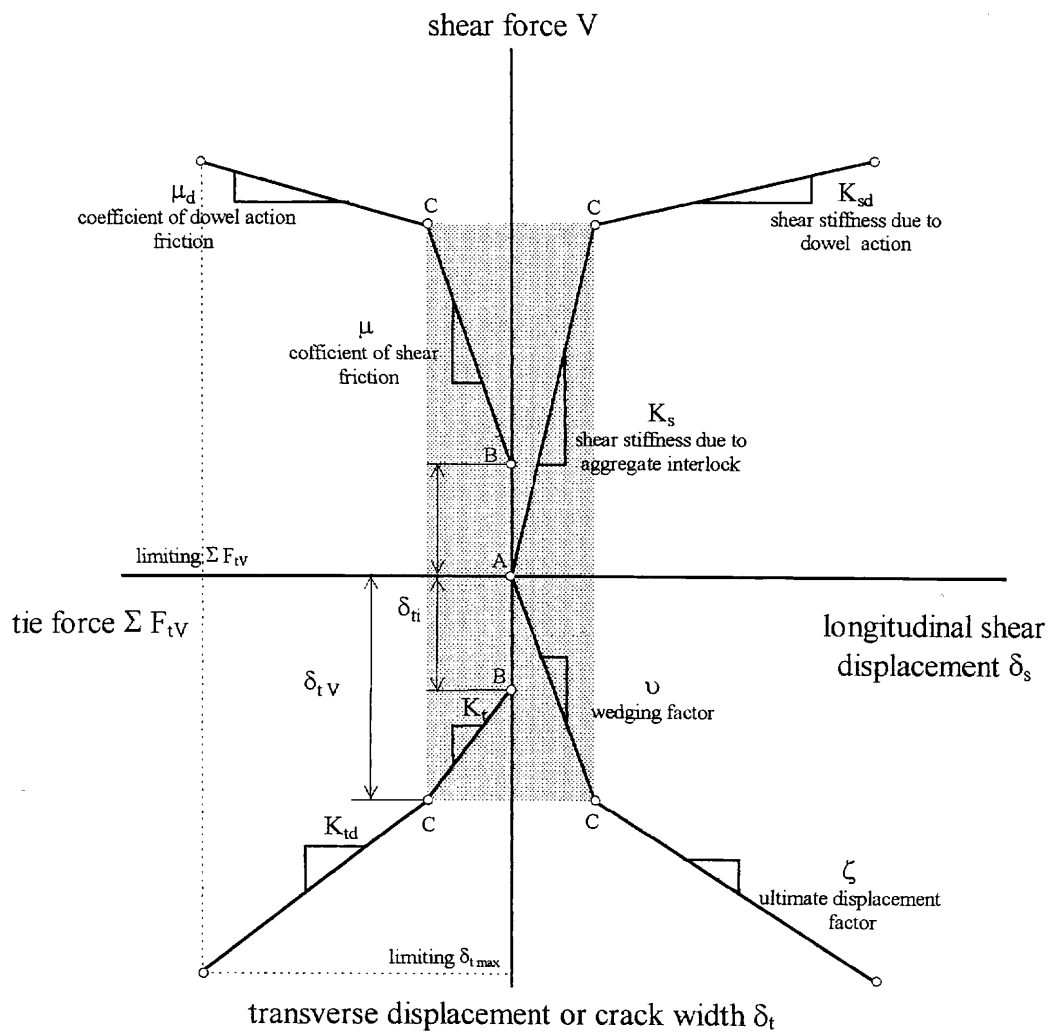


Fig. 4-11: Constitutive relationships between shear force V , transverse tie force ΣF_{tV} , longitudinal slip δ_s and transverse displacement δ_t .

4.4.2 Shear Wedging/Shear Friction Resistance

4.4.2.1 Strength due to Aggregate Interlock

Calculations for the capacity of the longitudinal joint, due to aggregate interlock, should prove that two following requirements are satisfied:

$$\tau_{v \max} = \frac{V}{A_{\text{eff}}} \leq \tau_u \quad (4-8)$$

$$\delta_{tV} = \frac{F_v}{K_t} + \delta_{ti} \leq \delta_{t \max} = 0,5 \text{ mm} \quad (4-9)$$

where:

- | | |
|-------------------|--|
| τ_v | applied shear stress |
| A_{eff} | effective shear transfer area |
| τ_u | maximum permitted design shear stress |
| δ_{ti} | initial crack width |
| $\delta_{t \max}$ | limiting crack width for aggregate interlock |

F_t maximum tie force (see formula [4-6])

K_t axial stiffness of the tie beam.

If even one from the above specified requirements is not satisfied the shear resistance R_d of the longitudinal joint should be determined according to dowel action model (see Subsection 4.4.3).

In computing τ_V , the effective depth of the diaphragm (see Fig. 4-6) can only be taken to the depth of the cast insitu / precast interface, i.e. $t - 30$ mm, in most types of hollow core slabs. The reason for this derives from observations made on the compaction of the insitu concrete in the joint [Elliott, Devies, Wahid Omar 1992¹⁴]. It is found that grout loss occurs in the bottom of the joint and that the lower 10 to 15 mm effectively remains ungrouted. Secondly, the lip at the bottom of the units, typically 10 to 15 mm deep, prevents full penetration, see (Fig. 4-6). The value also recognises that differential camber will be present - further reducing the net contact depth.

In many cases the point of maximum shear will coincide with minimum bending and therefore the full length b (Fig. 4-5) of the longitudinal joint may be used in calculating τ_V as follows:

$$A_{j\ eff} = b(t - 30) \text{ (mm units only)} \quad (4-10)$$

However where the maximum moment and shears coincide the length of the longitudinal joint is reduced to z (the lever arm) to allow for the decay in shear stress in the compression zone. Thus:

$$A_{j\ eff} = z(t - 30) \text{ (mm units only)} \quad (4-11)$$

The limiting value of τ_u is given in National Design Codes. Example values for τ_u are:

BS 8110 [15] $\tau_u = 0.23 \text{ N/mm}^2$

ACI 318 [16] $\tau_u = 0.275 \text{ N/mm}^2$

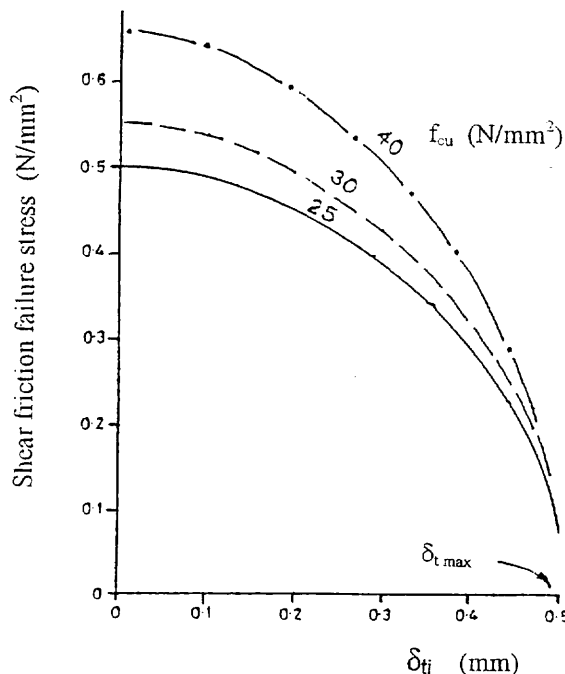


Fig. 4-12: Design graph for ultimate interface shear stress in longitudinal joints [14]

Eurocode 2 [18] formulates, indirectly, the maximum value of τ_u by following recommendation „ τ_{Rdj} “ for the average longitudinal shear between slab elements without indented joints should be limited to $0,1 \text{ N/mm}^2$ “

FIP Manual [17] $\tau_u = 0.14 \text{ N/mm}^2$ (i.e. working stress = 0.1 N/mm^2 and $\gamma_f = 1.4$)

EC2 [18] $\tau_u = 0.1 \text{ N/mm}^2$

In ref [14] a design graph for τ_u , (see Fig. 4-12) based on the maximum wedging displacement δ_t , has been derived.

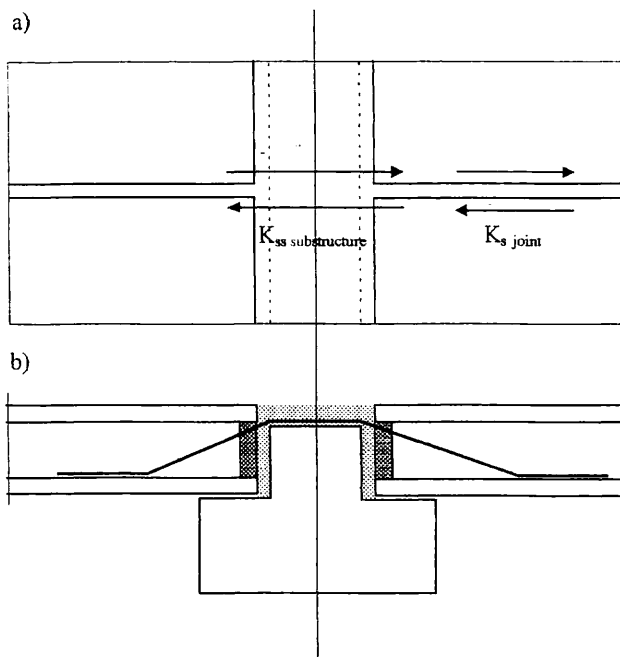


Fig. 4-13: Beam fulfilling the function of a shear member in the diaphragm (a) layout (b) section

In order to satisfy the requirement [8] the interaction of special shear members like the one shown in Fig. 4-13 can be taken into account. In such a case the value of the total shear force V generating F_{tM} force (see formula [4-5]) is reduced by the part of the substructure transferred by that shear member. The reduction of V is proportional to the ratios of shear stiffnesses K_{ss} of the shear member to the sum of the shear stiffnesses K_{ss} and the shear stiffness of the joint K_s .

The resulting compressive force F_{cM} , see Fig. 4-5, which is given by:-

$$|F_{cM}| = F_{tM} \quad (4-12)$$

brings two advantageous effects:

1° counteracts the tensile clamping force F_{tM} in the compressive tie beam

2° increases the resistance of the longitudinal joint, this effect can be considered in an equivalent way as the reduction of the applied shear force V . The requirement [4-8] will change to:-

$$\tau_{v\ max} = \frac{V - \sqrt{\mu} F_{cM}}{A_{j\ eff}} \leq \tau_u \quad (4-13)$$

where:

μ friction factor

Too high values of F_{cM} compressive force may result in the danger of local failure of a floor slab; the possibility of such failure should be eliminated according to principles foreseen for precast concrete structures subjected to alternating local compression.

In case of in plane moment action the requirement [4-9] will change to:

$$\delta_{t VM} = \frac{F_{tV} + F_{tM} \left(0,8 - \frac{1}{n_t \sqrt{\mu}} \right)}{K_t} + \delta_{ti} \leq \delta_{t max} = 0,5 \text{ mm} \quad (4-9a)$$

provided that: $\frac{F_{tV} + F_{tM}}{A_s} \leq f_y$

where:

n_t number of tie beams

4.4.2.2 Tie Steel Calculation

The axial stiffness of the tie beam, the one subjected to maximum tensile force (see formula [4-6]) should be large enough in order that the development length l_s is smaller than the width of a slab multiplied by coefficient 0,8, e.g. $l_{s max} = 0,8 \times 1,2 = 0,96 \text{ m}$. This distance, which is conservative, allows for the interference of shear transfer in the adjacent longitudinal joint.

Axial stiffness of the tie beam can be calculated according to following formula:

$$K_t = \frac{A_s E_s}{l_s} \quad (4-14)$$

where E_s is Young's modulus for tie steel, taken as 200 kN/mm² for bar and 190 kN/mm² for strand.

If K_t is insufficient to satisfy the requirement [4-9], A_s should be increased. The development length l_s is the least of:

$$l_s = 30 d \frac{A_s}{A_s \text{ provided}} \quad \text{for high tensile ribbed bar} \quad (4-15)$$

or

$$l_s = 54 d \frac{A_s}{A_s \text{ provided}} \quad \text{for mild steel plain bar} \quad (4-16)$$

and

$$l_s = 0,8 w \quad (4-17)$$

where:

w the width of the hollow core unit,

d the diameter of the bar.

The coupling bars of area A_{sv} cross the transverse joint between the floor slab and perimeter tie beam, see (Fig. 4-10 c). The effect of their deformation reduces K_t as follows:

$$K_t = \frac{E_s A_s A_{sv}}{l_s A_{sv} + l_{sv} A_s} \quad (4-18)$$

where:

l_{sv} bond length of the coupling bar.

If the edge beam remains in compression, i.e. when $|F_{cM}| > F_{tV}$, it is optional to include the stiffness of the concrete beam acting over the length of the hollow core unit in the expression for K_t . After the value of stiffness K_t is known the minimum tie steel A_s area can be calculated which should be applied to transfer the maximum total tensile force F_t denoted according to formula [4-6] and fulfilling the displacement limitation according to requirement [4-9].

4.4.2.3 Shear Stiffness due to Aggregate Interlock

The shear stiffness of a single longitudinal joint is given by K_s as follows:

$$K_s = \frac{V}{\delta_s} \quad (4-19)$$

According to the constitutive relationships in Fig. 4-11, K_s may be given by:

$$K_s = \mu \nu \Sigma K_t \quad (4-20)$$

where

μ friction factor (see Appendix 1)

ν wedging displacement factor

ΣK_t axial stiffness of tie reinforcement in all edge and interior beams

The wedging displacement factor ν concerns the increase in the transverse displacement, i.e. $\delta_t - \delta_{ti}$, where δ_{ti} is the initial crack width (see Table 1). The wedging factor is given by ν as:

$$\nu = \frac{\delta_t - \delta_{ti}}{\delta_s} \quad (4-21)$$

This factor is typically in the range $1 < \nu < 2$ (see Fig. 4-14), diminishing up to $\nu \ll 1$ if $\delta_t > 1$ mm. The relationship between δ_t and δ_s is as follows (see Fig. 4-14) [Elliott, Davies, Wahid Omar, 1992¹⁴]-

$$\delta_t = \delta_{ti} e^{(\beta \delta_s)} \quad (4-22)$$

where β is the gradient of a log δ_t vs. log δ_s graph and may be safely specified as $\beta = 3.0$. [Elliott, Davies, Wahid Omar, 1992¹⁴]. In order to determine δ_s a limit is imposed on δ_t . The test data show that a shear friction failure will occur when the crack width is limited to approximately 0.9 mm. Therefore a safe approach is given here to limit $\delta_{t max}$ to 0.5mm. Then

$$\delta_s = \frac{\log \frac{\delta_{t max}}{\delta_{ti}}}{\beta} \quad (4-23)$$

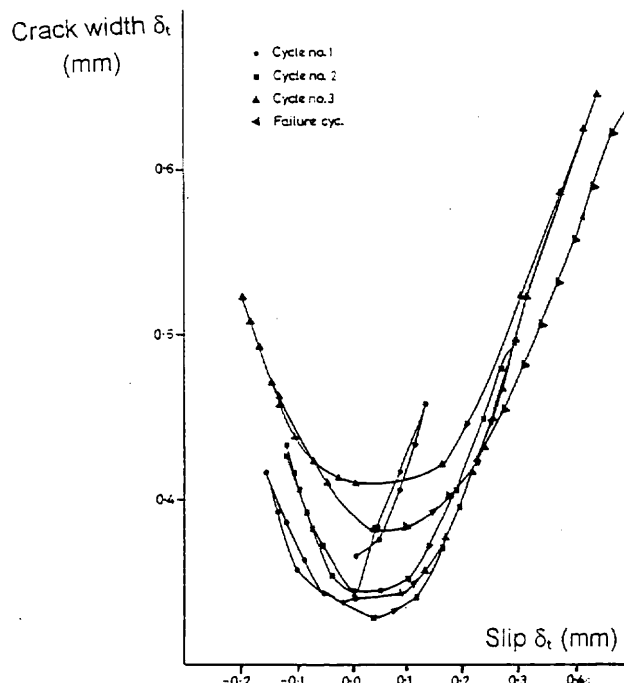


Fig. 4-14: Actual test data for crack width vs slip measurements [14]

4.4.3 Dowel Action

The term dowel action is used to describe the shear capacity of a reinforcing bar crossing a cracked plane. The behaviour is different for small and large displacements because of the breakdown of bond stress around the bar. At a relatively small displacement it can be assumed that the materials behave in an approximately linear elastic manner, which makes it possible to use a model based on an 'elastic foundation approach'.

4.4.3.1 Strength due to Dowel Action

If the applied shear force V is greater than the product of $A_{j,eff} \cdot \tau_u$ (see requirement [4-8]) the strength and stiffness of the diaphragm should be recalculated basing the design on the strength of the continuous reinforcement in the edge and interior beam(s). See (Fig. 4-15 a). This is called the dowel resistance, R_d .

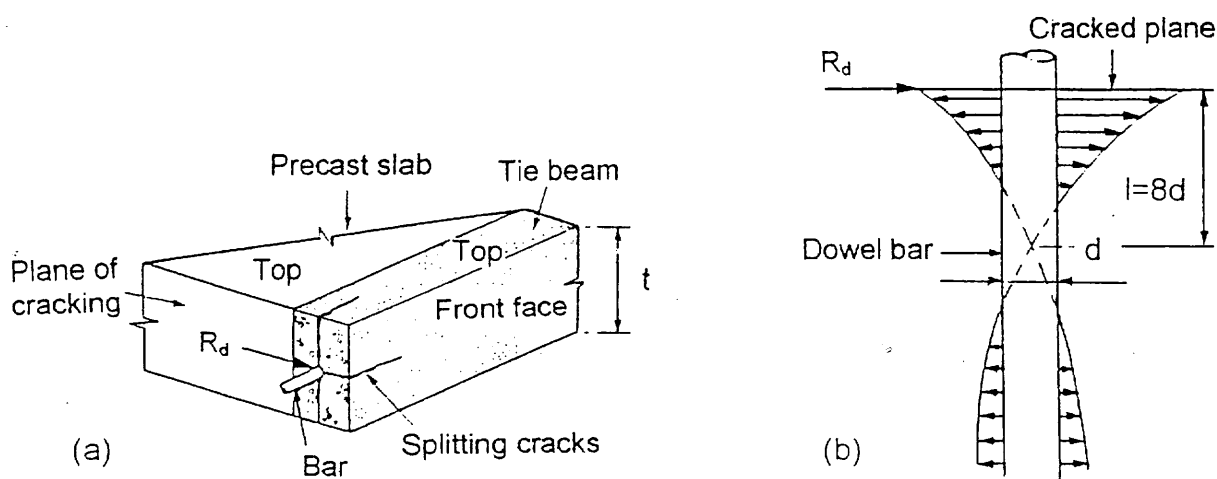


Fig. 4-15: Dowel action mechanism, (a) Splitting cracks around tie reinforcement at failure, (b) Stresses in the concrete around the bar in transverse section and stresses along the bar.

The magnitude of R_d may be determined by considering the resistance of the bar(s) when the insitu concrete fails by horizontal splitting; the shear strength of the bars themselves is never critical. Fig. 4-15 b shows the distribution of stresses in the transverse direction and along the length of the bar. When the concrete splits the resistance of the concrete is equal to a concrete splitting strength f_{ct} , which may be taken as $0.72\sqrt{f_{cu}}$ (i.e. about twice the normal code value) because of the large strain gradients across the critical section. The equilibrium of forces from (Fig. 4-15) gives the following [Elliott, Davies, Wahid Omar, 1992¹⁴]:

$$R_d \approx 4.0 n_t (t - kd) d f_{ct} \quad (4-24)$$

where

t depth of the edge beams,

n_t number of edge beams (at least 2),

d diameter of the bar,

k number of tie bars in each edge beams. Full scale experimental data [Elliott, 1996, Bensalem, 1996^{19,20}] confirm this result for bars diameters in the range 9 to 15 mm, and for concrete cube strengths of 25 N/mm² and 50 N/mm².

The calculations should show that the design shear force $V < R_d$.

4.4.3.2 Tie Steel Calculation due to Dowel Action

The steel area A_{sd} is given as follows:

$$A_{sd} = \frac{V}{\mu_d 0.6 f_y / \gamma_m} \quad (4-25)$$

where μ_d is the coefficient of friction for the effects of dowel action (a much lower value than for shear wedging). Hollow core slabs are considered as being untreated and smooth, hence $\mu_d = 0.7$. If vertical castellations of root depth 40 mm are present, then $\mu_d = 1.2$. The total area of steel is distributed equally between the number of tie beams present. The value 0.6 is the additional increasing coefficient for the shear resistance of a dowel.

4.4.3.3 Shear Stiffness due to Dowel Action

The shear displacement-force relationship is given by the sum of two parts, namely shear deformation of the concrete and bending of the steel bar. If the length of bar required for dowel action measured either side of longitudinal joint is $8d$ [Dulacska, 1972²¹], the total bending length is twice this distance $16d$, see (Fig. 4-15 b). Thus:

$$\delta_{sd} = \frac{V}{\frac{12E_s I_s}{(16d)^3} + 2\lambda^3 E_s I_s} \quad (4-26)$$

where

$$\lambda = \left\{ \frac{K_f d}{E_s I_s} \right\}^{0.25} \quad (4-27)$$

I_s is the second moment of area of the bar, d is the bar diameter, and K_f is the concrete deformability, taken as 500 N/mm³.



The transverse displacement δ_{td} is given by [Elliott, Davies, Wahid Omar, 1992^{14]}]

$$\delta_{td} = 0.3 + \zeta \delta_{sd} \quad (\text{mm units}) \quad (4-28)$$

where:

ζ = ultimate displacement factor determined empirically at the ultimate test load.

Taking the mean value from the eight tests by Wahid Omar [Elliott, Davies, Wahid Omar, 1992^{14]}] $\zeta = 0.15$.

At the ultimate limit state δ_{td} should not exceed a limiting crack width. If it does the area of steel must be increased in order to reduce δ_{sd} . A limit of $\delta_{td} < 1.0$ mm is suggested after taking surface roughness measurements in the edges of the precast units where the peak amplitude of the profile was in the order of 2 mm [Bensalem, 1996²⁰]. Shear stiffness of the joint is then:

$$K_{sd} = \frac{V}{\delta_{sd}} \quad (4-29)$$

4.4.4 Minimum Area of Tie Steel

The minimum tie steel A_{smin} (mm^2) is provided as a tie in EACH edge or internal beam. The tie should satisfy the perimeter of internal stability tie force F_T as determined from National Design Codes or FIP document [FIP 1988¹⁷] or Eurocode EC [Eurocode 2 1992¹⁸]

$$A_{smin} = \frac{F_T}{f_y/\gamma_m} \quad (4-30)$$

Note that $\gamma_m = 1.0$ in this situation. According to EC2 the minimum value of F_T in the edge beam should equal to larger value from following two ones: $|70| \text{ kN}$ or $\frac{(l_1 + l_2)}{2} |20| \text{ kN}$

4.5 Shear Stiffness of the Entire Diaphragm

The shear stiffness of the entire diaphragm is determined by the addition of the shear displacements δ_{si} in each longitudinal joint, see (Fig. 4-16). The effect of this displacement can be taken into account in approximative way by a reduction of shear modulus G as follows:

$$G^* = G \frac{wK_{si}}{wK_{si} + GA_{eff}} \quad (4-31)$$

where:

K_{si} shear stiffness of the joint i determined according to aggregate interlock or dowel action model

w width of each hollow core unit (usually 1,2 m)

A_{eff} contact area according to [4-10]

G shear modulus of insitu in fill concrete, typically grade C25.

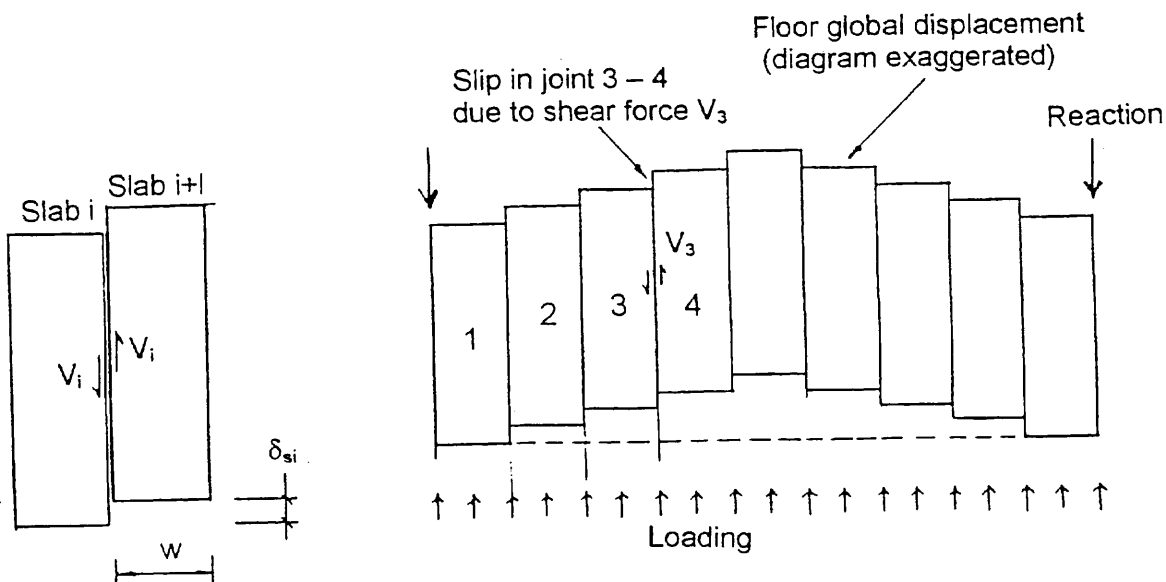


Fig. 4-16: Shear displacements in the total floor diaphragm.

4.6 Example Calculation

A longitudinal joint between adjacent hollow core units is subjected to design shear force $V=110\text{ kN}$. The purpose of this calculation is to determine the shear force capacity and the shear and transverse stiffness, and to design the transverse tie steel in the edge beams for the following data. It has been assumed that no bending moments are present and that the minimum edge beam tie force is 40 kN.

Depth of hollow core slab $t = 200 \text{ mm}$ Length of hollow core slab $b = 6000 \text{ mm}$

Initial crack width $\delta_{ti} = 0,2 \text{ mm}$ (table 1)

Final crack width, assumed primary to be equal $\delta_{tmax} = 0,5 \text{ mm}$

Number of tie beams $n_t = 2$

f_{cu} (infill concrete) = 25 N/mm^2 f_y (steel tie bars) = 500 N/mm^2 (high tensile ribbed bars)

E_s (steel tie bars) = 200 kN/mm^2

Wedging displacement factor $v = 1,5$ (see Fig. 4-14)

Maximum permitted design shear stress according to EC2, $\tau_u = 0,1 \text{ N/mm}^2$

$$A_{jet} = 6000 \cdot (200 - 30) \approx 1 \cdot 10^6 \text{ mm}^2$$

$$\text{Eq. 4-8} \quad \tau_{vmax} = \frac{110 \cdot 10^3}{1 \cdot 10^6} = 0,11 \frac{\text{N}}{\text{mm}^2} > 0,1 \frac{\text{N}}{\text{mm}^2}$$

The first one from two requirements [4-8] and [4-9] is primarily not satisfied therefore the further calculation is carried out in order to check more accurately the strength of the joint.

4.6.1 Aggregate Interlock

Strength calculation

$$\text{Eq. 4-23} \quad \delta_s = \frac{\log \frac{0,5}{0,2}}{3} = 0,3 \text{ mm} \quad \text{and} \quad \delta_{ti} = 0,2 \text{ mm}$$

$$\text{Eq. A. 4-7} \quad A_x = 0,5 (6,56 + 5,00) \times 10^{-3} = 5,78 \times 10^{-3} \text{ mm}^2/\text{mm}^2$$

$$A_y = 0,5 (17,40 + 1,25) \times 10^{-3} = 9,32 \times 10^{-3} \text{ mm}^2/\text{mm}^2$$

$$\text{Eq. A. 4-8} \quad f_c = 6,39 \times (25^{0,56}) = 38,75 \text{ N/mm}^2, \text{ and } \mu' = 0,4$$

$$\text{Eq. A. 4-5} \quad \tau = 38,75 (9,32 + 0,4 \times 5,78) \times 10^{-3} = 0,45 \text{ N/mm}^2$$

$$\text{Eq. A. 4-6} \quad \sigma = 38.75 (5.78 - 0.4 \times 9.32) \times 10^{-3} = 0.08 \text{ N/mm}^2$$

$$\text{Eq. A. 4-9} \quad \mu = \frac{0,45}{0,08} = 5,66$$

The value of μ is showing that the interface shear force is derived mainly from wedging rather than actual friction.

Restraining force

$$\text{Eq. 4-5} \quad F_{tV} = \frac{110}{2 \cdot 5,66} \cong 10 \text{ kN}$$

Use 1 no. 12 mm dia. tie bar in each edge beam (area = 113 mm² in each beam)

$$\text{Eq. 4-30} \quad A_{smin} \text{ per tie beam} = 40 \times 10^3 / 500 = 80 \text{ mm}^2 < 113 \text{ mm}^2 \text{ provided.}$$

$$\text{Eq. 4-15} \quad l_s = 30 \times 12 \frac{2 \cdot 80}{2 \cdot 113} = 254 \text{ mm} \ll 0,8 \cdot 1200 \text{ mm}$$

$$\text{Eq. 4-14} \quad K_t = \frac{113 \cdot 200 \cdot 10^3}{254} = 89 \frac{\text{kN}}{\text{mm}}$$

$$\text{Eq. 4-9} \quad \delta_{tV} = \frac{10}{89} + 0,2 = 0,31 \text{ mm} < 0,5 \text{ mm}$$

Calculations show that higher value of τ_u could be assumed (see the design graph in Fig. 4-12), although this is not permitted according to EC2. The requirement [4-9] is therefore satisfied.

Stiffness calculations:

$$\text{Eq. 4-20} \quad K_s = 5,66 \cdot 1,5 \cdot 2 \cdot 89 \cong 1510 \frac{\text{kN}}{\text{mm}}$$

As requirement [4-8] was not satisfied, the calculation according to dowel action model is here presented.

4.6.2 Dowel Action

Strength calculation:

$$f_{ct} = 0.72\sqrt{25.0} = 3.6 \text{ N/mm}^2$$

$$\text{Eq. 4-24} \quad R_d = 4.0 \times 2 \times (200 - 12) \times 12 \times 3.6 \times 10^{-3} = 65.0 \text{ kN} \text{ (for 2 no. edge beams)}$$

$R_d < V$, then increase bar diametr to 22 mm so that:

$$\text{Eq. 4-24} \quad R_d = 4.0 \times 2 \times (200 - 22) \times 22 \times 3.6 \times 10^{-3} = 112,78 \text{ kN} > V = 110 \text{ kN}$$

As expected the longitudinal strength R_d reduces dramatically when compared with R_v , the transverse force ΣF_{tV} increases evidently such that:

$$\text{Eq. 4-25} \quad A_{sd} = \frac{110 \cdot 10^3}{0,7 \cdot 0,6 \cdot 500} = 524 \text{ mm}^2 < 760 \text{ mm}^2 \text{ provided}$$

Stiffness calculation:

$$\text{Eq. 4-27} \quad \lambda = \left\{ \frac{500 \times 22}{200 \times 10^3 \times 11500} \right\}^{0.25} = 0.0468$$

$$\text{Eq. 4-26} \quad \delta_{sd} = \frac{110 \times 10^3}{\frac{12 \times 200 \times 10^3 \times 11500}{(16 \times 22)^3} + (2 \times 0.0468^3 \times 200 \times 10^3 \times 11500)} = 0.23 \text{ mm}$$

$$\text{Eq. 4-19} \quad K_s = 110 / 0,23 = 478 \text{ kN/mm}$$

$$\text{Eq. 4-28} \quad \delta_{td} = 0.3 + (0,15 \times 0,23) = 0,34 \text{ mm}$$

Total $\delta_t = 0,31 + 0,34 = 0,65 \text{ mm} < 1 \text{ mm permitted}$

4.6.3 Shear Stiffness of the Entire Diaphragm

Taking the lowest value of K_{si} , from the above, $K_s = 478 \text{ kN/mm}$ and the value of shear modulus of concrete $G = 10 \text{ kN/mm}^2$ the value of G^* calculated as

$$\text{Eq. 4-31} \quad G^* = 10 \cdot 10^3 \left[\frac{1200 \cdot 478 \cdot 10^3}{1200 \cdot 478 \cdot 10^3 + 1 \cdot 10^6 \cdot 10 \cdot 10^3} \right] = 600 \text{ N/mm}^2$$

Shear stiffness of the diaphragm is much reduced due to shear deformations of the longitudinal joints.

4.7 Experimental and Numerical Studies of Floor Diaphragms

Most of the experimental testing has been carried out in Scandinavia [22,23,24], Italy [6,7], UK [5,14,20,22,25], The Netherlands [26] and USA [27] and has involved either:

- (i) a detailed study of the shear behaviour of longitudinal joints between hollow core units [6,7,14,22,25-27], or
- (ii) testing of complete floor diaphragms subjected to shear, and shear and bending [5,22-24].

The numerical modelling has been carried out in Scandinavia [22] and The Netherlands [3,28]. Sarja [22] tested 5-slab diaphragms (i.e. 5 no precast units with 4 longitudinal joints) in 3-point bending. The results show that where the tie steel is 2 no. 10 mm diameter bars the lowest recorded shear stress is $\tau = 0.18 \text{ N/mm}^2$. The resulting average shear stress and bending moment at failure are given in Table 4-2. The results for the pure shear tests are clearly greater than in the case of combined bending and shear.

Table 4-2. Test Results on Hollow Core Floor Diaphragm in Bending and/or Shear [22]

Test ref	Loading regime	Tie steel bars	Shear force (kN)	Average shear stress (N/mm^2)	Bending moment (kNm)
1	3 point bending	2 x 10 mm	140	0.18	400
2			180	0.23	513
3			160	0.20	456
4			140	0.18	400
5	3 point bending	2 x 16 mm	247	0.32	705
6			287	0.37	819
7	pure shear	1 x 8	406	0.52	-
8			382	0.49	-

Table 4-3. Test Results on Hollow Core Floor Diaphragm in Shear [Elliott, Davies, Wahid Omar^{14]}

Test No.	No. of 12.5 mm strands	Dowel action present	Type of end beam*	In situ concrete cube strength f_{cu} N/mm ²	Initial crack width δ_{ti} mm	Shear stress and stiffness at shear friction failure Stress τ N/mm ²	Stiffness K_s kN/mm
1	1	Yes	Insitu	28	0.35	0.34	590
2	1	No	Insitu	28	0.24	0.38	1080
3	1	Yes	Insitu	27	0.27	0.25	1080
4	2	Yes	Insitu	29	0.11	0.41	4000
5	1	Yes	Precast	26	0.99	0.61	2870

* Insitu = 200 x 100 mm rectangular. Precast = 330 x 300 mm L shape.

Tests by Elliott *et al* [14,22,25] on 2-slab diaphragms (consisting of 4 m long x 200 mm deep units) recorded mean $\tau = 0.34$ N/mm², despite the presence of initial cracks in the interface up to 0.35 mm wide, see Table 4-3. In one test (Test 5) a reinforced precast concrete beam was used as the chord. The extra reinforcement in the beam increased both the strength and stiffness of the joint. Clamping forces normal to the precast floor units resulted in coefficients for the shear wedging and shear friction of at least $\mu = 5,0$.

Numerical finite element work by Sarja [22] showed the variation of the interface shear stress in the longitudinal joints. The largest stresses are due to compressive strut action and some arching stresses.

Bensalem [5,20] tested 4-slab diaphragms in such a way as to replicate the compressive arch action shown in Fig. 4-2 c. Under this regime is $\tau > 0.60$ N/mm². Moustafa [27] carried out similar tests on 3-slab diaphragms under reversible loading. The interface shear stresses at failure was $\tau_v = 0,1$ to $0,2$ N/mm² and shear friction factors were greater than 1.0.

Cederwall *et al* [23] tested 7-slab diaphragms in 4-point bending, and recorded $\tau = 0.14$ N/mm² in plain joints and 0.22 N/mm² in vertically indented joints, where the shear resistance was still active at crack widths of 3.1 mm.

Bensalem [20] has shown that the shear capacity is influenced by the roughness of the sides of the precast units. The roughness factor R_a is the arithmetical mean deviation of the edge profile (in mm), throughout the length of the precast unit. Values for R_a in typical hollow core production are between 0.2 mm and 0.3 mm. Shear tests were carried on slabs selected with different surface textures, and the resulting ultimate shear stress τ_u (N/mm²) expressed in terms of R_a (mm) is $\tau_u = 0.22 + 0.21 R_a$.

Menegotto [6,7] studied diaphragm action using precast units with undulated edge profiles Fig.[4-17] for the specific purpose of seismic activity. Approximately 30 samples, with three types of interface were tested according to so called pure shear models. The testing arrangement was characteristic because of the position of 4 restraining bars $d = 16$ mm being fixed outside of the shearing plane. That position of the restraining bars makes an essential difference in comparison to other pure shear tests in which the restraining bars were embedded in the tie beams (so remaining in the shearing plane). Similarly to other tests the joints were precracked.

The typical loading sequence was:

- first five cycles of small amplitude (slip displacements $\pm 1\text{mm}$)
- second five larger displacements ($\pm 10\text{mm}$)
- than final cycles of $\pm 20\text{mm}$.

The most important conclusions from that series of tests are:

- the average shear stress developed for displacements of $\pm 10\text{mm}$, in case of undulated profiled edges, was about $0,5 \text{ N/mm}^2$,
- very low figures characterize the strength and stiffness of the plain joints; the cycling loading brings a tremendous destruction of the wedging mechanism.

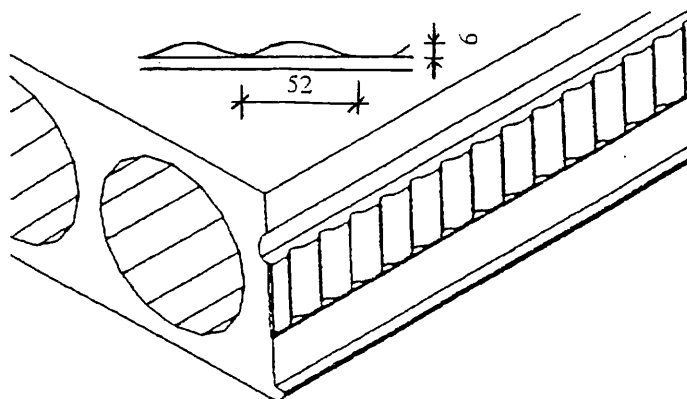


Fig. 4-17: The slab with undulated sinusoidaly edge - Menegotto tests [6] [7]

Tests on full-scale decks composed of five floor slabs, were carried out by M. Menegotto [6] [7] (see Fig. 4-17 and 4-18). The test showed that it is possible to use untopped deck with grouted joints as rigid diaphragms even under sever conditions (seismic action). The behaviour of longitudinul joints between slabs is sufficiently ductile and characterized by low sensitivity to cycling fatigue. This kind of the joint behaviour is guaranteed by the sinusoidaly profiled slabs edges and by the tie reinforcement bars which amount can be established according to following proposals [Menegotto 29]:

- pure friction coefficient $\mu' = 0,35$ (parallel to the waves)
- friction factor (incorporating improved wedge effect in case of sinusoidal profilation) $\mu = 0,50$.

Straman [28] and De Roo [3] modelled a large precast diaphragm consisting of precast units, longitudinal mortar joints, and transverse tie beams. The span to deflection ratio for the floor at failure was approximately 1/4000. Failure was due to yielding of the edge ties, with a factor of safety of 3.13 with respect to the design strength. The maximum compressive stress obtained was 3.6 N/mm^2 , and $\tau > 0.4 \text{ N/mm}^2$. The compressive stresses formed a triangular distribution giving a lever arm factor of 0.97, which suggests that the proposed value of 0.8 is conservative (see Section 4-1).

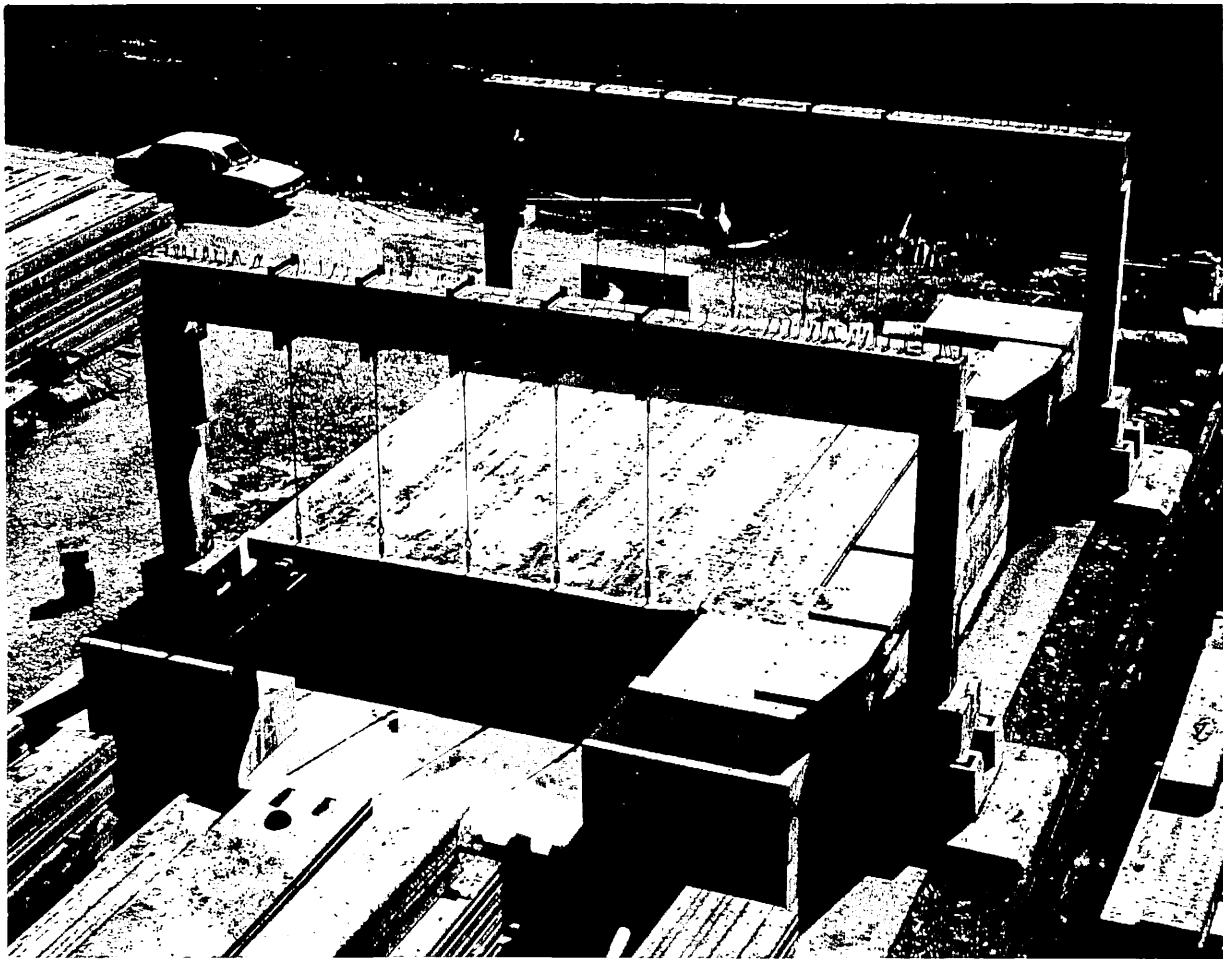
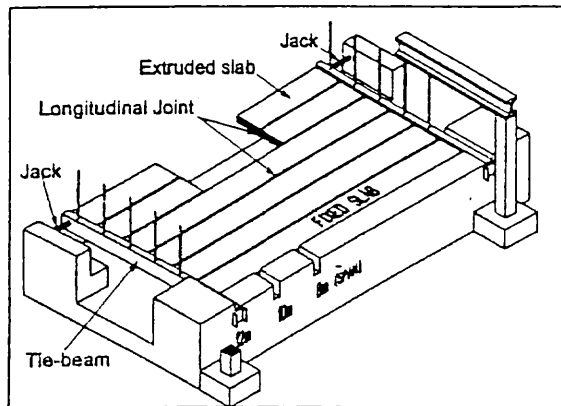


Fig. 4-18: Full - deck tests of M. Menegotto [6,7]

Appendix 1.

Analytical derivation of τ and σ values and friction factor μ .

The matrix may be assumed to be rigid-plastic with a yield stress f_c . Thus considering the stresses at the aggregate interface in Fig. 4-A-1[c]:

$$\tau' = \mu' f_c \quad (4-A.1)$$

where μ' is the coefficient of friction for the two phase model. Note μ' and τ' refer to the two-phase model only, not to the full longitudinal joint. The resultant radial and tangential forces F_r and F_{tan} derived from the radial stress f_c and the shear stress τ' are (Fig. 4-12 c):

$$F_r = 2 f_c R \sin \theta \quad (4-A.2 \text{ a})$$

and

$$F_{tan} = 2 \tau' R \sin \theta = 2 \mu' f_c R \sin \theta \quad (4-A.2 \text{ b})$$

In the longitudinal direction the components of F_r and F_{tan} are:

$$F_{rx} = 2 f_c R \sin \theta \cos \alpha \quad (4-A.3 \text{ a})$$

$$F_{tanx} = 2 \mu' f_c R \sin \theta \sin \alpha \quad (4-A.3 \text{ b})$$

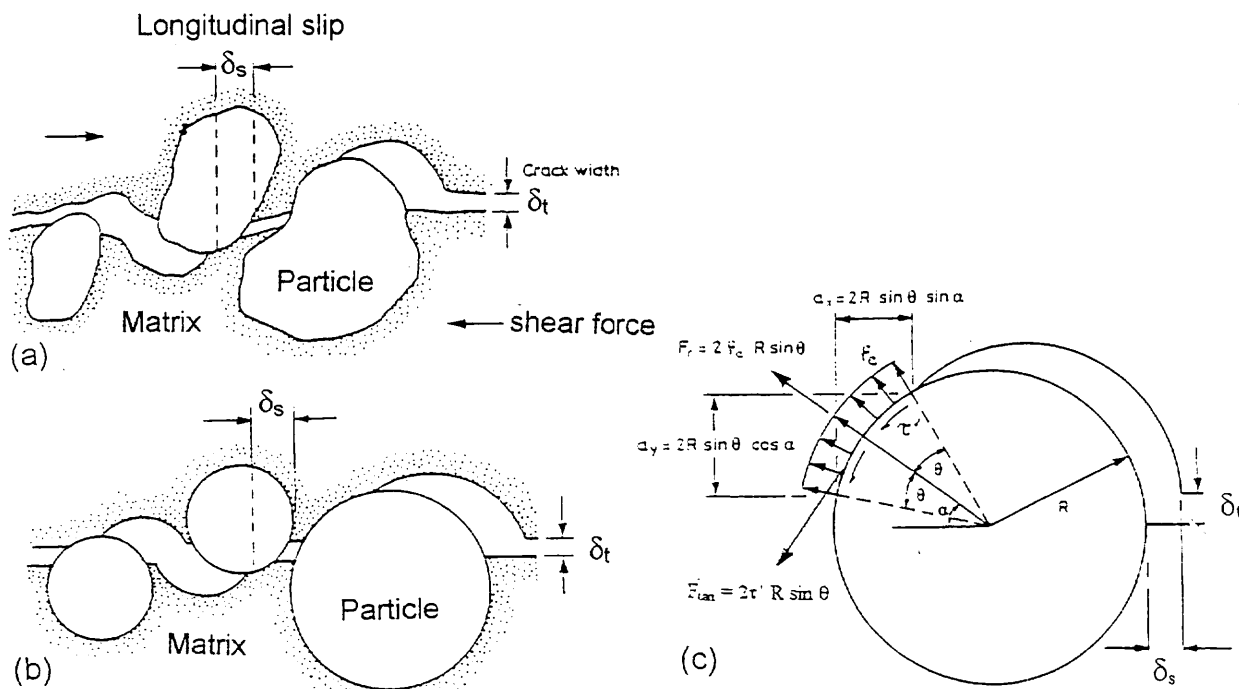


Fig. 4-A-1: Crack interface according a „two phase“ model, (a) Section perpendicular to crack plane, (b) Idealised „two phase“ model, (c) Stresses in a single aggregate particle.

The projected contact area in the longitudinal direction is $A_x = 2 R \sin \theta \sin \alpha$, such that the summation of the reaction forces F_x in this direction is equal to the shear resistance R_v as follows:

$$\Sigma F_x = f_c (\Sigma A_y + \mu' \Sigma A_x) = R_v \quad (4-A.4)$$

Dividing by the area of the crack plane A , gives the average shear stress resistance $\tau = R_v/A$ in the interface as follows:

$$\tau = f_c (A_y + \mu' A_x) \quad (4-A.5)$$

Where A_x and A_y are the total projected areas per unit area of crack plane along and transverse to the crack. A similar analysis of the forces acting normal to the interface gives the normal stress (y coordinate) $\sigma = \Sigma F_y / A$ as follows:

$$\sigma = f_c (A_x - \mu' A_y) \quad (4-A.6)$$

Using the test data from eight full scale tests by Elliott et al [14,22,25] A_x and A_y may be expressed empirically as a function of the cracked width δ_t and the slip δ_s as follows:

$$\begin{cases} A_x \\ \text{or} \\ A_y \end{cases} = 0.5 \left\{ \frac{\alpha_1 \delta_s}{\alpha_2 + \delta_s} + \frac{\alpha_3 \delta_t}{\alpha_4 + \delta_t} \right\} \quad (4-A.7)$$

for A_x : $\alpha_1 = 0.008$; $\alpha_2 = 0.067$; $\alpha_3 = -0.004$; $\alpha_4 = -0.9$ and

for A_y : $\alpha_1 = 0.022$; $\alpha_2 = 0.080$; $\alpha_3 = -0.001$; $\alpha_4 = -0.9$.

Values for f_c and μ' have been determined empirically by Walraven [11] and given as:

$$f_c = 6.39 f_{cu}^{0.56} \quad \text{and} \quad \mu' = 0.4 \quad (4-A.8)$$

Therefore the friction factor is equal to:-

$$\mu = \frac{\tau}{\sigma} \quad (4-A.9)$$

References

- 1 Bruggeling, A.S.G. and Huyghe, G.F., Prefabrication With Concrete, Balkema, Rotterdam, 1991, 380pp.
- 2 Walraven, J.C., Diaphragm Action in Floors, Prefabrication of Concrete Structures, International Seminar, Delft University of Technology, Delft University Press, Oct. 1990, pp 143-154
- 3 De Roo, A. M., Straman, J. P., Krachtsverdeling in en Vormverandering van een in Synvlak Belaste Prefab Vloerconstructie, PhD thesis, Delft Precast Concrete Institute, Delft University of Technology, 1991.
- 4 Svensson, S., Skivverkan i Elemenbyjalklag, Publication 88:1, Chalmers Technical University, Goteborg, Sweden, 1988.
- 5 Elliott, K.S., Davies, G. and Bensalem, K., Precast Floor Slab Diaphragms Without Structural Screeds, Concrete 200 - Economic and Durable Construction Through Excellence, Dundee, Sept 1993, pp 617 - 632
- 6 Menegotto, M., Seismic Resistant Extruded Hollow Core Slabs, International Symposium on Noteworthy Developments in Prestressed and Precast Concrete, Singapore, November 1989
- 7 Menegotto, M., Hollow Core Floors Tests for Seismic Action, FIP Symposium, Jerusalem, Sept 1988, pp 477 - 484.
- 8 Abdul-Wahab, H. and Sarsam, S., Strength of Vertical Plane Joints Between Large Precast Concrete Panels, The Structural Engineer, Vol 66, 14, July 1988.
- 9 FIP Recommendations, Planning and Design of Precast Concrete Structures, FIP Commission on Prefabrication, SEKO, Institution of Structural Engineers, London, May 1994.

- 10 Cholewicki, A., Shear Transfer in Longitudinal Joints of Hollow Core Slabs, Concrete Precasting Plant and Technology, B + FT, Vol 57, No4, April 1991, pp 58 - 67.
- 11 Walraven, J.C. and Reinhardt, H.W. 'Concrete mechanics: Part A: Theory and experiments on the Mechanical Behaviour of Cracks in Plain and Reinforced Concrete Subjected to Shear Loading', Heron, 26, No.1A, 1981, pp 1-68.
- 12 Millard, S.G. and Johnson, R.P. 'Shear Transfer Across Cracks in Reinforced Concrete due to Aggregate Interlock and to Dowel Action', Magazine of Concrete Research, 36, No.126, March 1984, pp9-21.
- 13 Münger F., Wicke M., Rndl N. „Design of shear transfer in concrete-concrete composite structures” International Conference „Composite Construction - Conventional and Innovative” IABSE and other organizations Innsbruck 1997.
- 14 Elliott K.S., Davies, G. and Wahid Omar, Experimental and Theoretical Investigation of Precast Hollow Cored Slabs Used as Horizontal Diaphragms, The Structural Engineer, Vol. 70, No.10, May 1992.
- 15 British Standards Institute, BS8110, The Structural Use of Concrete, BSI, London 1985.
- 16 ACI 318, Building Code Requirements for Reinforced Concrete, Detroit, American Concrete Institute, 1977.
- 17 FIP Recommendations, Precast Prestressed Hollow Cored Floors, FIP Commission on Prefabrication, Thomas Telford, London, 1988, 31pp.
- 18 Eurocode2 „Design of concrete structures” part 1-3 „Precast concrete elements and structures”, ENV 1992-1-3
- 19 Elliott, K. S., Multi Storey Precast Concrete Framed Structures, Blackwell Science, May 1996, 624 pp.
- 20 Bensalem, K., Structural Integrity of Precast Concrete Hollow Core Floor Diaphragms, PhD thesis, University of Nottingham, 1996.
- 21 Dulacska H., Dowel Action of Reinforcement Crossing Cracks in Concrete, Journal, American Concrete Institute, Vol.69, No.12, 1972, pp754-757.
- 22 Sarja, A., Analysis of the Statical In-plane Behaviour of Prefabricated Hollow Core Slabs Field, Concrete Laboratory Report No 51, Espoo, Finland, June 1978, 36pp.
- 23 Cederwall, K., Svensson, S. and Engstrom B., Diaphragm Action of Precast Floors with Grouted Joints. Nordisk Betong, Feb 1986, pp123-128.

5. Floors under seismic action

5.1 General

Earthquakes act upon buildings as a motion applied at their base, which causes the building structure to move accordingly.

If structures were rigid bodies, they would follow the ground displacement as a whole without deformation. In fact, as they are deformable, they usually respond with an amplified motion (Fig. 5.1).

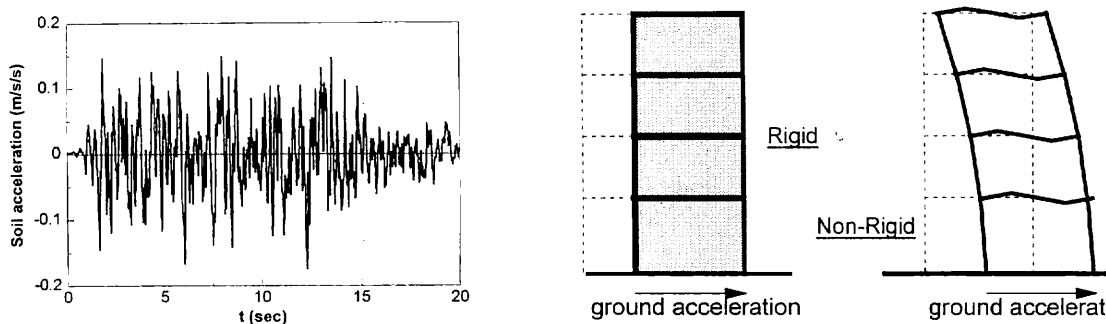


Fig. 5.1: Accelerogram. Rigid (left) and deformable (right) response of structures.

The forces transmitted through the structure are related to many parameters, dependent both on ground motion and on structural behaviour.

The expected intensity of an earthquake is uncertain. Therefore, it is recommended first to design qualitatively sound and robust structures. Quantitative design values of actions are given by codes.

The design earthquake may be defined by a given accelerogram (Fig. 5.1) or through its frequency content and the peak acceleration. "Response spectra" may also be used for synthesising typical accelerograms.

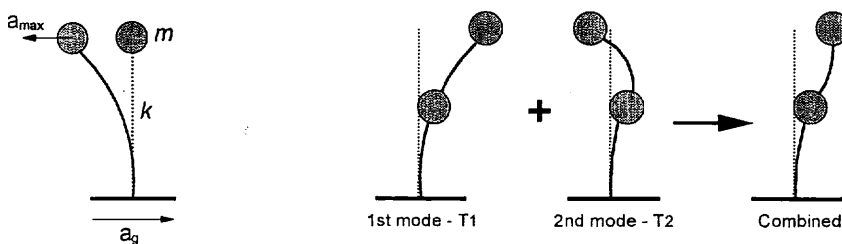


Fig. 5.2: One d.o.f. (left) and Two d.o.f.'s Structures (right).

As a more simple alternative to carrying out a dynamic analysis, its effects are often given in the form of design forces, derived from the site's data and the structure's main response parameters, self vibration periods and modes (Fig. 5.2) and ductility (Fig. 5.4).

Seismic forces have vertical and horizontal components.

Generally, structures are less sensitive to the former. Vertical components (up- and downwards) rarely affect well designed structures, which are generally able to withstand both overloading and deloading.

However, the combination of vertical and horizontal actions may be significant. In prefabricated structures for example, where friction is relied upon for the function of a joint under normal circumstances, the temporary removal of vertical load may lead to joint failure. Physical means of restraint should therefore always be provided in the form of ties. For a structure to remain within the elastic range during an earthquake, it would need to be designed with unrealistically high factors of safety, at least for any structure other than very low rise building. In actual fact, the horizontal force could well be greater than the force due to gravity.

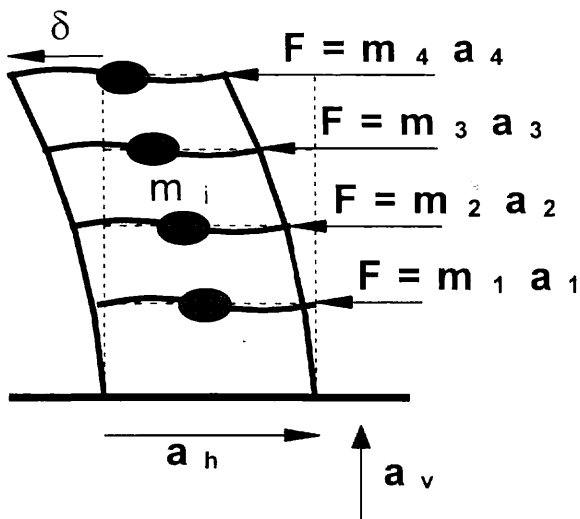


Fig. 5.3: Equivalent design (horizontal) forces.

Thus, safety standards are generally set such that, in normal cases, a structure should not collapse under the strongest (rare) earthquakes but could suffer even large damage, which is reasonable and economic; whereas, under low-intensity earthquakes there should not be any significant structural damage, i.e., all members should remain in the elastic range.

The relevant feature preventing the structure from collapsing during strong quakes, in spite of large damage, is the *ductility*.

Ductility is the ability of an element or a structure of undergoing large plastic deformations without a significant loss in strength. It provides the structure with the capacity of dissipating energy during strong motions, thus reducing its strength demand, and also avoids sudden (brittle) failures.

Strength and ductility are interchangeable in seismic resistance: Fig. 5.4 shows a typical criterion of equivalence between an elastic structure, with strength F_E , and an elasto-plastic structure of equal initial modulus E and ultimate deformation d_{max} , with strength F_Y .

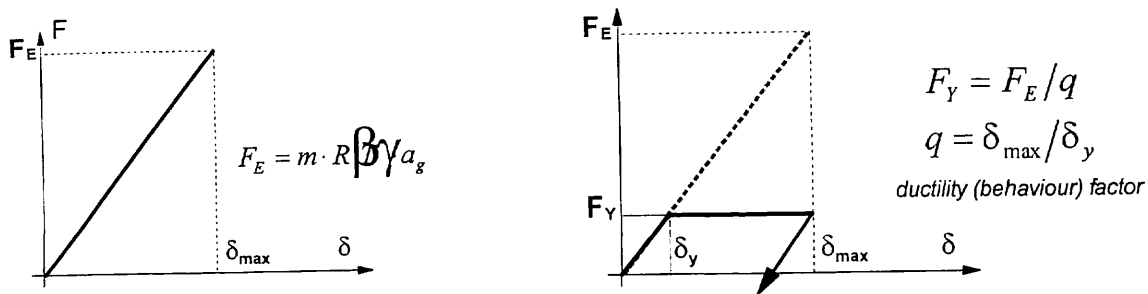


Fig. 5.4: Behaviour of equivalent structures: elastic (left) and elasto-plastic (right).

It is difficult to quantify precisely the ductility, especially for complex structures. Thus, structures are assigned conventional factors, according to type, shape, material, dimensioning, detailing (e.g., see Table below).

**Table 1. Basic values of ductility (behaviour)
q factor, after Eurocode 8.**

STRUCTURAL TYPE	Q
Frame system	5.0
Dual system:	
Frame equivalent	5.0
Wall equivalent, with coupled walls	5.0
Wall equivalent, with uncoupled walls	4.5
Wall system:	
With coupled walls	5.0
With uncoupled walls	4.0
Core system	3.5
Inverted pendulum system	2.0

Beyond the classification, designers should bear in mind the concept of ductility and design the structure in accordance to the principles outlined in these pages.

5.2 Diaphragm action

The main contribution required from decks (floors and roofs), with respect to the seismic performance of structures, is to act as diaphragms.

The primary function of a building structure, beginning from the decks, is to sustain service loads applied at various storeys. Decks are connected with vertical bearing elements (columns, walls) at nodes (joints).

An additional function of decks themselves is to link together the storey nodes, preventing their mutual displacements, which is called diaphragm action, giving rise to diaphragm forces.

These derive from internal constraints, tending to strain the deck's plane (temperature, shrinkage, creep, settlements, frame effects) and from external actions (wind, quakes).

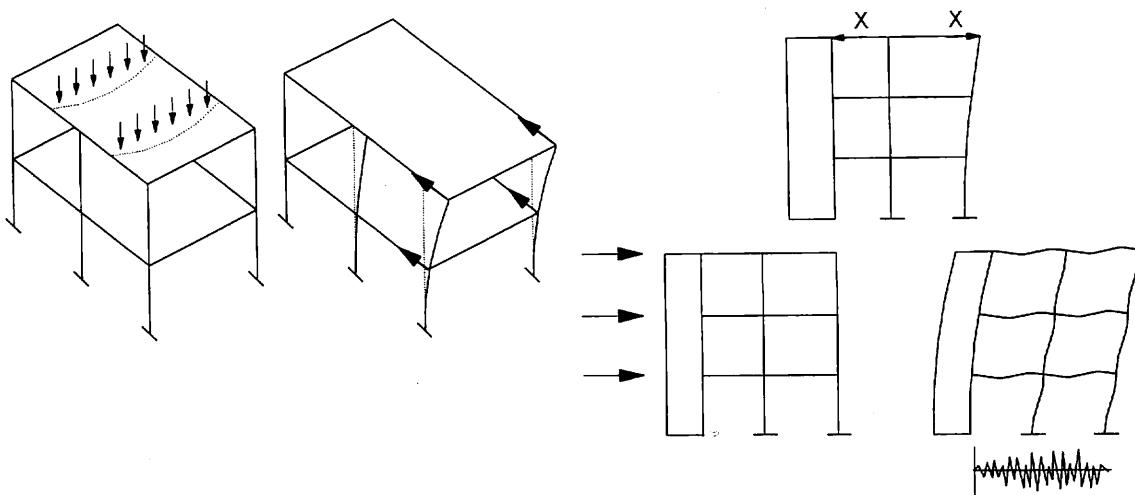


Fig. 5.5: Diaphragms functions (left) and typical actions (right).

Diaphragm action of floors is the in-plane action, whereas bearing actions are normal to the plane.

Diaphragms affect the distribution of horizontal forces among vertical frames and walls. The actual distribution may be calculated using an overall structural analysis. A diaphragm distributes not only the horizontal forces applied at its own level but all floor diaphragms react when a force acts at one level (see Fig. 5.6).

Floors are virtually rigid for in-plane shear and bending, with respect to horizontal deflections of vertical frames. Thus, structural analysis normally assumes perfect stiffness. However, non-rigid diaphragms may exist (e.g. discontinuous roofs, Fig. 5.7). In this case, vertical structures are partially independent.

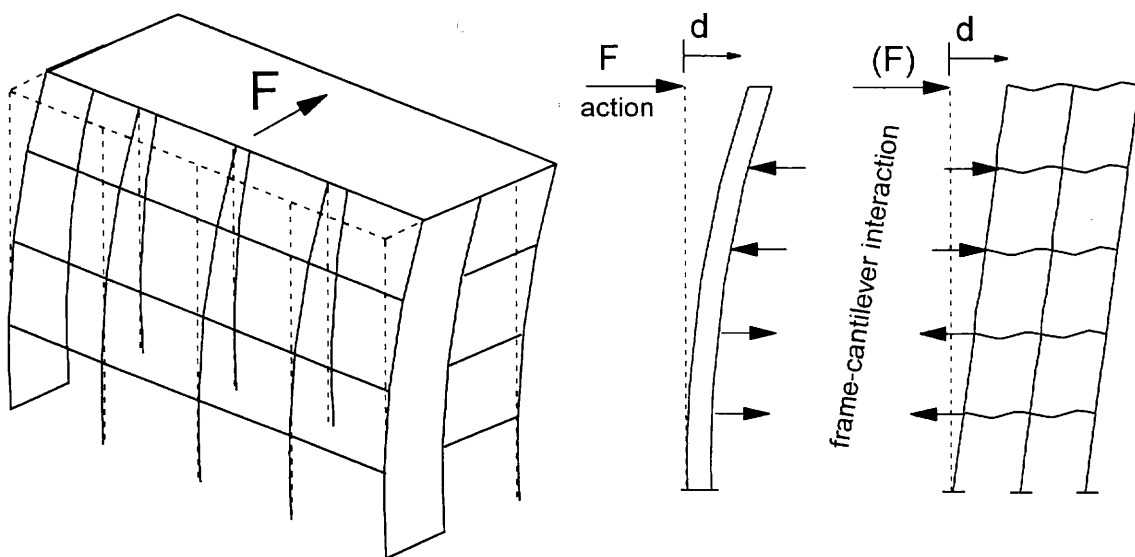


Fig. 5.6: Storey forces are given by global structural analysis.

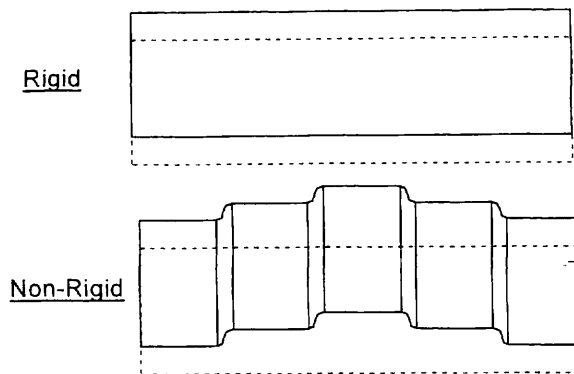


Fig. 5.7: Rigid and non-rigid models.

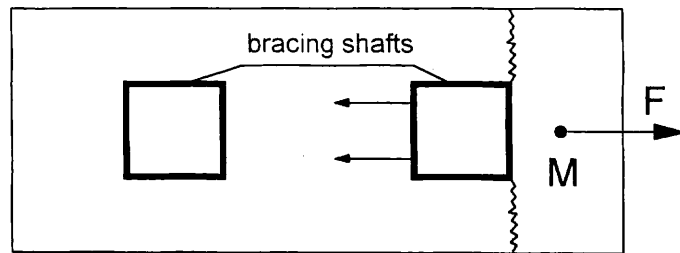
5.3 Seismic diaphragms

All variable actions are dynamic.

However, only seismic actions imply inelastic and cyclic deformations in structures

An essential difference with a seismic diaphragm is that it needs capacity to withstand inelastic deformations without loss of strength. It is a rather qualitative difference, as dissipation takes place to elements other than diaphragms.

Another important point is that forces are applied at strong points within the structure, i.e., within the diaphragm, producing tensile forces (Fig. 5.8).

Fig. 5.8: The inertial force F of mass M produces tension in diaphragm .

Stress states in diaphragms are basically not critical, even in seismic conditions, provided that the structure has:

- regular layout (bi-symmetric, compact, ..., see Fig. 5.9)
- regular elevation shape (continuous vertical elements)
- uniform distribution of stiffness and mass
- reasonable proportions

and diaphragms are continuous and well connected.

Under these circumstances the function of the diaphragm can be considered as satisfactory.

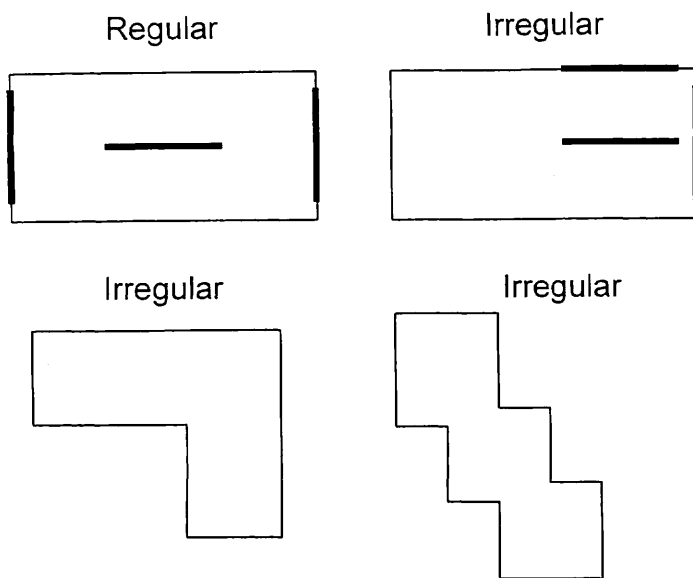


Fig. 5.9: Regular and irregular layout of buildings.

In contrast, the stresses increase, becoming locally critical and initiating cracks, when the structure has

- large spans on flexible bearings with distant bracings (e.g., dual structures)
- non-compact layout (which excites torsional modes)
- vertical elements interrupted at mid height (Fig. 5.10)
- large openings, inlets, concave corners in floors (Fig. 5.10)
- mechanical gaps, like supports and joints (of special relevance in prefabrication)
- previous cracks of other origin (slab action, shrinkage, ...)

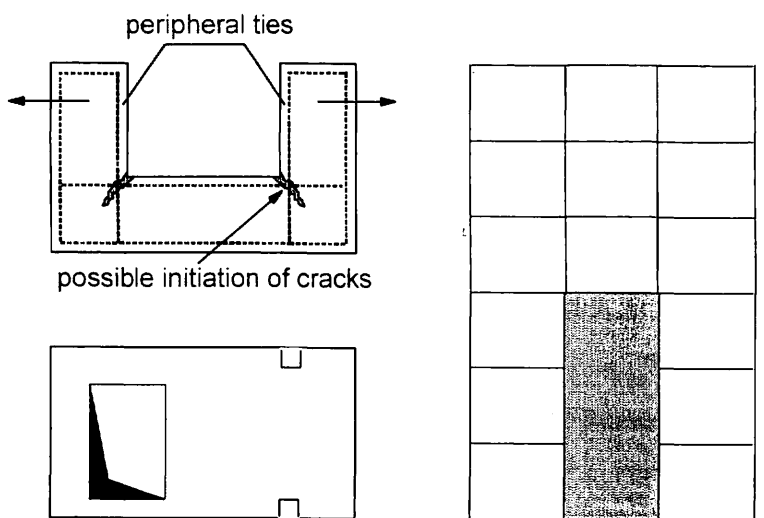


Fig. 5.10: Concave corners in plan, openings and inlets, shear walls interrupted

5.4 Design criteria

When the forces applied at each story have been established as discussed in previous paragraph, the diaphragms may be designed. It may well be that the capacity of the diaphragm will be very large relative to the forces to be absorbed. The actual design criterion to be considered is likely to be the actual resistance of the ductile main frame (capacity design criterion).

Struts-and-ties models are well suited for bi-dimensional (in-plane) problems.

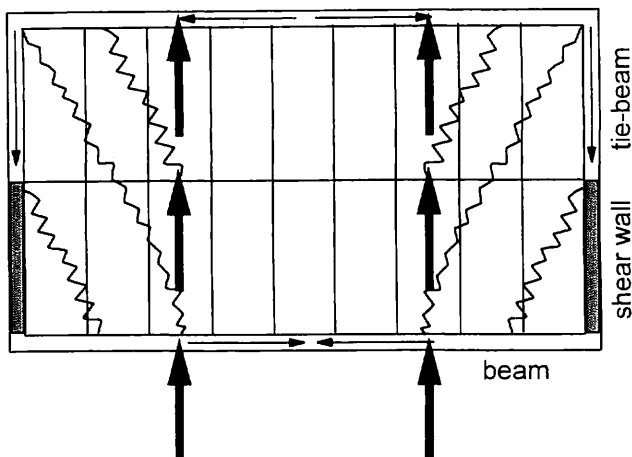


Fig. 5.11: Struts-and-ties idealization of diaphragm forces.

In today's construction, for economic reasons many floors are precast, even in cast-in-situ buildings. Particularly suitable are Hollow-Core Slabs floors, with or without structural topping.

Structural topping, provided with good reinforcement detailing, may be of some benefit for ensuring continuity to the whole diaphragm, where it is of complex shape. However, it introduces additional mass, without fully exploiting the slabs' capacity in bending. Toppings are min 50 mm deep, reinforced with fabric mesh. Ultimate conditions may be related to:

- failure of connection with shear walls
- buckling of concrete struts, under combined plate and slab stresses (adhesion to prefab slabs is critical)
- brittle failure of small diameter rebars (due to excess of bond).

Untopped floors are lighter and perform diaphragm action through their full depth in joints.

Joints (slab-to-slab, slab-to-beam, slab-to-bracing, ties) are crucial and require accuracy in design and execution.

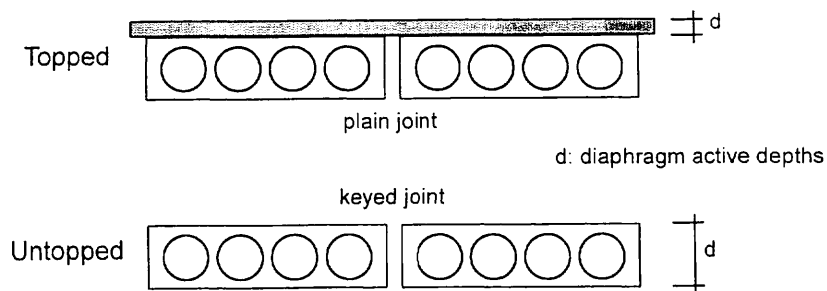


Fig. 5.12: Scheme of precast HCS floors, with/without structural topping.

In non-seismic buildings, joints may be justified by their strength established from test or calculation.

In seismic buildings, the capacity of maintaining strength after severe load reversals and possible "ductility" are of paramount importance, too.

Systems meeting the above pre-requisites have been developed and practically applied, after extensive experimental research.

Joints must show the following features:

- high shear resistance
- strain-hardening behaviour in shear vs. sliding
- possible energy dissipation during loading cycles
- very limited degradation after severe load reversals.

Plain joints in untopped floors are not recommended, neither are sharply keyed joints, as interlocking of cracked faces cannot be relied upon, after the smoothing out of indentations due to cyclic friction.

An example of a slab-to-slab joint, fulfilling the above requirements for untopped floors, is the continuous wave-profiled slab edge, infilled with mortar to form the shear-joint (Fig. 5.13).

Slab-to-beam joints must be provided with reinforcement anchored to the ties and protruding into at least two grouted cores per slab, dimensioned according to the criterion of capacity design.

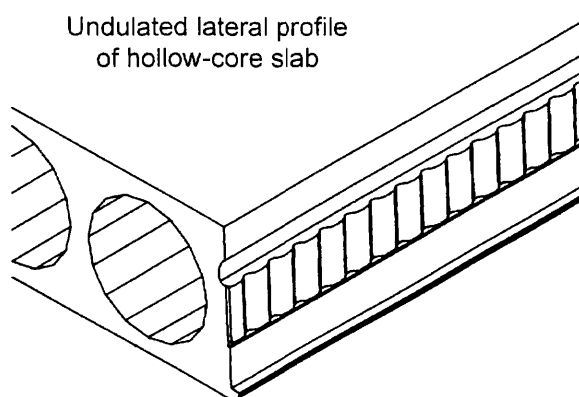


Fig. 5.13: Waved profile of Hollow Core Slab edge.

The connection of the diaphragm to the vertical seismic resistant elements (shear walls, bracings, ...) is provided by tie-beams, connected to the slabs via the joints.

A mechanically continuous tying system of steel bars must be provided, following the layout of struts-and-ties or the results of other type of analysis (see for example Fig. 5.10 and 5.11). If splices are overlapped, they are to be located in areas unlikely to crack.

Sophisticated models for numerical non-linear analysis of complex shape diaphragms do exist, but their use is mainly suited for research purpose. Given that floors must be checked for diaphragm action according to the criteria of robustness and capacity design, a well drawn struts-and-ties model is a good basis for adequate detailing.

Appendix: Calculation examples

The seismic forces acting on diaphragms should be calculated according to an overall structural analysis and eccentricities of the masses, as required by codes and should take account of eccentricities of force due to the layout and form of the structure.

For the sake of simplicity, the acting forces in the following examples will be considered independent of the rest of the structures and no eccentricities will be introduced. This would be acceptable also in common practice, because the internal forces within the diaphragms itself do not vary a great deal and due to the uncertainties of the actions and of the model. It is normally acceptable to consider the forces on an overall basis.

However, it is important to determine not only an overall resultant acting force on the diaphragm but several resultant, properly located. It should be noted that a wrongly located force could incorrectly indicate tensile forces when in fact compressive forces exist.

Once the acting forces are found, the reactions at the bracing points can be determined. In "dual structures", frequent in prefabrication, where columns are relatively deformable compare with bracing shear walls that are present, the reactions can be assigned entirely to the latter elements.

Once all acting and reacting forces are established, a system of ties should be designed, according to a strut-and-tie model. Drafting the lay-out of the struts and ties is left to the designer's judgement. Analysis of the internal forces is easily performed and enables the designer to dimension the steel reinforcement in ties and to work out shear and other forces in joints.

Some examples are given, (figures 2, 3, 4, 5,) showing typical diaphragm shapes, with various length-depth ratios L/H, positions of bracings and direction of quake forces.

Seismic forces F acting along a line, and referring to one floor field, are divided into upper, middle and lower forces F_u , F_m , F_d , according to their position on the floor. F_m represent the inertia force due to permanent loads of the floor plus a given part of the live loads.

F_u and F_d represent approximately the outer walls, beams and columns.

F_u , F_m and F_d mobilize the additional parallel tensile forces (S), that can be shared among slabs (see Figs. 1 and 2). These need connections through the slab cores, that work also in the shear transmission mechanisms between slabs and beams (fig. 1).

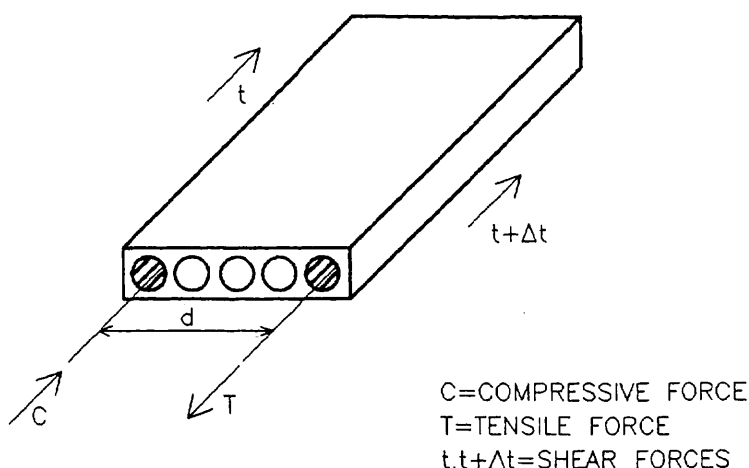


Fig. 1

The figures show possible strut-and-tie patterns for some typical floors, starting from the simplest ones. Struts may be taken at 45° . The patterns of strut-and-ties trusses are indicated, as well as the values of their internal forces - compressive (C) or tensile (T), respectively - forces F_u , F_m and F_d may be summed up for simplicity in order to have only nodal forces on the truss. Depending upon how the truss is analyzed, forces S may need to be added to tensile forces T.

In the schemes of figs. 2, 3 and 4, the diaphragm works as a horizontal deep beam, being restrained at both ends; in fig. 5 and 6, as a cantilever, clamped at one end. All have the slabs parallel to the external forces F.

@Seismicisolation

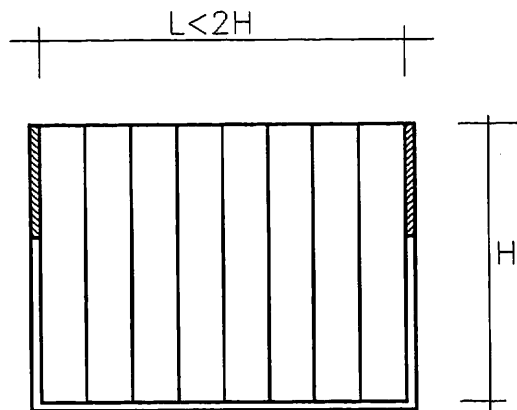
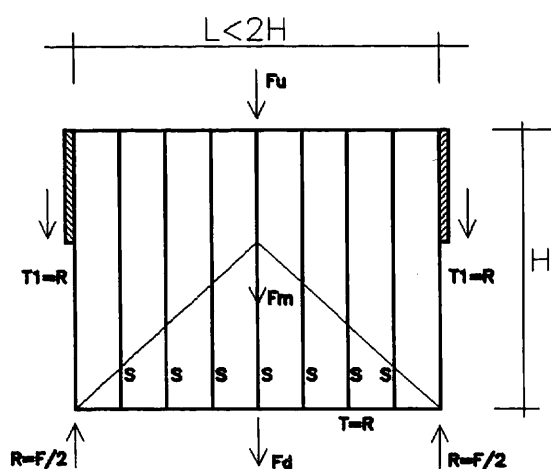


Fig.2A



SEISMIC FORCE (APPLIED)
 $F = F_u + F_m + F_d$
 $S = \text{TENSILE FORCES IN PARALLEL TIES}$
 $T = \text{TENSILE FORCE IN CHORD TIE BEAM}$
 $\Sigma S = \Sigma F_m + \Sigma F_d + \Sigma F_u$
 $R = \text{HORIZONTAL REACTIONS ON BRACINGS}$
 $T_1 = \text{ACTION ON SHEAR WALL}$

Fig.2B

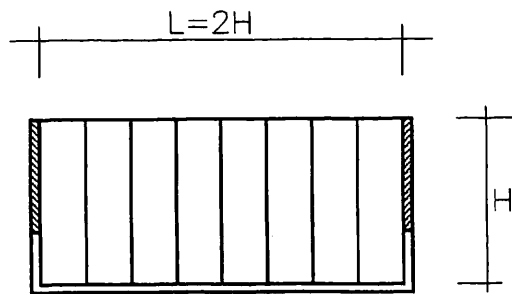
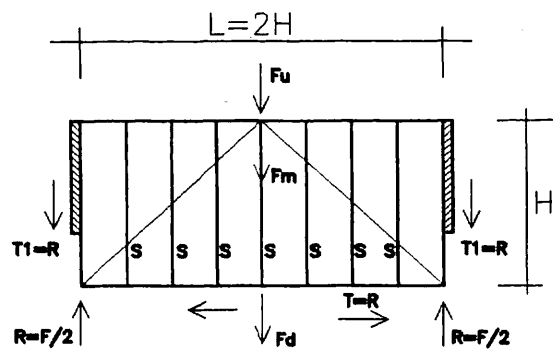


Fig.3A—EXAMPLE OF FLOOR



SEISMIC FORCE (APPLIED)
 $F = F_u + F_m + F_d$
 S=TENSILE FORCE IN PARALLEL JOINTS
 T=TENSILE FORCE IN CHORD TIE BEAM
 $\Sigma S = \Sigma F_m + \Sigma F_d + \Sigma F_u$
 R=HORIZONTAL REACTIONS ON BRACINGS
 $R = T_1$

Fig.3B —STRUT-AND-TIES-PATTERN

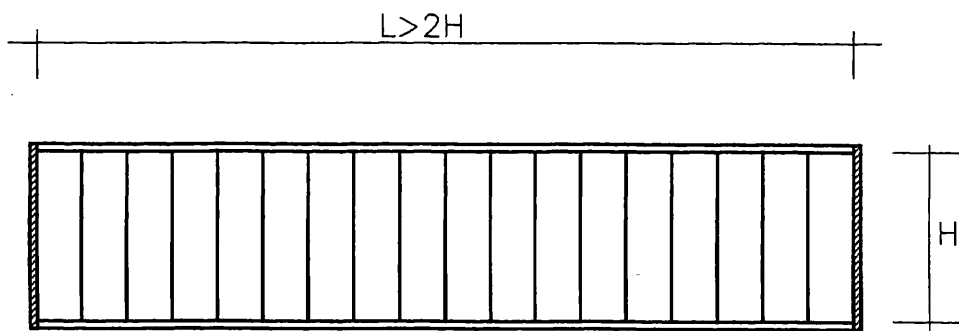
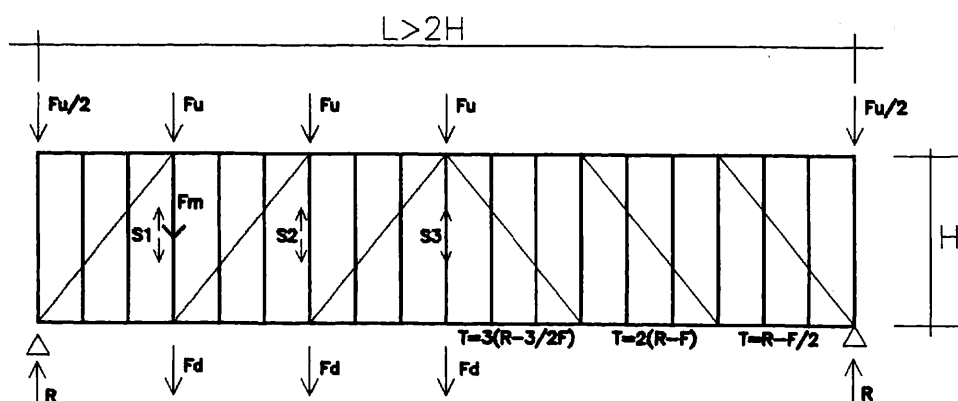
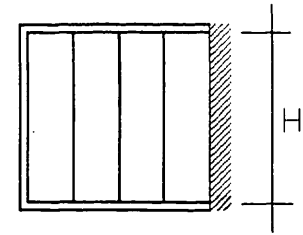


Fig.4A – EXAMPLE OF FLOOR



$$\begin{aligned} F &= F_u + F_m + F_d \\ R &= 3F \\ S_1 &= R + F_m + F_d \\ S_2 &= R + F + F_m + F_d \\ S_3 &= F_m + F_d \end{aligned}$$

Fig.4B – STRUT-AND-TIES PATTERN



$L=H$

Fig.5A

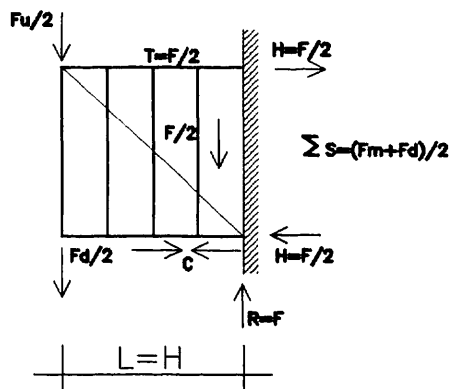
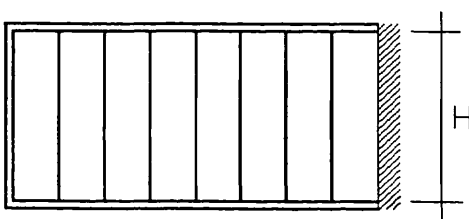


Fig.5B



$L=2H$

Fig.6A

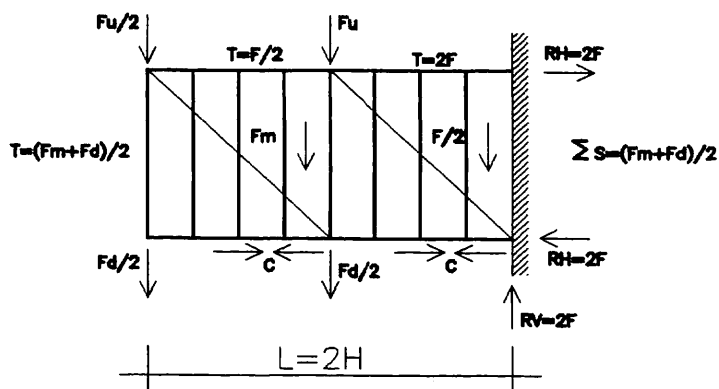


Fig.6B
@Seismicisolation

Fig. 7A show a typical deep beam type floor, where Fig. 7B its strut-and-ties model.

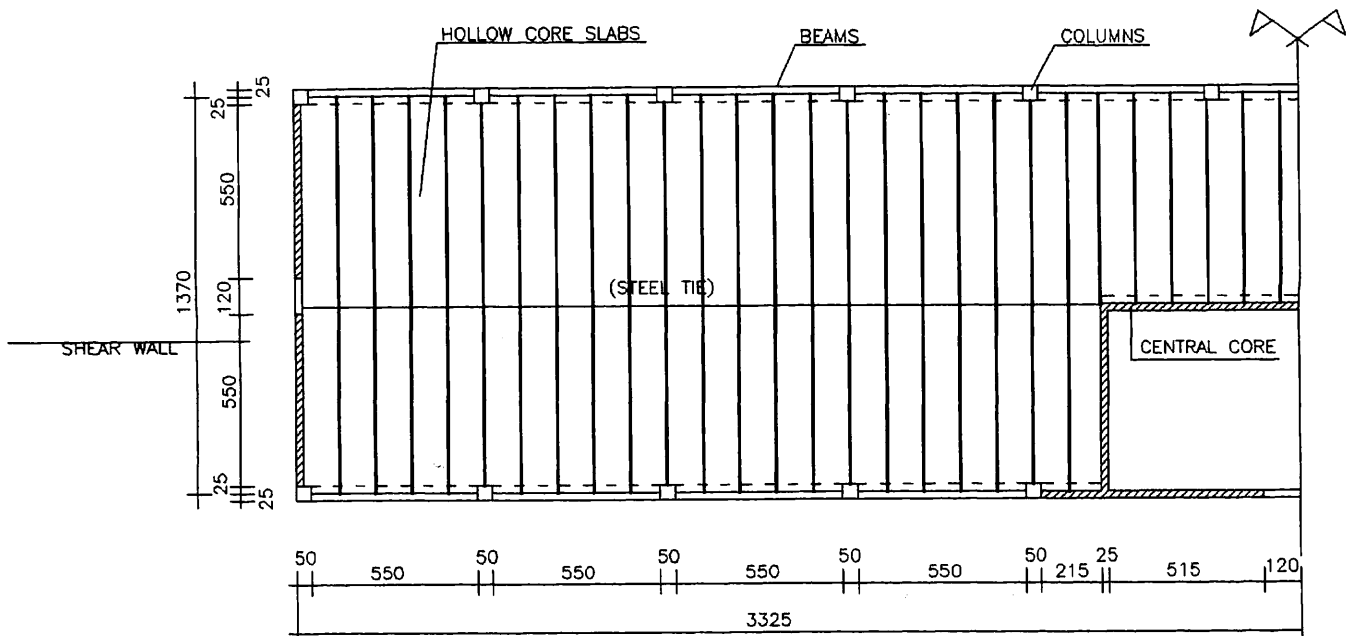


Fig.7A – BUILDING WITH CENTRAL CORE AND LATERAL SHEAR WALLS

In absence of a central beam and of a reinforced topping, as in this case, with long span slabs, a steel tie is advisable, in order to make it possible the strut-and-tie system as in fig. 7B.

The tie is made of steel tendons or sheathing bars laid upon the slabs. If neither a beam and a tie is placed to split the span, a different, unfavorable strut-and-tie system develops.

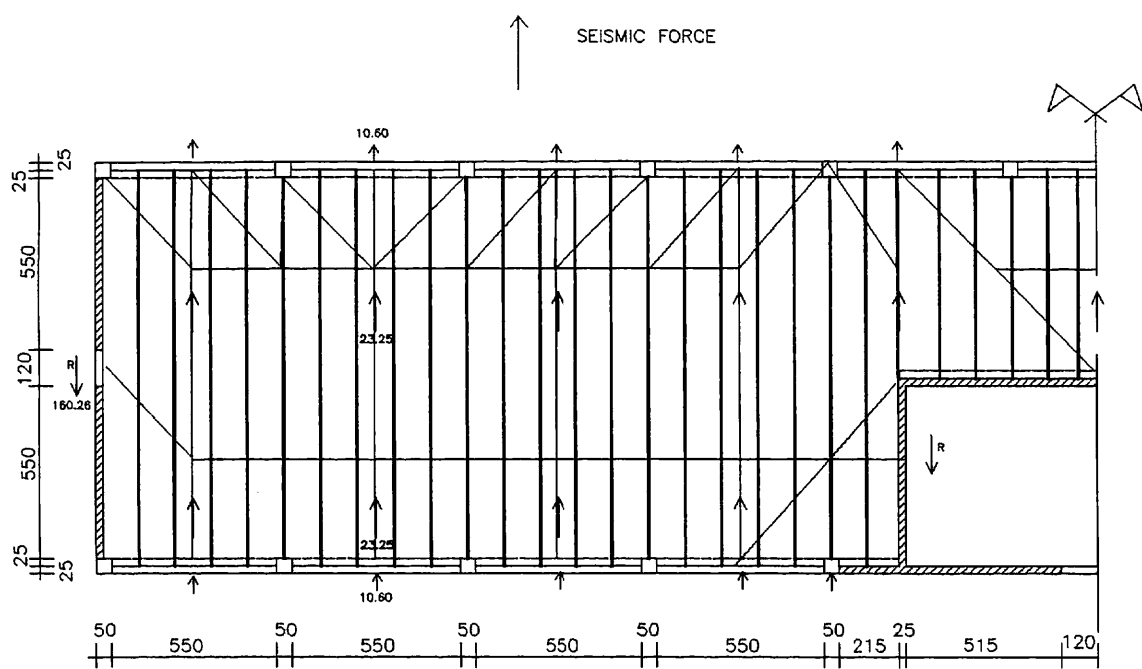


Fig. 7B

The example represents the 4th floor of a building. The acting seismic forces have been calculated following the equivalent static analysis and gives, for the typical field, values are follow

$$F_u = 10.6 \text{ KN}$$

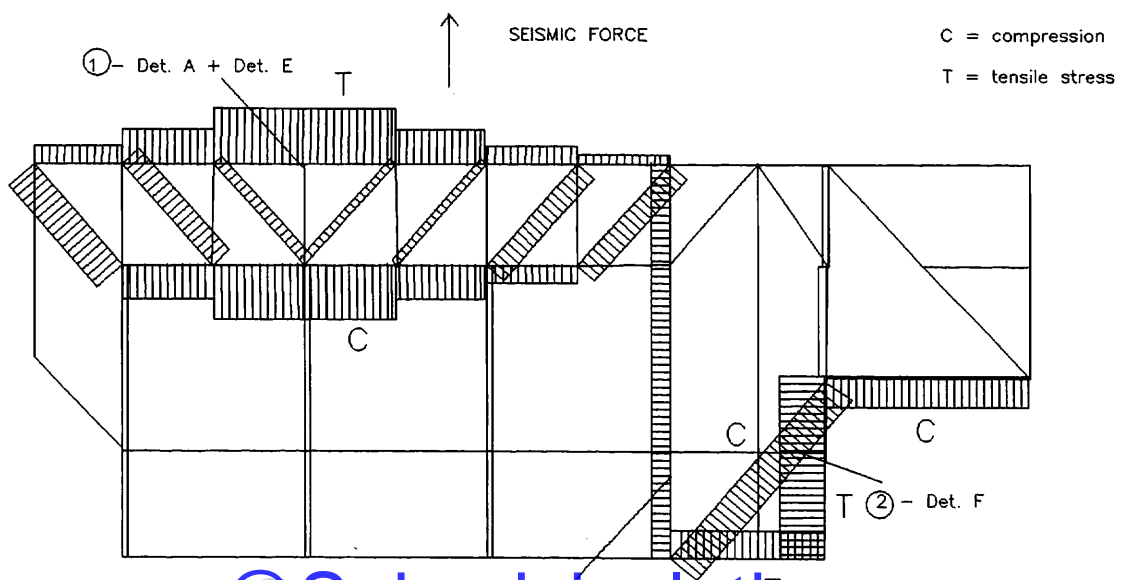
$$F_m = 46.5 \text{ KN}$$

$$F_d = 10.6 \text{ KN}$$

In fig. 7B the corresponding internal forces are shown.

According to the Italian code, those forces are to be considered as "service forces", to be checked against allowable stresses. A similar principle could be followed using limit state methods.

The allowable stress for reinforcing steel is taken at 260 Mpa. Thus, the reinforcement in tie-beams is determined, as follows.



@Seismicisolation

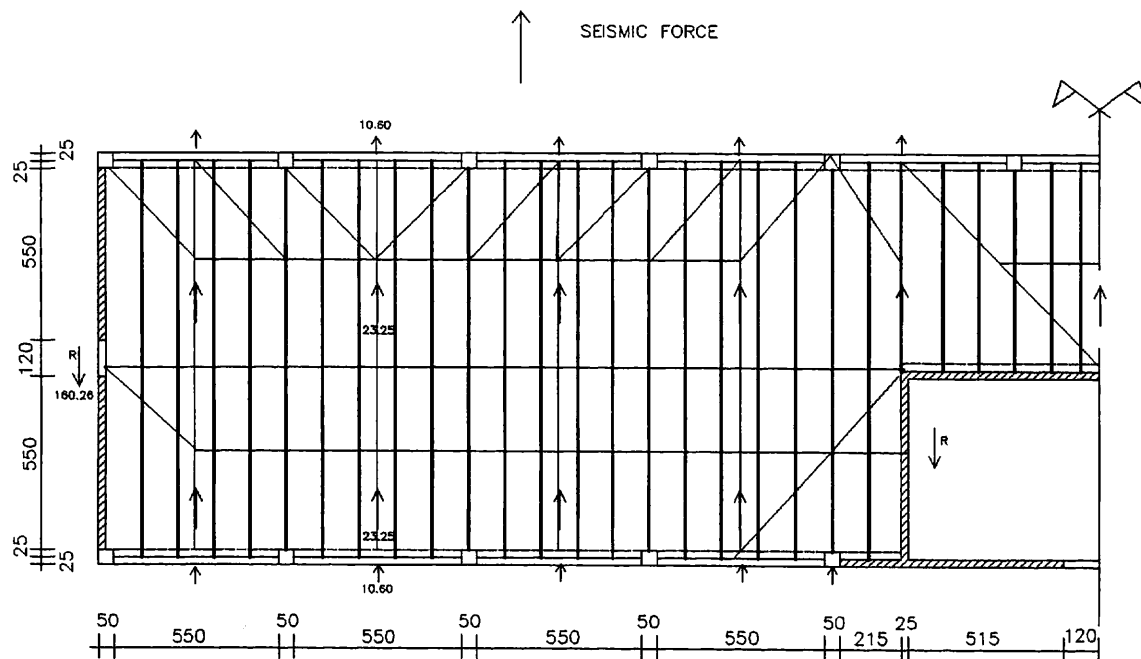


Fig.7C – example with steel tie

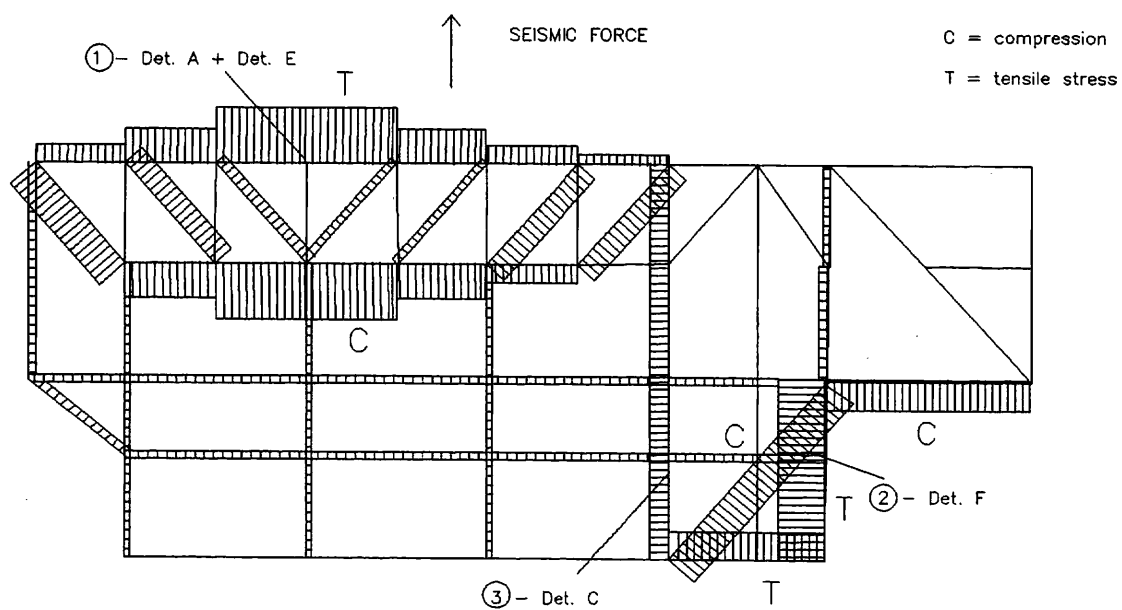


Fig.7D
@Seismicisolation

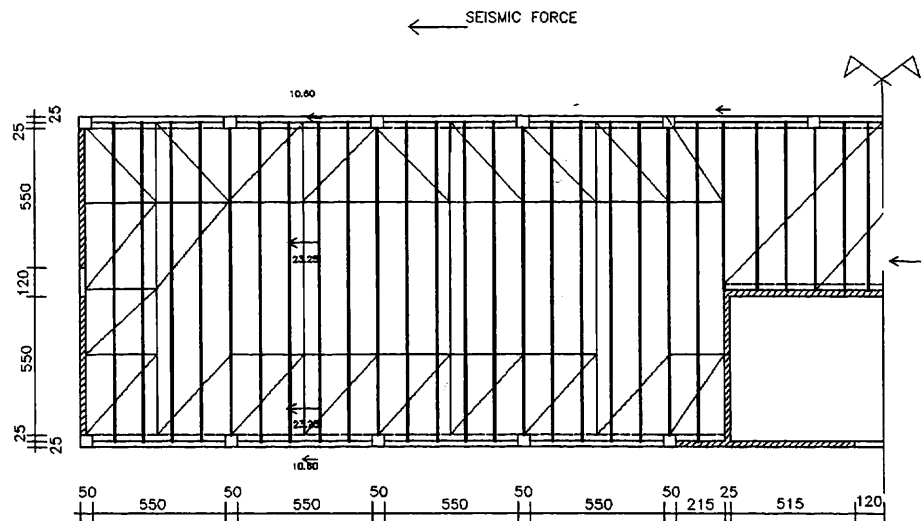


Fig. 7E – example without steel tie

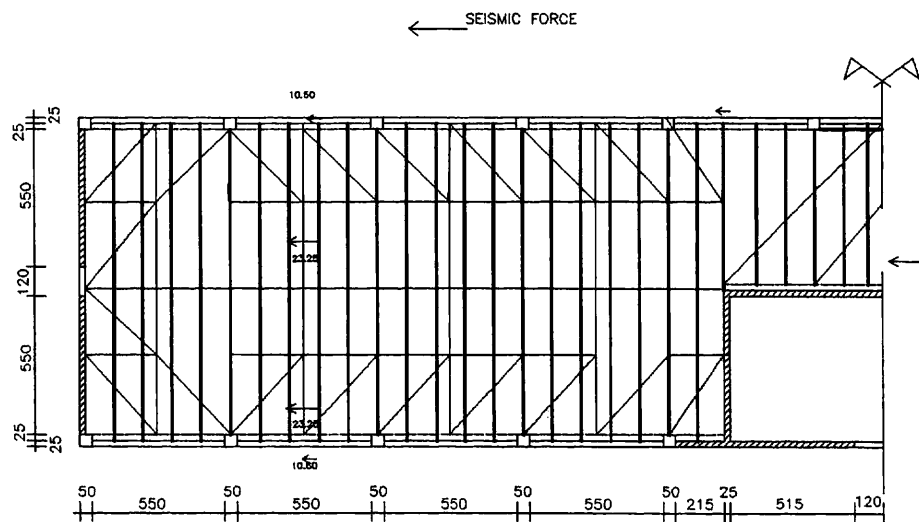
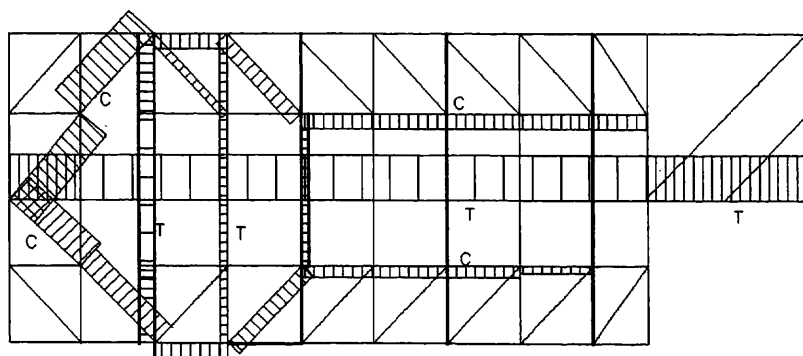


Fig. 7F – example with steel tie



C = compression
T = tensile stress

Fig. 7G

EXAMPLES OF DESIGN (fig. 7)

①

$$T_1 = 221 \text{ KN}$$

$$A_{s1} = 221000 / 260 = 850 \text{ mm}^2 \rightarrow 4 \text{ bars of } 8 \text{ mm. dia (detail A + det. E fig.10)}$$

②

$$T_2 = 177 \text{ KN}$$

$$A_{s2} = 17700 / 260 = 680 \text{ mm}^2 \rightarrow 3 \text{ bars of } 8 \text{ mm. dia (detail F fig.10)}$$

③

$$T_3 = 110 \text{ KN}$$

$$A_{s3} = 11000 / 260 = 423 \text{ mm}^2 \rightarrow 3 \text{ bars of } 14 \text{ mm. dia (detail C fig.10)}$$

- Connecting reinforcement (detail B fig. 10)

$$\Delta t = 4 \cdot 23.25 / 4 = 5.81 \text{ KN}$$

$$T = M / d = \Delta t = 1200 / 900 = 7.75 \text{ KN}$$

$$A_s = 7750 / 260 = 29 \text{ mm}^2 \rightarrow 2 \text{ bars of } 12 \text{ mm. dia. (detail B fig.10)} \\ (\text{required for shear capacity of slab})$$

- Reinforcement in shear wall (detail F fig. 10)

$$A_s = R / 260 = 160250 / 260 = 620 \text{ mm}^2 \rightarrow 3 \text{ bars of } 18 \text{ mm. dia}$$

A similar example is shown as in figs. 8A, B, which still has forces parallel to the slabs, but is a cantilever type (one end free).

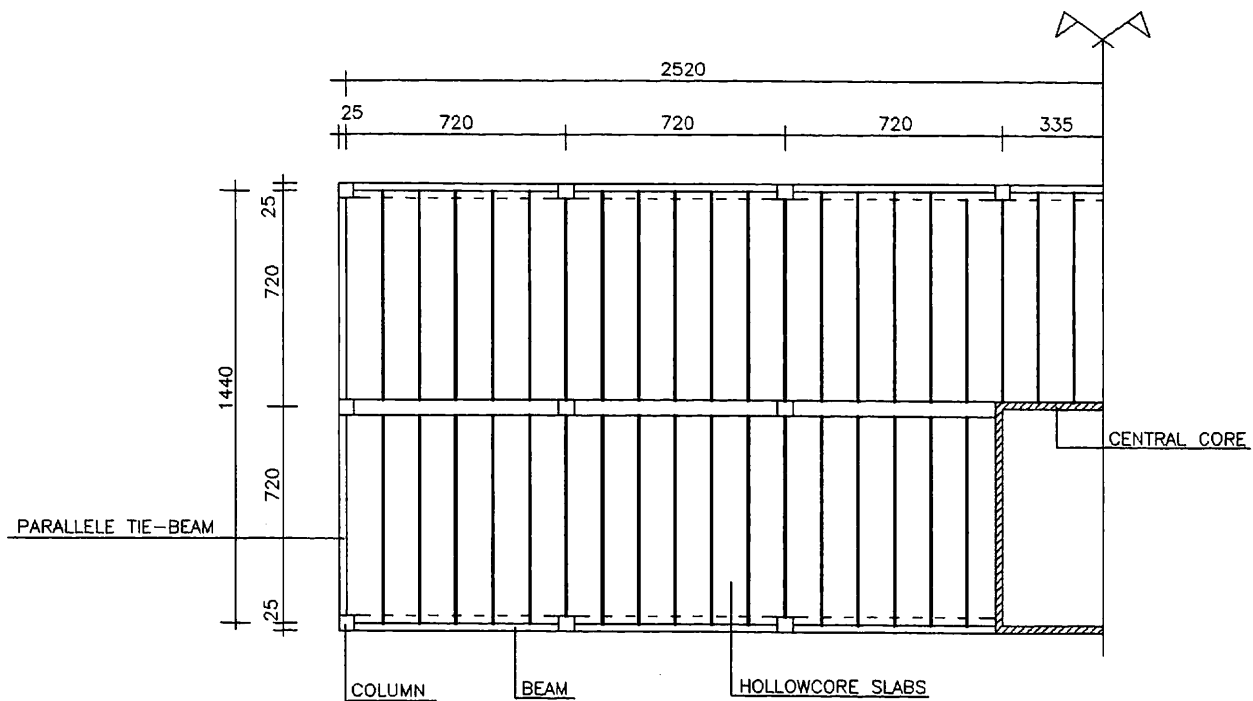
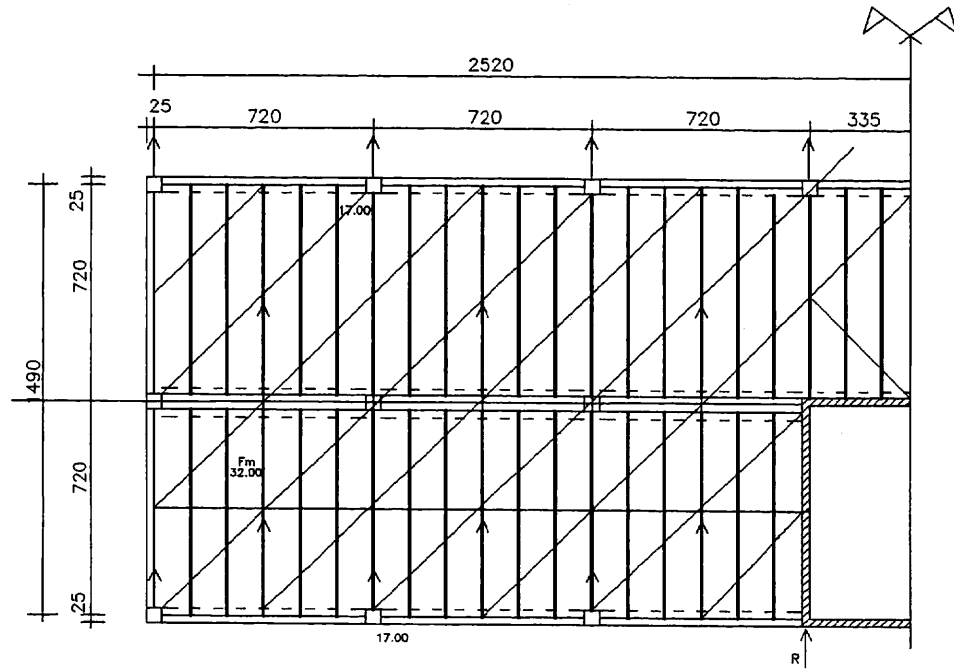


Fig.8A - BUILDING WITH CENTRAL CORE



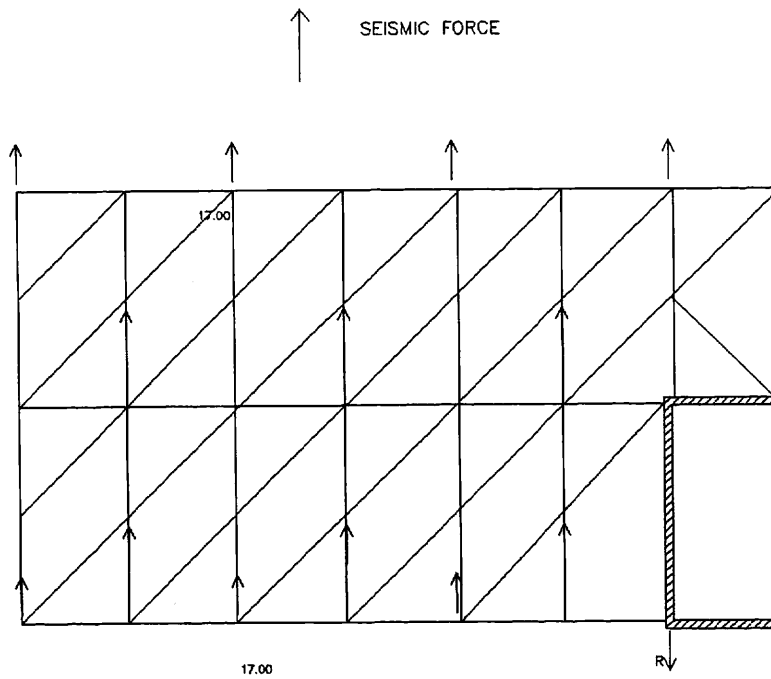


Fig.8C

C = compression

T = tensile stress

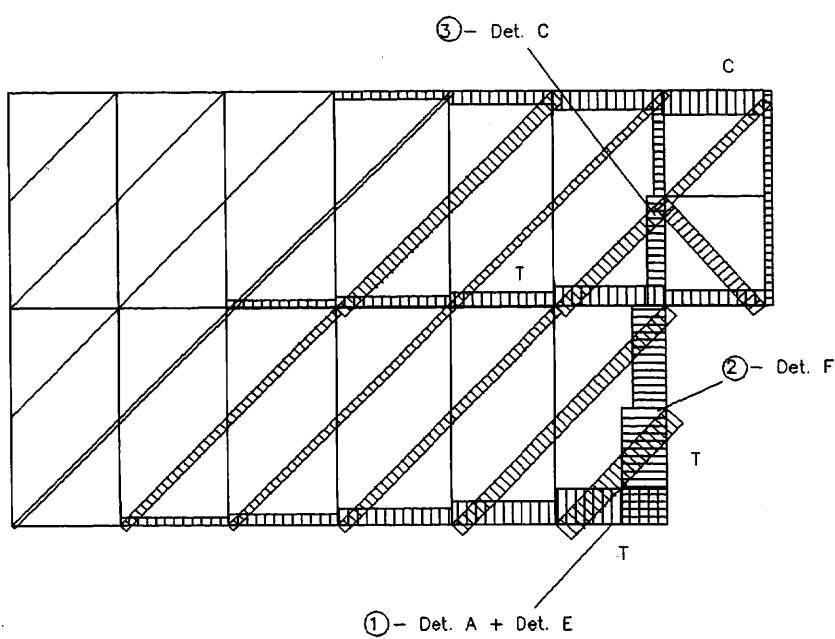


Fig.8D

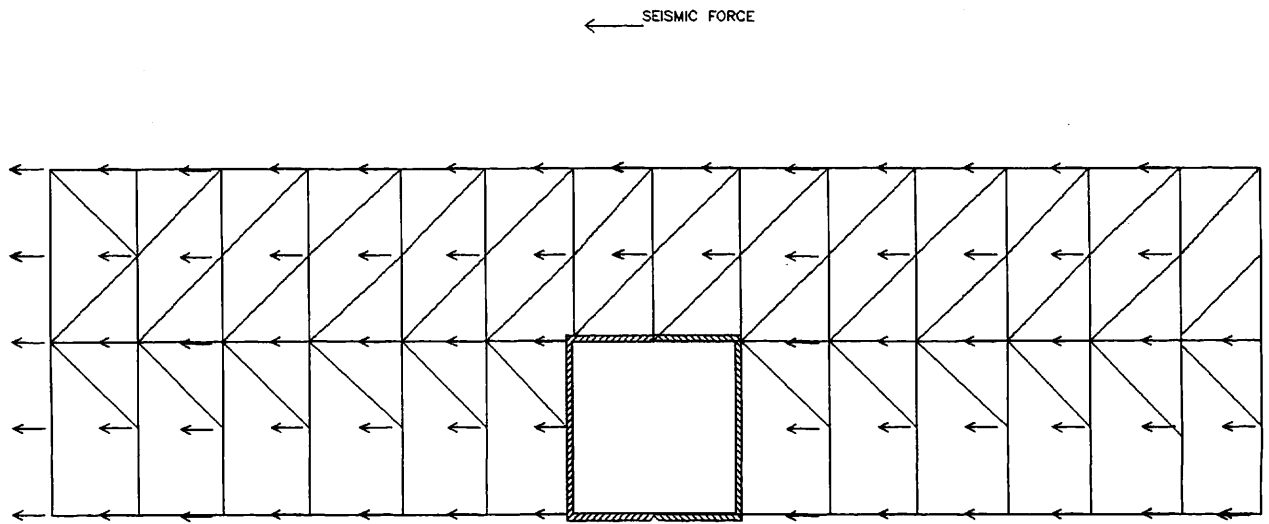


Fig.8E

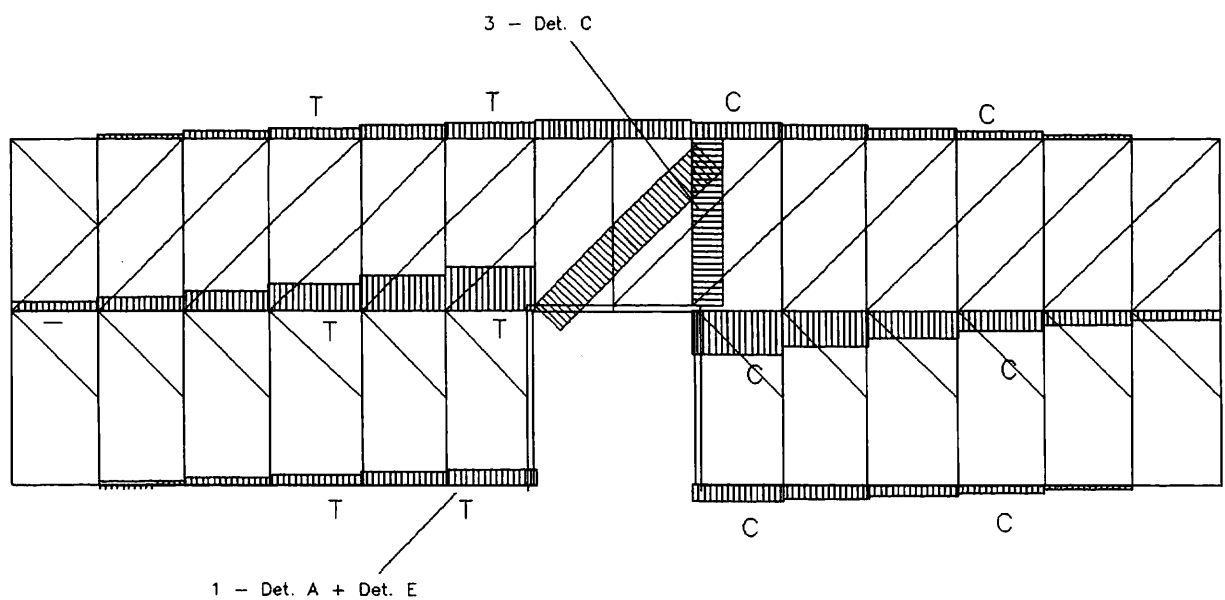


Fig.8F

The forces, in tie-beams result

-FIG . 8C

①

$$T_1 = 325 \text{ KN}$$

$$A_{s1} = 325000 / 260 = 1250 \text{ mm}^2 \rightarrow 4 \text{ bars of } 20 \text{ mm. dia (detail A + det. E fig.10)}$$

②

$$T_2 = 240 \text{ KN}$$

$$A_{s2} = 240000 / 260 = 920 \text{ mm}^2 \rightarrow 3 \text{ bars of } 20 \text{ mm. dia (detail F fig.10)}$$

③

$$T_3 = 140 \text{ KN}$$

$$A_s = 140000 / 260 = 538 \text{ mm. } 3 \text{ bars of } 16 \text{ mm. dia (detail C fig.10)}$$

The situation with forces perpendicular to the slab direction is analyzed in the schemes shown in Fig. 9.

It would be complicated to plot on the same drawing all forces together. Thus, the effects have been divided into the forces acting on each floor field. The idealized example assumes that a central force $F_m = 20$ KN and edge forces F_b (as previous F_u and F_d) are applied at one field (Fig. 9/A).

Effects of edge forces F_b are easy to calculate, thus only forces F_m are considered.

EXAMPLES OF DIFFERENT POSITIONS OF F_m (MIDDLE SEISMIC FORCE)

Assuming $F_m = 20$
 (Lower $F_m/2$ (=10) effects not shown)
 (s [fig. 7/B] is not shown)

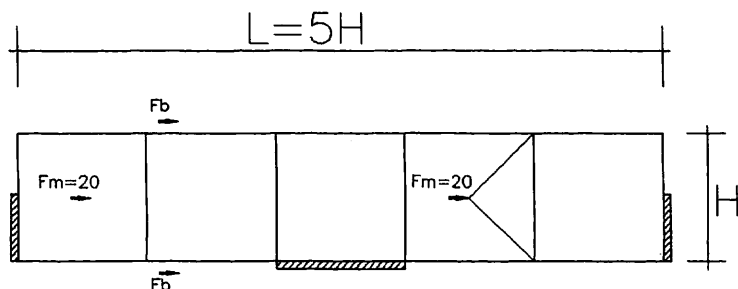


FIG. 9A

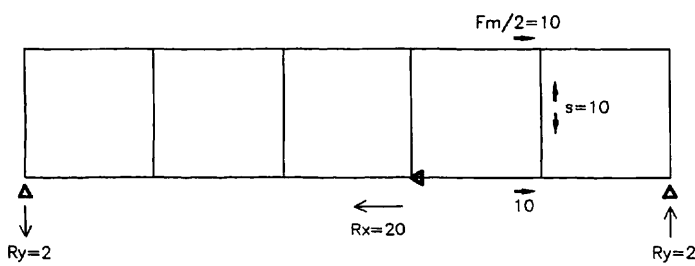


FIG. 9B

Fig. 9/B schematically shows the reactions R_x and R_y due to F_m applied to the fourth field, which divides into twice $F_m/2$ at the edges via two struts, as well as the local chord force $S = F_m/2 = 10$. The effects of the upper $F_m/2$ in two different position are shown in Fig. 9/C and 9/D, respectively, in terms of all internal forces in the idealized truss model.

Thus, the effects of F_m on all fields must be superimposed, including chord forces S .

The effects of F_m are to be superimposed, also and the summarised set of internal forces is shown in Fig. 9/E.

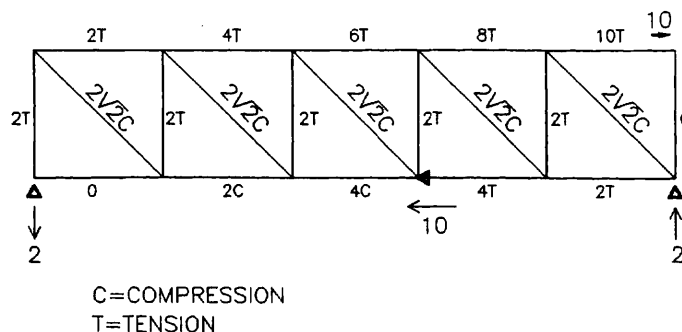


FIG. 9C

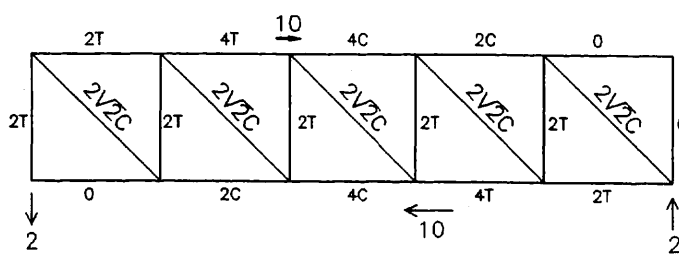
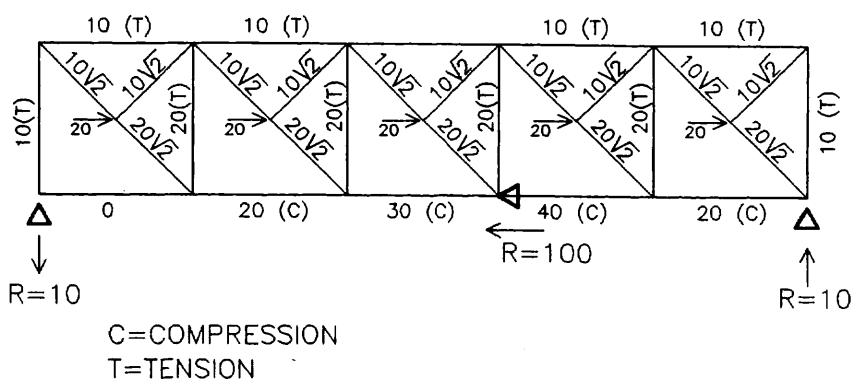


FIG. 9D



The tensile connection between slab and tie beam deserves some observations.

Until the diaphragm is monolithic, tensile tie forces are assigned to the slabs, which are connected to beams by re-bars anchored in some of their cores. If slab-to-slab joints are allowed to move, a different mechanism takes place. If joints fail completely, it tends to become a Vierendeel model, where slabs are the only shear connectors between compressive and tensile flanges, thus being subject to bending and shear. For this condition, although an extreme one, it is advisable to optimize the bending capacity of the connection, by anchoring possibly the connecting re-bars in the outer cores of the slabs (Fig. 1).

Anchoring the re-bars in the slab-to-slab joints is not recommended. In fact, they may disturb the joint filling and impair the joint's shear capacity, by adding bond to shear stresses, also any crack opening in the joint would destroy the bond. This could happen under ultimate severe conditions but, in seismic structures, this possibility should be assumed even if not suggested by mathematical analysis.

Some typical reinforcement and connections details are shown in Fig.10.

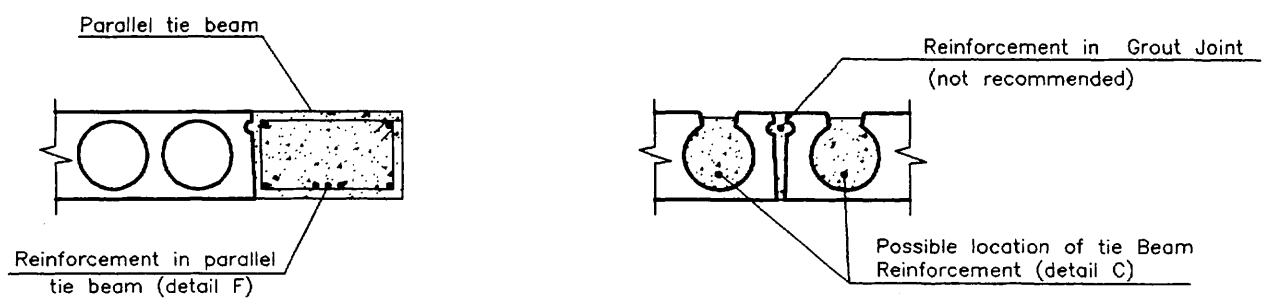
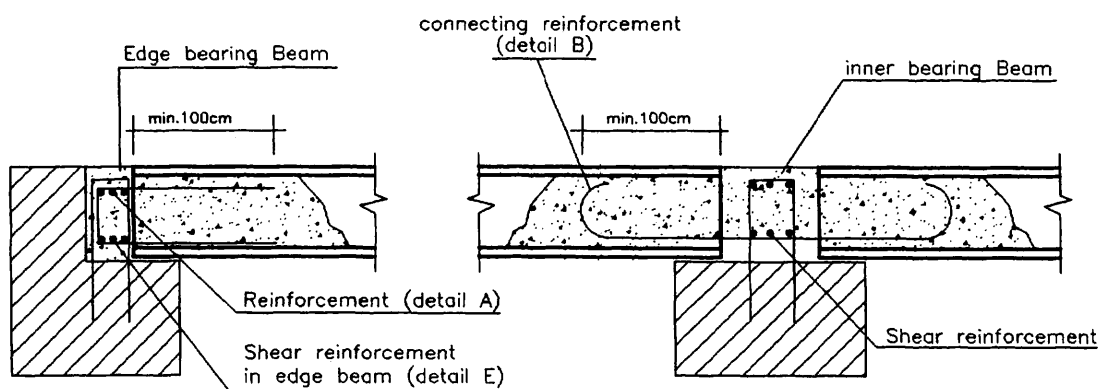
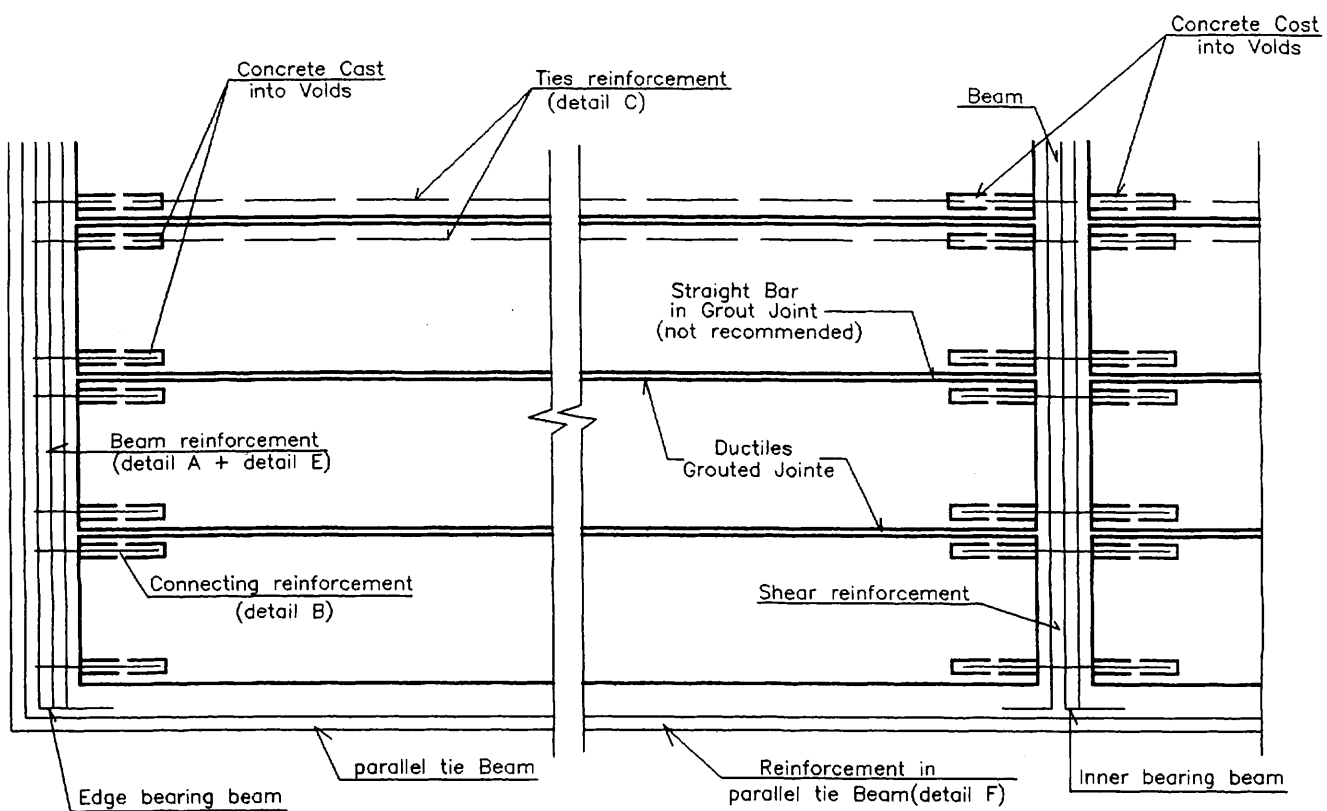


Fig. 10
@Seismicisolation